



MISO : Multimodal Investigation of Stroke Origin

Cyril Dargazanli

► To cite this version:

| Cyril Dargazanli. MISO : Multimodal Investigation of Stroke Origin. Human health and pathology. Université de Montpellier, 2022. English. NNT : 2022UMONT076 . tel-04650608

HAL Id: tel-04650608

<https://theses.hal.science/tel-04650608>

Submitted on 16 Jul 2024

HAL is a multi-disciplinary open access archive for the deposit and dissemination of scientific research documents, whether they are published or not. The documents may come from teaching and research institutions in France or abroad, or from public or private research centers.

L'archive ouverte pluridisciplinaire **HAL**, est destinée au dépôt et à la diffusion de documents scientifiques de niveau recherche, publiés ou non, émanant des établissements d'enseignement et de recherche français ou étrangers, des laboratoires publics ou privés.

THÈSE POUR OBTENIR LE GRADE DE DOCTEUR DE L'UNIVERSITÉ DE MONTPELLIER

En Biologie Santé

École doctorale CBS2, SCIENCES CHIMIQUES ET BIOLOGIQUES POUR LA SANTÉ

Unité de recherche : Institut de Génomique Fonctionnelle
UMR 5203 CNRS - U 1191 INSERM, Montpellier

MISO : Multimodal Investigation of Stroke Origin

Présentée par Cyril DARGAZANLI
Le 2 décembre 2022

Sous la direction de Vincent COSTALAT
et la co-direction de Nicola MARCHI

Devant le jury composé de

Romain BOURCIER, PU-PH, CHU de Nantes

Président du Jury

Frédéric CLARENÇON, PU-PH, CHU de Paris La Pitié-Salpêtrière

Rapporteur

Vincent COSTALAT, PU-PH, CHU de Montpellier

Directeur de thèse

Nicola MARCHI, Docteur, Institut de Génomique Fonctionnelle, Montpellier

Membre du Jury

Christophe HIRTZ, Professeur, CHU de Montpellier

Membre invité

Philippe MARIN, Docteur, Institut de Génomique Fonctionnelle, Montpellier

Membre invité



UNIVERSITÉ
DE MONTPELLIER

REMERCIEMENTS

*Je remercie tout d'abord l'équipe de l'**Institut de Génomique Fonctionnelle** de Montpellier, pour cette collaboration fructueuse qui a rendu ce travail possible :*

Au Docteur Nicola Marchi, pour cet accompagnement sans faille, tes remarques, corrections, et ta disponibilité.

Au Docteur Frédéric de Bock, à Emma Zub et Marine Blaquièvre : je ne vous remercierai jamais assez car sans votre aide, je n'aurai pas pu conduire ce travail. Léonie : merci pour m'avoir aidé dans le démarrage de cette thèse.

A la plateforme de Protéomique et en particulier au Docteur Philippe Marin pour avoir facilité l'accès à votre expertise. A Mathilde Decourcelle : merci pour ta contribution et tes apports sur la partie spectrométrie de masse.

Mes remerciements vont ensuite à l'équipe de Neuroradiologie de Gui de Chauliac :

A mon directeur de thèse, Professeur Vincent Costalat : ton dynamisme sans limites, tes idées qui m'ont porté depuis bientôt 10 ans ;

Aux praticiens, qui de jour comme de nuit m'ont permis d'obtenir des prélèvements d'une grande valeur : Docteur Imad Derraz, Docteur Razvan Alexandru Radu, Docteur Grégory Gascou, Docteur Mehdi Mahmoudi, Docteur Pierre-Henri Lefèvre.

Au Docteur Jérémy Deverdun, pour ton expertise sur le SVM.

Au Docteur Marinette Moynier et à Pauline Luchez : sans vous, le recueil des données cliniques n'aurait pas été le même.

Au Docteur Francesca Rapido : ce travail scientifique est lié au tien, et inversement.

Merci aux manipulateurs de Neuroradiologie, qui ont joué le jeu des prélèvements malgré la pression importante qui est la leur lors des thrombectomies...

Je remercie également l'équipe de Protéomique Clinique du Professeur Christophe Hirtz : la deuxième partie de cette thèse est permise grâce à cette nouvelle collaboration.

Je remercie chaleureusement les Professeurs Romain Bourcier et Frédéric Clarençon de me faire l'honneur d'être membres du jury. Je ne doute pas un instant de la pertinence de leurs remarques.

Enfin, Elodie, je te remercie de m'avoir supporté pour cette deuxième thèse, nous qui ne savions pas encore où la vie nous mènerait lors de la première il y a maintenant 6 ans. Que de chemin parcouru depuis !

RESUME DE THESE

L'infarctus cérébral (IC) est un problème majeur de santé publique. Il pose de multiples défis diagnostiques, thérapeutiques et pronostiques.

Sur le plan thérapeutique, le traitement endovasculaire (TEV) de l'IC a connu une révolution majeure, en 2015, à la suite de la validation des techniques mécaniques (stent-retriever, aspiration ou combinaison des 2 techniques) permettant une recanalisation des occlusions artérielles proximales intracrâniennes de la circulation antérieure, ces dernières comptant pour 30 à 40% des IC.

De façon parallèle au bénéfice majeur sur le pronostic fonctionnel des patients victimes d'IC, le TEV de l'IC a permis un accès jusque-là impossible à du matériel biologique intracrânien.

Les premières recherches biologiques dans ce contexte ont porté sur le thrombus intracrânien extrait par TEV, permettant principalement une description histologique et une corrélation de la composition histologique et de l'aspect radiologique du thrombus intracrânien.

Plusieurs études ont tenté une corrélation histologique du thrombus intracrânien avec l'origine étiologique de l'IC, et ce en raison d'un taux important (30-40%) de bilan étiologique exhaustif négatif après survenue d'un IC, impactant de façon négative la prévention secondaire et le risque de récurrence ischémique.

Ces études, se basant principalement initialement sur l'histologie standard, ont apporté des résultats inhomogènes, soulevant des limites méthodologiques liées à une absence de consensus permettant une classification histologique reproductive des thrombus intracrâniens.

L'histoire de notre travail commence en 2015 par une approche immunohistologique du thrombus intracrânien, corrélant le nombre de cellules CD3+ au sein du thrombus à l'origine cardioembolique ou athérothrombotique de l'IC.

Elle se poursuit par une analyse protéomique du thrombus intracrânien, en utilisant la spectrométrie de masse et l'apport d'une analyse statistique avec machine à vecteurs de support pour la différenciation de l'origine cardioembolique ou athérothrombotique de l'IC.

Enfin, la dernière partie du travail se porte sur l'analyse d'un large panel de marqueurs (cytokines, chémokines et molécules d'adhésion) prélevés en intracrânien sur une cohorte patients victimes d'IC, en secteur artériel ischémique en aval de l'occlusion vasculaire, les corrélant avec les données clinico-radiologiques initiales et de suivi.

Au total, notre travail s'intègre dans le sens de la littérature actuelle, affirmant qu'une compréhension biologique, allant au-delà de la recanalisation, est indispensable à une prise en charge optimale des IC chez les patients avec occlusion artérielle proximale intracrânienne.

Mots clés : accident vasculaire cérébral, infarctus cérébral, thrombectomie cérébrale, traitement endovasculaire, thrombus, neuroradiologie, spectrométrie de masse, protéomique, biomarqueurs

THESIS ABSTRACT

Acute Ischemic Stroke (AIS) is a major public health burden, involving several diagnostics, therapeutics and prognostic concerns.

Endovascular treatment (EVT), using stent-retriever, aspiration, or a combination of both techniques, has been validated in 2015 for patients presenting with AIS involving large vessel occlusion (LVO) of the anterior circulation, which can represent 30–40% of AIS. Besides a major clinical impact on AIS prognostic, EVT has allowed access to biological material sampled at the intracranial level.

Initial studies have focused on the intracranial thrombus retrieved by EVT, describing the variable histological architecture of cerebral thrombi, or the correlation between the gross histological composition of intracranial thrombi and their radiological appearance.

Several studies have tried to correlate the histological composition of intracranial thrombi and stroke etiology because a high proportion (30-40%) of strokes remains cryptogenic despite an exhaustive work-up, and secondary prevention (impacting stroke recurrence risk) is based on stroke etiology. However, these studies used standard histological techniques, with conflictual results and concerns due to the lack of consensus allowing reproductive histological classification of intracranial thrombi. Our research program began in 2015 with an immunohistochemical study focusing on CD3+ T-cell content in intracranial thrombi retrieved from AIS patients with LVO, relating that marker to the stroke etiology (either cardioembolic or atherosclerotic).

In this Thesis, we first focused on the proteomic analysis of cardioembolic and atherothrombotic thrombi, using mass-spectrometry, and applying a support-vector machine learning routine to identify protein candidates segregating the two selected populations.

Next, we analyzed a large panel of biomarkers (cytokines, chemokines, and adhesion molecules) in blood samples obtained intracranially beyond the arterial occlusion in a cohort of patients with AIS and LVO; we determined correlations between these soluble biomarkers post-clot, baseline, and follow-up clinicopathological data.

In conclusion, our work is in line with recent research, claiming that a biological approach, beyond proximal recanalization, is mandatory to achieve an optimal management of AIS in patients with LVO.

Keywords: acute ischemic stroke, thrombectomy, endovascular treatment, thrombus, clot, neuroradiology, mass-spectrometry, proteomics, biomarkers

SUMMARY

RESUME DE THESE	2
THESIS ABSTRACT	6
LIST OF FIGURES.....	11
LISTE OF TABLES.....	13
ABBREVIATIONS	14
INTRODUCTION	16
General context	16
Main causes of ischemic strokes	19
Thirty-year evolution of stroke management, from intravenous thrombolysis to endovascular treatment	20
Endovascular treatment revolution.....	22
Early experience (1998-2013)	22
Demonstration of major clinical impact (2015)	25
EVT as an opportunity to learn more about AIS pathology	26
Global Description of the PhD work	37
Support Vector Machine.....	46
SAMPLING WORKFLOW	51
Inclusion criteria	51
Imaging protocol.....	52
Timing	55
Endovascular treatment procedure.....	56
ADAPT	57
Stent-retriever	57
Anesthesia	60
Patient consent.....	60
Measures and Main Outcome	62
PROTEOMIC ANALYSIS OF INTRACRANIAL THROMBUS.....	63
Basics on proteomics principles and workflow	63
Overview of the proteomics workflow	63
What is Mass Spectrometry?	65
Angiography suite and freezing process	67
Laboratory	67
Published article	72
Commentary.....	84
SECOND PART: PERICLOT BLOOD ANALYSIS.....	85
Context.....	85
Material and methods	87
Inclusion criteria	87
Imaging	87

Blood sampling	89
Feasibility analysis.....	90
Flow of samples	92
Statistical analysis.....	92
Results.....	94
Baseline characteristics.....	94
MESOSCALE Panel.....	99
Discussion.....	111
Deciphering the role of intracranial post-clot blood inflammation in AIS	115
Study Limits.....	118
CONCLUSION AND PERSPECTIVES	121
REFERENCES.....	128
SUPPLEMENTAL DATA	144
Supplemental File 1: Ethics committee approval	144
Supplemental File 2: model of informed consent	146
Supplemental file 3: anesthesia protocol during EVT.....	150
Supplemental Table 1: Association between MESOSCALE central biomarkers and stroke outcome (modified Rankin Score), univariate analysis	151
Supplemental Table 2: Association between MESOSCALE central biomarkers and stroke outcome (modified Rankin Score), multivariate analysis (NIHSS/ASPECTS adjusted).....	152
Supplemental Table 3: Association between MESOSCALE biomarkers and favorable outcome (mRS 0-2 or mRS prestroke=90-day mRS), univariate analysis	153
Supplemental Table 4: Association between MESOSCALE biomarkers and favorable outcome (mRS 0-2 or mRS prestroke=90-day mRS), multivariate analysis	154
Supplemental Table 5: Association between MESOSCALE central biomarkers and 24-hours NIHSS change, univariate analysis	155
Supplemental Table 6: Association between MESOSCALE central biomarkers and 24-hours NIHSS change, multivariate analysis.....	156
Supplemental Table 7: Association between MESOSCALE biomarkers and infarct volume at 24 hours. Univariate analysis.....	157
Supplemental Table 8: Association between MESOSCALE biomarkers and infarct volume at 24 hours. Multivariate analysis.....	158
Supplemental Table 9: Association between MESOSCALE biomarkers and infarct volume change at 24 hours. Univariate analysis.	159
Supplemental Table 10: Association between MESOSCALE biomarkers and infarct volume change at 24 hours. Multivariate analysis.	160
Supplemental Table 11: Association between MESOSCALE central biomarkers and cardioembolic etiology	161
Supplemental Table 12: Association between MESOSCALE biomarkers and any hemorrhagic transformation, univariate analysis.....	162
Supplemental Table 13: Association between MESOSCALE biomarkers and any hemorrhagic transformation, multivariate analysis	163

LIST OF FIGURES

Figure 1: Modal anatomy of the supra-aortic vessels	17
Figure 2: Modal anatomy of the major intracranial arteries	17
Figure 3: Multicellular deconstruction at the cerebrovascular interface, potential impact of neurovascular targeting, and modulation of neuroinflammation.....	18
Figure 4: First-generation devices dedicated to Endovascular Treatment of Stroke: the Merci retriever devices.....	23
Figure 5: The Penumbra System.....	24
Figure 6: Hematoxylin and eosin-stained section of two intracranial thrombi	30
Figure 7: "Cardioembolic" thrombus.....	31
Figure 8: "Atherosclerotic" thrombus	31
Figure 9: Summary of sample sources, proteomics methods and applications of stroke proteomics studies performed in animal models and patients.....	37
Figure 10: Number of published articles focusing on intracranial thrombus between 2006 and 2021.....	40
Figure 11: Overview of MESOSCALE features.....	46
Figure 12: Illustration of SVM hyperplane.....	48
Figure 13: Illustration of the SVM soft margin	49
Figure 14: illustration of kernel transformation	50
Figure 15: Illustration of ASPECTS score	53
Figure 16: Illustration of areas used for assessment of pc-ASPECTS scores	54
Figure 17: Illustration of semiautomated infarct core segmentation	54
Figure 18: Pathways for management of patients with acute ischemic stroke from symptom onset to endovascular treatment.....	55
Figure 19: : Illustration of Direct Aspiration First Pass Technique (ADAPT) technique	58
Figure 20: Stent-retrievers used in the study	59
Figure 21: Illustration of the combined technique	59
Figure 22: Overview of a typical proteomics workflow.....	64
Figure 23: Illustration of a thrombus retrieved by a combined technique	67
Figure 24: Coomasie-blue gels.....	68
Figure 25: Gels obtained after using a Hemoglobin Depletion Kit	69
Figure 26: Illustration of manual excision of Hemoglobin band.....	70
Figure 27: Final optimized protocol from clot retrieval to MS/MS Spectrometry.....	70
Figure 28: Feasibility study after hemoglobin depletion protocol	71
Figure 29: CT perfusion imaging processed by RAPID software showing the ischemic core and perfusion deficit	88
Figure 30: MR perfusion imaging processed by RAPID software showing the ischemic core and perfusion deficit	89
Figure 31: Central post-thrombus blood sampling with a 3-cc syringe	90
Figure 32: feasibility results on 5 samples of intracranial and peripheral blood without depletion	91
Figure 33: feasibility results on 5 samples of intracranial and peripheral blood after most abundant protein depletion	92
Figure 34: Flow-chart of the study	94
Figure 35: Association of MESOSCALE biomarkers with 90-day mRS.....	100
Figure 36: Distribution of the 3 biomarkers significantly associated with 90-day mRS	101

Figure 37: Association of MESOSCALE biomarkers with 24-hours NIHSS change (difference between H24 and admission NIHSS)	104
Figure 38: Association of MESOSCALE biomarkers with 24-hours Infarct Volume.....	105
Figure 39: Association of MESOSCALE biomarkers with 24-hours Infarct Volume change (difference between H24 and admission infarct volume)	107
Figure 40: Association of MESOSCALE biomarkers with cardioembolic etiology	108
Figure 41: Association of MESOSCALE biomarker with any intracranial hemorrhage.....	109

LISTE OF TABLES

Table 1: Summary of Recommended Diagnostic Workup in Acute Ischemic Stroke	27
Table 2: Overview of Non-Contrast CT, CTA, and MR imaging data and correlation with histological data and therapeutic response.	29
Table 3: Review of primary studies on analysis of intracranial thrombus.....	36
Table 4: Review of proteomic studies focusing on intracranial thrombus	39
Table 5: Review of studies analyzing blood samples obtained by microcatheter aspiration during EVT.	44
Table 6: The modified Thrombolysis in Cerebral Infarction reperfusion scale	57
Table 7: the modified Rankin Score (mRS)	62
Table 8: Main baseline characteristics and outcomes of study sample (N=72).	98
Table 9: Association between MESOSCALE biomarkers and stroke outcome (90-day mRS), univariate analysis	101
Table 10 : Association between MESOSCALE biomarkers and stroke outcome (90-day mRS), multivariate analysis.....	102
Table 11: Association between MESOSCALE biomarkers and favorable outcome (mRS 0-2 or mRS prestroke=90-day mRS).....	103
Table 12: Correlation of IL-6 and FLT1 with NIHSS 24-hours change	104
Table 13: Correlation of ICAM-1 with final stroke volume at 24 hours.....	106
Table 14: Correlation of ICAM-1 with stroke volume change at 24 hours	107
Table 15: Correlation of Eotaxin and TARC with any hemorrhagic transformation	110
Table 16: Overview of biomarkers quantified in the present study	115

ABBREVIATIONS

ADAPT: direct Aspiration First Pass Technique

AIS: Acute Ischemic Stroke

ASPECTS: Alberta Stroke Program Early CT Score

BBB: Blood Brain Barrier

BCA: Bicinchoninic Acid Assay

CE: Cardiac Embolism

CSC: Comprehensive Stroke Center

CT: Computed Tomography

CTA: Computed Tomography Angiography

DDA: Data-Dependent Acquisition

ECG: Electrocardiogram

ESI: Electrospray Ionization

ETIS: Endovascular Treatment in Ischemic Stroke Follow-up Evaluation

EVT: Endovascular Treatment

GA: General Anesthesia

H&E: Hematoxylin and Eosin

HU: Hounsfield Units

ICA: Internal Carotid Artery

IL: Interleukin

IVT: Intravenous Thrombolysis

LC: Liquid Chromatography

LVO: Large Vessel Occlusion

MCA: Middle Cerebral Artery

MISO: Multimodal Investigation of Stroke Origin

MRI: Magnetic Resonance Imaging

mRS: Modified Rankin Score

MS: Mass spectrometry

mTICI: modified Thrombolysis in Cerebral Infarction

NIHSS: National Institutes of Health Stroke Scale

NNT: Number Needed to Treat

PCA: Posterior Cerebral Artery

pc-ASPECTS: posterior circulation Acute Stroke Prognosis Early Computed Tomography Score

RIPA: Radioimmunoprecipitation Assay

RBC: Red Blood Cell

RPLC: Reversed-Phase Liquid Chromatography

rtPA: Recombinant Tissue-type Plasminogen Activator

SDS-PAGE: Sodium Dodecylsulfate Polyacrylamide Gel Electrophoresis

SDS: Sodium Dodecyl Sulfate

sICH: Symptomatic Intracranial Hemorrhage

SVM: Support Vector Machine

SVS: Susceptibility Vessel Sign

TAI: Thrombus Attenuation Increase

TCR: T-cell antigen receptor

TOF: Time Of Flight

tPA: Tissue-type Plasminogen Activator

WBC: White Blood Cell

INTRODUCTION

General context

According to the World Health Organization, stroke is a significant public health burden and the second most common cause of death worldwide following coronary artery disease,^{1–3} with an incidence and a prevalence of 12.2 and 30.7 million. It is a heterogeneous disease, referring to any damage to the brain caused by impairment of blood supply, with more than 150 causes identified.¹

Acute Ischemic Stroke (AIS) is a subtype of stroke caused by vessel occlusion or decreased perfusion at the arterial level, leading to deprivation of oxygen, glucose, and other essential nutrients to the brain, finally resulting in necrotic cerebral tissue. Arterial occlusion is mainly secondary to embolism and may involve either small arteries, arterioles, or large arteries, depending on size and nature of the embolic material. Sometimes, *in situ* thrombosis is the cause of the arterial occlusion. Arteries guarantee the arterial supply of the brain (Figure 1) from the anterior circulation (internal carotid artery, anterior and middle cerebral arteries) and the posterior circulation (vertebral arteries, basilar arteries). These arteries build the so-called circle of Willis at the base of the brain, which provides a primary collateral anastomotic connection between the anterior and posterior circulation, protecting against ischemia in the event of arterial impairment (Figure 2). Another anastomotic network is formed by the leptomeninges anastomoses, including pial arteries connecting branches between two major cerebral arteries supplying two different cortical territories.⁴

Among the ischemic strokes (accounting for 87% of stroke cases)⁵, AIS due to large vessel occlusion (LVO) is associated with the worst outcome, with a more than doubled risk of death or dependence compared to AIS without LVO.⁶ There is no consensual definition of LVO, but the one widely accepted is an obstruction in the intracranial internal carotid artery (ICA), M1 or M2 segment of the middle cerebral artery (MCA), A1 segment of the anterior cerebral artery, intracranial vertebral artery, P1 segment of the posterior cerebral artery, or basilar artery. When considering this definition, LVO accounts for 24 to 38% of AIS.^{7,8} We should remember that although called LVO, we deal with small-diameter arteries; the MCA at its origin ranged from 2.4 to 4.6 mm (average 3.9 mm), around twice the diameter of the anterior cerebral artery.⁹

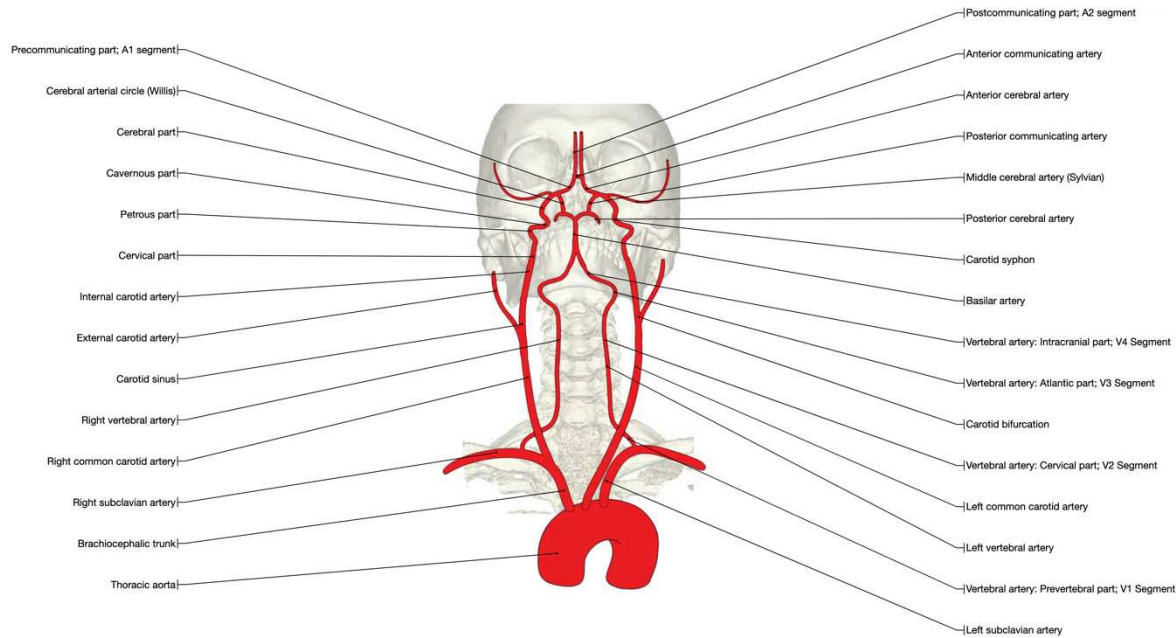


Figure 1: Modal anatomy of the supra-aortic vessels

Reproduced with permission of Imaios. Micheau A, Hoa D, e-Anatomy, www.imaios.com, DOI: 10.37019/e-anatomy

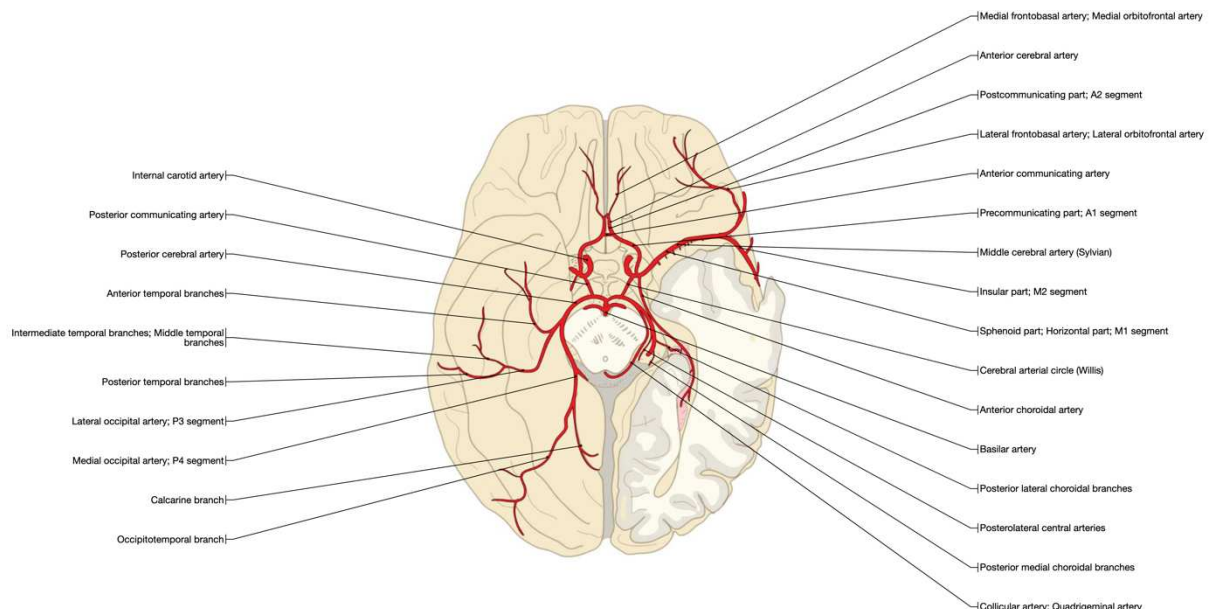


Figure 2: Modal anatomy of the major intracranial arteries

Reproduced with permission of Imaios. Micheau A, Hoa D, e-Anatomy, www.imaios.com, DOI: 10.37019/e-anatomy

At the cellular level, the outer wall of the brain vascular endothelium is enclosed by mural cells (smooth muscle cells or pericytes) and astrocyte end-feet, anatomically assembled to

guarantee blood-brain barrier (BBB) functions. Deconstruction and reactivity of mural and glial cells around the brain endothelium occur in response to ischemic insult, impacting vascular permeability and participating in neuroinflammation.¹⁰ Understanding the multicellular reactivity and plasticity around the vascular endothelium during central nervous central diseases is essential to develop BBB repair and anti-inflammatory therapeutic strategies. As a hypothesis, sealing a leaky cerebrovasculature (and BBB) may decrease the accumulation of blood-derived products into the brain parenchyma, allowing the neurovascular system to recover physiological interstitial homeostasis, thus curbing inflammation and improving neuronal functions. As a corollary hypothesis, combining neuronal and glio-vascular anti-inflammatory drugs will enable efficient therapeutic outcomes. A schematic representation of cerebrovascular players and multicellular (astrocytes, microglia, pericytes, etc.) reactivity under pathological insult is shown in Figure 3.

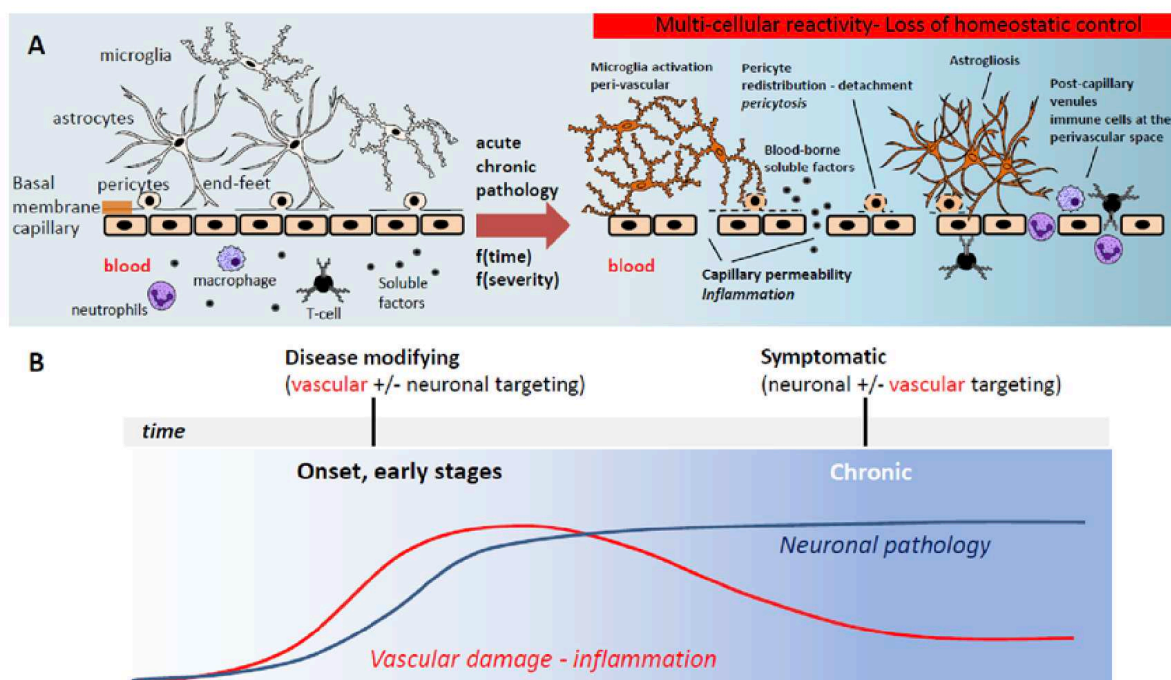


Figure 3: Multicellular deconstruction at the cerebrovascular interface, potential impact of neurovascular targeting, and modulation of neuroinflammation

From Giannoni P, Badaut J, Dargazanli C, De Maudave AF, Klement W, Costalat V, et al. The pericyte-glia interface at the blood-brain barrier. *Clin Sci.* 2018 Feb 14;132(3):361–74.

Used with permission of Portland Press

Main causes of ischemic strokes

Determining the cause of stroke is one of the main objectives when evaluating a stroke patient in clinical practice.

Cardiac causes of brain embolism include atrial fibrillation, acute myocardial infarction, severe systolic heart failure, sinoatrial disease, endocarditis (infective or marantic), valvular diseases, patent foramen ovale, and rarely, cardiac tumors. Cardiac embolism (CE) causes more severe strokes than other etiologies, and this subset of patients has high rates of both early and long-term recurrence.¹¹ Atrial fibrillation, the most common cardiac arrhythmia,¹² is commonly found during the etiologic work-up of stroke patients. One-fourth of all strokes after age 40 are caused by atrial fibrillation.^{13,14} Overall, patients with atrial fibrillation harbor 3 to 5 times greater risk for ischemic stroke. It has been known for a long time that atrial fibrillation may cause cardiac thrombi in the left atrium.^{15,16} Thrombogenic events in atrial fibrillation are related to several underlying pathophysiological mechanisms, which can be summarized in abnormal changes in flow (blood stasis), vessel wall, and blood hemostasis and coagulation (platelet activation, inflammation, and growth factor disturbances).¹⁷ Treatment with oral anticoagulation can prevent up to 70% of recurring strokes in those patients.

Another cause of large vessel occlusion and AIS is embolism from a carotid atherosclerotic plaque. Carotid plaques are typically slow growing or quiescent for a long time. However, they may suddenly develop ruptures, fissures, or endothelial ulcerations. These lesions will lead to platelet aggregation and thrombus formation, which may cause *in situ* occlusion or embolization to more distal vessels. It has been shown that some markers of unstable plaque (cap rupture, large lipid core, plaque infiltration of inflammatory cells) were more frequent in patients with recent ischemic lesions.^{18,19}

In the context of LVO, atherosclerotic lesions are represented by tandem occlusions or *in situ* thrombosis of an intracranial plaque. Acute atherosclerotic tandem occlusions are defined by occlusion or sub-occlusion of both the extracranial ICA and intracranial ICA/MCA. They are a severe form of ischemic stroke associated with high rates of disability and death (morbidity rates up to 70%, mortality rates up to 55%)²⁰ and represent approximately 20% of patients with an intracranial LVO of the anterior circulation.²¹

Symptomatic intracranial atherosclerotic stenosis is not rare in the European population but occurs with a higher prevalence in Asians.²² Most lesions occur in the distal ICA, the intracranial ICA bifurcation, and the M1 segment of the MCA.²³ This condition is associated with a high risk of hemodynamic ischemic events.²⁴ Despite that since the SAMMPRIS trial, having found that aggressive medical management was superior to intracranial stenting (with the Wingspan system) for patients harboring intracranial atherosclerotic stenosis, some of these patients still present with acute LVO and are potentially concerned by EVT of stroke.

Thirty-year evolution of stroke management, from intravenous thrombolysis to endovascular treatment

Patients suffering from stroke have been described by the earliest Greek, Roman, and Persian physicians. The term “apoplexy” was employed to describe that condition, and various usage of herbs, diet, and surgery was proposed.²⁵

The significant change in AIS patient management began in 1995. Before, no specific treatment was available, and patients were frequently observed in the emergency department. There was no fundamental need for cerebral imaging because the result would not have changed the patient’s management. Differentiating ischemic stroke and cerebral hemorrhage was not relevant.

The National Institute of Neurological Disorders and Stroke (NINDS) tissue-type plasminogen activator (tPA) trial demonstrated that treatment with intravenous t-PA within 3 hours of the onset of ischemic stroke improved clinical outcomes at three months.²⁶ After this pilot trial, six randomized controlled studies published between 1995 and 2002 assessed tPA versus placebo in various time windows 0 to 6 hours from stroke symptom onset. However, no trial showed benefits beyond 4.5 hours.²⁷

Besides life-threatening consequences, the socio-economic burden of stroke is considerable, with an increasing cost due to an ageing population.²⁸ Hence, a recent study of the economic burden of stroke across 32 European countries showed a 60 billion € cost each year. These findings are probably underestimated because several categories of health care costs (public health activities, supportive treatments, home adjustments, home care) are not routinely

tracked in health care statistics.²⁹ Around 50% of the stroke survivors will need, at least to some extent, the assistance of others in their daily life.³⁰

The neuropsychological impact of stroke is considerable. 40% of stroke survivors may have long-term depression symptoms that are associated in stroke survivors with a physical disability.^{31,32} Late neurological impairment may include seizures and epilepsy. Estimates of the rate of early post-AIS seizures range from 2% to 33%, while late seizures are 3% to 67%, and the prevalence of post-AIS epilepsy is around 3%.³³ An extensive proportion of 5-year stroke survivors harbors neuropsychological deficits, including memory, executive function, information processing speed, visuoperceptual/construction ability, and language.³⁴ Occurrence of stroke in young people may be devastating, with fewer than half of these subjects returning to work.³⁵

Up to now, cerebral thrombi were inaccessible (except postmortem), and intravenous thrombolysis (IVT) with recombinant tissue plasminogen activator (alteplase-rtPA) was the only treatment available.³⁶ Time window for IVT administration remains limited. However, two recent meta-analyses of five randomized control trials (RCTs-WAKE-UP [Efficacy and Safety of MRI-Based Thrombolysis in Wake- Up Stroke], EXTEND [Extending the Time for Thrombolysis in Emergency Neurological Deficits], ECASS-4 [European Cooperative Acute Stroke Study-4], THAWS [Thrombolysis for Acute Wake-Up and Unclear-Onset Strokes With Alteplase], and EPITHET [Echoplanar Imaging Thrombolytic Evaluation Trial] showed a benefit of intravenous alteplase over standard medical treatment in patients with stroke 4.5 to 9 hours from the onset, or unknown time of onset, or wake-up stroke with salvageable brain tissue (imaging mismatch), despite an increased risk of symptomatic intracranial hemorrhage (sICH).^{37,38}

Besides this short therapeutic window limitation, the success of IVT for LVO recanalization largely depends on the occlusion site, with a low success rate in proximal locations such as the carotid terminus.³⁹

Endovascular treatment revolution

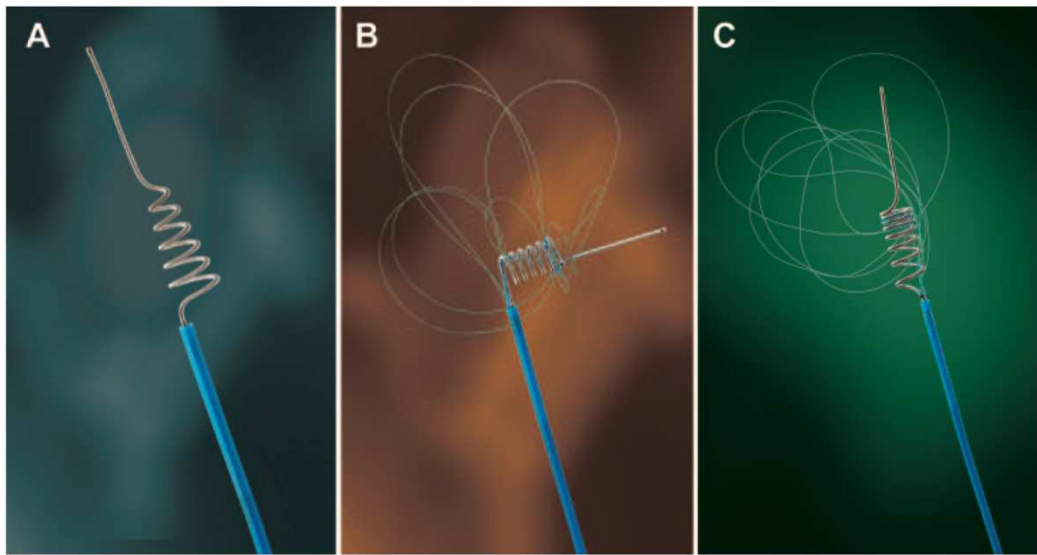
Early experience (1998-2013)

The first EVT approach for AIS used intra-arterial thrombolysis (IAT).

The PROACT trials (published in 1998 and 1999) focused on the intra-arterial infusion of pro-urokinase.

- PROACT I was a randomized study that showed that intra-arterial administration of 6 mg pro-urokinase in patients with M1 or M2 occlusions allowed higher recanalization rates compared to placebo. However, all patients had concomitantly intravenous heparin, and clinical outcomes were not assessed.⁴⁰
- PROACT II studied patients with angiographically proven proximal MCA occlusions, randomized to receive either IAT with 9 mg of pro-urokinase within six hours of symptoms onset, associated with heparin, or heparin only in the control arm. Both clinical and angiographical outcomes were better in the IAT group, with 40% of patients achieving modified Rankin Score (mRS, an ordinal scale with 7 possible values, Table 7) of 2 or better versus 25% in the control arm. Recanalization rates occurred at 66% versus 18%, respectively.⁴¹ Despite these results, IAT with urokinase has never been integrated into stroke guidelines because FDA asked for a confirmatory RCT which has never been realized.

After these PROACT trials, a dedicated EVT device was developed, the MERCI retriever device (Figure 4), the first cleared by the U.S. Food and Drug Administration in 2004, to retrieve intracranial thrombi in patients suffering from an AIS with LVO. Recanalization rates ranged from 46% in the first MERCI trial, published in 2005,⁴² to 55% in the MULTI-MERCI trial, published in 2008.⁴³



The first-generation X series (A) had a tapered design without filaments. The Merci second-generation L-series (B) incorporated a "side-winder" 90-degree angle with added filaments. The Merci third-generation V series (C) is available in soft and firm configurations and incorporates a variable spring rate design along the coil for optimal clot retention. Permission to use photographs was granted by Stryker.

Figure 4: First-generation devices dedicated to Endovascular Treatment of Stroke: the Merci retriever devices

From Alshekhlee A, Pandya DJ, English J, Zaidat OO, Mueller N, Gupta R, et al. Merci mechanical thrombectomy retriever for acute ischemic stroke therapy: Literature review. *Neurology*. 2012 Sep 25;79(Issue 13, Supplement 1):S126–34.

Reproduced with permission of Wolters Kluwer Health, Inc.

The second dedicated device was the Penumbra System (Figure 5), offering two recanalization options, using, in the first instance, thrombus debulking and aspiration, followed by direct thrombus withdrawal if aspiration failed. A high recanalization rate of 82% was reported in this study, but functional outcomes remained poor, with 25% of patients achieving functional independence at three months ($mRS \leq 2$). Moreover, the complication rate was substantial, with 12.8% of patients experiencing procedural difficulties.

The third-generation devices were the SOLITAIRE and TREVO retrievable stent devices, allowing promising recanalization and clinical outcomes published in the SWIFT and TREVO 2 trials.^{44,45}

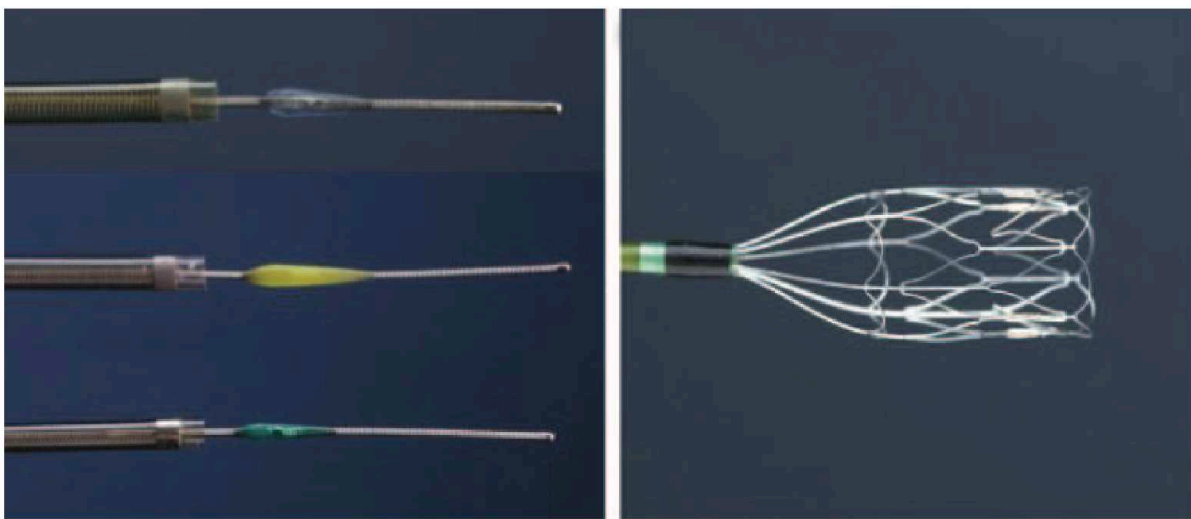


Figure 5: The Penumbra System

From The Penumbra Pivotal Stroke Trial Investigators. The Penumbra Pivotal Stroke Trial: Safety and Effectiveness of a New Generation of Mechanical Devices for Clot Removal in Intracranial Large Vessel Occlusive Disease. Stroke. 2009 Aug;40(8):2761–8.

Reproduced with permission of Wolters Kluwer Health, Inc.

2013 was the year of three negative endovascular treatment randomized controlled studies (RCT): SYNTHESIS, MR RESCUE, and IMS III, which were presented at the International Stroke Conference in Hawaii and subsequently published in the same issue of the New England Journal of Medicine. MR RESCUE has been conducted using the MERCI retriever or PENUMBRA system over eight years, comparing patients receiving EVT versus those receiving standard medical care.⁴⁶ Good clinical outcome (mRS 0–2) was only demonstrated in 14%, with no outcome difference between groups. IMS III was also disappointing, showing no difference in outcome between EVT and IVT alone groups (41% good clinical outcome EVT arm versus 39% in the BMT arm).⁴⁷ SYNTHESIS trial did not show difference in good clinical outcomes between the 2 arms (42% in the EVT arm versus 46% in the IVT arm) as well.⁴⁸ We should note that devices or techniques (intra-arterial thrombolysis with rtPA, manipulation of clot with use of a guidewire or microcatheter, or a combination of these approaches) used in these 3 studies were relatively limited in their ability to achieve recanalization and the new generation retrievable stents were used in a small number of patients.

Demonstration of major clinical impact (2015)

In 2015, a Multicenter Randomized Clinical Trial of Endovascular Treatment for Acute Ischemic Stroke in the Netherlands (MR CLEAN),⁴⁹ Endovascular Revascularization with Solitaire Device versus Best Medical Therapy in Anterior Circulation Stroke within 8 h (REVASCAT),⁵⁰ Endovascular Treatment for Small Core and Proximal Occlusion Ischemic Stroke (ESCAPE),⁵¹ Solitaire™ FR as Primary Treatment for Acute Ischemic Stroke (SWIFT PRIME)⁵² and Extending the Time for Thrombolysis in Emergency Neurological Deficits with Intra-Arterial Therapy (EXTEND IA)⁵³ had demonstrated the superiority of endovascular management on best medical treatment for patients harboring large vessel occlusion (LVO) in the anterior circulation. Subsequently, in 2016 and 2017, 2 additional studies, Mechanical thrombectomy after intravenous alteplase versus alteplase alone after stroke (THRACE)⁵⁴ and Endovascular therapy for acute ischaemic stroke: the Pragmatic Ischaemic Stroke Thrombectomy Evaluation (PISTE)⁵⁵ confirmed these results.

EVT was a significant revolution both for stroke management and patient outcome. Indeed, the number of patients to treat (NNT) for functional independence at 90 days is low, ranging from 4 in SWIFT-Prime⁵² to 7.4 in MR-CLEAN⁴⁹. Although initially proven for patients treated within the 6 hours after the onset of stroke symptoms, in 2018 2 randomized controlled studies (DWI or CTP Assessment with Clinical Mismatch in the Triage of Wake-Up and Late Presenting Strokes Undergoing Neurointervention with Trevo trial [DAWN])⁵⁶ and DEFUSE 3 (Endovascular Therapy Following Imaging Evaluation for Ischaemic Stroke 3)⁵⁷ showed the benefit of EVT in carefully selected AIS-LVO patients presenting within 6–24 hours after symptoms onset and having substantial tissue at risk. Indeed, the Number Needed to Treat (NNT) for functional independence was even lower in these two studies (2.8 and 3.6, respectively).

One limitation of EVT is its accessibility: fewer than 10% of AIS patients would meet the eligibility criteria,⁵⁸ and not all stroke centers have sufficient resources and expertise to provide EVT.⁵⁹

EVT as an opportunity to learn more about AIS pathology

Besides this huge step forward regarding stroke management, EVT allows access to intracerebral thrombi and peri-clot ischemic blood, enabling their systematic analysis.

Initially (2015-2016), a few studies on intracranial thrombi focused on the variable architecture of cerebral thrombi with different components such as fibrin, red blood cells (RBC), and platelets,^{60,61} which are the main components of the intracranial thrombus. At this time, no advanced subtype classification of blood components was performed.

Studying the histopathologic clot composition of intracranial thrombi could potentially have high clinical relevance. This is for two main reasons: a significant proportion (30%) of strokes are cryptogenic despite an exhaustive work-up;⁶² secondly, clot composition may influence the efficacy of fibrinolysis (RBC-rich thrombi being more responsive to tPA than fibrin-rich or platelet-rich thrombi)^{63–65} or affect the success rate of EVT and outcome. Fibrin-rich thrombus are associated with an increased number of recanalization attempts, longer procedure time and less favorable clinical outcomes compared to RBC-rich clots.⁶⁶ Importance of thrombus composition on the effectiveness of EVT is highlighted by recent industrial efforts, with a novel EVT device (Geometric Clot Extractor NIMBUS; Cerenovus, Galway, Ireland), specifically designed to retrieve resistant fibrin-rich thrombi.^{67,68}

Because secondary prevention is based on the stroke etiology, we may assume that one-third of the patients receive only a probabilistic medication. Furthermore, there is some evidence that stroke etiology may impact the effect of EVT in AIS.⁶⁹ Hence, identifying the etiology of acute ischemic stroke is essential for effective secondary prevention. We may classify stroke etiologic work-up into six categories of investigations (Table 1):

1. brain imaging
2. vascular imaging
3. cardiac rhythm analysis
4. cardiac structure analysis
5. laboratory analyses
6. other

Type of exam	Patient subset	Technique
Brain imaging	All patients	At least CT MRI whenever possible (superior to CT regarding sensitivity and ability to identify the etiology of the stroke)
Vascular imaging	All patients	CTA or MRA from the aortic arch to vertex
Cardiac rhythm	All patients	At least 12-lead ECG 24-hour ECG monitoring recommended
	AIS of undetermined source with baseline short-term ECG monitoring without atrial fibrillation, but the cardioembolic mechanism is suspected	Prolonged ECG monitoring
Cardiac structure	Suspicion of cardiac source or patients without an apparent cause	Echocardiography (2D or transesophageal)
Laboratory and other investigations	All patients	Complete blood count, coagulation, glucose, troponin
	Young patients	Evaluation of autoimmune diseases, homocysteine levels, coagulopathy, screening for thrombophilia and genetic profile

Table 1: Summary of Recommended Diagnostic Workup in Acute Ischemic Stroke

The incomplete molecular understanding of stroke pathophysiology negatively impacts patients' management, follow-up, and secondary prevention.^{3,70} A recent consensus indicates that examining patients' intracranial thrombi could help unveil novel disease mechanisms.⁷¹ Indeed, studying the intracranial thrombi composition could advance our knowledge of the molecular mechanisms of local cerebrovascular cell damage in this disease setting.^{72–75}

We have begun to analyze the basic histological or immunohistochemical features of intracranial thrombi, describing thrombus architecture or reporting the presence of fibrin and leucocytes. The most frequently used conventional histological stains were hematoxylin and eosin (H&E), Martius Scarlet Blue, Elastica van Gieson, Prussian blue, Masson and Von Kossa. Primary studies having focused on gross histological or immunohistochemical analysis of intracranial thrombi are shown in Table 3. For an exhaustive review of the literature on the potential insights given by intracranial thrombosis composition for AIS etiology understanding, we here refer to the recent article of Aliena-Valero el al.⁷⁶

Additional articles focused on the correlation between thrombus composition and imaging.^{61,77–80} Both CT and MRI have been used. On CT, clot composition has been correlated to clot x-ray attenuation (lower Hounsfield units are associated with fibrin- and/or platelet-rich clots, and higher Hounsfield units associated with RBC-rich clots) and clot perviousness (reflecting clot "porosity"). On MRI, the susceptibility vessel sign (SVS, a linear intravascular hypointense focus on gradient-echo or susceptibility-weighted-imaging) has been correlated to the paramagnetic properties of deoxygenated hemoglobin of RBC-rich thrombi, as well as with a more favorable clinical outcome when using stent retriever (compared to ADAPT) in first instance.⁸¹

	Measured parameter	Histologic correlation	Increased therapeutic response
Non-contrast CT	Hounsfield Units (HU)	High HU=RBC rich clots	Higher HU
Arterial contrast-enhanced CT	Thrombus attenuation increase (TAI)	No consensus	Increased TAI
MRI	Susceptibility vessel sign	SVS +=RBC rich	SVS +

Table 2: Overview of Non-Contrast CT, CTA, and MR imaging data and correlation with histological data and therapeutic response.

As a clinical team managing stroke patients routinely, we had to manage the frustration of observing 30% of our patients discharged from the hospital without clear stroke etiology even after exhaustive in-hospital work-up.⁸²

In 2015, a few studies on intracranial thrombi were undertaken. They mainly reported variable architecture of cerebral thrombi with different components such as fibrin, red blood cells (RBC) and platelets.^{60,61} No advanced subtype classification of blood components was performed, and there was no consensual definition for what makes a thrombus rich or poor in a given histologic component.

Since 2015, even if an increasing number of studies have focused on investigating the composition of thrombi in patients with AIS (Table 3), it is still unclear whether cardioembolic thrombi are fibrin-rich, and non-cardioembolic thrombi RBC-rich thrombi.⁶⁶ Furthermore, the processes that would lead to cardioembolic thrombi being fibrin platelet-rich, and non-cardioembolic thrombi RBC-rich, are unknown.

Only three studies analyzed white blood cells in the intracranial thrombi without differentiating their subtypes.^{60,80,83} We considered that Immunochemistry might allow precise analysis of white cells sub-types, already identified as potential biomarkers of the vulnerable atheromatous lesion.⁸⁴ Because T-cells had already been shown to be a significant

component of vulnerable atherosclerotic carotid lesions,⁸⁵ we previously attempted to associate the histopathologic T-cells content of thrombi to the stroke etiology, using immunochemistry with anti-CD3. The central hypothesis of our past study was that CD3+ cell content inside intracranial thrombi could aid in screening for an atherothrombotic stroke, with the final goal being the utilization of immunochemistry on intracranial thrombi as an etiological biomarker.

We investigated 54 consecutive thrombi retrieved after EVT in acute stroke patients. Formalin-fixed specimens were embedded in paraffin and consecutive 3-mm thick slices on the entire specimen were cut and stained with hematoxylin and eosin. Figure 6 shows examples of fibrin-dominant and erythrocyte-dominant patterns.

In this study, a cell was considered positive for CD3+ marker when fulfilling three criteria: successful staining with cells marked, compatible size, and visible nucleus. We found that thrombi of “atherosclerotic” origin demonstrated significantly more CD3+ cells than the other groups (mainly cardioembolic; Figures 7 and 8).⁸⁶

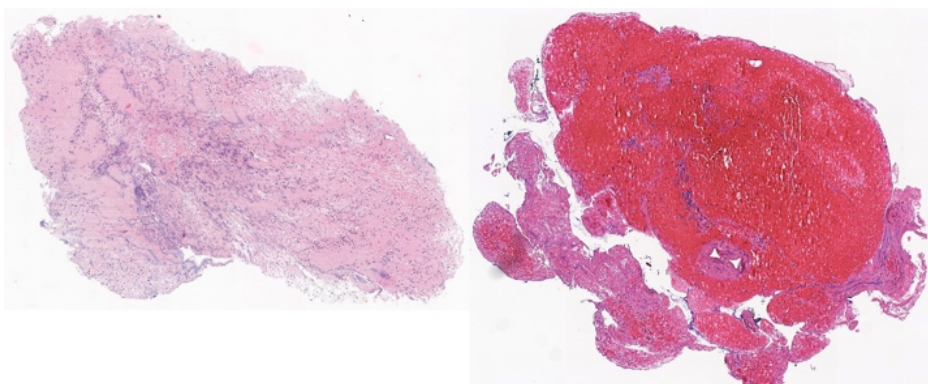


Figure 6: Hematoxylin and eosin-stained section of two intracranial thrombi

Fibrin-dominant thrombus (left) and erythrocyte-dominant thrombus (right).

From Dargazanli C, Rigau V, Omer E. High CD3+ cells in intracranial thrombi represent a biomarker of atherothrombotic stroke. PLoS ONE. 2016.

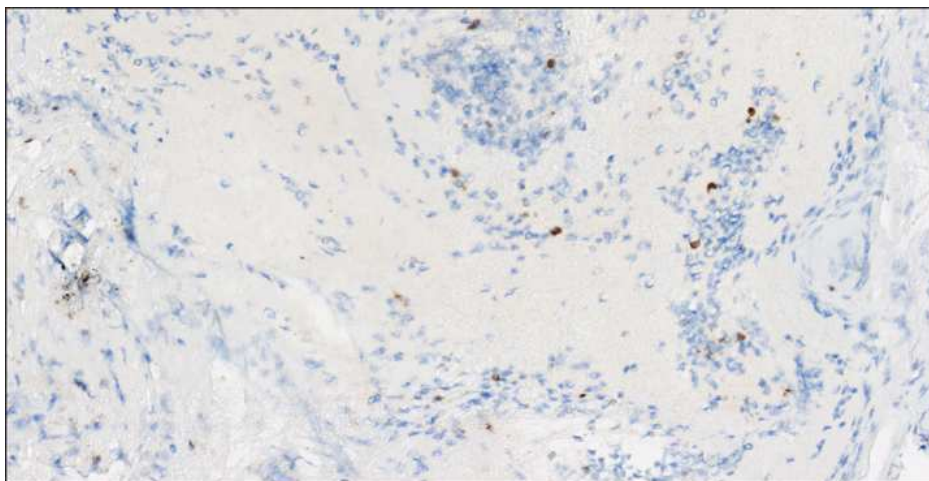


Figure 7: "Cardioembolic" thrombus

CD3+ cells (brown) corresponding to T cells in a "cardioembolic" thrombus.

From Dargazanli C, Rigau V, Omer E. High CD3+ cells in intracranial thrombi represent a biomarker of atherothrombotic stroke. PLoS ONE. 2016.

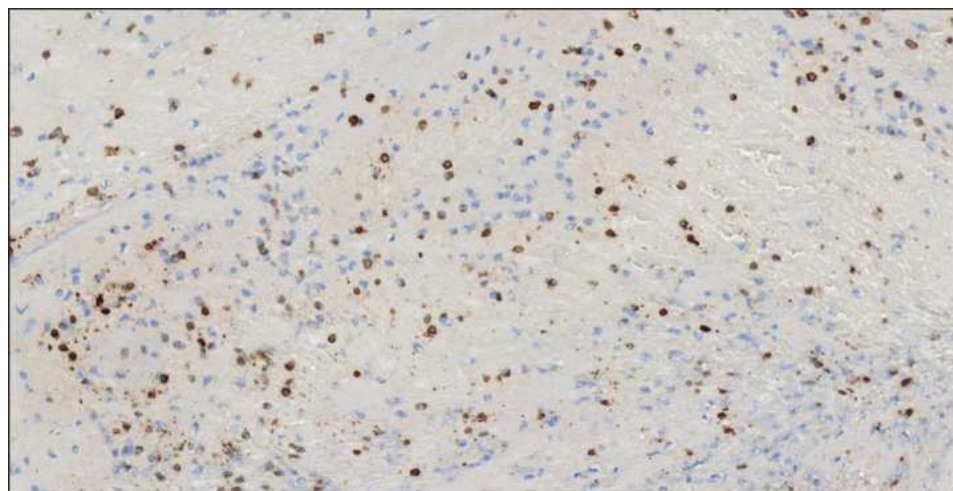


Figure 8: "Atherosclerotic" thrombus

CD3+ cells (brown) corresponding to T cells in an "atherosclerotic" thrombus.

From Dargazanli C, Rigau V, Omer E. High CD3+ cells in intracranial thrombi represent a biomarker of atherothrombotic stroke. PLoS ONE. 2016.

Besides innovative results, this preliminary work allowed us to assimilate and be comfortable with administrative and legislative duties relative to biobanks. However, our histological biomarker (CD3+) has been established and tested on the same cohort, limiting its validity. Second, although manual counting on each slice provided reproducibility for T-cells identification, this approach is semi-quantitative. Moreover, the use of CD3+ does not allow

to differentiate the different subpopulations of T cells, i.e., CD4+ (helper/inducer) T cells, CD4+ regulator T cells (Tregs, identified by expression of transcription factor forkhead box P3 [Foxp3]), cytotoxic/suppressor CD8+ T cells, NK cells, and double negative T cells. A significant differentiation, given that T cells subpopulation may have different roles in AIS. It has been shown that total circulating T cells is stable after stroke. On the other hand, CD4⁺ helper T cells slightly and shortly increased after AIS, while CD8⁺ cytotoxic T cells were unchanged.⁸⁷ Their role is also different: diminution of brain infiltration by CD4-positive T cells in mice delays cerebral infarct progression,⁸⁸ while CD8+ T cells are implicated in post stroke demyelination.⁸⁹ Tregs have shown protective effects via IL-10 signaling.⁹⁰

Because of these limitations, we decided to move forward and explore a cohort of intracranial thrombus using more advanced techniques to unravel molecular-levels compositions and possibly associations to etiology. This quest was possible thanks to a strong collaboration between the Gui de Chauliac Hospital Neuroradiology Department (Pr. Vincent Costalat), the Cerebrovascular and the Cerebrovascular and Glia Research laboratory, Department of Neuroscience, Institute of Functional Genomics (UMR 5203 CNRS—U 1191 INSERM), University of Montpellier (Dr. Nicola Marchi), and the Functional Proteomics Platform (Institut de Génomique Fonctionnelle, Univ. Montpellier, UMR 5203 CNRS - U 1191 INSERM, Montpellier, France) University of Montpellier (Dr. Philippe Marin) for the first part of the work.

Next, in the second part of this work, we analyzed blood samples obtained by microcatheter aspiration beyond the intracranial occlusion, investigating a large set of soluble biomarkers and correlating to patient's outcome (Clinical Proteomics Platform, Institute for Regenerative Medicine & Biotherapy (IRMB), Saint Eloi Hospital, Montpellier, France; Pr. Christophe Hirtz). We here underscore that a biomarker is: "a characteristic that is objectively measured and evaluated as an indicator of normal biological processes, pathogenic processes, or pharmacologic responses to a therapeutic intervention".⁹¹ To date, despite more than 150 candidate stroke biomarkers have been studied in diagnosis or prognosis,⁹² blood-based molecules are not routinely used in stroke (unlike in other emergency conditions such as myocardial infarction or pulmonary embolism); most biomarkers are measured in peripheral blood only, therefore introducing significant confounding factors regarding specificity and

source of the biomarker. Our study focuses on the direct examination of intracranial biological material (clot and blood), a novel approach that could allow reaching sufficient diagnostic accuracy, for example, to discriminate cause, and then outcome, hemorrhagic or ischemic stroke and stroke from stroke mimics (which are conditions simulating stroke at the acute phase)⁹³

Publication (First author, year)	N.	Etiology of stroke	Histological Technique	Thrombus gross organization	Thrombus composition or description
Marder et al., 2006	25	AS=16% CE=64% Other=12% ND=8%	H&E, Gomori Methenamine silver	Layered=32% Serpentine=36% Fibrin-rich=12% RBC-rich=12%	Description: Linear deposits of nucleated cells, atheromatous material
Almekhlafi et al., 2008	5	AS=60% CE=20% ND=20%	H&E, Martius scarlet blue, Masson trichrome, von Kossa	Fibrin-dominant=80% Mixed=20%	Quantification: fibrin/RBCs ratio, endothelialization, calcifications, Description: leukocytes
Liebeskind et al., 2011	50	ND	H&E	Fibrin-dominant=44% RBC dominant=26% Mixed=30%	Quantification: RBCs, fibrin, leukocytes
Singh et al., 2013	48	AS=38% CE=60 % ND=2%	H&E, Prussian-blue, Elastica-van-Gieson, Kossa, PAS, IHC (CD34)	Mixed=42% RBC-dominant=31% Fibrin-dominant=27%	Description: leukocytes, endothelial cells
Kim et al., 2015	37	CE=59% AS=22% ND=19%	H&E IHC=CD61		Quantification : leucocytes RBCs, fibrin, platelets
Sallustio et al., 2015	28	AS=61% CE=39%	H&E, phosphotungstic acid-hematoxylin	Serpentine =54% Layered=39% Erythrocytic 7%	Quantification=fibrin
Simons et al., 2015	40	CE=53%	H&E IHC=CD34	Early-phase analysis: RBC dominant=27.5%, RBC equal to fibrin= 27.5% Late phase pathology: organized fibrin=27.5%, fibrin-dominant =17.5%,	
Niesten et al., 2016	22	AS= 36% CE 27% Other 14% ND 23%	H&E, Mallory phosphotungstic acid-hematoxylin IHC=glycophorin A, CD31	Mixed 64% Fresh (\leq 1 day) = 73%; Lytic (1–5 days) = 18% Organized (\geq 5 days) =9%	
Boeckh-Behrens and al., 2016	34	CE 47% ND 26% Other 18% AS 9%	H&E, Elastica van Gieson	Fibrin dominant=50% Mixed= 38% RBC-dominant=12%	Quantification: RBCs, fibrin, WBCs Description: surface endothelialization
Qureshi et al., 2016	18	ND	H&E	RBCs-dominant 39% Mixed 33% Fibrin-dominant 28%	Quantification: RBC aggregates, eosinophilic deposits, mixed regions and basophilic components
Schuhmann et al., 2016	37	CE=51% AS=37% ND=32%	H&E, Martius scarlet blue IHC=CD4, CD68, vWF	Serpentine=51% Layered=30% Erythrocytic=19% Fibrin/collagen dominant=38% RBC dominant=35% Mixed=27%	
Boeckh-Behrens et al., 2016	137	CE=49% ND= 27% AS=16% Other=8%	H&E		Quantification : RBCs, fibrin/platelets ratio, leukocytes

Dargazanli et al., 2016	54	CE=46% Other + ND=35% AS=19%	H&E IHC=CD3	Mixed=46% RBC-dominant=28% Fibrin-dominant=26%	Quantification: CD3 cells
Denorme et al., 2016	36	CE =64% ND 17% AS =11% Other=8%	H&E, Martius Scarlet Blue IHC=vWf		Quantification: RBCs, fibrin, vWf
Hashimoto et al., 2016	83	CE 77% ND 12% Artery to artery embolism=7% Dissection 1% In situ occlusion 2%	H&E, Masson trichrome	Erythrocyte-dominant =41% Organization=23% Atheromatous components=8%	Quantification: RBCs, fibrin/platelet ratio Description: atheromatous components
Boeckh-Behrens et al., 2017	122	CE=47% ND=23% AS=19% Other=11%	H&E IHC=CD31		Quantification : RBCs, fibrin/platelets, leukocytes, CD31 + cells
Sporns et al., 2017	187	CE=41% ND=34% AS=19% Other =6%	H&E, Elastica van Gieson, Prussian blue IHC=CD3, CD20, CD68/ KiM1P		Quantification : RBCs, fibrin, leukocytes, CD3 + cells, CD20 + cells, CD68/ KiM1P + cells
Laridan et al., 2017	68	CE=59% ND=22% AS=10% Other= 9%	H&E IHC=CD66b and NE, H3Cit (NETs marker)	Fresh (\leq 1 day) =47% Old (\geq 1 day) = (53%)	Quantification: neutrophils, NETs
Ducroux et al., 2018	74	CE=49% ND=34% AS=13% Other=4%	H&E IHC: MPO, H4Cit (NETs marker)		Quantification: NETs Description: polymorphonuclear leukocytes
Maegerlain et al., 2018	64	CE=55% ND=28% AS=14% Other=3%	H&E, Elastica van Gieson		Quantification : RBCs, fibrin/platelets ratio, leukocytes
Maekawa et al., 2018	43	CE=70% ND=16% AS=12% Other=2%	H&E	Fibrin-rich=58% RBC-rich=42%	Quantification: RBCs, fibrin, leukocytes
Choi et al., 2018	52	CE=62% ND=23% AS=15%	H&E, Martius scarlet blue		Quantification: RBCs, fibrin, leukocytes
Prochazka et al., 2018	90	ND	H&E, Carstairs method, IHC: vWf, CD31, CD15		Quantification : Fibrin, platelets, vWf, CD31+ cells Description : neutrophils
Funatsu et al., 2018	101	AS=11% CE=78% ND + Other=11%	H&E, Masson trichrome, Elastica van Gieson	Vascular wall components in 22%	Quantification : RBCs, fibrin/platelets ratio
Berndt et al., 2018	32	CE=59% ND=25% AS=13% Other=3%	H&E		Quantification: RBCs, platelets, fibrin, neutrophils
Park et al., 2019	48	Active cancer=16 Inactive cancer=16 No history of cancer=16	IHC=CD42b, antifibrinogen, glycophorin A, MPO, histone H3 (Nets)		Quantification: RBCs, platelets, fibrin, NETs, neutrophils
Fitzgerald et al., 2020	612	CE=47.4%	Martius Scarlett Blue		Quantification : RBCs, leukocytes,

		AS=26.1% ND=22.9% Other=3.6%			fibrin, platelets, collagen
Genchi et al., 2021	80	CE=55% ND=22% AS=14% Other=9%	IHC=Histone H3, MPO	cell-dominant, filopodia-dominant, web-dominant	Quantification: NETs, neutrophils
Wang and al., 2022	94	CE=60 AS=40%	H&E IHC=CD3, CD20, CD105 (endothelial cells), actin	RBC dominant Mixed Fibrin dominant Organized	Quantification: T- cells, B-cell, endothelial cells, actin expression

Table 3: Review of primary studies on analysis of intracranial thrombus

*AS=atherosclerotic, CE=cardioembolic, ND= not determined, H&E= hematoxylin-eosin,
RBC=red blood cell, PAS=Periodic acid-Schiff, IHC=immunohistochemistry, vWF=von
Willebrand factor, NETs= Neutrophil extracellular traps, MPO=Myeloperoxidase*

Global Description of the PhD work

The project unfolds as two consecutive studies.

The first part of this work was based on proteomic analysis of intracranial thrombi retrieved by EVT, using proteomics and, for the first time in this field, artificial intelligence (support-vector-machine, SVM). “Machine Learning Analysis of the Cerebrovascular Thrombi Proteome in Human Ischemic Stroke: An Exploratory Study” was published in *Frontiers in Neurology* in 2020.⁹⁴

At the time of investigation (2019-2020), only two proteomic studies had been performed on intracranial thrombus. We will not detail proteomics studies that had been performed on other AIS samples (brain, blood, cerebrospinal fluid, urine, extracellular vesicles, Figure 10).⁹⁵

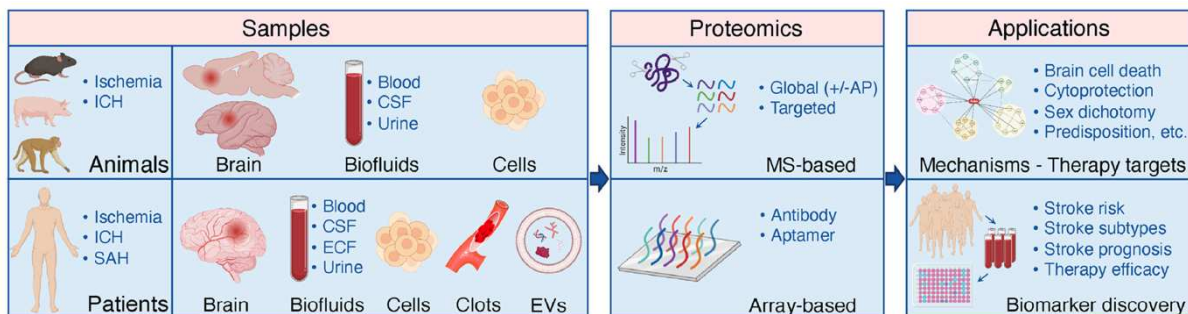


Figure 9: Summary of sample sources, proteomics methods and applications of stroke proteomics studies performed in animal models and patients

*Used with permission of Wolters Kluwer Health, Inc.
From Hochrainer K, Yang W. Stroke Proteomics: From Discovery to Diagnostic and Therapeutic Applications. Circ Res. 2022 Apr 15;130(8):1145–66.*

A first proteomic investigation was performed in 2017 on 20 consecutive acute stroke patients, analyzing fractionated peptides by nano-liquid chromatography with tandem mass spectrometry.⁹⁶ Stroke etiology was atrial fibrillation (n=11), atherosclerosis (n=4), cryptogenic (n=2), and other identified cause (n=3). After initial freezing at -80°C, sonication, and trypsin digestion, fractionated peptides underwent nano-liquid chromatography with tandem mass spectrometry (nLC-MS/MS) analysis.

They correlated two inflammation-associated proteins (integrin alpha-M and mitochondrial superoxide dismutase) to high blood LDL.⁹⁶ Mitochondrial superoxide dismutase was previously associated with unstable carotid plaques.⁹⁷ Eighty-one common proteins (e.g., hemoglobin, fibrin, actin) were found in all 20 emboli.

A second study, published in 2018, analyzed four thrombi, with ~1,600 proteins identified, with 341 proteins commonly detected in all patients.⁹⁸ From a functional point of view, the authors found several significantly enriched pathways in their thrombotic proteome dataset (as remodeling of epithelial adherens junctions, protein ubiquitination pathway, mitochondrial dysfunction, acute phase response signaling, clathrin-mediated endocytosis signaling, integrin signaling, caveolar-mediated endocytosis signaling, phagosome maturation, leukocyte extravasation signaling, among others).

A proteomic study was previously conducted on coronary clots and published in 2014.⁹⁹ A total of 708 unique proteins were identified. Authors showed that five proteins (fermitin homolog 3, thrombospondin-1, myosin-9, beta parvin and ras-related protein Rap-1b) co-expressed within the coronary thrombus with CD41 (integrin alpha-IIb/beta-3, a receptor present in platelets responsible for platelet aggregation and interaction with extracellular matrix), indicating the potential activation of a focal adhesion pathway within thrombus platelets during coronary thrombus formation.

Finally, even if histological techniques remain the most used to study intracranial thrombi in the last few years, an increasing number of teams report using more advanced biological techniques in this field (Figure 11).

First author, year	Number of samples	Techniques	Findings
Alonso-Orgaz and al., 2014	20	3 techniques of tandem mass spectrometry	A total of 708 proteins in the coronary thrombus Correlation of 5 proteins (fermitin homolog 3,

			thrombospondin-1, myosin-9, beta parvin and ras-related protein Rap-1b) with CD41 (platelets)
Rao and al., 2017	20	Nano-liquid chromatography with tandem mass spectrometry	Correlation of Serum LDL levels with thrombus proteins: -inflammation related (alpha-M and mitochondrial superoxide dismutase) -metabolism related (Phosphoglycerate Kinase 1, Integrin Alpha-M, Glucose-6-phosphate dehydrogenase)
Munoz and al., 2018	4	Nano-liquid chromatography with tandem mass spectrometry	Identification of around 1600 different protein species in thrombotic material

Table 4: Review of proteomic studies focusing on intracranial thrombus

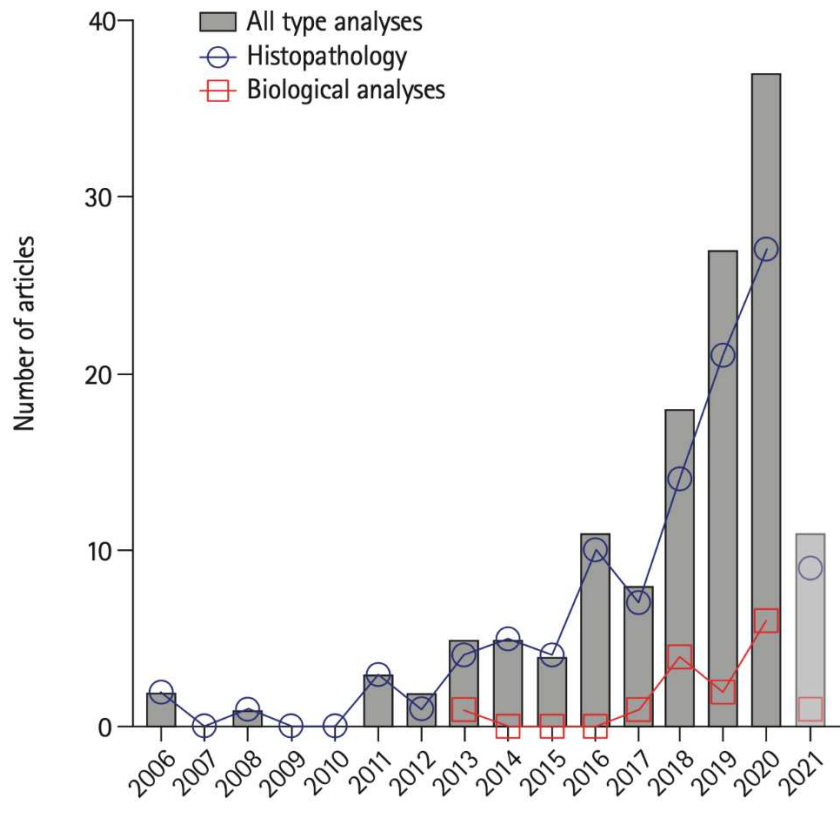


Figure 10: Number of published articles focusing on intracranial thrombus between 2006 and 2021.

From Aliena-Valero A. and al., Clot Composition Analysis as a Diagnostic Tool to Gain Insight into Ischemic Stroke Etiology: A Systematic Review. J Stroke. 2021.

Reproduced with the permission of Journal of Stroke.

The second part of this work focuses on understanding the molecular composition of post-thrombus intracranial blood samples obtained by microcatheter aspiration during EVT of AIS.

At the time of investigation (2020-2022), very few studies (performed by two teams) had analyzed ischemic blood, i.e., sampled beyond the intracranial occlusion level.

Kollikowski and al. (2020), analyzed microcatheter aspiration of 40 blood samples within the core of the occluded vascular compartment (beyond the intracranial occlusion), compared to blood samples from carotid-femoral. Cell counting was performed after red blood cell lysis and white blood cell (WBC) staining with Tuerk solution using a Fuchs-Rosenthal counting

chamber. Chemokine and cytokine Quantification (IL-8, IP-10, Eotaxin, TARC, MCP-1, RANTES, MIP-1a, MIG, CXCL-5 (ENA-78), MIP-3a, GRO α , CXCL-11 (I-TAC), and MIP-1b in samples were performed using a fluorescent bead immunoassay (LEGENDplex; Biolegend, San Diego, CA).

The authors found that the total number of leukocytes significantly increased at the brain level, and neutrophils predominantly drove this increase. Significant increases were also described for lymphocytes and monocytes, associated with locally elevated plasma levels of the T-cell chemoattractant CXCL-11.¹⁰⁰ This exciting paper was the first direct human evidence that neutrophils, lymphocytes, and monocytes, as well as specific chemokine upregulation, may accumulate in the ischemic arterial bed during acute ischemic stroke.

This increase in total leukocyte counts driven by neutrophils within the occluded ischemic cerebral vasculature was confirmed in a subsequent study by the same team (2021).¹⁰¹ Furthermore, this finding may have a predictive value because leukocyte influx was associated with reduced retrograde collateral flow and greater infarct extent.

Another study by Kollikowski and al., published in 2021, pointed out the cerebral platelet activation and platelet-neutrophil interactions in post-clot ischemic blood. Microcatheter aspiration of 1 ml of post-clot ischemic blood and systemic arterial blood samples (self-control) was performed. Local chemokines CXCL4 and CXCL7 levels were higher compared with peripheric blood. Local platelet counts were lower, whereas neutrophil counts were elevated higher. Local platelet and neutrophil counts and CXCL7 and MPO levels were correlated.¹⁰²

Another team, which described the BACTRAC protocol in 2019 (a protocol isolating intracranial blood within the artery immediately downstream of the clot, in the clot itself, and systemic blood proximal to the clot, clinicaltrials.gov NCT03153683),¹⁰³ explored how the protein expression of 25 AIS patient's intracranial blood compared with the protein expression of their systemic arterial blood. They published their results in 2020. Their analysis was performed using a cardiometabolic panel (92 protein biomarkers) and an inflammatory panel (immune assay of 92 inflammation-related protein biomarkers). Their main results showed that 42 cardiometabolic and 53 inflammatory proteins had significantly different expressions in central versus peripheric blood. All these 95 proteins exhibited lower expression at the

central (post LVO) level. Among them, endopeptidase, phospholipid transfer protein (PITP), uromodulin (UMOD), ficolin-2 (FcN2), c-c motif chemokine 19 (ccl19), c-c motif chemokine 20 (ccl20), fibroblast growth factor 21, c-c motif chemokine (ccl23).

Another study by the BACTRAC team, published in 2022 on 16 patients, showed that intracranial ischemic blood harbored significant increases in T cell amount, whereas myeloid and macrophage cells decreased compared to patient carotid artery blood samples.¹⁰⁴

Finally, this same team analyzed proteins obtained from intracranial (distal to clot) and systemic arterial blood (carotid) on 42 AIS patients.¹⁰⁵ They correlated increased systemic ($p<0.001$) and intracranial ($p=0.013$) levels of VCAM1 with the presence of systemic hypertension. Interestingly, intracranial VCAM1 level was a prognostic factor, positively correlated to infarct volume and brain edema volume. Moreover, $\% \Delta$ in NIHSS from admission to discharge was significantly correlated to both systemic and intracranial ($p=0.011$; VCAM1 levels, suggesting that elevated levels of systemic and intracranial VCAM1 were associated with less clinical improvement. VCAM1 is a vascular adhesion molecule induced by several mediators, including pro-inflammatory cytokines like TNF α , reactive oxygen species (ROS), turbulent blood flow, microbial stimulation of toll-like receptors, high glucose concentrations, and shear stress.¹⁰⁶

First author, year	Number of samples	Techniques	Findings (post-thrombus blood compared to control/peripheral blood)
Martha and. al, 2020	28	Relative concentrations of mRNA for gene expression in 84 inflammatory molecules in arterial blood distal and proximal to the intracranial thrombus	CR4, IFNA2, IL-9, CXCL3, Age, T2DM, IL-7, CCL4, BMI, IL-5, CCR3, TNF α , and IL-27 predicted infarct volume.

			IFNA2, IL-5, CCL11, IL-17C, CCR4, IL-9, IL-7, CCR3, IL-27, T2DM, and CSF2 predicted oedema volume.
Kollikowski and al., 2020	40	leukocyte counting and differentiation, platelet counting, the quantification of 13 proinflammatory human chemokines/cytokines	↑ total number of leukocytes predominantly driven by neutrophils ↑ lymphocytes and monocytes ↑ T-cell chemoattractant CXCL-11
Maglinger and al., 2020	25	Olink Proteomics (Olink Proteomics, Boston, Massachusetts, USA)	↓ of a majority of proteins
Kollikowski and al., 2021	58	Leukocyte counting and differentiation, assessment of collateral flow	↑ total number of leukocytes predominantly driven by neutrophils Association of Leukocyte influx with reduced retrograde collateral flow and greater infarct extent
Maglinger and al., 2021	42		VCAM1 is associated with systemic hypertension, infarct volume, brain oedema volume and reduced clinical improvement

Kollikowski and al., 2021	70	leukocyte counting and differentiation, platelet counting, quantification of platelet-derived neutrophil-activating chemokine CXCL4(PF-4), neutrophil attractant CXCL7(NAP-2), and myeloperoxidase (MPO)	↑ mean local CXCL4 ↑ neutrophils count ↓ platelets count Correlation between local platelet and neutrophil counts and between CXCL7 and MPO
Shaw and al., 2022	16	Flow cytometry panel identifying B cells, T cells, dendritic cells, NK cells, macrophages, monocytes, granulocytes, platelets, and endothelial cells	↑ T cell count ↓myeloid/macrophage count
Schuhmann and al., 2022	36	Immediate flow-cytometry analysis of leukocyte populations	High proportion of granulocytes, local shift towards CD4+ T cells

Table 5: Review of studies analyzing blood samples obtained by microcatheter aspiration during EVT.

We used an innovative quantitative technique (MESOSCALE) to analyze post-clot blood samples to examine a panel of 37 chemokines, cytokines, and angiogenic/vascular-related factors. This high-sensitive technique uses electrochemiluminescent labels conjugated to detect antibodies, and light intensity is measured to quantify the targeted analytes. For this technique, a plate is coated with capture antibodies (immobilized on a working electrode surface) on independent and well-defined spots. The sample and a solution containing detection antibodies conjugated with electrochemiluminescent labels (MSD SULFO-TAG™) are added, emitting light when electrochemically stimulated. Analytes in the sample bind to capture antibodies, and the sandwich is completed by recruitment of the detection antibodies by the bound analytes. A voltage applied to the plate electrodes causes the captured labels to

emit light. The instrument measures the intensity of emitted light (proportional to the amount of analyte present in the sample), providing a quantitative measure of each analyte in the sample. Subsequently, signal processing algorithms quickly convert the measured signal into valuable data, keeping read time fast, even for high-density plate formats. This technique has high sensitivity than conventional ELISA (MULTI-ARRAY Technology).

Our study used the V-PLEX Neuroinflammation Panel 1, Cytokine Panel 1, Proinflammatory Panel 1, Vascular Injury Panel 2, Angiogenesis Panel 1, and Chemokine Panel 1 Kits (MSD, Gaithersburg, MD, USA). This panel provides assay-specific components for the quantitative determination of 37 human biomarkers, combining proinflammatory, cytokine, chemokine, and angiogenesis panels (CRP, Eotaxin, Eotaxin-3, FGF (basic), ICAM-1, IFN- γ , IL-1 α , IL-1 β , IL-2, IL-4, IL-5, IL-6, IL-7, IL-8, IL-10, IL-12/IL-23p40, IL-13, IL-15, IL-16, IL-17A, IP-10, MCP-1, MCP-4, MDC, MIP-1 α , MIP-1 β , PIGF, SAA, TARC, Tie-2, TNF- α , TNF- β , VCAM-1, VEGF-A, VEGF-C, VEGF-D, VEGFR-1/Flt-1).

This method has previously been used to demonstrate an increase of biomarkers of neuroinflammation and cerebrovascular dysfunction in Alzheimer's disease; in another study of post-COVID-19 patients with neurological symptoms,^{107,108} to quantify biomarkers of neuronal and oxidative damage in traumatic brain injury.^{109,110} Mesoscale technique has been validated for biomarkers quantification.¹¹¹ We should note that CRP, Interleukin-6, Interleukin-1 β , and Tumor necrosis factor- α have been previously identified as potential cardioembolic stroke biomarkers,¹¹² suggesting a marked role of systemic inflammation in both pathophysiology and prothrombotic state in atrial fibrillation.^{113,114}

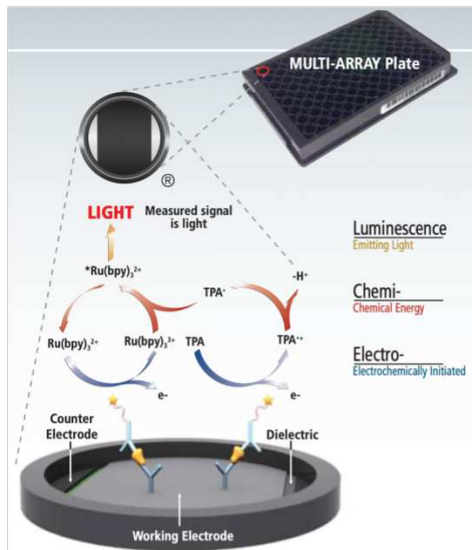


Figure 11: Overview of MESOSCALE features

Support Vector Machine

Support Vector Machine (SVM) was used to analyze the combination of clinical and analytical data; to address the classification of intracranial thrombi in cardioembolic versus atherosclerotic groups, and to correlate post-clot soluble factors with the outcome and patients' characteristics.

SVM is a machine learning method that can address various classification problems.¹¹⁵

It is a computer algorithm (classifier) that learns by example to assign labels to objects. Two general principles are aimed at optimizing the classifier's accuracy (maximizing the percentage of correct labels assigned to new samples) and optimizing its reproducibility (warranting that classifier may apply to new data).

The three steps necessary for SVM analysis are:

1. Feature selection: this step will transform the original raw training data into a set of “features” used as input for SVM
2. Training and testing the classifier

Evaluation of the classifier's performance: sensitivity, specificity, and accuracy.

Logically, the ultimate test of model performance is on unseen data. Then, the preferred method is to split the dataset into train and test groups early.

One advantage of classification learning methods is that they can be predictive; once a classifier such as an SVM is generated, it can then be applied to new samples to predict to which group they belong. Effective use of SVM in our fields does not require an in-depth understanding of its mathematical principles. Still, we will provide some basic concepts to understand SVM general principles better. Hence, the four fundamental concepts that should be understood are:¹¹⁶

1. the separating hyperplane
2. the maximum-margin hyperplane
3. the soft margin
4. the kernel function

Classification in the machine learning approach is supervised learning, used to analyze a given data set, leading to a model that separates data into a desired and specific number of classes. During training, the model maps input data to output data based on many examples of input-output pairs. In this phase, SVM is trained using example observations where we know the label assignments (e.g., cardioembolic or atherosclerotic thrombi) of the examples in advance. Features corresponding to observations can be used to train a decision function that generates class assignments (or labels).

The separating hyperplane

The decision function is represented by an optimal hyperplane separating (or classifying) observations belonging to one class from another based-on patterns of data about those observations called features. That hyperplane will subsequently be used to define the most probable label for unseen data. Features used to define the hyperplane are referenced by coordinates according to their relationships to each other and form the so-called support vectors (Figure 13).

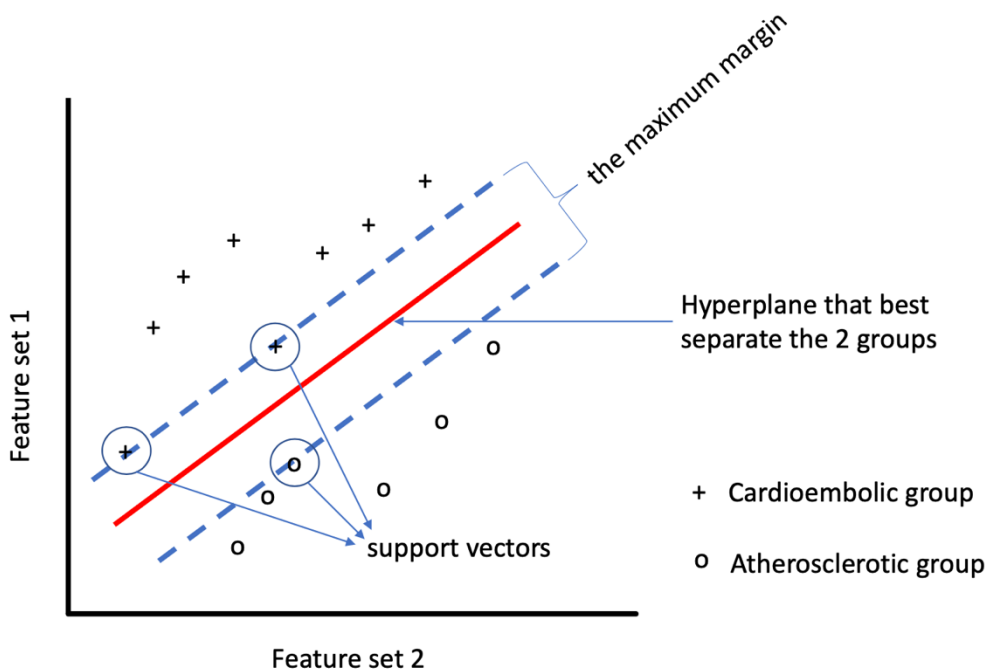


Figure 12: Illustration of SVM hyperplane

The hyperplane that maximally separates the support vectors corresponding to each of the two to-be-predicted classes. Here, cardioembolic samples (x) and atherosclerotic samples (o). The closest points are called the support vectors, because they are the data observations that “support”, or determine, the decision boundary.

The maximum-margin hyperplane

The optimal hyperplane is the one that maximizes the distance (i.e., the “margin”) between the support vectors of both class labels, in order to predict the correct classification of previously unseen examples. In other terms, we must maximize the distance separating the closest pair of data points belonging to opposite classes.

A hyperplane may be a line when two feature dimensions are studied, or a two-dimensional plane when three features are used.

The soft margin

One limitation of SVM is overfitting, corresponding to the loss of learning generalization capability of a classifier. In this instance, a classifier may achieve some good diagnostic results on training data, but it has no way to generalize the good classification ability to new test data (Figure 14).¹¹⁷

A soft margin formulation may help to avoid the overfitting problem.

Proteomics special characteristics (mainly small number of samples and large number of variables) may theoretically increase the likelihood of an SVM classifier's overfitting in classification.

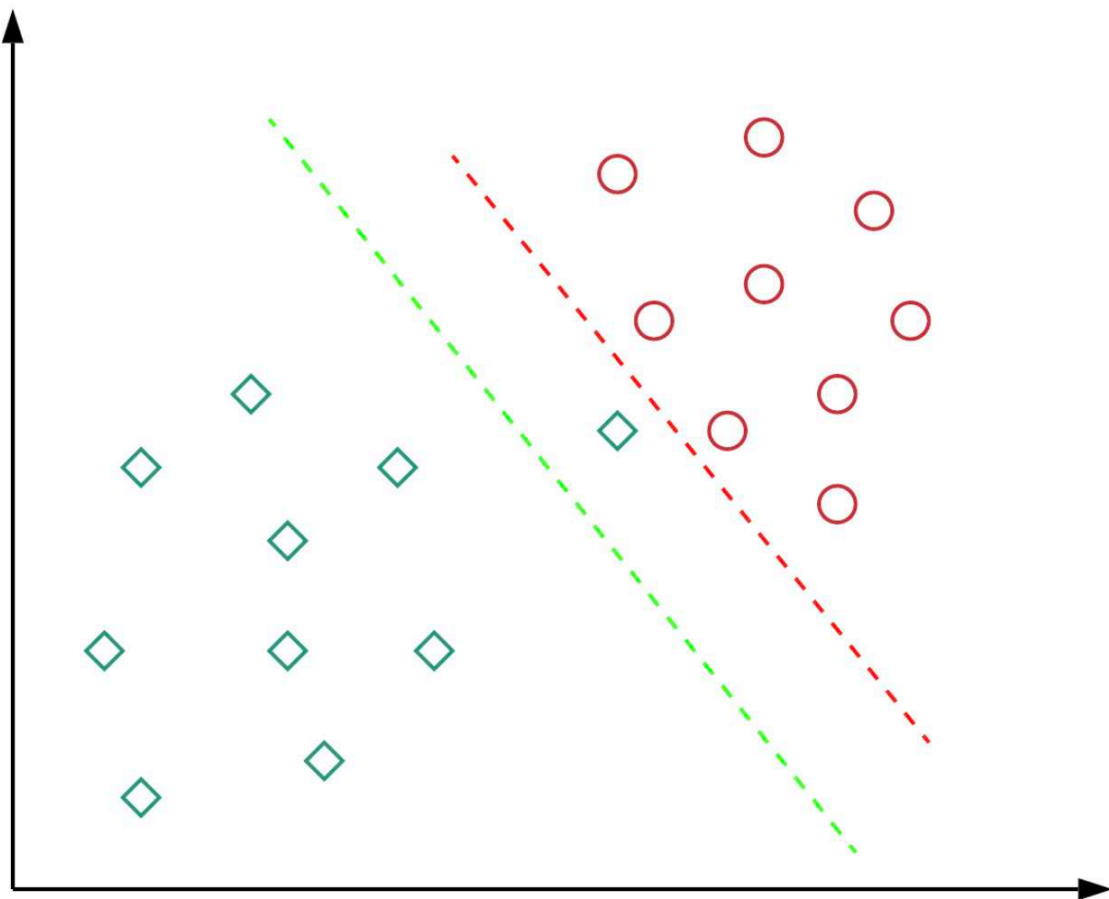


Figure 13: Illustration of the SVM soft margin

The red hyperplane perfectly separates all the training points. However, the green hyperplane has a softer margin, and may be better to generalize on unseen data. In other terms, allowing the classifier to misclassify (here the green square misclassified using the hyperplane represented by the green dashed line) may allow for greater generalizability to new data

The kernel function

The kernel function is a mathematical transformation allowing to project data from a low-dimensional space to a space of higher dimension and separation of data otherwise non-

separable in a lower dimensional space (Figure 15). In other terms, If the data is not linearly separable in the original, space, we apply transformations to the data, which map the data from the original space into a higher dimensional feature space. Generally, statisticians begin with a simple SVM, before trying some “standard” kernel function. Figure 15 shows an example of basic kernel transformation allowing linear separation of data.

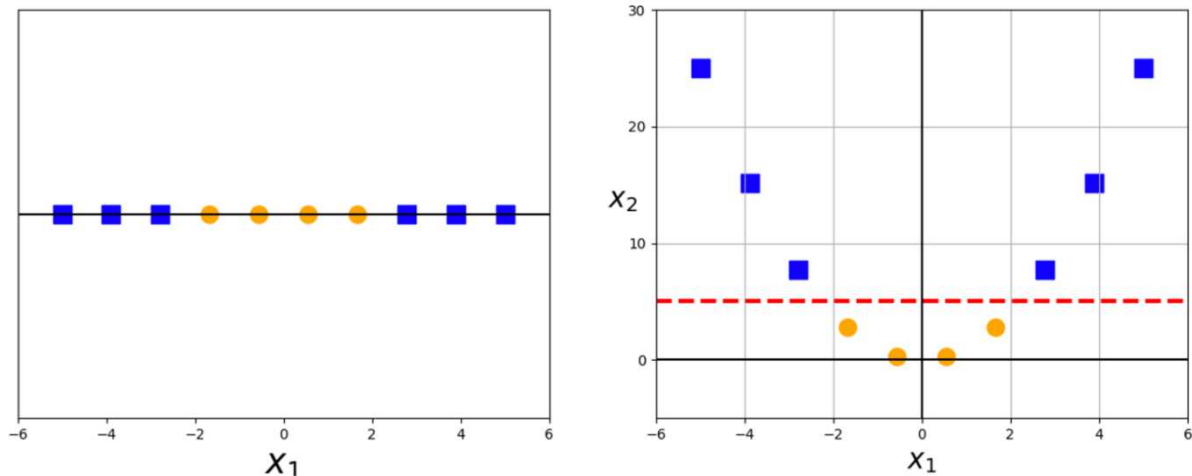


Figure 14: illustration of kernel transformation

In 1-dimension, the data is not linearly separable. After applying the transformation $\phi(x) = x^2$ and adding a second dimension to the feature space, the classes become linearly separable.

We will first describe the material and methods common to the two studies, before detailing the specificities of each work.

SAMPLING WORKFLOW

Inclusion criteria

Our inclusion criteria correspond with the 2019 Update to the 2018 Guidelines for the Early Management of Acute Ischemic Stroke guidelines.¹¹⁸

Patients of age 18 and older with suspected AIS secondary to an LVO were recruited without upper or lower limits of the neurological severity (NIHSS) at baseline. Patients were required to present imaging evidence of occlusion of the internal carotid artery (ICA, cervical or intracranial part), the M1 or M2 branches of the middle cerebral artery (MCA), the basilar artery, or a tandem atheromatous occlusion defined by the occlusion of both cervical carotid artery and intracranial artery (carotid artery or MCA). Intravenous thrombolysis (IVT) treatment was allowed and administrated according to current guidelines.¹¹⁹

All patients were included in the Endovascular Treatment in Ischemic Stroke Follow-up Evaluation (ETIS) registry, a multicenter (14 French centers), open, observational, and prospective trial (ClinicalTrials.gov Identifier: NCT03776877). The primary objective of the ETIS registry is to assess clinical outcomes and different factors (clinical, imaging) that may affect clinical outcomes, such as systems of care associated with the use of acute reperfusion treatment or medical treatment alone intended to restore blood flow in patients experiencing an acute ischemic stroke due to large intracranial vessel occlusion. Secondary objectives of this registry include:

- Study of the relationship between efficacy (recanalization rate at the end of the procedure), complications (procedural and H24 bleeding) and functional status of patients at 3 months (modified Rankin Score, mRS).
- Search for prognostic factors of good functional status at 3 months post-intervention: management delay, type of stroke (occlusion site, concomitant treatment, wake-up stroke, patient > 80 years, and initial severity), complications of thrombectomy.
- Search for prognostic factors of safety (Complication rate) and efficacy (Recanalization and reperfusion rates).
- Assess the reliability of pre- and post-diagnostic imaging.

- Search of biomarkers of stroke recovery and stroke etiology (analysis of baseline plasmatic biomarkers and correlation with the functional status of patients at three months and efficacy/safety of the endovascular procedure of the acute ischemic stroke). MISO study is in line with this objective, adding specific samples and biomarkers exploration to the one already collected and analyzed in the ETIS registry (Fibrinolysis markers [D-dimer, PDF, fibrinogen, plasmin-anti-plasmin complexes], , circulating von Willebrand factor, activation and platelet aggregation markers [serotonin, p-selectin...], neutrophils activation markers [MPO, MMP-9, neutrophil elastase...], presence of NETS [free DNA, H3 citrullinated histones]).
- Assess the neurocognitive outcomes of patients 3 months post-stroke

Imaging protocol

A well-established imaging protocol is implemented in our comprehensive stroke center (CSC). CTA perfusion is preferred whenever possible, especially for patients with severe symptoms at admission and a known time of symptom onset. This modality is sometimes chosen for patients with MRI incompatible devices and implants.

MRI was performed on 1.5-Tesla Aera or 3-Tesla Skyra scanners (Siemens, Erlangen, Germany). MRI is preferred:

- For wake-up stroke, or when the onset of symptoms is not clear
- For minor or mild symptoms of stroke patients (NIHSS <6)
- For the oldest patients (>85 years old), to assess microbleeds burden before IVT.

Alberta Stroke Program Early CT Score (ASPECTS) is a topographic scoring system for assessment of the extent of early ischemic changes in MCA territory, divided into 10 regions, validated for predicting radiological and neurological outcome. Each region scores 1 point if normal and 0 if abnormal; thus, a normal scan or MRI scores 10, and a total MCA territory infarct scores 0 (Figure 16). The posterior circulation Acute Stroke Prognosis Early Computed Tomography Score (pc-ASPECTS) is used for grading infarct core in the vertebrobasilar system (Figure 17).¹²⁰

Infarct core volumes at baseline and on follow-up imaging were measured using a semiautomated segmentation method with an FDA-approved software (Centricity, GE

Healthcare, Chicago, Illinois, USA), or using RAPID software (iSchemiaView, Redwood city, California, USA), which is a fully automated post processing software application used for quantitative stroke analysis.

On CT, ischemic core was defined as brain volume with CBF under 30% of the CBF of the homologous zone in the contralateral hemisphere.

On MRI, ischemic core was defined by RAPID software as brain volume with apparent diffusion coefficient (ADC) below $620 \times 10^{-6} \text{ mm}^2/\text{s}$.

An illustration of semiautomatic segmentation of infarct score is provided in Figure 18.

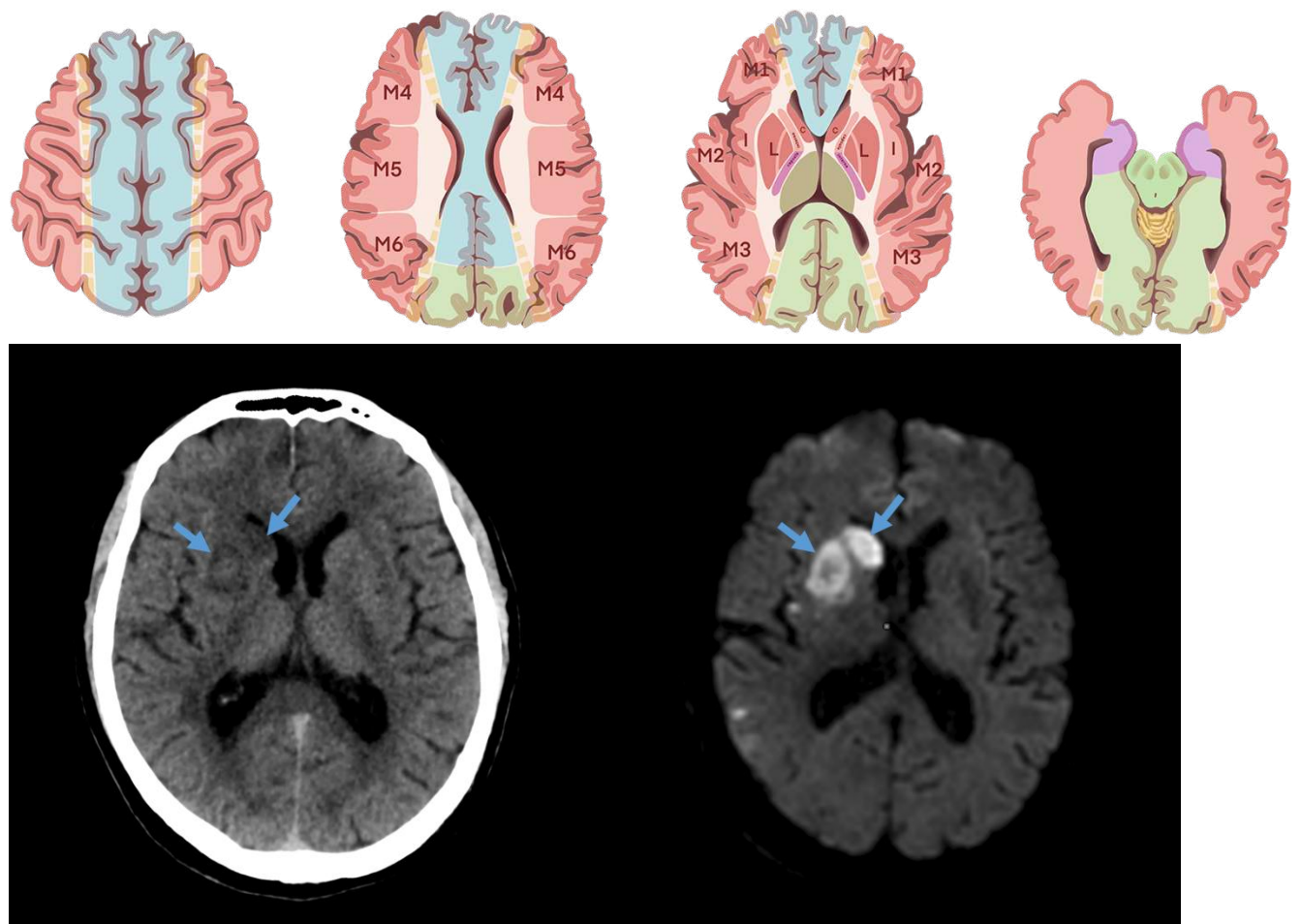


Figure 15: Illustration of ASPECTS score

An Alberta Stroke Program Early CT Score (ASPECTS) of 8 is depicted in this patient with a right MCA stroke

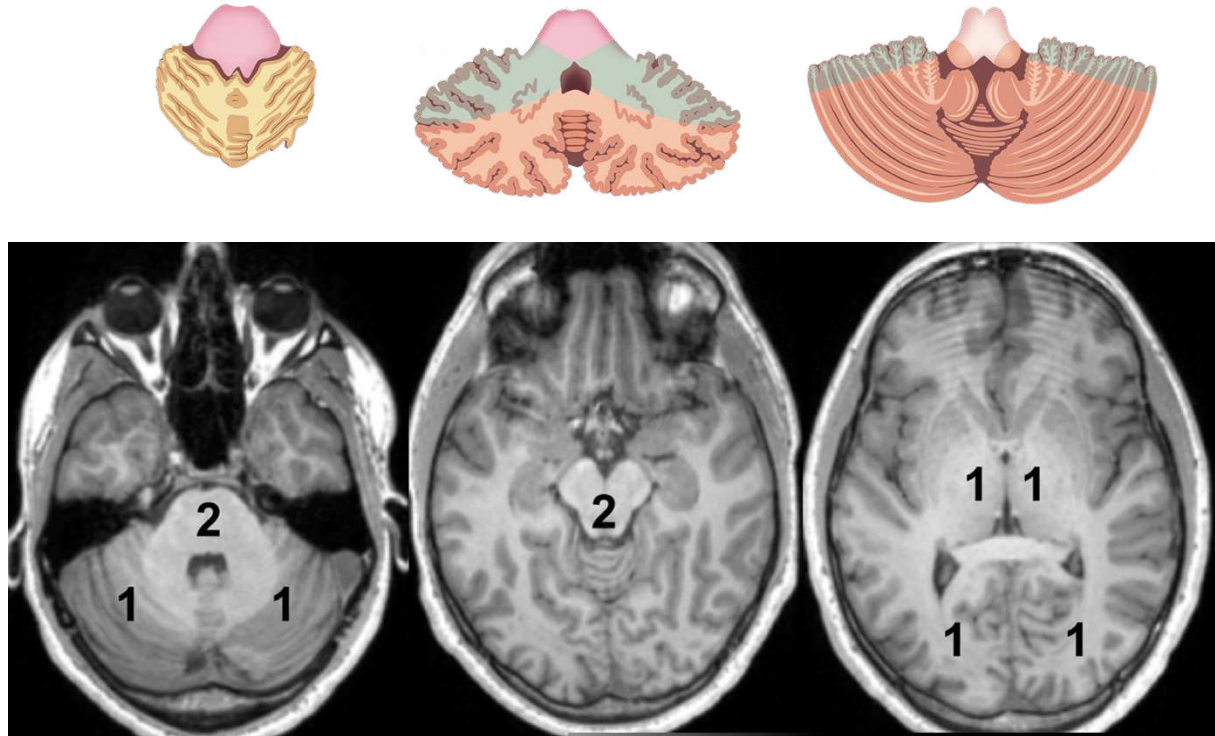


Figure 16: Illustration of areas used for assessment of pc-ASPECTS scores

2 points are considered for mesencephalon and protuberance, 1 for thalamus, occipital lobe and cerebellum hemisphere

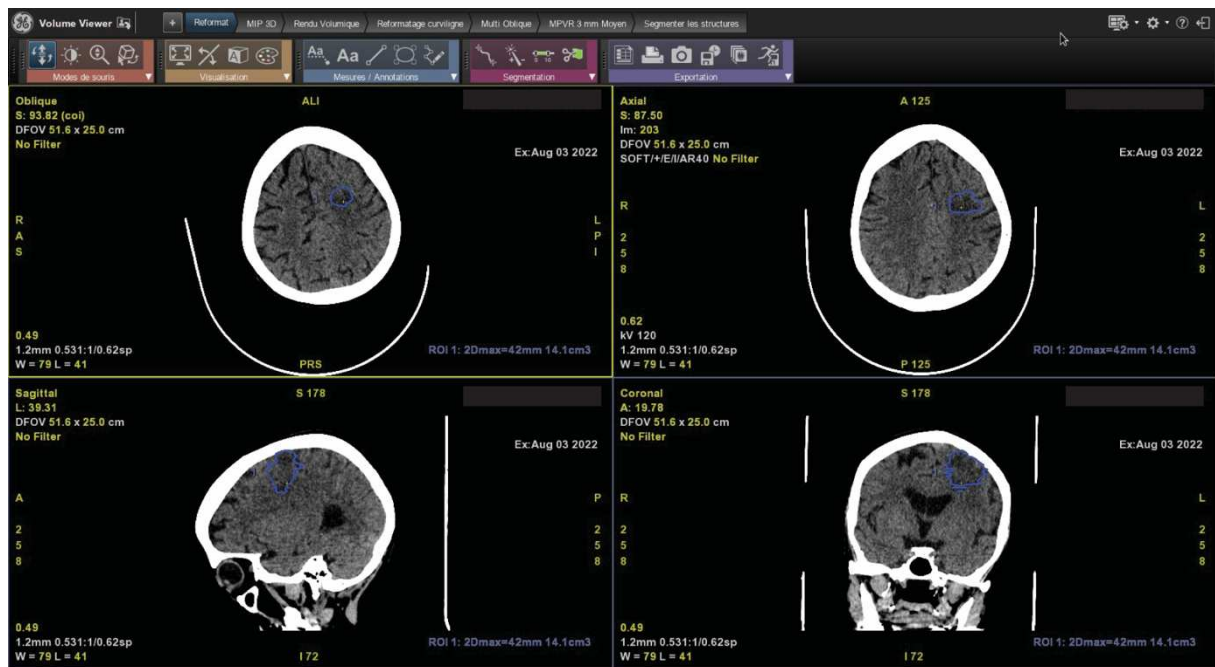


Figure 17: Illustration of semiautomated infarct core segmentation

An infarct core of 14.1 cm³ is calculated on this follow-up CT performed one day after EVT

Timing

Pre-hospital and in-hospital delays of patient's management were calculated in minutes. The studied delays were the following: symptoms onset to admission, symptoms onset to groin puncture, groin puncture to reperfusion, and symptoms onset to reperfusion.

Figure 19 provides an overview of global pathway for managing patients with acute ischemic stroke from symptom onset to endovascular treatment.

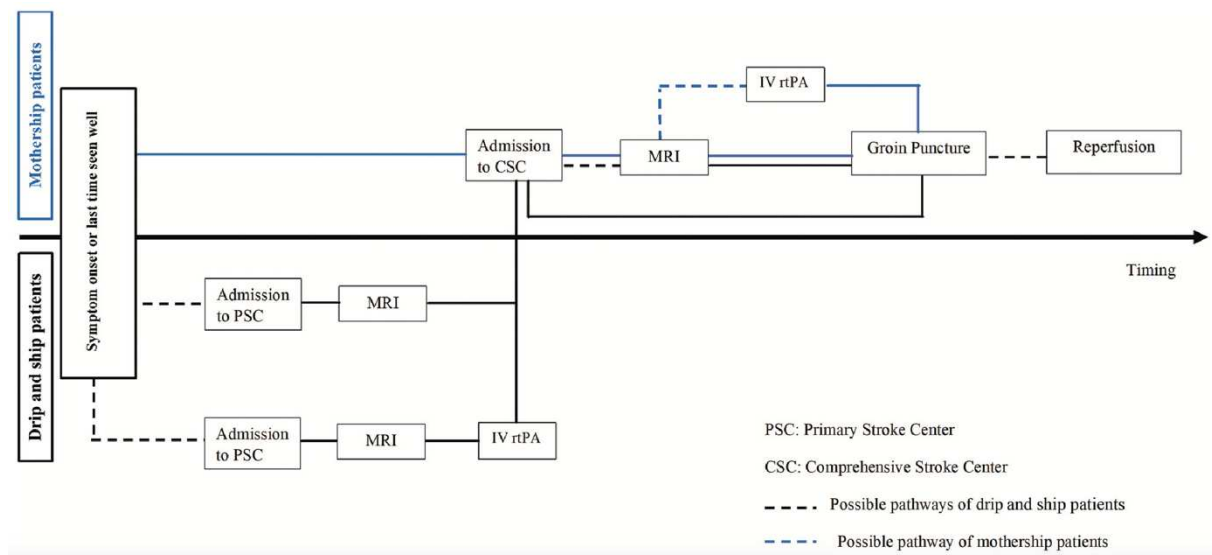


Figure 18: Pathways for management of patients with acute ischemic stroke from symptom onset to endovascular treatment

From Benali A, Moynier M, Dargazanli C, Deverdun J, Cagnazzo F, Mourand I, et al. Mechanical Thrombectomy in Nighttime Hours: Is There a Difference in 90-Day Clinical Outcome for Patients with Ischemic Stroke? AJNR Am J Neuroradiol. 2021 Mar;42(3):530–7.

Reproduced with permission of WILLIAMS & WILKINS CO., American Society of Neuroradiology

Endovascular treatment procedure

Here we provide details on the endovascular treatment (EVT) procedure for the non-interventional neuroradiologic audience and readers.

Much technical progress has been made since 1927 and the E. Moniz's presentation at the Congress of the Neurological French Society in Paris of his first experiences with a new method to study the cerebral vessels, that he called "l'encéphalographie artérielle." The catheter technique was introduced in 1953 (Seldinger), and the subtraction technique was in 1963 (Ziedses des Plantes). Later, in the 1980s, the basis of the endovascular treatment aimed at treating extracranial pathologies was first followed by intracranial ones, thanks to the evolution of catheters, guide wires, and the technical skills of interventional neuroradiologists. Nowadays, interventional neuroradiology may address a broad scope of vascular diseases of the central nervous system (acute strokes, brain or spinal dural arteriovenous fistulas, arteriovenous malformations, brain aneurysms, carotid stenosis, cerebral venous diseases, brain or head, and neck tumors embolization).

EVT in our studies was performed mainly via the femoral artery approach (groin puncture). In a few instances, the radial or direct carotid approach was used. Procedures were performed by board-certified neurointerventional radiologists or by supervised neurointerventional fellows in a mono or biplane neuroangiography suite (Siemens, Erlangen, Germany). In the anterior circulation, a 9-French balloon guide catheter (Merci Balloon Guide Catheter; Concentric Medical, Stryker, Kalamazoo, USA) was introduced through a femoral sheath into the concerned carotid artery.

In the posterior circulation (basilar artery occlusion), a 6-French Neuron Max (Penumbra, California, USA) guide catheter was placed into the dominant or most navigable vertebral artery.

EVT approach was based on the operator's preference, and included direct Aspiration First Pass Technique (ADAPT)¹²¹ or the use of a stent-retriever, under general or local anesthesia. Reperfusion results were reported by using the modified Thrombolysis in Cerebral Infarction Scale (mTICI).^{122,123}

mTICI score	Definition
0	No reperfusion
1	Minimal reperfusion
2A	Partial filling <50% territory
2B	Partial filling >50% territory
2C	Near complete reperfusion (>90%) except slow-flow or few distal cortical emboli
3	Complete reperfusion

Table 6: The modified Thrombolysis in Cerebral Infarction reperfusion scale

ADAPT

A large bore aspiration catheter (Sofia 5 or 6, Microvention, California, USA) is positioned just proximal to the level of occlusion and then connected to a syringe or automatic aspiration pump. Once attached to the suction system, the catheter is advanced into the proximal end of the thrombus, and suction is initiated (Figure 20). Forward pressure is provided to ensure adequate apposition. The catheter's engagement with the thrombus is confirmed when there is no backflow through the suction tubing. The thrombus is then either aspirated through the catheter or becomes stuck at the catheter tip, and the catheter may be withdrawn back into the guide catheter. Importantly, this technique does not allow accessing blood distal to the thrombus.

Stent-retriever

This technique allows to retrieve clot and to sample local blood distal to the thrombus. A 0.21-inch internal diameter microcatheter (Headway; Microvention, or Trevo Pro Vue 18; Stryker) was navigated distal to the occlusion over a 0.014-inch steerable microwire (Synchro 2 Standard, Stryker). The microwire was retrieved from the microcatheter, allowing exchange with the stent-retriever (Figure 21).

Then, the microcatheter was unsheathed, allowing stent-retriever deployment (Trevo; Stryker, Solitaire FR; Medtronic, Embotrap II or III; Cerenovus). The device was left in place for 2 minutes, allowing full expansion of the nitinol stent through the thrombus. The aspiration

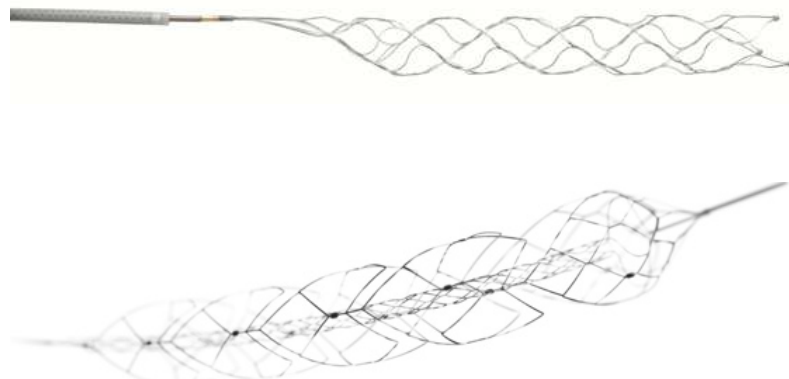
catheter is then advanced to the proximal face of the clot, and the aspiration pump is connected and activated. The stent retriever and aspiration catheter are then withdrawn into the guide catheter as a unit (Figure 22). Before this retrieval, the balloon guide catheter was inflated to reduce distal emboli.¹²⁴ Rarely, where no backflow is observed within the guide catheter, the guide catheter is also retrieved under aspiration to remove the entrapped thrombus, which is generally massive in this instance.

Groin punctures were routinely closed with a vascular closure system (Angio-Seal [St. Jude Medical, St. Paul, MN], or FemoSeal [Terumo]), radial punctures using the Terumo TR-band system.

Peri-procedural complications [embolization in a new territory (defined as an angiographic occlusion in a previously unaffected vascular territory observed on the angiogram after clot removal), arterial dissection or perforation, vasospasm, and subarachnoid hemorrhage] were recorded.



Figure 19: : Illustration of Direct Aspiration First Pass Technique (ADAPT) technique



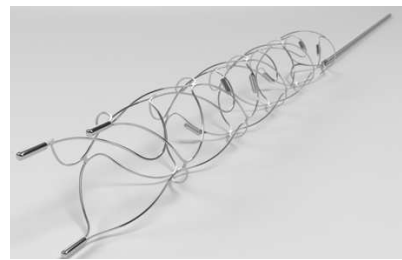


Figure 20: Stent-retrievers used in the study

Top to bottom: Trevo NXT (Stryker), Embotrap III (Cerenovus), Solitaire X (Medtronic). Images used with permission of Stryker, Cerenovus and Medtronic

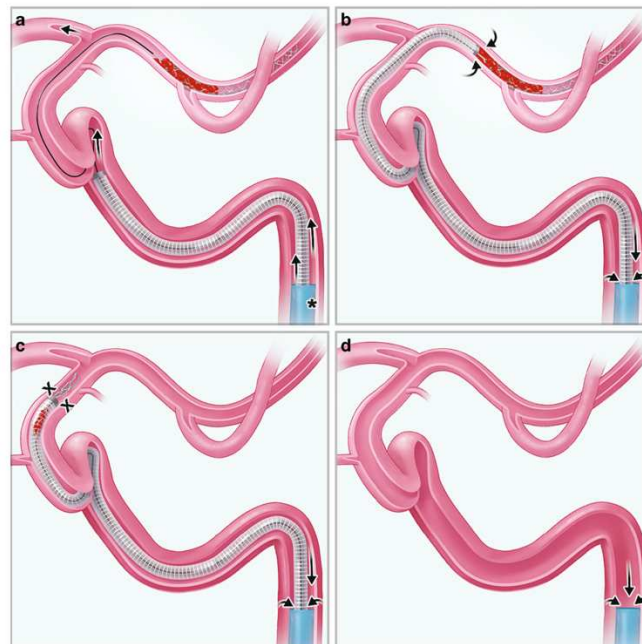


Figure 21: Illustration of the combined technique

This technique was the most used in our studies. a. A guiding catheter (Asterisk) is placed distally in the internal carotid artery. The stent retriever is advanced and deployed primarily distally to the clot and only the proximal one-third interacts with the clot. b. The aspiration catheter is advanced to the face of the clot and aspiration with the pump is started. The stent retriever is retrieved while the aspiration catheter is pushed simultaneously until a wedge position is reached. The vacuum within the aspiration catheter is preserved with the pump. c, d. Stent retriever and aspiration catheter are withdrawn into the guide catheter as a unit.

Reproduced with the permission of Springer Nature. From Maus V, Behme D, Kabbasch C, Borggrefe J, Tsogkas I, Nikoubashman O, et al. Maximizing First-Pass Complete Reperfusion with SAVE. Clin Neuroradiol. 2018 Sep;28(3):327–38.

Anesthesia

EVT was performed under local anesthesia with conscious sedation or general anesthesia (GA). The choice was indicated by the patient's medical history, level of occlusion (GA was preferred for tandem or distal occlusions), and patient's cooperation and tolerance.

Medications used during the procedure for all patients included analgesics (paracetamol), antiemetics (ondansetron), and vasoconstrictors (noradrenaline), the latter given in order to maintain blood pressure in the 140-180 mmHg range before recanalization.

For GA, induction of anesthesia was performed using hypnotics (etomidate, propofol), curare (rocuronium), and opioids (remifentanil). None of the included patients received heparin intravenously.

The detailed protocol used by the anesthesiology team is given in the Appendix (Supplemental File 2).

Unfractionated heparin was not administered neither intravenously nor added to the 1,000ml rinsing fluid (standard 0.9% saline solution) during EVT.

Patient consent

According to French legislation, the patient's consent to pursue research was mandatory to perform analysis on intracranial thrombi and peripheral and central blood samples. It was not a straightforward task, mainly for the following reasons.

1. Study inclusion was most often made in an emergency context.
2. Our patients were often severe, harboring both cognitive, language (fluency or understanding) disturbances
3. Because we treat stroke patients from all the Languedoc-Roussillon area, they often return to the remote neurovascular unit on day 1 or 2. It is often too early to obtain informed consent, when a patient has not recovered yet from neurological impairment.
4. When the patient leaves the neurovascular unit for the rehabilitation center, it is often complex to reach him directly.
5. Unfortunately, phone numbers are not always recorded in the emergency files and are very difficult to find. Sometimes, the recorder number was not correct at the time we used it.

6. Some patients had no relatives at all nor designed trusted persons.

In practice, we asked either the patient (when both comprehension and expression were preserved) or his/her relatives whenever possible, i.e., before its discharge from our center. Otherwise, we phone-called each patient or relative at home to explain the purpose of the research and obtain informed consent. It was also possible to use samples from deceased patients. After oral consent, a document explaining the protocol was sent to their domicile. We sometimes had to call referring physicians to obtain valid contact details. Both studies (reference study RECHMPL 18_0236, N° ID-RCB: 2018-A02651-54) were approved by the local ethics committee (Comité de Protection des Personnes [CPP] SUD-MEDITERRANEE III, UFR MEDECINE 186, chemin du Carreau de Lanes CS 83021 30908 NIMES Cedex 2) and registered on clinicaltrials.gov (NCT04421326). Local ethics committee approval (for the second part of the thesis), and informed consent model are provided in the supplemental data section (Supplemental Files 1 and 2).

Measures and Main Outcome

Follow-up imaging was performed between 16 and 30 hours after EVT to assess intracranial hemorrhage. Symptomatic intracranial hemorrhage (sICH) was defined as any hemorrhage occurring within 24 hours associated with an increase of ≥ 4 points in the NIHSS score or that caused death.³⁶

The mRS was collected during a phone visit by an investigator collaborator within 3 months (+/- 15 days) following the stroke. This evaluation was carried out by a trained study team member certified in mRS evaluation, independent of the management of the patient. A favorable functional outcome was defined as an mRS ≤ 2 .

0	No symptoms.
1	No significant disability. Able to carry out all usual activities, despite some symptoms.
2	Slight disability. Able to look after own affairs without assistance, but unable to carry out all previous activities.
3	Moderate disability. Requires some help but can walk unassisted.
4	Moderately severe disability. Unable to attend to own bodily needs without assistance and unable to walk unassisted.
5	Severe disability. Requires constant nursing care and attention, bedridden, incontinent.
6	Dead.

Table 7: the modified Rankin Score (mRS)

PROTEOMIC ANALYSIS OF INTRACRANIAL THROMBUS

Basics on proteomics principles and workflow

Overview of the proteomics workflow

The proteome corresponds to all proteins or modified proteins produced by a biological entity. This term was introduced in 1994 by Wilkins et al. to characterize proteins as a complement to genomic data.¹²⁵

Proteomics encompasses the application of techniques used to identify and quantify protein content in a cell, tissue, or organism. Mass spectrometry (MS)-based proteomics has led to the possibility of characterizing and quantifying the protein profile of biological specimens and discovering their interactions in numerous pathologies. It has led to the possibility of characterizing complex interactions and has dramatically helped advancement in protein analysis for both fundamental and clinical research.

Figure 9 shows the typical steps of a proteomics workflow, from the sample of interest to the protein identification.

Proteases are necessary to digest proteins into peptides with a predictable terminus, which are subsequently analyzed in an MS/MS device. Their mass-to-charge ratio and predicted sequence allow describing the proteins in the sample. Peptides are preferred to proteins because ionization and separation by reversed-phase liquid chromatography (RPLC) is easier, and their fragmentation is more predictable,¹²⁶ named “bottom-up” approaches. Only a few of those peptides are needed to identify a particular protein. Trypsin is the most used protease for protein digestion, with a high catalytic activity achieving peptides with a basic arginine or lysine at the C-termini, adequate for tandem mass spectrometry (MS) analysis.¹²⁷ After trypsin digestion, peptides with size between 5 and 20 amino acids can be detected by mass spectrometry depending on charges number they wear.

Unfolded proteins are necessary for easy access for proteases. To do so, a buffer containing strong denaturants (urea, guanidine) and ionic detergents (sodium dodecyl sulfate, SDS, or deoxycholate-SDC) is applied to tissue or cell lysis of interest. In some instances, protein

depletion may be necessary, to remove high-abundance proteins such as hemoglobin for thrombi, or albumin for serum or plasma samples, and different methods are available.¹²⁸ We will detail this point in the material and methods section. Subsequently, several methods (such as dialysis, buffer exchange, size exclusion, protein precipitation, chromatography, or electrophoresis) are available to remove molecules that may have been added in the extraction/depletion processes (“sample clean-up strategies”) or to fractionate sample to reduce the dynamic range of sample.¹²⁹

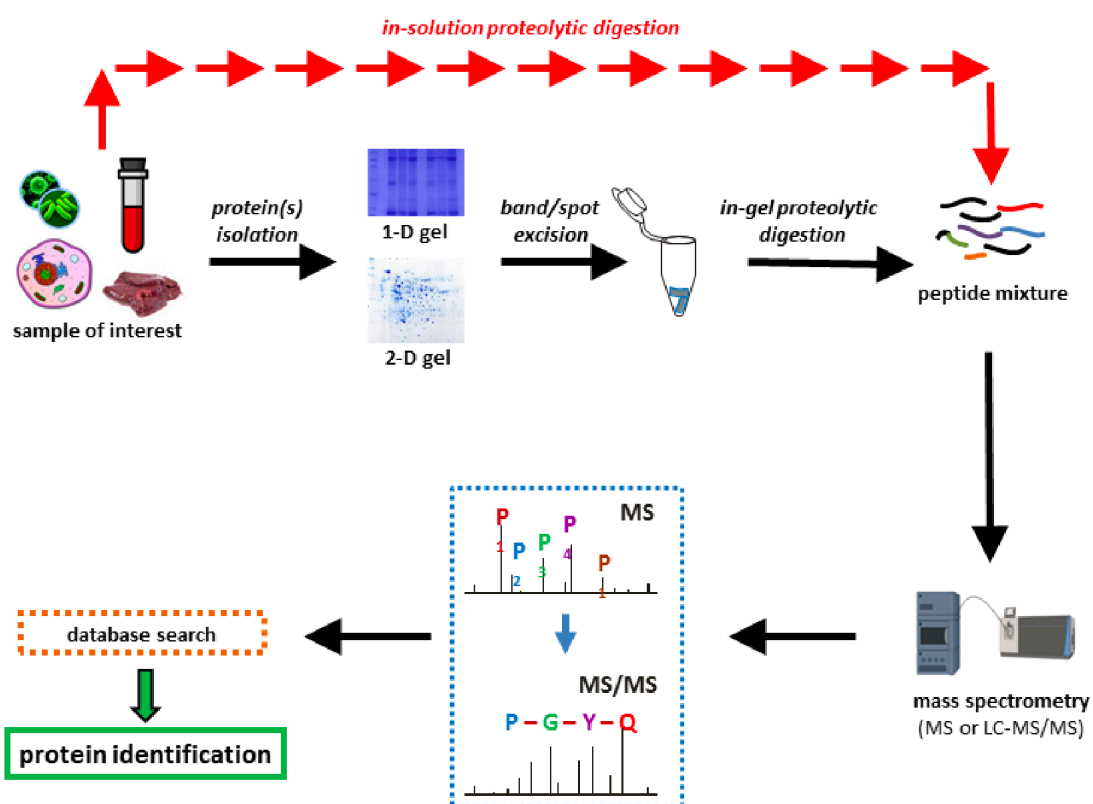


Figure 22: Overview of a typical proteomics workflow.

From Dupree EJ, Jayathirtha M, Yorkey H, Mihasan M, Petre BA, Darie CC. A Critical Review of Bottom-Up Proteomics: The Good, the Bad, and the Future of This Field. *Proteomes*. 2020 Jul 6;8(3):14.

What is Mass Spectrometry?

MS-based proteomics is one of the key techniques allowing complex protein sample analysis.

The mass spectrometer involves:

- **an ionization source** to ionize the analytes, converting analytes of interest into gas-phase ions. Electrospray ionization (ESI)¹³⁰ is the most used technique to ionize peptides, and is the technique used in our study. A strong electric current is applied to the solution, causing the ejection of liquid droplets into the gas phase, followed by desolvation and the accumulation of charge on the protein surface. After ionization, charged droplets move towards the mass analyzer of the spectrometer under high vacuum. An advantage of ESI is the availability to couple a Liquid Chromatography (LC) column to the electrospray needle (LC-MS), allowing separation of peptides or proteins before the mass spectrometer, separates molecules in a liquid mobile phase using a solid stationary phase. This is particularly relevant when analyzing of complex peptide samples. In our studies, nano-liquid chromatography was performed with a RSLC U3000 device (ThermoFisher Scientific).
- **a mass analyzer** Allows the transmission or separation of analytes according to their ratio m/z, using different principles. We should note that “mass spectrometry” is a misnomer, because it is the mass-to-charge ratio (m/z) which is determined, and mass is not what is measured. Different types of mass analyzers are currently used in proteomics: low resolution like ion trap, quadrupole and time of flight (TOF), or high resolution like Fourier transform ion cyclotron (FT-MS) and Orbitrap. They will measure the ion mass spectra of peptides (MS spectra) and from peptides fragments (MS/MS spectra). A hybrid quadrupole-Orbitrap mass analyzer (Q-Exactive HF, Thermo Fisher Scientific) has been used in our study.
- **a detector** that identifies the number of ions for each m/z value. It transforms ion signal to electric signal. The signal is proportional to the received charges.
- **tandem mass spectrometry (MS/MS)**: to obtain more information about ions structure, mass spectrometry in tandem is useful. Two or more analyzers are combined. Firstly, ions are separated and measured according to their m/z (MS). Then,

some ions (m/z) are selected and fragmented in products ions from precursors which are analyzed in a second time (MS/MS). In our work, proteomic data were analyzed using data-dependent acquisition (DDA), which selects the most abundant precursor ions for MS/MS analysis, allows to minimize redundant peptide precursor selection and increases the depth of proteome coverage.¹³¹

The mass-spectrometer products a file giving a peak list, the mass to charge ratio of precursor ions with their relative intensity and charge, as well as the mass to charge ratio of its fragment ions and their relative intensities. This file will be compared to a target database containing theoretical peptide sequences, obtained by computationally performing theoretical digestions and MS/MS analysis of all the possible proteins or resulting peptides from a given genomic dataset. Finally, a list of peptide-spectrum matches is obtained and used to identify individual peptides and subsequently, the proteins present in the sample. The Maxquant software was the one used in our work.¹³²

Angiography suite and freezing process

In the angiography room, after retrieval (Figure 23), thrombi were immediately frozen at -80°C in a dedicated transportable azote freezer (Voyager, Air Liquide). A primary concern was maintaining a constant temperature for several days. For that reason, the freezer was reloaded every week in the Cellular Therapy Department of our hospital (Dr. John De Vos). Before refilling, the samples previously collected were transferred to the -80°C ultra low-temperature freezer of the Pathology department (Pr. Valérie Rigau).

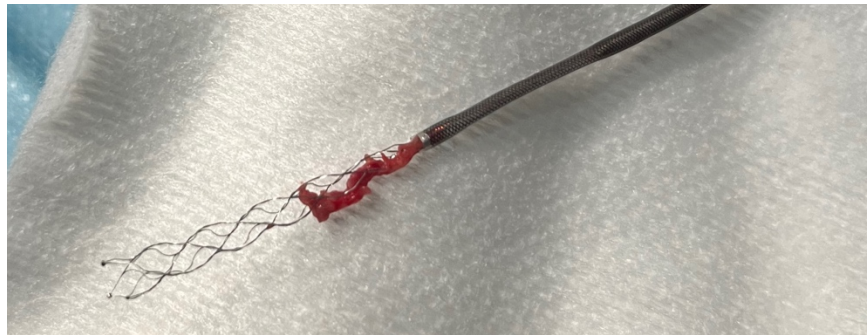


Figure 23: Illustration of a thrombus retrieved by a combined technique

The thrombus is embedded in the stent-retriever and aspiration catheter.

Laboratory

The first step was to perform quality control of our samples to validate their protein content and to find the best protocol to extract proteins. Six macroscopic samples were randomly chosen for this initial research:

1. Thrombus weigh
2. Application of a lysis buffer (radioimmunoprecipitation assay, RIPA 13 µl/mg) including two ionic detergents and one non-ionic detergent under sonication (10 strokes), combined with a protease inhibitor cocktail
3. Centrifugation: 12000rpm, 10mn, 4°C and removal of the supernatant
4. A second application of RIPA
5. Protein dosage by BCA method (Bicinchoninic acid assay)
6. SDS-PAGE electrophoresis
7. Fixation and coloration with Coomassie Blue

The first results showed (not surprisingly) that hemoglobin was present in all thrombi and suggested that this ubiquitous protein may “hide” other proteins of interest (Figure 24), potentially reducing the sensitivity of the MS/MS analysis.

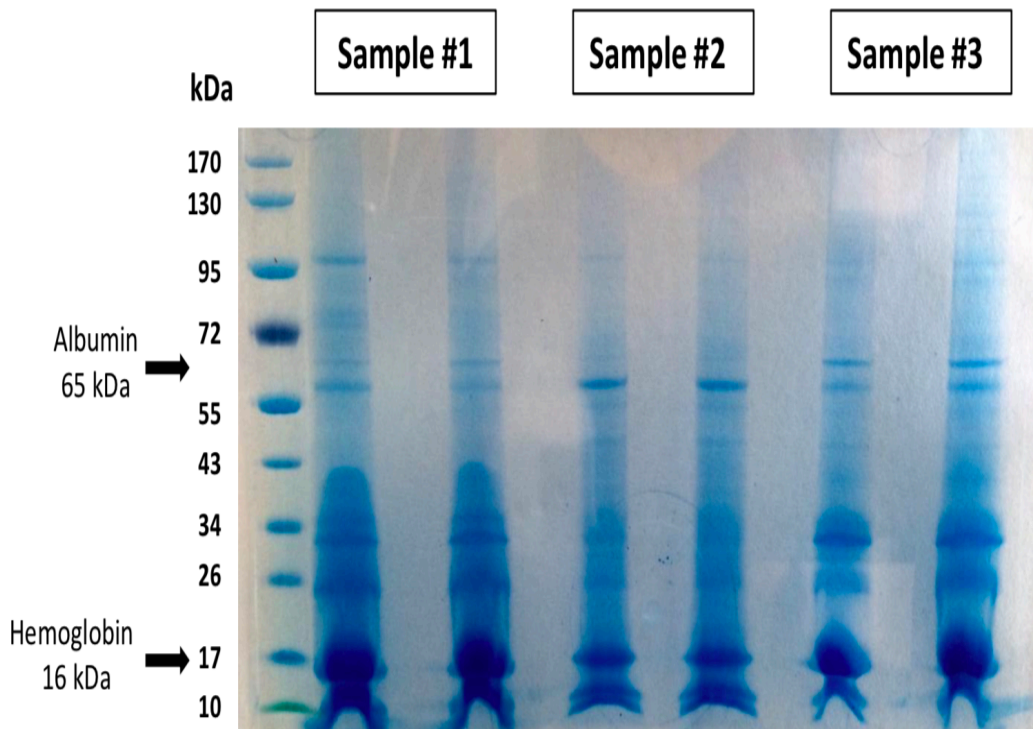


Figure 24: Coomasie-blue gels

A large band of Hemoglobin is present at the bottom of the gels

Finding the best Hemoglobin depletion protocol

Hemoglobin depletion kit

We next proceed by depleting the hemoglobin. We initially used the HemogloBind™ Hemoglobin Depletion Kit (reference H0145-05; Biotech Support Group, Monmouth Junction NJ, USA). Preparation consisted of 250 μ l of clot sample + 250 μ l Hemoglobin depletion. Stir 10 minutes at 4°C, centrifugation at 2min at 9000rpm, and supernatant recovery.

However, as depicted in Figure 25, this method led to a sample-dependent and variable protein depletion, negatively impacting proteins other than hemoglobin. In a volume of

2.25 μ L, the protein content was 20ug before and 1.12ug after depletion.

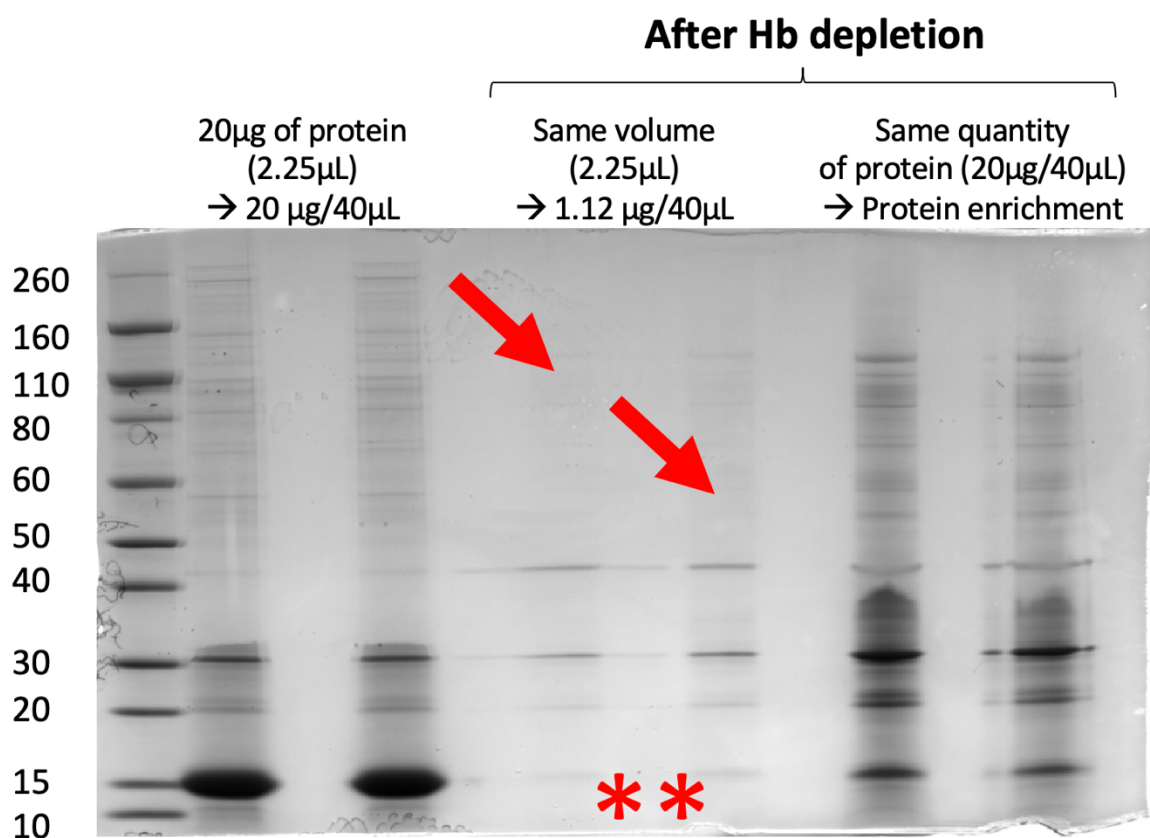


Figure 25: Gels obtained after using a Hemoglobin Depletion Kit

Red arrows indicate regions of the gel where proteins other than hemoglobin were depleted.

Excision of the hemoglobin band directly on the gel

We abandoned the depletion method, and clot samples were processed using a short gel migration to facilitate the excision of the Hemoglobin band and identify the proteins to be analyzed by MS/MS (Figure 26).

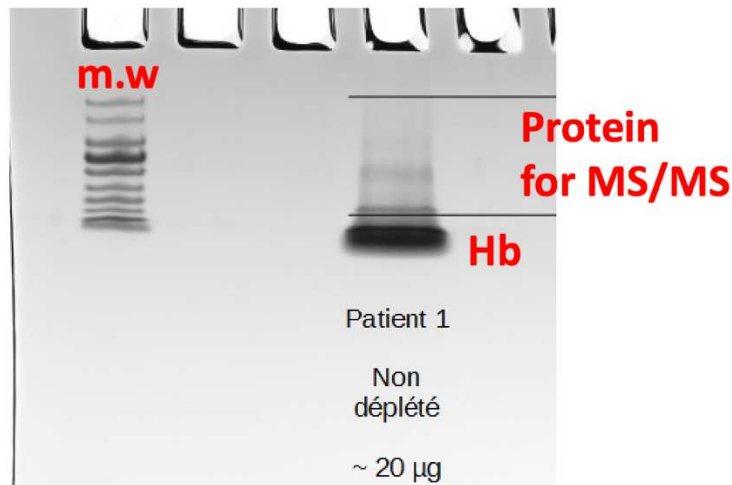


Figure 26: Illustration of manual excision of Hemoglobin band

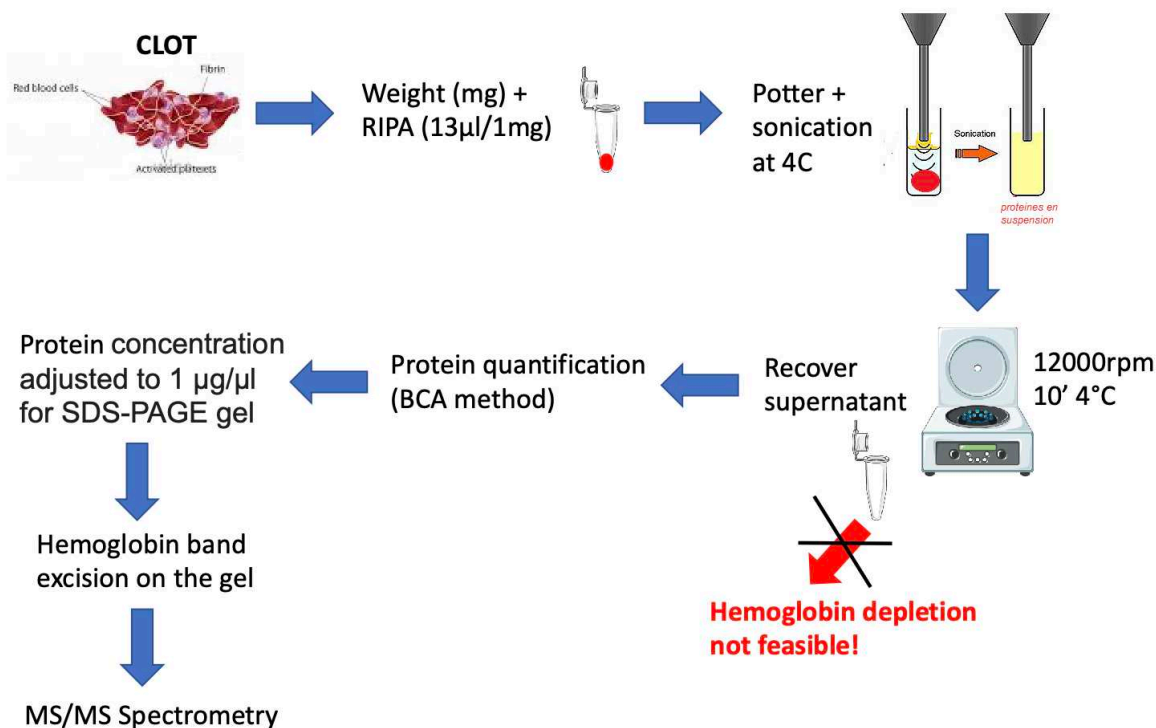


Figure 27: Final optimized protocol from clot retrieval to MS/MS Spectrometry

This optimized protocol (Figure 27) was subsequently used to prepare two samples for a preliminary proteomic run, with encouraging results: 605 and 683 proteins were found. 421 proteins were commonly detected (Figure 28). Hence, we established our standard protocol of thrombus protein extraction after that analysis (May 2018).

Total number of clot proteins identified: 605 and 683

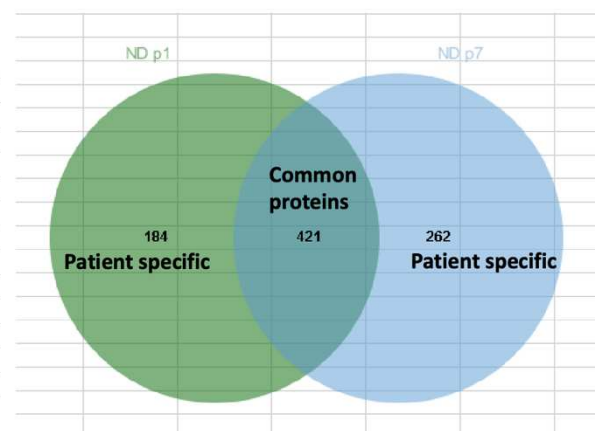
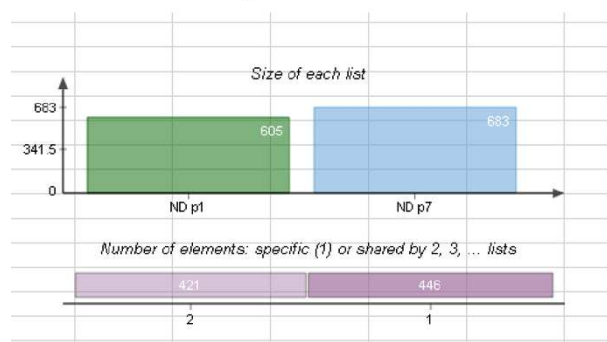


Figure 28: Feasibility study after hemoglobin depletion protocol

Optimized protocol applied on 2 samples showing 605 and 683 proteins.

Published article



Machine Learning Analysis of the Cerebrovascular Thrombi Proteome in Human Ischemic Stroke: An Exploratory Study

OPEN ACCESS

Edited by:

Bruce Campbell,
The University of Melbourne, Australia

Reviewed by:

Simon F. De Meyer,
KU Leuven, Belgium
Hidetoshi Kasuya,
Tokyo Women's Medical University

Medical Center East, Japan
Miriam Priglinger-Coorey,
Royal North Shore Hospital, Australia

*Correspondence:

Nicola Marchi
nicola.marchi@igf.cnrs.fr
Vincent Costalat
v-costalat@chu-montpellier.fr
Cyril Dargazanli
c-dargazanli@chu-montpellier.fr

[†]These authors have contributed
equally to this work

Specialty section:
This article was submitted to
Stroke,
a section of the journal
Frontiers in Neurology

Received: 23 June 2020
Accepted: 30 September 2020
Published: 05 November 2020

Citation:
Dargazanli C, Zub E, Deverdun J, Decourcelle M, de Bock F, Labreuche J, Lefèvre P-H, Gascou G, Derraz I, Riquelme Bareiro C, Cagnazzo F, Bonafé A, Marin P, Costalat V and Marchi N (2020) Machine Learning Analysis of the Cerebrovascular Thrombi Proteome in Human Ischemic Stroke: An Exploratory Study. *Front. Neurol.* 11:575376.
doi: 10.3389/fneur.2020.575376

Cyril Dargazanli^{1,2*}, Emma Zub¹, Jeremy Deverdun³, Mathilde Decourcelle⁴, Frédéric de Bock¹, Julien Labreuche⁵, Pierre-Henri Lefèvre², Grégory Gascou², Imad Derraz², Carlos Riquelme Bareiro², Federico Cagnazzo², Alain Bonafé², Philippe Marin¹, Vincent Costalat^{1,2*} and Nicola Marchi^{1,2†}

¹ Institut de Génomique Fonctionnelle, Univ Montpellier, UMR 5203 CNRS - U 1191 INSERM, Montpellier, France

² Diagnostic and Interventional Neuroradiology Department, Gui de Chauliac Hospital, Montpellier, France, ³ I2FH, Institut d'Imagerie Fonctionnelle Humaine, Gui de Chauliac Hospital, Montpellier, France, ⁴ BioCampus Montpellier, CNRS, INSERM, Université de Montpellier, Montpellier, France, ⁵ Santé Publique: Épidémiologie et Qualité des Soins, CHU Lille, University of Lille, Lille, France

Objective: Mechanical retrieval of thrombotic material from acute ischemic stroke patients provides a unique entry point for translational research investigations. Here, we resolved the proteomes of cardioembolic and atherothrombotic cerebrovascular human thrombi and applied an artificial intelligence routine to examine protein signatures between the two selected groups.

Methods: We specifically used $n = 32$ cardioembolic and $n = 28$ atherothrombotic diagnosed thrombi from patients suffering from acute stroke and treated by mechanical thrombectomy. Thrombi proteins were successfully separated by gel-electrophoresis. For each thrombi, peptide samples were analyzed by nano-flow liquid chromatography coupled to tandem mass spectrometry (nano-LC-MS/MS) to obtain specific proteomes. Relative protein quantification was performed using a label-free LFQ algorithm and all dataset were analyzed using a support-vector-machine (SVM) learning method. Data are available via ProteomeXchange with identifier PXD020398. Clinical data were also analyzed using SVM, alone or in combination with the proteomes.

Results: A total of 2,455 proteins were identified by nano-LC-MS/MS in the samples analyzed, with 438 proteins constantly detected in all samples. SVM analysis of LFQ proteomic data delivered combinations of three proteins achieving a maximum of 88.3% for correct classification of the cardioembolic and atherothrombotic samples in our cohort. The coagulation factor XIII appeared in all of the SVM protein trios, associating with cardioembolic thrombi. A combined SVM analysis of the LFQ proteome and clinical data did not deliver a better discriminatory score as compared to the proteome only.

Conclusion: Our results advance the portrayal of the human cerebrovascular thrombi proteome. The exploratory SVM analysis outlined sets of proteins for a proof-of-principle characterization of our cohort cardioembolic and atherothrombotic samples. The integrated analysis proposed herein could be further developed

and retested on a larger patients population to better understand stroke origin and the associated cerebrovascular pathophysiology.

Keywords: stroke, thrombus, cerebrovascular, mechanical thrombectomy, proteome, support vector machine learning, neuroradiology

INTRODUCTION

Stroke is a major public health burden and the second most common cause of death worldwide (1–3). Currently, the incomplete molecular understanding of stroke pathophysiology negatively impacts patients' management, follow-up, and secondary prevention (3, 4). A recent consensus indicates that examinations of patients' intracranial thrombi could help unveil novel disease mechanisms (5). Studying the intracranial thrombi composition could advance our knowledge of the molecular mechanisms of local cerebrovascular cell damage in this disease setting (6–9).

Mechanical thrombectomy (MT) is a standard of care for patients presenting with acute ischemic stroke (AIS) due to large vessel occlusion (LVO) (10). MT allows the retrieval of cerebral thrombi from brain arteries, enabling subsequent samples storage and analysis. A few studies have analyzed the histological composition of intracranial thrombi (11, 12), describing architecture or reporting the presence of fibrin and leucocytes (13). However, an in depth characterization of the thrombi molecular components is currently lacking (11).

Here, we performed a quantitative proteomic analysis of intracranial thrombi retrieved using MT from a cohort of $n = 32$ cardioembolic and $n = 28$ atherothrombotic diagnosed AIS patients. We resolved the thrombi proteomes for our cohort samples and next applied a support-vector machine (SVM) learning approach to estimate whether specific sets of proteins, alone or in combination with available clinical data, could help differentiate the cardioembolic from atherothrombotic origin in our selected population.

MATERIALS AND METHODS

Inclusion Criteria

Patients with suspected ischemic stroke secondary to an LVO were prospectively recruited at a high-volume, comprehensive stroke center in France. Patients were required to present imaging evidence of occlusion of the internal carotid artery (ICA, cervical or intracranial part), the M1 or M2 branches of the middle cerebral artery (MCA), the basilar artery, or a tandem atheromatous occlusion defined by the occlusion of both cervical carotid artery and intracranial artery (carotid artery or MCA). Use of intravenous thrombolysis (IVT) treatment was allowed and administrated according to current guidelines (10). Stroke cause was defined by a stroke neurologist blinded to the proteomics analysis, according to the TOAST (Trial of ORG 10172 in Acute Stroke Treatment) (14) classification, after an exhaustive in-hospital workup (15) including at least computed tomography and magnetic resonance imaging, duplex sonography of the cervical arteries, blood coagulation

tests, long-term electrocardiography, and transthoracic or transesophageal echocardiography. Stroke etiology was defined as "atherothrombotic tandem" when CT angiography and MR angiography demonstrated >50% stenosis or occlusion of the cervical carotid artery with associated intracranial ICA or MCA occlusion ipsilateral to the symptomatic hemisphere, in addition to exclusion of potential sources of cardiac embolism. Stroke etiology was defined as "cardioembolic" when at least one cardiac source for an embolus was identified after a complete cardiological work-up including Holter monitoring and echocardiography, in the absence of any stenosis of ipsilateral large extracranial arteries or atherosclerosis, excluding atrial fibrillation with non-cardioembolic strokes.

Exclusion criteria for the present study were: (1) failure of thrombus retrieval (failure of catheterization, patients with spontaneous reperfusion at the beginning of the procedure), (2) patients non-suitable for MT with a pre-stroke modified Rankin Scale (mRS) score of >3; (3) patients with non-atheromatous or non-cardioembolic tandem occlusions (intimal dysplasia/web, dissection), (4) patients having had MT but with a thromboembolic material unsuitable for proteomic analyses (mainly due to insufficient material amounts retrieved), (5) patients with no clear etiology or "undefined etiology" (defined as at least two possible etiologies found after a complete clinical, laboratory, and imaging work-up).

The study was approved by the local ethics committee, with the patients providing written informed consent in acute phase whenever possible. Otherwise, the consent form was signed by the patient's relatives.

Patient Characteristics

Patient demographics, vascular risk factors, imaging data, vital signs before treatment, severity of ischemic stroke, and clinical outcomes were collected with a structured questionnaire. Age, sex, cardiovascular risk factors (hypertension, dyslipidemia, diabetes mellitus, and smoking habits), time of symptom onset, National Institutes of Health Stroke Scale (NIHSS) at baseline, use of IVT, and its time from symptom onset were collected (see Table 1). The Alberta Stroke Program Early CT Score (ASPECT) on diffusion-weighted magnetic resonance or CT imaging was assessed by a neuroradiologist.

Endovascular Procedure

All patients were treated in a dedicated neuroangiography suite under general anesthesia or conscious sedation, after evaluation by the anesthesiology team.

Most of the procedures were performed using the Trevo[®] device (Stryker, Kalamazoo, Michigan) or the Solitaire FRTM device (Medtronic, Dublin, Ireland) via the femoral artery

TABLE 1 | Patients data, Treatment Characteristics, Complications, and Outcomes according to stroke etiology.

Characteristics	Cardioembolic (n = 32)	Atherothrombotic (n = 28)	P-Values
Age, years	79.5 (72.0–85.5)	67.5 (57.5–77.5)	0.005
Men	18/32 (56.3)	20/28 (71.4)	0.22
Medical history			
Hypertension	16/32 (50.0)	20/28 (71.4)	0.091
Diabetes	6/32 (18.8)	3/28 (10.7)	0.48
Hypercholesterolemia	10/32 (31.3)	8/28 (28.6)	0.82
Current smoking	6/32 (18.8)	10/28 (35.7)	0.14
Alcohol abuse	3/32 (9.4)	4/28 (14.3)	0.70
Coronary artery disease/Myocardial Infarction	5/32 (15.6)	3/28 (10.7)	0.71
Previous stroke or TIA	8/32 (25.0)	2/28 (7.1)	0.088
Cardiac failure	6/32 (18.8)	0/28 (0.0)	0.047
Coronary stent	1/32 (3.1)	1/28 (3.6)	NA
Coronary bypass	1/32 (3.1)	1/28 (3.6)	NA
Carotid endarterectomy	0/32 (0.0)	0/28 (0.0)	NA
Atrial fibrillation	20/32 (62.5)	1/28 (3.6)	<0.001
Previous antithrombotic medications	20/32 (62.5)	11/28 (39.3)	0.073
Aspirin	10/32 (31.3)	8/28 (28.6)	0.82
Clopidogrel	1/32 (3.1)	2/28 (14.3)	NA
Vitamin K Antagonist	7/32 (21.9)	0/28 (0.0)	0.0110
New oral anticoagulant	3/32 (9.4)	0/28 (0.0)	NA
Current stroke event			
Systolic blood pressure, mmHg	136 (111–151)	152 (139–170)	0.006
Diastolic blood pressure, mmHg	80 (65–90)	90 (76–96)	0.033
Heart rate	76 (64–90)	80 (70–96)	0.51
Weight, kg	71 (60–81)	79 (64–88)	0.18
Body Mass Index	24.4 (23.0–27.7)	26.0 (23.5–30.2)	0.23
Glycemia, mmol/L	6.8 (6.2–7.5)	6.8 (5.7–8.1)	0.77
NIHSS score	19 (10–24)	19 (14–23)	0.85
Pre-stroke mRS≥1	6/32 (18.8)	2/28 (7.1)	0.26
ASPECTS	8 (6–10)	8 (7–9)	0.84
Site of occlusion			
MCA (M1 or M2)	18/32 (56.3)	2/28 (7.1)	<0.001
Intracranial ICA	11/32 (34.4)	1/28 (3.6)	
Tandem	1/32 (3.1)	24/28 (85.7)	
Basilar artery	1/32 (3.1)	0/28 (0.0)	
Cervical ICA	1/32 (3.1)	1/28 (3.6)	
Complete blood count			
Hemoglobin	13.5 (12.4–14.9)	13.8 (12.8–14.7)	0.65
Platelets	203 (177–237)	250 (212–301)	0.011
White cells	8.9 (6.6–12.0)	10.3 (8.5–11.6)	0.15
Treatment characteristics			
Intravenous rt-PA	13/32 (40.6)	15/28 (53.6)	0.32
General anesthesia	9/32 (28.1)	15/28 (53.6)	0.45
Onset to groin puncture time, min	173 (147–327)	289 (184–693)	0.034
Onset to Intravenous rt-PA, min	130 (110–180)	130 (105–180)	0.58
Total number of passes	1 (1–2)	1 (1–2)	0.55
Reperfusion success	29/32 (90.6)	28/28 (100.0)	NA
Groin puncture to reperfusion, min	40 (31–59)	72 (50–97)	0.002
Adverse events			
Per-procedural complication	1/20 (5.0)	3/20 (15.0)	NA

(Continued)

TABLE 1 | Continued

Characteristics	Cardioembolic (n = 32)	Atherothrombotic (n = 28)	P-Values
Any ICH	12/32 (37.5)	11/28 (39.3)	0.89
PH or symptomatic ICH	0/32 (0.0)	0/28 (0.0)	NA
Functional outcome			
Favorable outcome (mRS 0–2)	10/32 (31)	14/28 (50)	0.14

Values expressed as no/total no. (%), or median (interquartile range).

ASPECTS, Alberta stroke program early computed tomography score; CT, computed tomography; ICA, internal carotid artery; ICH, Intracranial hemorrhage; MCA, middle cerebral artery; mRS, modified Rankin scale; NIHSS, national institutes of health stroke scale; PH, parenchyma hematoma; rt-PA, recombinant tissue plasminogen activator; TIA, transient ischemic attack.

approach. A balloon catheter was positioned in the ICA to allow flow arrest during thrombus retrieval. The stent retriever was delivered through a microcatheter and deployed across the thrombus. A distal aspiration during the stent retrieval was performed, according to the SAVE technique (16). A control angiogram was obtained to assess recanalization and reperfusion. This sequence was repeated until mTICI 2b or mTICI 2C/3 flow (defined as successful reperfusion) was established (17). The “retrograde approach” (also known as the distal-to-proximal or intracranial-first approach), aiming to recanalize the distal and symptomatic intracranial occlusion before addressing the cervical carotid lesion, was generally chosen for tandem occlusions. The interventional neuroradiologist used another thrombectomy device in the case of reperfusion failure (mTICI <2b) with the first stent retriever. Reperfusion results were reported by using the mTICI score (18). Peri-procedural complications [embolization in a new territory (defined as an angiographic occlusion in a previously unaffected vascular territory observed on the angiogram after clot removal), arterial dissection or perforation, vasospasm, and subarachnoid hemorrhage] were recorded.

Follow-Up and Outcome

All patients underwent cross-sectional imaging (computed tomography or magnetic resonance imaging) within a range of 18–24 h after the procedure. Intracranial hemorrhage was classified according to the ECASS (European Cooperative Acute Stroke Study) criteria (19). Symptomatic intracranial hemorrhage was defined as any intracerebral hemorrhage with an increase of at least four NIHSS points within 24 h, or resulting in death. The mRS at 90 days was assessed by trained research nurses unaware of the study group assignments, during face-to-face interviews, or via telephone conversations with the patients, their relatives, or their general practitioners.

Collection and Processing of Intracranial Thrombi

In the angiography room, after retrieval (Figure 1E), thrombi were immediately frozen at -80°C in a dedicated transportable azote freezer (Voyager, Air Liquide). In the laboratory, samples were prepared for mass spectrometry analysis. After initial mashing in a glass potter at 4°C in RIPA buffer, thrombi were further dissolved using an ultrasonic liquid processor (10 applications of 1 second each at 4°C ; Vibra-cell VCX130PB,

VWR) and then centrifuged (Eppendorf 5427R) at 1,200 RPM for 10 min at 4°C . Protein concentration was assessed by a bicinchoninic acid (BCA) assay. Protein extracts (20 μg) were separated by SDS-PAGE using a short (2 cm) migration. Single pieces of gel including separated proteins except hemoglobin were excised for each sample and proteins were digested in-gel using Trypsin (Trypsin Gold, Promega), as previously described (20).

Mass Spectrometry

The resulting peptide samples were analyzed online using Q-Exactive HF mass spectrometer coupled with an Ultimate 3000 RSLC (Thermo Fisher Scientific) fitted with a stainless-steel emitter (Thermo Fisher Scientific). Desalting and pre-concentration of samples were performed online on a Pepmap® pre-column (0.3 mm \times 10 mm, Thermo Fisher Scientific). A gradient consisting of 2–40% of buffer B in 123 min, then 90% of buffer B during 5 min (A: 0.1% formic acid in water; B: 0.1% formic acid 80% ACN) at 300 nL/min was used to elute peptides from the capillary reverse-phase column (0.075 mm \times 500 mm, Pepmap® C18, Thermo Fisher Scientific). Spectra were acquired with Xcalibur software (v4.1 Thermo Fisher Scientific). MS/MS analyses were performed in a data-dependent mode with standard settings. MS data analysis was performed using the MaxQuant software with default settings (v1.5.5.1) (21). All MS/MS spectra were searched using the Andromeda search engine (22) against the UniProtKB Reference proteome UP000005640 database for Homo sapiens (release 2019_03, <https://www.uniprot.org/>) and the contaminant database in MaxQuant. Default search parameters were applied. Oxidation (Met) and Acetylation (N-term) were used as variable modifications and Carbamidomethyl (Cys) was used as fixed modification. FDR was set to 1% for peptides and proteins. A representative protein ID in each protein group was automatically selected using an in-house bioinformatics tool (Leading v3.2). First, proteins with the most numerous identified peptides were isolated in a “match group” (proteins from the “Protein IDs” column with the maximum number of “peptides counts”). For the match groups where more than one protein ID were present after filtering, the best annotated protein in UniProtKB [reviewed entries rather than automatic ones, highest evidence for protein existence, most annotated protein according to the number of Gene Ontology Annotations (UniProtKB-GOA, made on 20190416)]

was defined as the “leading” protein. Graphical representation and statistical analysis of MS/MS data were performed using Perseus (v1.6.1.1). Label-free quantification (MaxQuant LFQ) was used to highlight proteins differentially expressed between samples (23).

The mass spectrometry proteomics data have been uploaded to the ProteomeXchange Consortium via the PRIDE partner repository with the dataset identifier PXD020398 (24).

Data Analysis

Descriptive Analysis

Data in **Table 1** are presented as median (range) for quantitative variables, and percentage (count) for categorical variables. Baseline and treatment characteristics, complications and outcomes were compared according to stroke etiology using Chi-Square or Fisher’s exact tests for categorical variables and the Mann-Whitney *U*-test for quantitative variables. No statistical comparisons were done for categorical variables with frequency <5. Statistical testing was done at the 2-tailed α level of 0.05. Data were analyzed using the SAS package, release 9.4 (SAS Institute, Cary, NC).

A support-vector machine (SVM) approach was implemented using MATLAB (r2018a, MathWorks, Natick, MA, USA). The SVM algorithm analyzes and learns from the dataset (**Supplementary Table 2**) to identify the hyperplanes for the best segregation of data according to a known discriminatory characteristic (25). In our work, the relatively small sample size prevents from achieving a correct validation step and SVM was used as a statistical tool to examine whether hyperplanes exist splitting our two groups. Here, we specifically tested whether samples segregation is attainable using combinations of up to 3 proteins (trios) from those commonly detected in all samples. Each possible combinations of three proteins from the data set in **Supplementary Table 2** was tested ($n = 13,908,836$), the corresponding X/Y/Z hyperplanes were defined by the SVM (see **Figure 3A**), and the percentage of correct sample classification was obtained. The protein combinations achieving the best discriminatory score for our populations were retained. SVM analysis was also performed using clinical data in **Table 1**.

RESULTS

Clinical Data, Peripheral Blood and Thrombi Characteristics

Baseline clinical data, treatment characteristics, early complications and outcomes are provided in **Table 1**. In the selected population, subjects suffering from atherothrombotic stroke were younger (67.5 vs. 79.5 years old, $p = 0.005$), presented no cardiac failure (0 vs. 18.8%, $p = 0.047$), no significant atrial fibrillation (3.6 vs. 62.5%, $p < 0.001$), and displayed higher systolic and diastolic blood pressure at admission (152 and 90 mmHg vs. 136 and 80 mmHg, $p = 0.006$ and 0.033). M1 occlusions were more frequent in the cardioembolic group (56.3 vs. 7.1%, $p < 0.001$). Groin puncture to reperfusion time was longer in the atherothrombotic group, which included 85.7% of tandem occlusions (72 vs. 40 min., $p = 0.002$). Complete blood count at admission indicated that platelet levels were higher

in the atherothrombotic group ($250 \times 10^9/\text{L}$ vs. $203 \times 10^9/\text{L}$, $p = 0.011$; **Table 1**). Weight of the retrieved thrombi was 31.2 mg for the cardioembolic group (range 5.8–206.2 mg) and 36 mg for the atherothrombotic group (range 3.2–136.2; $p = 0.85$). Total protein concentrations were $11.20 \mu\text{g}/\mu\text{l}$ (5.3–22.1) and $11.1 \mu\text{g}/\mu\text{l}$ (4–26.5; $p = 0.82$) for the cardioembolic and atherothrombotic groups, respectively.

Analysis of the Intracranial Human Thrombi Proteome

All thrombus samples were individually processed by SDS-page chromatography and the hemoglobin band excised (**Figures 1 A–F**). Mass spectrometry analysis identified a total of 2,455 proteins in the samples analyzed. The complete list of all proteins detected in each sample is provided in **Supplementary Table 1**. A total of 438 proteins were commonly present in all the samples analyzed (**Supplementary Table 2**). Analysis of ClueGO annotations of the thrombi proteome, according to UniProtKB or EBI GOA databases, showed protein clusters for key biological pathways including metabolic processes, cytokines production, and cell proliferation, activation, or motility (**Figure 2A**). Indicating an inflammatory track are proteins associated with leukocytes activation, migration, and cell adhesion (**Figure 2B; high definition zoom-in**). This dataset constitutes the largest human thrombus proteome available and a shared library for the investigation of the molecular mechanisms of thrombus formation and ischemic stroke pathophysiology.

Exploring the Use of Support-Vector-Machine Learning to Analyse the Thrombi Proteome

The proteomic LFQ data obtained from our samples cohort were analyzed using a SVM routine to mathematically examine potential signatures existing between the cardioembolic and atherothrombotic proteomes. The SVM algorithm does not handle missing data across samples and the analysis was performed using the proteins commonly detected in all thrombi (438 proteins; **Supplementary Table 2**). In our SVM study we specifically aimed at identifying small set of discriminatory elements, here up to 3 proteins (see Methods). As a result, proteins trios were found by SVM providing a 88.3% accuracy of correct classification of our two sample groups. Proteins and their biological functions are detailed in **Table 2**. Factor XIII, which catalyzes the last step of the coagulation cascade by crosslinking fibrin fibers, was present in all combinations. **Figure 3A** shows an illustration of the SVM hyperplane classification for the cardioembolic and atherothrombotic samples according to the protein trio Eukaryotic translation initiation factor 2 subunit 3, Ras GTPase-activating-like protein IQGAP2, and Coagulation factor XIII. Using this specific setting, four and three patients were misclassified (light green squares in **Figure 3A**) as cardioembolic and atherothrombotic, respectively. In univariate analysis (Wilcoxon test), the coagulation Factor XIII, the Eukaryotic translation initiation factor 2 subunit 3, and the Myosin light chain kinase levels were significantly

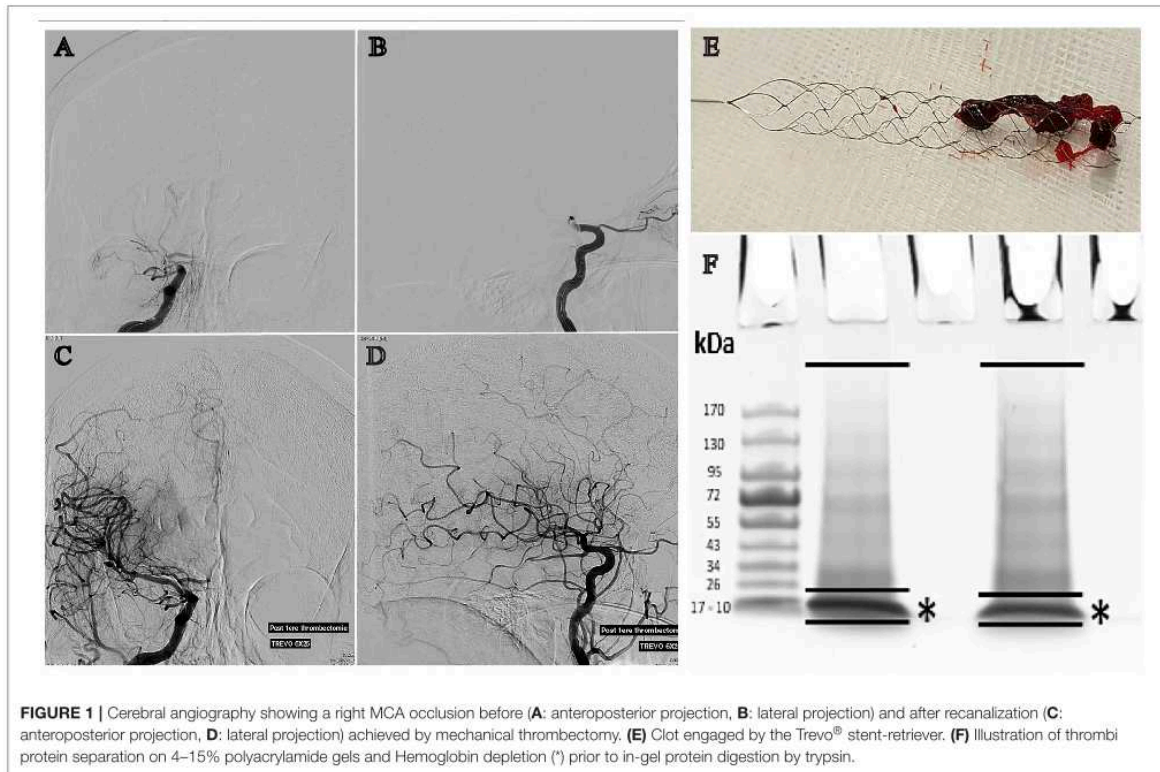


FIGURE 1 | Cerebral angiography showing a right MCA occlusion before (**A**: anteroposterior projection, **B**: lateral projection) and after recanalization (**C**: anteroposterior projection, **D**: lateral projection) achieved by mechanical thrombectomy. (**E**) Clot engaged by the Trevo® stent-retriever. (**F**) Illustration of thrombi protein separation on 4–15% polyacrylamide gels and Hemoglobin depletion (*) prior to in-gel protein digestion by trypsin.

different between the cardioembolic and atherothrombotic groups, with respective *p*-values of 0.002, 0.04, and 0.01 (see Table 2). These results have a dual value, suggesting potential molecular differences between cardioembolic and atherothrombotic thrombi while supporting the notion of protein biomarkers to understand clot origin.

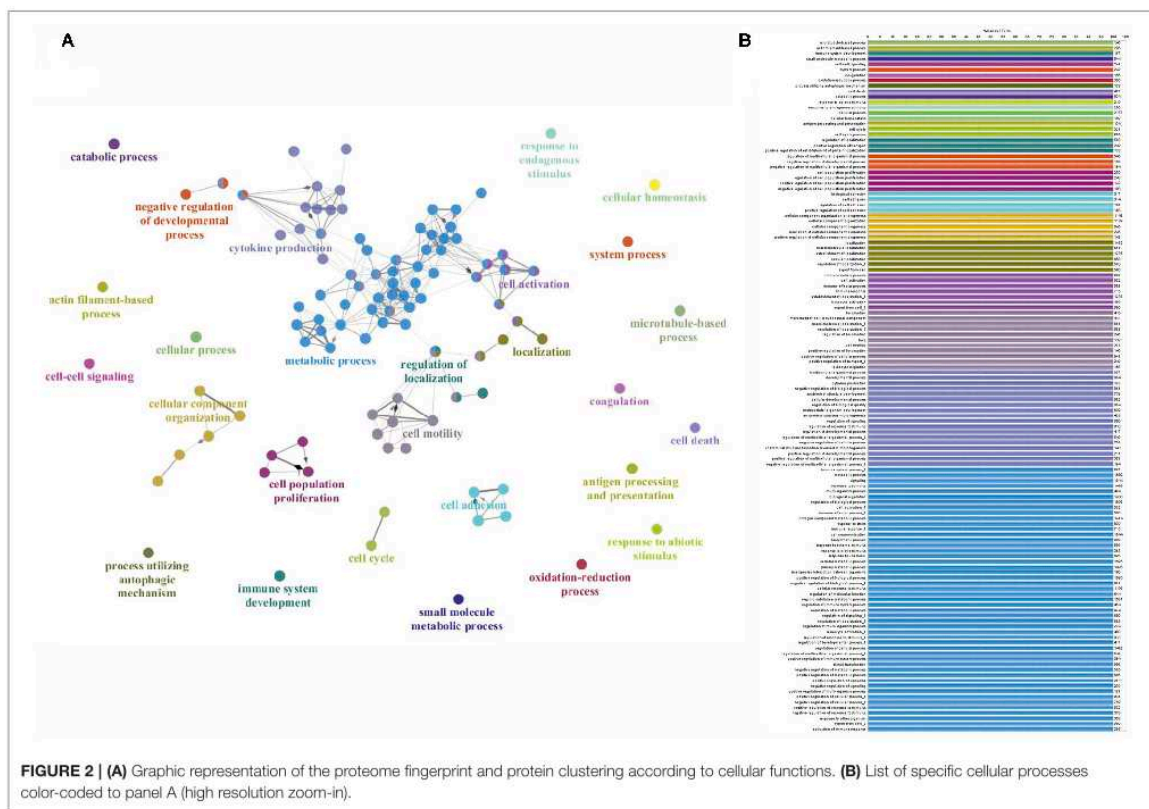
Integrating SVM Analyses of Clinical Data and Thrombi Proteome

In an attempt to identify additional SVM differentiation factors, we performed an analysis using patients clinical data (Table 1; age, sex, history of cardiac failure or atrial fibrillation, previous antithrombotic medication, glycemia, weight and BMI, thrombus weight and global protein concentration, hemoglobin, leucocytes, and platelet rate). SVM identified history of cardiac failure and atrial fibrillation as variables differentiating the two population with an 81.36% accuracy. This result is obvious considering our study design and because history of cardiac failure was used as one of the criteria to diagnose etiology at enrollement (see Methods). Cardiac failure and atrial fibrillation are two known risk factors linked to cardioembolic stroke (3). Interestingly, when atrial fibrillation was excluded from the SVM analysis, patient age and thrombus protein concentration provided a differentiation level of 74.58% within our sample cohorts. The latter results

indicate thrombus total protein concentration as a new SVM analytical variable. Addition of a third variable did not improve the SVM score (*not shown*). We do acknowledge that combining the protein trio 1 (see Table 2), history of cardiac failure, and protein concentration we obtained a SVM score of 96.6%.

Testing Proteome Using LFQ Statistics

The selected SVM method tests all combinations of three inter-dependent proteins, obtaining solutions for data clusterization that are not executable using LFQ and standard statistics (26). Thus, a Student's *T*-test (Perseus algorithms) analysis on the proteins (log2 transformed) detected in all samples did not deliver significant difference between the studied cardioembolic and atherothrombotic populations. Furthermore, we applied a conventional method where proteomes (Supplementary Table 1) are filtered to include proteins with at least 50% of valid LFQ values. By using this approach, Student's *t*-test identified four proteins (PHB, SLC25A11, ATP5A1, and APOE; see Table 3) that display an abundance in cardioembolic as compared to atherothrombotic thrombi (volcano plot in Figure 3B). However, LFQ *T*-test difference was low (*x*-axis = -1.2; red dots in Figure 3B) with the crucial caveat that, because of method design, these proteins were undetectable in an elevated number of



samples (**Supplementary Table 1**), therefore impeding group discrimination. These results support the relevance and the efficiency of SVM to analyze the proteome thrombi dataset in our experimental settings.

DISCUSSION

Our study advances the knowledge of the human cerebrovascular thrombi composition by delivering the largest proteome dataset available to date. We focused on the proteomic analysis of cardioembolic and atherothrombotic thrombi and we applied a support-vector machine learning routine in an exploratory, proof-of-concept, attempt to identify protein candidates segregating the two selected populations. Our research supports the general notion that direct analysis of the thrombi material could unveil, in the future, new disease players and candidate biomarkers potentially aiding stroke diagnosis. The SVM method used herein was set to identify combinations of protein trios (**Table 2**) in the intracranial thrombi, and it allowed for an 88.3% correct classification of our selected cardioembolic and atherothrombotic populations (**Table 1**). We here underscore that histological, cellular (e.g., red blood cells, platelets, white blood cells), and molecular (omics) analyses

should be all integrated to obtain a complete and multi-level depiction of the thrombi structure and biology.

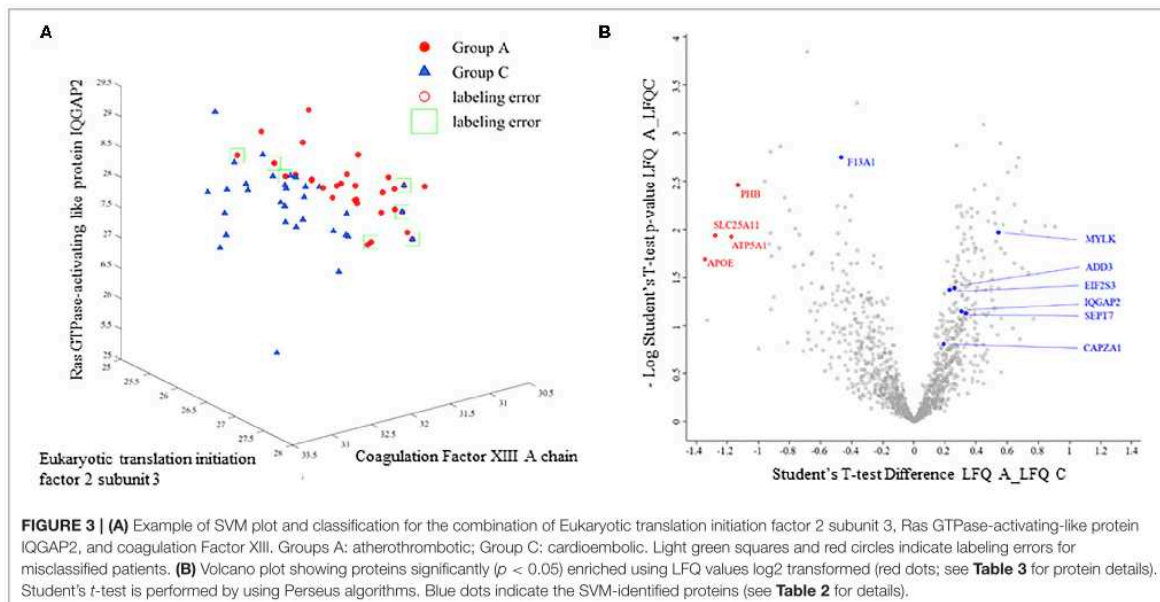
Understanding the composition of the human clot was previously attempted in two studies, although limited in sample size or lacking SVM analysis (12, 27). A first proteomic investigation correlated 2 inflammation-associated proteins (integrin alpha-M and mitochondrial superoxide dismutase) to high blood LDL (27). Mitochondrial superoxide dismutase was previously associated to unstable carotid plaques (28). These proteins were detected in our study, although without significant differences between cardioembolic and atherothrombotic thrombi. A second study analyzed 4 thrombi, with ~1,600 proteins identified (12). An earlier investigation, focused on human coronary thrombi in patients with ST-segment elevation in acute myocardial infarction, identified 708 proteins. The implication of platelet activation during the formation of thrombus causing acute coronary syndrome was suggested (29).

Combining Mass-Spectrometry With SVM Analysis: Initial Feasibility and Proposed Applicability to Human Ischemic Stroke

An innovative aspect of the presented study is the methodological combination of large-scale proteomic tools and machine learning

TABLE 2 | SVM protein trios allowing 88.3% accuracy of correct classification of cardioembolic and atherothrombotic thrombi.

Trio combinations	Proteins	Protein function (40)	Univariate p-value (bilateral Wilcoxon rank sum test)
1	<ul style="list-style-type: none"> Coagulation factor XIII Eukaryotic translation initiation factor 2 subunit 3 Ras GTPase-activating-like protein IQGAP2 	<p>Catalyzes the last step of the coagulation cascade by crosslinking fibrin fibers</p> <p>Involved in the early steps of protein synthesis</p> <p>Binds to activated CDC42 and RAC1. Associates with calmodulin</p>	0.0022 0.0439 0.1326
2	<ul style="list-style-type: none"> Coagulation factor XIII F-actin-capping protein Myosin light chain kinase 	<p>Catalyzes the last step of the coagulation cascade by crosslinking fibrin fibers</p> <p>Binds to the fast-growing ends of actin filaments in a Ca^{2+} independent manner</p> <p>Calcium/calmodulin-dependent kinase implicated in smooth muscle contraction via phosphorylation of myosin light chains</p>	0.0022 0.1752 0.0142
3	<ul style="list-style-type: none"> Coagulation factor XIII Septin-7 Gamma-adducin 	<p>Catalyzes the last step of the coagulation cascade by crosslinking fibrin fibers</p> <p>Filament-forming cytoskeletal GTPase. Required for normal organization of the actin cytoskeleton</p> <p>Membrane-cytoskeleton-associated protein that promotes the assembly of the spectrin-actin network</p>	0.0022 0.1897 0.0589



models or algorithms to define and potentially categorize the thrombi proteomes (3). In our patients' cohort, the fibrin stabilizing or coagulation Factor XIII (FXIII) was identified by SVM as one potential differentiating element between the cardioembolic and atherothrombotic thrombi analyzed (Table 2). FXIII is a key enzyme in the coagulation cascade that allows the cross-linking of fibrin chains with subsequent increase of mechanical clot strength and resistance to fibrinolysis (30).

FXIII was also reported in embolized thrombi from the cardiac left atrial appendage in atrial fibrillation patients (31).

Interestingly, it has been recently shown that FXIII levels are higher after myocardial injury and that FXIII harbors an important role in cardiac healing and remodeling (32). Moreover, valine-to-leucine (V34L) single-nucleotide polymorphism (SNP), which is associated with higher levels of FXIIIa, appears to be associated with a lower risk of pathological thrombosis in

TABLE 3 | LFQ (log₂ transformed) of single proteins enriched in cardioembolic as compared to atherothrombotic thrombi.

Gene	Uniprot Identification (40)	Protein name	Main known protein function (40)	Subcellular Location	Student's T-test Difference	-log P-value
					Log2 LFQ intensity Atheroma_Log2 LFQ intensity Cardioembolic	
SLC25A11	Q02978	Mitochondrial 2-oxoglutarate/malate carrier protein	Catalyzes the transport of 2-oxoglutarate at mitochondrial membrane	Mitochondrion	-1.278498	1.94
APOE	P02649	Apolipoprotein E	Lipid transport between organs via the plasma and interstitial fluids	Extracellular	-1.34310437	1.69
PHB	P35232	Prohibitin	Inhibits DNA synthesis	Mitochondrion	-1.1333107	2.46
ATP5A1	P25705	ATP synthase subunit alpha	Produces ATP from ADP	Mitochondrion, plasma membrane	-1.1749357	1.93

ischemic heart disease (33, 34). Importantly, atrial fibrillation or atrial cardiopathies that share a common mechanism of thrombus formation in the left atrial appendage should be identified as soon as possible after stroke occurrence to initiate anticoagulation therapy (35). Our SVM learning analysis also identified proteins involved in the cellular cytoskeleton assembly (**Table 2**), namely the myosin light chain kinase and F-actin-capping protein. In general, the large scale proteomic analysis of human clots here executed discloses pathways and molecular players of clot-endothelium interplay and local inflammation related to cerebrovascular damage (**Figure 2**). The latter is important because cerebrovascular breakdown contributes to the development of central nervous system disease (6–8, 36), in this case potentially enabling post-stroke sequelae.

Study Limitations and Prospectives

To further explore the utility of the protein candidates here discovered (**Table 2**) a validation step using an independent, and larger sample population will be necessary to define reproducibility and accuracy parameters (e.g., sensitivity, specificity, positive ad negative predictive values). Our SVM analysis, due to a relatively small sample size, only allowed accuracy estimation. A compelling question is whether our integrated proteomic-SVM method could be next used to examine specific signatures in case of cryptogenic stroke. We are aware that the proteins here identified may be not helpful in a population of cryptogenic stroke that includes etiologies other than the two studied here. We are aware that an efficient transition from SVM proteome analysis to clinical laboratory tools (e.g., Elisa) could be challenging and time consuming. (12, 27). The latter will be possible only when definitive molecular candidate(s) will be confirmed in larger populations with results replicated across stroke centers. Nevertheless, our study provide a proof of principle model that could be further developed and applied. Our proteome results (**Supplementary Tables 1, 2**) are shared and available to be re-analyzed using more advanced or alternative SVM methods.

We here recognize that the cohort used in the present study is heterogeneous in respect to age and blood platelet levels. Although blood platelet levels have been associated to stroke

outcome (37), it is unknown whether a correlation with stroke etiology exists. One study showed that high platelet content of intracranial thrombi associates with large artery atherosclerosis. However, the authors did not study the correlation between blood platelet content and stroke cause (38). Another possible limitation of our approach concerns the retrieved material that may not represent the entire thrombus, although the analyses presented here were performed on the largest portion of clots retrieved at one pass of the thrombectomy device. IVT may also alter the samples, although this effect is likely to be limited due to the short time between IVT and thrombus extraction and processing. Finally, pre-stroke antithrombotic therapy may alter thrombus proteome composition (39).

Conclusions

In summary, quantitative proteomics and SVM analysis can be feasibly combined to examine the variation of intracranial human thrombi proteomes. If further developed and tested on larger cohorts, these methods have the potential to discover precise and novel pathophysiological players and biomarkers, with the ideal goal of aiding cerebrovascular stroke diagnosis and secondary prevention.

DATA AVAILABILITY STATEMENT

The mass spectrometry proteomics data have been deposited to the ProteomeXchange Consortium via the PRIDE [1] partner repository with the dataset identifier PXD020398.

ETHICS STATEMENT

The studies involving human participants were reviewed and approved by Comité de Protection des Personnes «Sud-Méditerranée IV», Centre Hospitalier Universitaire de Montpellier, hôpital Saint-Eloi, 34295 Montpellier Cedex 5. The patients/participants provided their written informed consent to participate in this study.

AUTHOR CONTRIBUTIONS

CD, JD, PM, VC, and NM: conception and design of the study, analysis of data, and drafting of the manuscript. EZ, MD, FB, and JL: acquisition and analysis of data, drafting of the manuscript, and figures. PH-L, GG, ID, CR, FC, and AB: acquisition of data. CD and VC: emergency surgery interventions, samples collection and patients' approval. All authors contributed to the article and approved the submitted version.

FUNDING

Funds from Stryker Neurovascular were used to performed this study. Stryker was not involved in study design, monitoring, data collection, statistical analysis or interpretation of results.

REFERENCES

- Amarenco P, Bogousslavsky J, Caplan LR, Donnan GA, Hennerici MG. Classification of stroke subtypes. *Cerebrovasc Dis Basel Switz.* (2009) 27:493–501. doi: 10.1159/000210432
- Ornello R, Degan D, Tiseo C, Carmine CD, Perciballi L, Pistoia F, et al. Distribution and temporal trends from 1993 to 2015 of ischemic stroke subtypes: a systematic review and meta-analysis. *Stroke.* (2018) 49:814–9. doi: 10.1161/STROKEAHA.117.020031
- Yaghi S, Bernstein RA, Passman R, Okin PM, Furie KL. Cryptogenic stroke: research and practice. *Circ Res.* (2017) 120:527–40. doi: 10.1161/CIRCRESAHA.116.308447
- Jickling GC, Sharp FR. Biomarker panels in ischemic stroke. *Stroke J Cereb Circ.* (2015) 46:915–20. doi: 10.1161/STROKEAHA.114.005604
- De Meyer SF, Andersson T, Baxter B, Bendszus M, Brouwer P, Brinjikji W, et al. Analyses of thrombi in acute ischemic stroke: a consensus statement on current knowledge and future directions. *Int J Stroke.* (2017) 12:606–14. doi: 10.1177/1747493017709671
- Sweeney MD, Zhao Z, Montagne A, Nelson AR, Zlokovic BV. Blood-brain barrier: from physiology to disease and back. *Physiol Rev.* (2019) 99:21–78. doi: 10.1152/physrev.00050.2017
- Librizzi L, de Cutio M, Janigro D, Runtz L, de Bock F, Barbier EL, et al. Cerebrovascular heterogeneity and neuronal excitability. *Neurosci Lett.* (2018) 667:75–83. doi: 10.1016/j.neulet.2017.01.013
- Giannoni P, Baudat J, Dargazanli C, De Maudave AF, Klement W, Costalat V, et al. The pericyte-glia interface at the blood-brain barrier. *Clin Sci Lond Engl* (1979). (2018) 132:361–74. doi: 10.1042/CS20171634
- Nation DA, Sweeney MD, Montagne A, Sagare AP, D’Orazio LM, Pachicano M, et al. Blood-brain barrier breakdown is an early biomarker of human cognitive dysfunction. *Nat Med.* (2019) 25:270–6. doi: 10.1038/s41591-018-0297-y
- Furie KL, Jayaraman MV. 2018 guidelines for the early management of patients with acute ischemic stroke. *Stroke.* (2018) 49:509–10. doi: 10.1161/STROKEAHA.118.020176
- Brinjikji W, Duffy S, Burrows A, Hacke W, Liebeskind D, Majoi CB, et al. Correlation of imaging and histopathology of thrombi in acute ischemic stroke with etiology and outcome: a systematic review. *J NeuroInterventional Surg.* (2017) 9:529–34. doi: 10.1136/neurintsurg-2016-012391
- Muñoz R, Santamaría E, Rubio I, Ausín K, Ostolaza A, Labarga A, et al. Mass spectrometry-based proteomic profiling of thrombotic material obtained by endovascular thrombectomy in patients with ischemic stroke. *Int J Mol Sci.* (2018) 19:498. doi: 10.3390/ijms19020498
- Dargazanli C, Rigau V, Omer E. High CD3+ cells in intracranial thrombi represent a biomarker of atherothrombotic stroke. *PLoS ONE.* (2016) 11:e0154945. doi: 10.1371/journal.pone.0154945
- Adams HP, Bendixen BH, Kappelle LJ, Biller J, Love BB, Gordon DL, et al. Classification of subtype of acute ischemic stroke. Definitions for use in a multicenter clinical trial. TOAST. trial of org 10172 in acute stroke treatment. *Stroke.* (1993) 24:35–41. doi: 10.1161/01.STR.24.1.35
- McMahon NE, Bangie M, Benedetto V, Bray EP, Georgiou RF, Gibson JME, et al. Etiologic Workup in Cases of Cryptogenic Stroke. *Stroke.* (2020) 51:1419–27. doi: 10.1161/STROKEAHA.119.027123
- Maus V, Behme D, Kabbsch C, Borggrefe J, Tsogkas I, Nikoubashman O, et al. Maximizing first-pass complete reperfusion with save. *Clin Neuroradiol.* (2018) 28:327–38. doi: 10.1007/s00062-017-0566-z
- Dargazanli C, Fahed R, Blanc R, Gory B, Labreuche J, Duhamel A, et al. Modified thrombolysis in cerebral infarction 2c/thrombolysis in cerebral infarction 3 reperfusion should be the aim of mechanical thrombectomy: insights from the aster trial (contact aspiration versus stent retriever for successful revascularization). *Stroke.* (2018) 49:1189–96. doi: 10.1161/STROKEAHA.118.020700
- Fugate JE, Klunder AM, Kallmes DF. What is meant by “tici”? *Am J Neuroradiol.* (2013) 34:1792–7. doi: 10.3174/ajnr.A3496
- Hacke W, Kaste M, Fieschi C, Toni D, Lesaffre E, von Kummer R, et al. Intravenous thrombolysis with recombinant tissue plasminogen activator for acute hemispheric stroke. The European cooperative acute stroke study (ECASS). *JAMA.* (1995) 274:1017–25. doi: 10.1001/jama.1995.03530130023023
- Shevchenko A, Tomas H, Havlis J, Olsen JV, Mann M. In-gel digestion for mass spectrometric characterization of proteins and proteomes. *Nat Protoc.* (2006) 1:2856–60. doi: 10.1038/nprot.2006.468
- Cox J, Mann M. MaxQuant enables high peptide identification rates, individualized p.p.b.-range mass accuracies and proteome-wide protein quantification. *Nat Biotechnol.* (2008) 26:1367–72. doi: 10.1038/nbt.1511
- Cox J, Neuhauser N, Michalski A, Scheltema RA, Olsen JV, Mann M. Andromeda: a peptide search engine integrated into the MaxQuant environment. *J Proteome Res.* (2011) 10:1794–805. doi: 10.1021/pr101065j
- Tyanova S, Temu T, Sinitcyn P, Carlson A, Hein MY, Geiger T, et al. The perseus computational platform for comprehensive analysis of (proteo)omics data. *Nat Methods.* (2016) 13:731–40. doi: 10.1038/nmeth.3901
- Perez-Riverol Y, Csordas A, Bai J, Bernal-Llinares M, Hewapathirana S, Kundu DJ, et al. The PRIDE database and related tools and resources in 2019: improving support for quantification data. *Nucleic Acids Res.* (2019) 47:D442–50. doi: 10.1093/nar/gky1106
- Gholami R, Fakhari N. Support vector machine: principles, parameters, applications. In: Samui P, Sekhar S, Balas VE, editors. *Handbook of Neural Computation.* Academic Press (2017). p. 515–35. doi: 10.1016/B978-0-12-811318-9.00027-2
- Tyanova S, Albrechtsen R, Kronqvist P, Cox J, Mann M, Geiger T. Proteomic maps of breast cancer subtypes. *Nat Commun.* (2016) 7:10259. doi: 10.1038/ncomms10259

ACKNOWLEDGMENTS

Mass spectrometry experiments were carried out using facilities of the Functional Proteomics Platform of the Proteomics Pole of Montpellier. We would like to thank Leonie Runtz for initial testing. We also thank Marine Blaquierre (IGF) for her technical involvement.

SUPPLEMENTARY MATERIAL

The Supplementary Material for this article can be found online at: <https://www.frontiersin.org/articles/10.3389/fneur.2020.575376/full#supplementary-material>

Supplementary Table 1 | Complete list of proteins and mass-spectrometry data for each sample.

Supplementary Table 2 | List of proteins commonly present in all samples.

27. Rao NM, Capri J, Cohn W, Abdaljaleel M, Restrepo L, Gornbein JA, et al. Peptide composition of stroke causing emboli correlate with serum markers of atherosclerosis and inflammation. *Front Neurol.* (2017) 8:427. doi: 10.3389/fneur.2017.00427
28. Lepedda AJ, Ciglano A, Cherchi GM, Spirito R, Maggioni M, Carta F, et al. A proteomic approach to differentiate histologically classified stable and unstable plaques from human carotid arteries. *Atherosclerosis.* (2009) 203:112–8. doi: 10.1016/j.atherosclerosis.2008.07.001
29. Alonso-Orgaz S, Moreno-Luna R, López JA, Gil-Dones F, Padial LR, Moreu J, et al. Proteomic characterization of human coronary thrombus in patients with ST-segment elevation acute myocardial infarction. *J Proteomics.* (2014) 109:368–81. doi: 10.1016/j.jprot.2014.07.016
30. Muszbek L, Yee VC, Hevessy Z. Blood coagulation factor XIII: structure and function. *Thromb Res.* (1999) 94:271–305. doi: 10.1016/S0049-3848(99)00023-7
31. Gosk-Bierska I, McBane RD, Wu Y, Mruk J, Tafur A, McLeod T, et al. Platelet factor XIII gene expression and embolic propensity in atrial fibrillation. *Thromb Haemost.* (2011) 106:75–82. doi: 10.1160/TH10-11-0765
32. Frey A, Gassenmaier T, Hofmann U, Schmitt D, Fette G, Marx A, et al. Coagulation factor XIII activity predicts left ventricular remodelling after acute myocardial infarction. *ESC Heart Fail.* 7:2354–64. doi: 10.1002/eihf.2.12774
33. Bagoly Z, Koncz Z, Hársfalvi J, Muszbek L. Factor XIII, clot structure, thrombosis. *Thromb Res.* (2012) 129:382–7. doi: 10.1016/j.thromres.2011.11.040
34. Wartiovaara U, Mikkola H, Szöke G, Haramura G, Kárpáti L, Balogh I, et al. Effect of Val34Leu polymorphism on the activation of the coagulation factor XIII-A. *Thromb Haemost.* (2000) 84:595–600. doi: 10.1055/s-0037-1614073
35. Kamel H, Okin PM, Elkind MSV, Iadecola C. Atrial fibrillation and mechanisms of stroke: time for a new model. *Stroke.* (2016) 47:895–900. doi: 10.1161/STROKEAHA.115.012004
36. Clement W, Blaquierre M, Zub E, deBock F, Boux F, Barbier E, et al. A pericyte-glia scarring develops at the leaky capillaries in the hippocampus during seizure activity. *Epilepsia.* (2019) 60:1399–411. doi: 10.1111/epi.16019
37. Yang M, Pan Y, Li Z, Yan H, Zhao X, Liu L, et al. Platelet count predicts adverse clinical outcomes after ischemic stroke or TIA: subgroup analysis of CNSR II. *Front Neurol.* (2019) 10:370. doi: 10.3389/fneur.2019.00370
38. Fitzgerald S, Dai D, Wang S, Douglas A, Kadirkal R, Layton KF, et al. Platelet-rich emboli in cerebral large vessel occlusion are associated with a large artery atherosclerosis source. *Stroke.* (2019) 50:1907–10. doi: 10.1161/STROKEAHA.118.024543
39. Marcone S, Dervin F, Fitzgerald DJ. Proteomic signatures of antiplatelet drugs: new approaches to exploring drug effects. *J Thromb Haemost.* (2015) 13:S323–31. doi: 10.1111/jth.12943
40. UniProt Consortium T. UniProt: the universal protein knowledgebase. *Nucleic Acids Res.* (2018) 46:2699. doi: 10.1093/nar/gky092

Conflict of Interest: The authors declare that the research was conducted in the absence of any commercial or financial relationships that could be construed as a potential conflict of interest.

Copyright © 2020 Dargazanli, Zub, Deverdun, Decourcelle, de Bock, Labreuche, Lefèvre, Gascou, Derraz, Riquelme Bareiro, Cagnazzo, Bonafé, Marin, Costalat and Marchi. This is an open-access article distributed under the terms of the Creative Commons Attribution License (CC BY). The use, distribution or reproduction in other forums is permitted, provided the original author(s) and the copyright owner(s) are credited and that the original publication in this journal is cited, in accordance with accepted academic practice. No use, distribution or reproduction is permitted which does not comply with these terms.

Commentary

One proteomic study performed on 31 patients was published (after ours) in 2022.¹³³ The authors analyzed (by label-free quantitative liquid chromatography-tandem mass spectrometry LC-MS/MS) 16 cardioembolic and 15 large artery atherosclerotic thrombi, identifying 1581 proteins. They reported 14 significantly differentially abundant protein groups between the two etiologies. Remarkably, factor XIII A chain was one of the most abundant proteins found in CE clots, in line with our results.

Here, we acknowledge some shortcomings of our study. For example, we cannot exclude thrombus modifications induced by IVT. A recent analysis performed on 1430 retrieved thrombi of AIS patients suggested no interaction between IVT administration and thrombus composition;¹³⁴ however, only standard histological compositions (Martius Scarlett Blue staining) were examined (RBC, fibrin and platelet density, leukocytes).

Moreover, our proteomics data are a “snapshot” of the thrombus proteome at the time of thrombectomy. The proteome of a given biological entity is not a “steady-state” process; it is instead dynamic, possibly adapting its composition to environmental changes through multiple processes (transcriptional, translational, post-translational, and degradational).

SECOND PART: PERICLOT BLOOD ANALYSIS

Context

Endovascular treatment (EVT) of acute ischemic stroke (AIS) gives access to both intracranial thrombus and peri-thrombus blood, allowing an immediate and localized investigation of cellular and molecular processes of the AIS immune response.⁷⁶ Therefore, new biomarkers sampled at the intracranial level are of interest.

Importantly, neuroinflammation is a mechanism for neuronal loss and brain damage, and it has a crucial role in stroke pathology. During AIS, proinflammatory mediators are released from activated white blood cells and, in the brain, resident astrocytes or microglial cells. After clot retrieval, the reperfusion damage (e.g., at the downstream microcirculation, blood-brain barrier, and correspondent brain territory) could be contingent on the presence of local and specific pro-inflammatory molecules or cells, negatively impacting the outcome. Furthermore, evidence suggests that neuron cells can rapidly respond to ischemic and inflammatory conditions by secreting molecules implied in neuroprotection.¹³⁵

As background, an increase of neutrophil counts in the ischemic (post-thrombus) blood is associated with stroke outcome,¹⁰⁰ supporting experimental evidence that immune cells contribute to ischemic brain damage at the acute phase.¹³⁶ A vascular adhesion molecule, VCAM1, sampled in the ischemic arterial bed, is positively correlated to infarct and oedema volume and reduced NIHSS improvement.¹⁰⁵ The platelet-derived neutrophil-activating chemokine C-X-C-motif ligand (CXCL) 4 (PF-4), also sampled intracranially in the post-thrombus ischemic blood, is associated with the angiographic degree of reperfusion following recanalization, and functional outcome at discharge is correlated with local myeloperoxidase (MPO) level.¹⁰²

Here, we performed a quantitative analysis of a large panel of cytokines, chemokines, vascular growth factors, and adhesion molecules in the intracranial blood collected from AIS patients. We used post-clot blood samples obtained by microcatheter aspiration distally to the large vessel occlusion (LVO) in a prospective cohort of patients undergoing EVT.

Material and methods

Inclusion criteria

Our inclusion criteria were the same as in the sampling workflow section. All consecutive patients undergoing EVT of AIS were potentially enrolled.

Imaging

Infarct volume was automatically measured with the RAPID software (iSchemaView, Redwood City, California, USA) on either computed tomography perfusion (CTP) imaging or on magnetic resonance imaging (MRI) with a diffusion-weighted-imaging (DWI) sequence. When baseline imaging was performed in a remote center where RAPID software was not implemented, baseline infarct volume was (semi-)manually delineated using GE PACS console for the study purpose.

Perfusion mismatch (corresponding to a chosen ratio between core volume and perfusion deficit volume) was assessed when available, i.e., for patients who had Perfusion MRI or CT at baseline.

Perfusion mismatch was defined using Rapid Software (Figures 29 and 30) using a mismatch ratio of at least 1.2 and minimal penumbra volume of 10 mL, in addition to a maximum core and severely hypoperfused tissue volume (respectively, DWI lesion and Tmax \geq 8 seconds volume <100 mL), according to DEFUSE criteria.¹³⁷

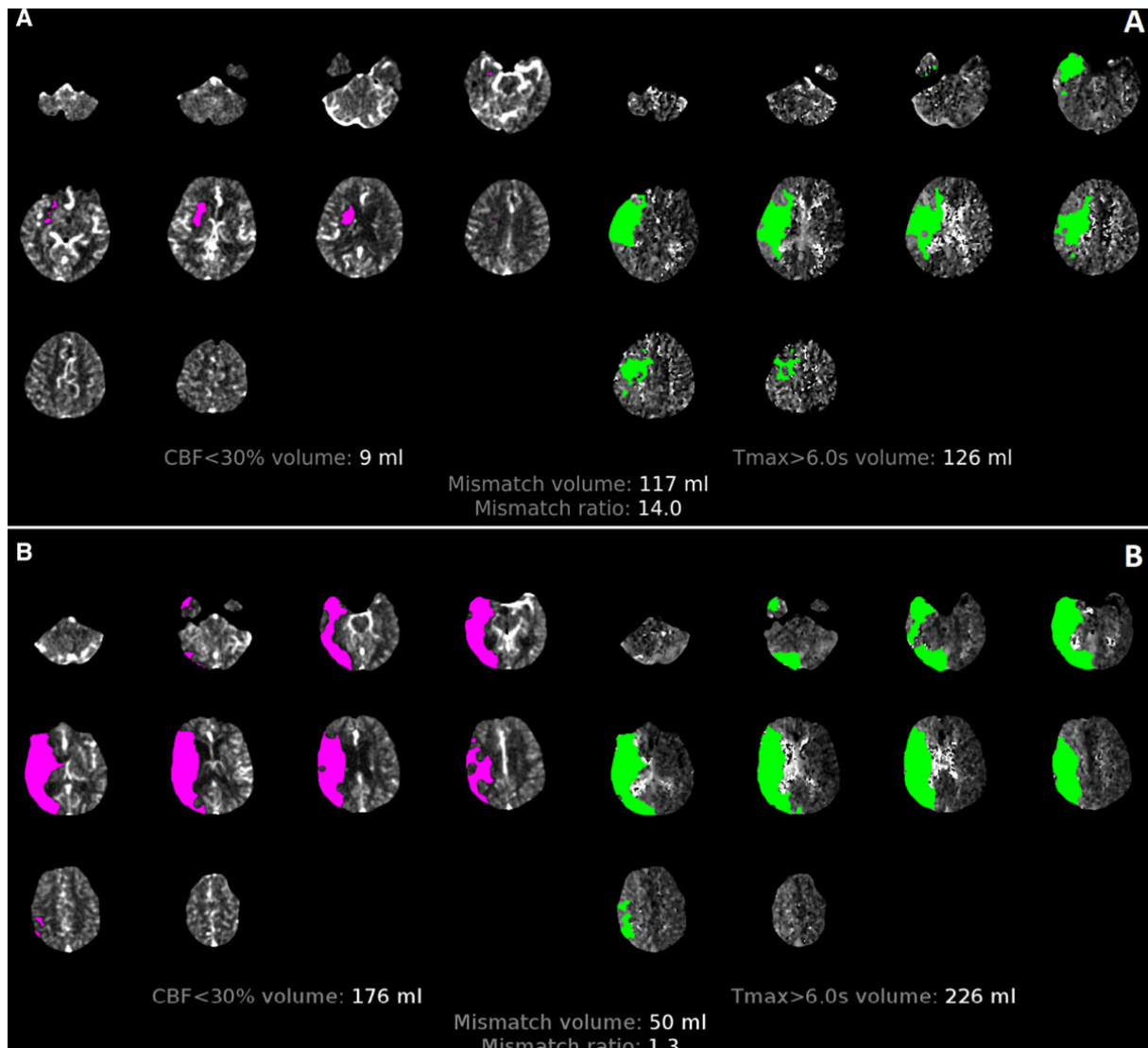


Figure 29: CT perfusion imaging processed by RAPID software showing the ischemic core and perfusion deficit

A: a patient with an occlusion of the M1 segment of the right MCA. Small ischemic core (pink), considerable tissue at risk for infarction (green) and a large mismatch ratio (14).

B: a patient with a right sided M1 occlusion and a malignant perfusion profile. This patient has a large ischemic core (pink) which largely overlaps the perfusion deficit (green).

CBF indicates cerebral blood flow.

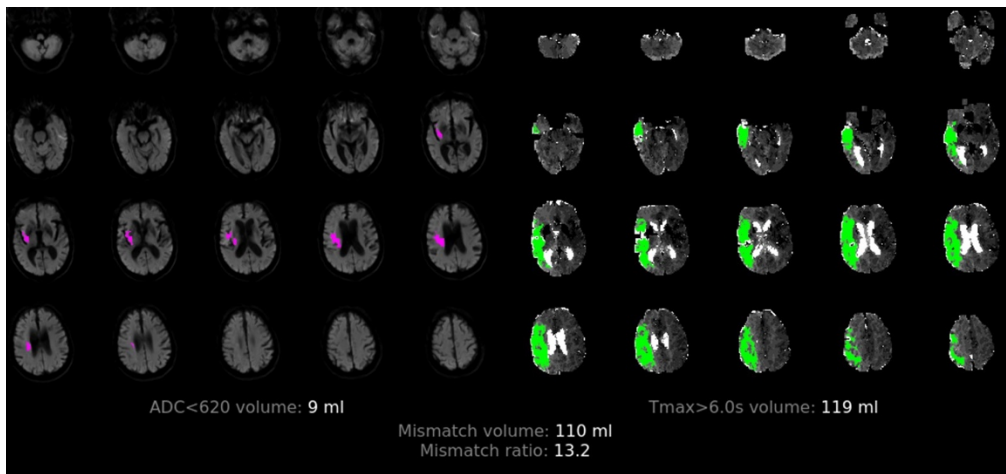


Figure 30: MR perfusion imaging processed by RAPID software showing the ischemic core and perfusion deficit

A patient with an occlusion of the M1 segment of the right MCA. Small ischemic core (pink), considerable tissue at risk for infarction (green) and a large mismatch ratio (13,2).

Blood sampling

A first sample (5cc of arterial blood) was taken at the puncture site immediately after the groin access (peripheric blood).

After thrombus was crossed with either a 0.021in (Headway 21, Microvention, or Trevo Pro 18, Stryker) or less frequently a 0.027in (Headway 27; Microvention) inner lumen diameter microcatheter, mounted on a 0.014in microwire, a 1 or 3cc syringe was connected to the hub of the microcatheter. Thereafter, before deploying the stent-retrieval device, dead space volume was aspirated and discarded (0.027in = 0.7ml dead space, 0.021in = 0.5ml dead space). Subsequently, a sample of a minimum of 0.5ml of ischemic blood was drawn (Figure 31), and then EVT procedure took over. When central sampling was not possible, the patient was excluded from the study, and the EVT procedure was continued without any delay.

At the end of the procedure, before sheath removal and artery closure, 5cc of arterial blood was withdrawn for another ongoing study (ANAIS, Dr. Francesca Rapido).

All samples were immediately transferred into a purple EDTA tube inverted manually around five times to ensure that the anticoagulant was evenly dispersed.

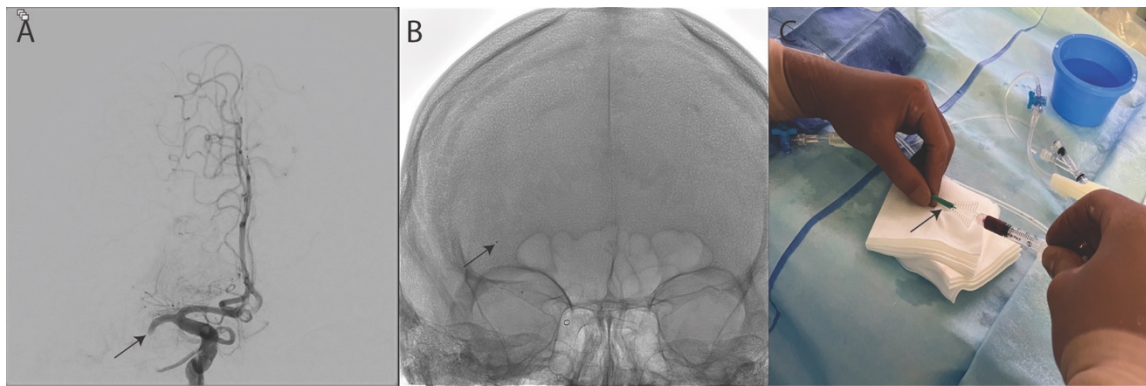


Figure 31: Central post-thrombus blood sampling with a 3-cc syringe

A: Digital subtraction angiography of the right ICA showing occlusion of the M1 segment of the MCA (black arrow). B: Sampling situation. The distal tip of the microcatheter (black arrow) in place in the distal insular segment of the right MCA, beyond the occlusion level. C: Blood aspiration with a 3ml luer lock syringe according to the sampling protocol after discarding the specific microcatheter dead space volume.

Feasibility analysis

The initial step was to assess the intracranial blood sample quality. To this end, we randomly choose 5 samples. SDS polyacrylamide gel separations were performed with or without the depletion of the most abundant proteins (Figures 32 and 33). Thus, blood analysis is often complicated by high-concentration proteins, including albumin and IgG, that represent more than 70% of total serum protein. Hence, removing albumin, immunoglobulins, and other abundant proteins is essential to allow the visualization in a gel of the less abundant or smaller proteins. Here, we used the “ThermoScientific High Select HSA/Immunoglobulin and Top 14 Abundant Protein depletion spin columns” (ThermoFisher Scientific, Waltham, Massachusetts, USA) to deplete serum albumin (HSA), albumin, IgG, IgA, IgM, IgD, IgE, kappa and lambda light chains, alpha-1-acid glycoprotein, alpha-1-antitrypsin, alpha-2-macroglobulin, apolipoprotein A1, fibrinogen, haptoglobin, and transferrin.

Figures 32 and 33 show the feasibility results (and the presence of protein signals) on five intracranial and peripheral blood samples.

Importantly, sample quality was maintained after both night storage and protein depletion. In the depleted samples (Figure 33), SDS gels showed the presence of high molecular weight proteins, not damaged or cleaved by proteases.

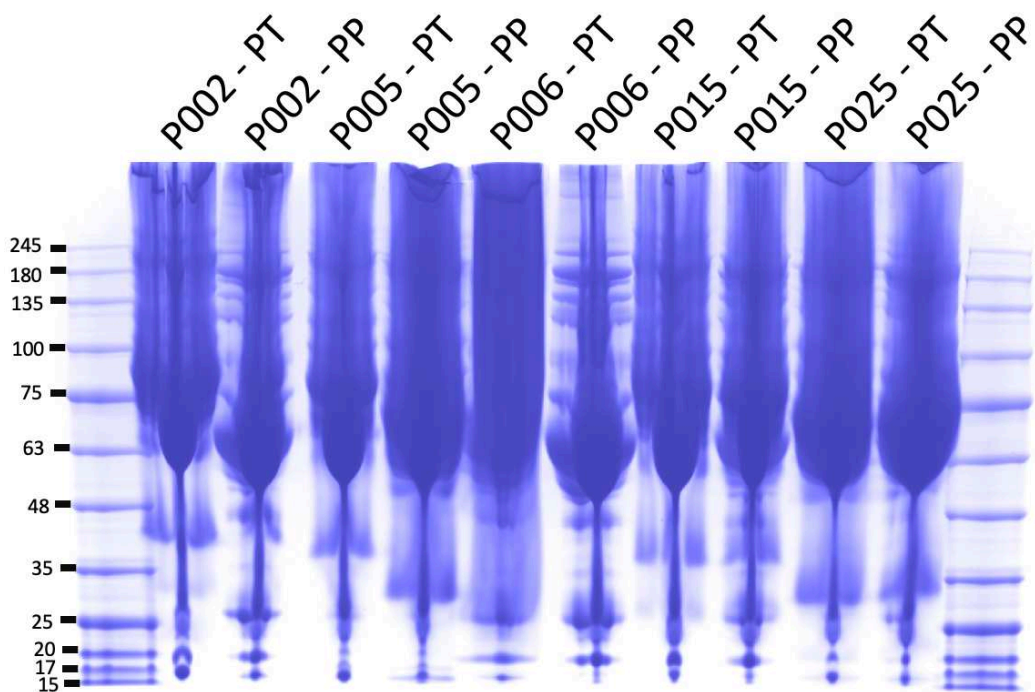


Figure 32: feasibility results on 5 samples of intracranial and peripheral blood without depletion

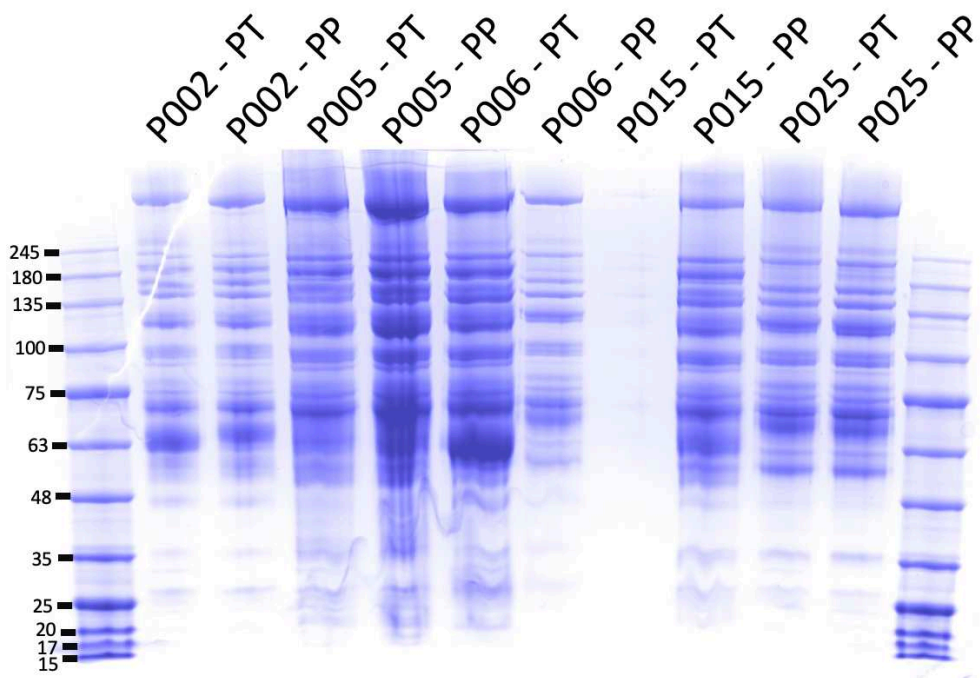


Figure 33: feasibility results on 5 samples of intracranial and peripheral blood after most abundant protein depletion

Of note, technical failure on P015 patient after depletion. PT: perithrombus blood. PP: peripheral blood

Flow of samples

Immediately after the procedure, a message alert was sent to the “MISO WhatsApp group” to schedule initial processing. For sample processing, a time window of a maximum of 24 hours (at 4°C) after initial sampling was allowed because our initial feasibility study showed no impact on the protein content (Figures 32 and 33). Samples were centrifuged, and the plasma was stored at -80C (C. Hirtz, PPC).

Statistical analysis

Data are presented as mean (SD) or median (interquartile range [IQR]) for quantitative variables according to the normality of distribution and numbers (percentage) for categorical variables. The normality of distribution was assessed using histograms and the Shapiro-Wilk test.

Due to the high skewness of distributions for several biological parameters, associations of biological parameters with cardioembolic etiology and main outcomes (90-day mRS, 24-hours Infarct Volume, 24-hours change in infarct volume and NIHSS, any intracranial hemorrhage) were investigated using non-parametric analyses. For cardioembolic etiology and any intracranial hemorrhage, the associations were assessed using Mann-Whitney U tests, and standardized mean differences with their 95% confidence intervals (CIs) were calculated on rank-transformed biological values as effect sizes. For 90-day mRS, 24-hours Infarct Volume, 24-hours change in infarct volume and NIHSS outcomes, the associations were assessed using Spearman's rank correlation coefficients by reporting the 95%CI of correlation coefficients estimated using Fisher z transformation. Associations of biological parameters with outcomes were further investigated after adjustment on admission NIHSS and ASPECTS by using Partial Spearman's correlation analyses (quantitative outcomes) or non-parametric covariance analyses (binary outcome). Since 37 biological parameters were tested, a correction for multiple testing were done for each outcome by using the False Discovery Rate controlling procedure.

For the biological parameters significantly associated with 90-day mRS after correction for multiple testing, we assessed the distributions of the biological parameters according to patients with and without favorable outcomes at 90-day (90-day mRS 0-2 or equal to pre-stroke) and calculated the ORs of favorable outcome per one-standard deviation in log-transformed biological values estimated from multivariable logistic regression models adjusted for admission NIHSS and ASPECTS. Statistical testing was done at the two-tailed α level of 0.05. Data were analyzed using the SAS software package, release 9.4 (SAS Institute, Cary, NC).

Results

Baseline characteristics

Between March 2021 and March 2022, 380 patients with AIS were treated by EVT in our comprehensive stroke center (CSC). Of these, 110 patients were eligible to be included in the present study (Flow-chart of the study, Figure 34).

Patients not having undergone EVT ($n=10$) because of early recanalization, treated with ADAPT technique in first instance ($n=92$), or patients where microcatheter aspiration was not attempted ($n=168$) were excluded. The aspiration of 1ml of ischemic blood was attempted in 110 patients and succeeded in 75 patients. A total of 72 samples of 40 patients entered laboratory analyses, after exclusion of 3 samples due to processing delay $>24\text{h}$.

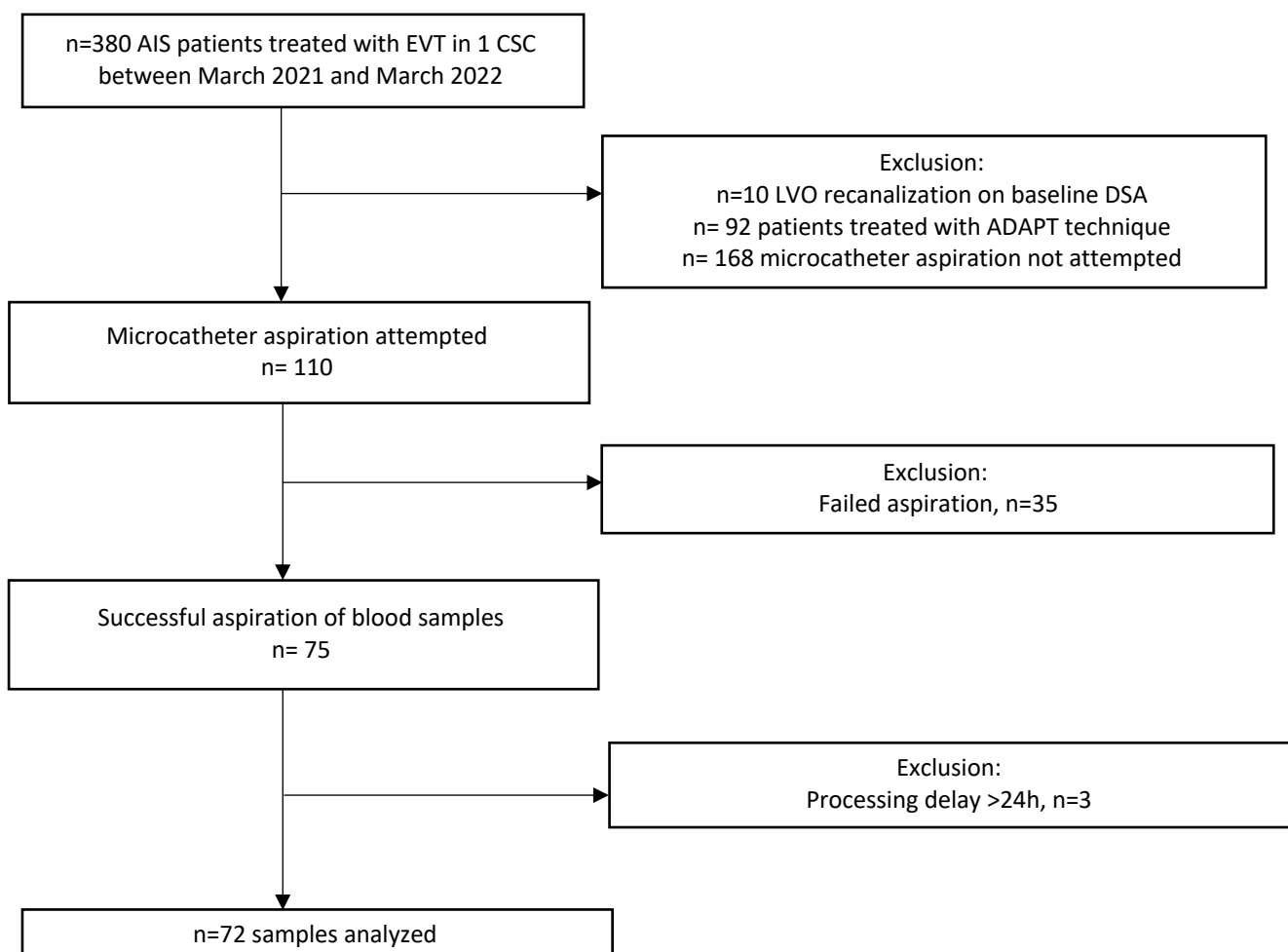


Figure 34: Flow-chart of the study

AIS = Acute Ischemic Stroke. EVT = Endovascular Treatment. LVO = Large Vessel Occlusion. DSA = Digital Subtraction Angiography. ADAPT = A Direct Aspiration

Baseline characteristics, treatment characteristics, and outcomes are described in Table 8. Briefly, the mean patient age was 75 years ($SD \pm 11$), 58.2% of patients were, 41.8% women. The most prevalent comorbid disease was hypertension (58.3%), followed by hypercholesterolemia (25%).

Median NIHSS at presentation was 17 (IQR = 11–21).

The median preprocedural ASPECTS at presentation was 8 (IQR = 6–9).

Twenty-six patients (36.1%) received IV rt-PA treatment before the EVT. The median time from symptom onset to groin puncture was 290 minutes (IQR = 183–380). On the initial angiogram, 40 (55.6%) patients showed MCA occlusion, 18 (25%) an ICA-T, 12 (16.7%) a tandem occlusion, 1 (1.4%) and 1 (1.4%) a basilar occlusion and a cervical carotid occlusion.

Technically successful reperfusion (defined as mTICI 2b or 3) was achieved in 67 patients (93.1%) after a median of 1 (IQR = 1–2) EVT attempts, and a median time of reperfusion after symptom onset of 316 minutes (IQR = 216–424).

Symptomatic intracranial hemorrhage was observed in 5 (7.2%) patients.

Median infarct core at day-1 was 19 mL (5-70).

	N	Values
Baseline		
Age, yrs., mean (SD)	72	75 ± 11
Men	72	42 (58.3)
BMI, kg/m ² , mean (SD)	68	26.3 ± 4.5
Medical history		
Hypertension	72	42 (58.3)
BP-lowering treatment	72	42 (58.3)
Diabetes	72	10 (13.9)
Hypercholesterolemia	72	18 (25.0)
Active smoking	72	8 (11.1)
Prior Stroke	72	11 (15.3)
Prior myocardial infarction	72	12 (16.7)
Prior cardiac insufficiency	72	7 (9.7)
Atrial fibrillation	72	19 (26.4)
Thrombectomy medications	72	32 (44.4)
Aspirin	72	20 (27.8)
Plavix	72	3 (4.2)
Vitamin K antagonist	72	3 (4.2)
New oral anticoagulants	72	10 (13.9)
Ticagrelor	72	1 (1.4)
Examination findings		
Pre-stroke mRS		
0	72	63 (87.5)
1		6 (8.3)
2		2 (2.8)
3		1 (1.4)
Admission NIHSS	72	17 (11 to 21)
Admission ASPECTS	71	8 (6 to 9)
Admission Systolic BP, mmHg, mean (SD)	72	148 ± 27
Admission Diastolic BP, mmHg, mean (SD)	72	80 ± 16

Infarct volume at initial imaging, ml	68	14.0 (1.0 to 39.5)
Pretreatment glucose, mmol/l	70	7.0 (5.9 to 8.4)
Admission cardiac frequency, mean (SD)	72	81 ± 19
Cardioembolic stroke	72	48 (66.7)
Perfusion imaging	72	52 (72.2)
Mismatch	52	48 (92.3)
Occlusion level		
MCA	72	40 (55.6)
ICA terminus		18 (25.0)
Basilar artery		1 (1.4)
Tandem		12 (16.7)
Cervical carotid artery		1 (1.4)
Acute stroke treatment		
Fibrinolysis	72	26 (36.1)
Onset to Fibrinolysis time, minutes	25	180 (145 to 210)
General anesthesia	72	19 (26.4)
Onset to groin puncture, minutes	69	290 (183 to 380)
Number of MT device passes	72	1 (1 to 2)
Outcomes		
mTICI ≥2b (successful reperfusion)	72	67 (93.1)
2b	72	13 (18.1)
2c	72	16 (22.2)
3	72	38 (52.8)
Onset to successful reperfusion time, minutes	66	316 (216 to 424)
90-day mRS	72	4 (2 to 6)
90-day favorable outcome*	72	26 (36.1)
Hemorrhagic complication	70	32 (45.7)
Symptomatic ICH	69	5 (7.2)
24-hours Change in NIHSS†	69	-3 (-9 to 0)
24-hours Infarct Volume, ml	68	19 (5 to 70)

24-hours change in infarct volume, ml†	67	5 (0 to 18)
--	----	-------------

Values are number (%) or median (IQR) unless otherwise is indicated.

* Defined as 90-day mRS 0-2 or equal to pre-stroke mRS

† Difference between 24-hours and baseline measure

Abbreviations: ASPECTS=Alberta stroke program early computed tomography score; BP=blood pressure; ICA=internal carotid artery; ICH=intracranial cerebral hemorrhage; IQR=interquartile range; MCA=middle cerebral artery; mRS=modified rankin scale; MT=mechanical thrombectomy; mTICI=modified thrombolysis in cerebral infarction; NIHSS=national institutes of health stroke scale; SD=standard deviation.

Table 8: Main baseline characteristics and outcomes of study sample (N=72).

MESOSCALE Panel

Association between MESOSCALE biomarkers with stroke outcome (90-day mRS)

- **In univariate analysis** and before correction for multiple comparisons, eight intracranial blood biomarkers (IL-10, IL-6, IL-8, TARC, FLT1, SAA, ICAM-1, VCAM-1) were correlated with stroke outcome assessed by 90-day mRS (Table 9, Supplemental Table 1).

After correction for multiple comparisons, only intracranial blood IL-6 remained significantly correlated with stroke outcome (Spearman's rank correlation coefficient =0.40580; p=0.0129; Figure 35 and Table 9).

- **In multivariate analysis** (adjustment on admission ASPECTS and NIHSS) and after correction for multiple comparisons, three intracranial blood biomarkers remained significantly associated with 90-day mRS (Figures 35 and 36; Table 10).
 - IL-6 (Spearman's rank correlation coefficient=0.37283; p=0.0294)
 - TARC (Spearman's rank correlation coefficient= -0.35379; p=0.0354)
 - SAA (Spearman's rank correlation coefficient= 0.38745; p=0.0294)

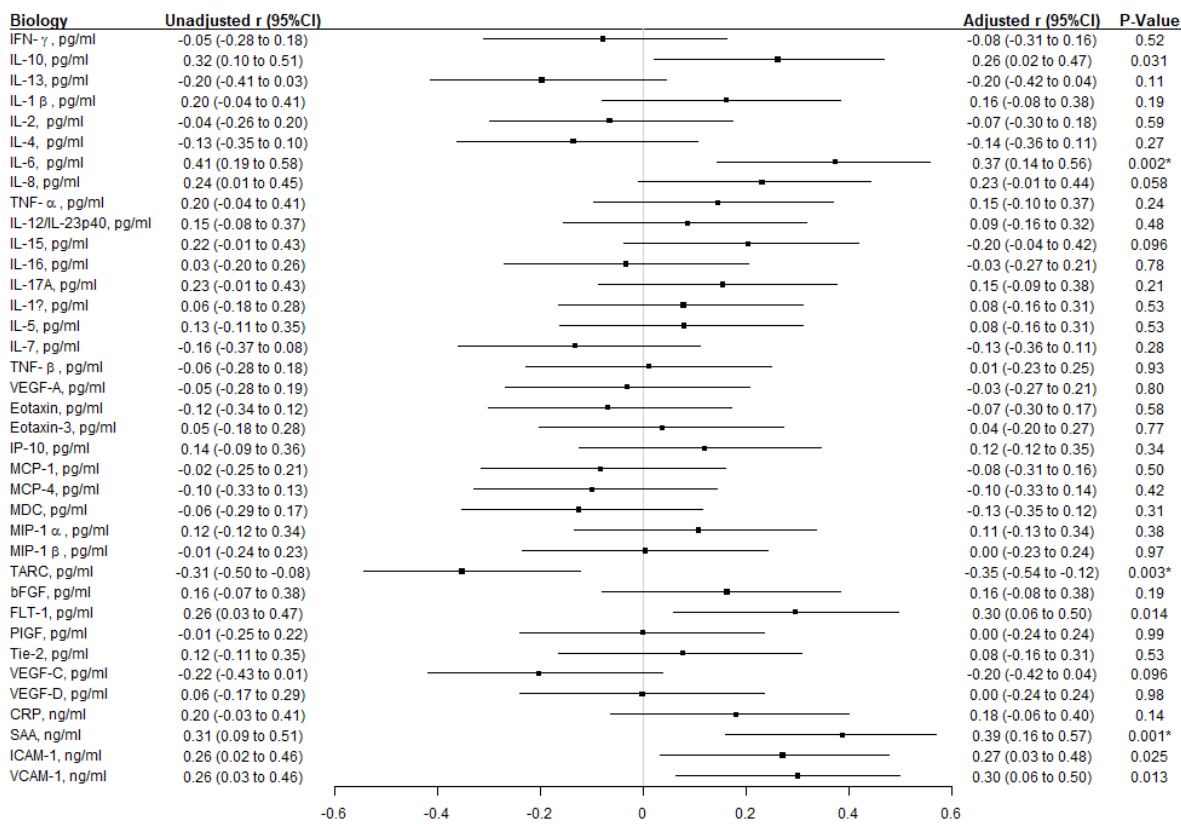


Figure 35: Association of MESOSCALE biomarkers with 90-day mRS

Spearman's rank correlation coefficients (r) before and after adjustment on admission NIHSS and ASPECTS are reported

* $p<0.05$ after correction for multiple testing using False Discovery Rate controlling procedures

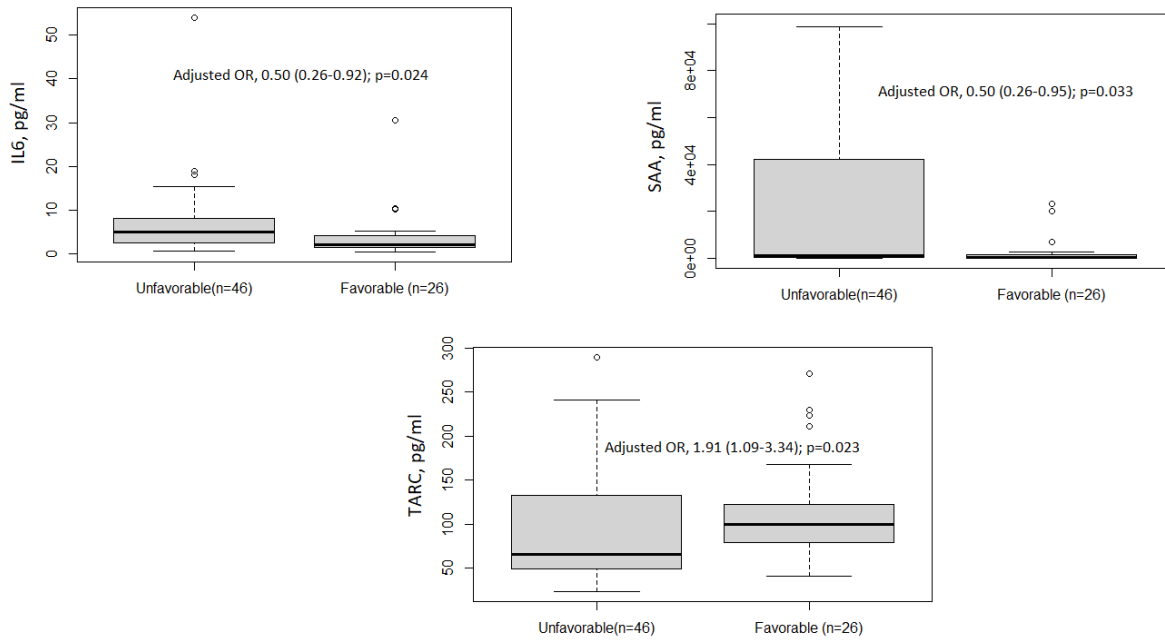


Figure 36: Distribution of the 3 biomarkers significantly associated with 90-day mRS

After multiple testing correction according to favorable status defined as 90-day mRS 0-2 or equal to pre-stroke mRS. The odds ratios (OR) per one standard deviation increase in biological parameters (log-transformed) adjusted for admission NIHSS and ASPECTS are reported.

Biomarker	Correlation	Correlation_lowerCI	Correlation_upperCI	pValue	PvalueCor
IL10	0.32344	0.096945	0.514738	0.0053	0.0739
IL6	0.40580	0.189449	0.580801	0.0003	0.0129
IL8	0.24466	0.012052	0.449407	0.0380	0.1759
TARC	-0.30892	-0.502857	-0.081041	0.0080	0.0739
FLT1	0.26336	0.030142	0.466441	0.0261	0.1587
SAA	0.31296	0.085458	0.506173	0.0071	0.0739
ICAM_1	0.25542	0.023450	0.458459	0.0300	0.1587
VCAM_1	0.26248	0.030960	0.464374	0.0256	0.1587

Table 9: Association between MESOSCALE biomarkers and stroke outcome (90-day mRS), univariate analysis

Biomarker	Correlation	Correlation_lowerCI	Correlation_upperCI	pValue	PvalueCor
IL10	0.26118	0.022321	0.468801	0.0311	0.1644
IL6	0.37283	0.144797	0.559448	0.0016	0.0294
TARC	-0.35379	-0.544293	-0.123396	0.0029	0.0354

Biomarker	Correlation	Correlation_lowerCI	Correlation_upperCI	pValue	PvalueCor
FLT1	0.29587	0.059600	0.497424	0.0139	0.1031
SAA	0.38745	0.161376	0.571001	0.0010	0.0294
ICAM_1	0.27138	0.033215	0.477264	0.0248	0.1531
VCAM_1	0.29979	0.063859	0.500635	0.0126	0.1031

Table 10 : Association between MESOSCALE biomarkers and stroke outcome (90-day mRS), multivariate analysis

Adjusted on baseline ASPECTS and NIHSS

Association between MESOSCALE biomarkers and favorable outcome (mRS 0-2 or mRS prestroke=90-day mRS)

- **In univariate analysis** and before correction for multiple comparisons, two biomarkers (IL-13, TARC) were associated with favorable stroke outcome ($p=0.0138$ and $p=0.0288$, respectively); three biomarkers (IL-10, IL-6, SAA) were associated with unfavorable stroke outcome ($p=0.0069$, $p=0.0058$, $p=0.0160$). After correction for multiple comparisons, any of these remained significantly associated with favorable or unfavorable outcome (Table 11).
- **In multivariate analysis** and before correction for multiple comparisons, two biomarkers (IL-13, TARC) were associated with favorable stroke outcome ($p=0.0151$ and $p=0.0179$, respectively); three biomarkers (IL-10, IL-6, SAA) were associated with unfavorable stroke outcome ($p=0.0157$, $p=0.0097$, $p=0.0088$). After correction for multiple comparisons, any of these remained significantly associated with favorable or unfavorable outcome (Table 11).

Biomarker	EffectSize	EffectSize_lowerCI	EffectSize_upperCI	Pvalue	PvalueCor
IL10	-0.69679	-1.19097	-0.20260	0.0069	0.1273
IL13	0.62891	0.13716	1.12066	0.0138	0.1479
IL6	-0.71364	-1.20847	-0.21882	0.0058	0.1273
TARC	0.55316	0.06385	1.04248	0.0288	0.2130
SAA	-0.61414	-1.10539	-0.12288	0.0160	0.1479

Biomarker	EffectSize	EffectSize_lowerCI	EffectSize_upperCI	Pvalue	PvalueCor
IL10	-0.59850	-1.08237	-0.11464	0.0158	0.1322

Biomarker	EffectSize	EffectSize_lowerCI	EffectSize_upperCI	Pvalue	PvalueCor
IL13	0.61027	0.12035	1.10020	0.0151	0.1322
IL6	-0.64130	-1.12471	-0.15788	0.0097	0.1322
TARC	0.59635	0.10510	1.08761	0.0179	0.1322
SAA	-0.66023	-1.15207	-0.16839	0.0088	0.1322

Table 11: Association between MESOSCALE biomarkers and favorable outcome (mRS 0-2 or mRS prestroke=90-day mRS)

List of biomarkers associated with favorable stroke outcome before correction for multiples comparisons, in univariate (up) and multivariate (bottom)

Association between MESOSCALE biomarkers with NIHSS 24-hours change

There was no significant association between the MESOSCALE biomarkers and NIHSS change at 24 hours in univariate and multivariate analysis (Figure 37, Supplemental Tables 5 and 6).

- In univariate analysis, IL-6 was correlated with NIHSS 24-hours change before correction for multiple comparisons ($p=0.0328$), but was not significant after correction for multiple comparisons ($p=0.6072$; Table 12)
- In multivariate analysis, IL-6 was correlated with NIHSS 24-hours change before correction for multiple comparisons ($p=0.0372$) but was not significant after correction for multiple comparisons ($p=0.6456$).
- FLT-1 was correlated with NIHSS 24-hours change before and after correction for multiple comparisons in univariate analysis ($p=0.0003$ and $p=0.0118$) but did not remain significant after correction for multiple comparisons in multivariate analysis ($p=0.0883$; Table 12).

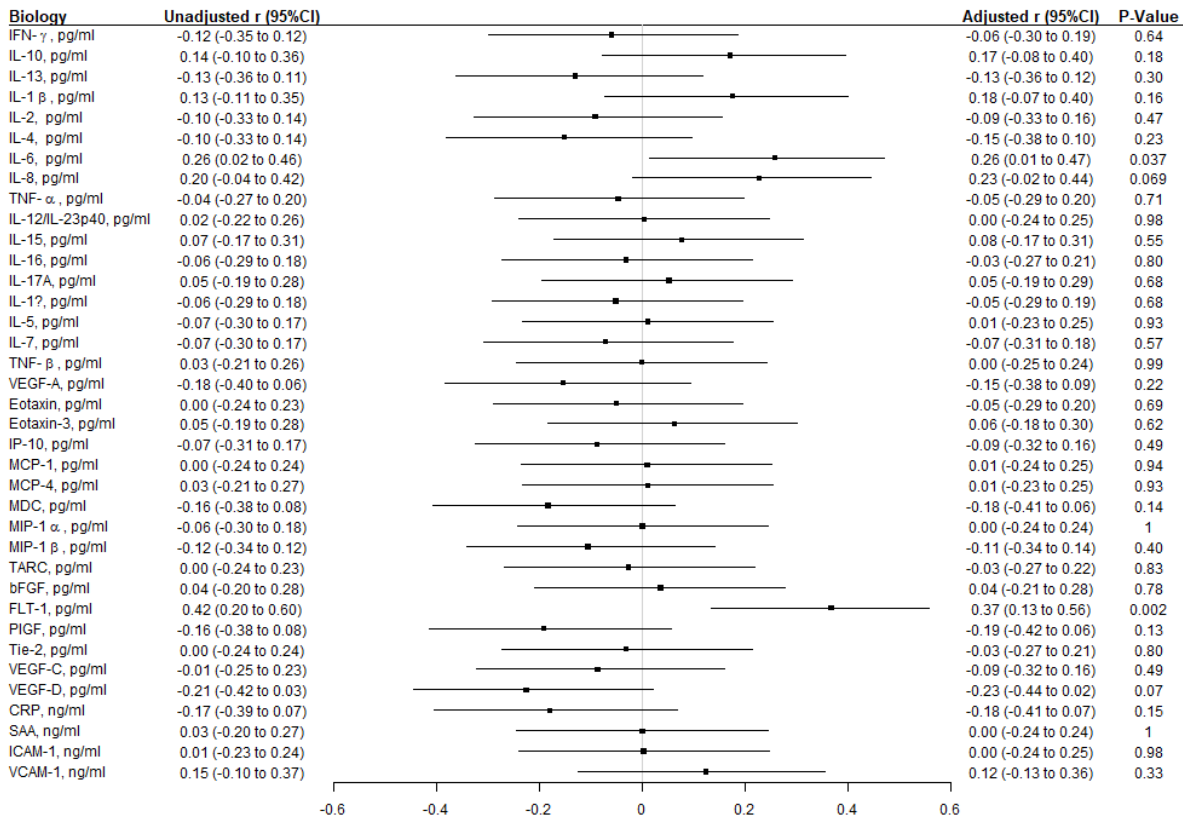


Figure 37: Association of MESOSCALE biomarkers with 24-hours NIHSS change (difference between H24 and admission NIHSS)

Spearman's rank correlation coefficients (r) before and after adjustment on admission NIHSS and ASPECTS are reported. No p-values reached the significance level after applying False Discovery Rate controlling procedures.

Biomarker	Correlation	Correlation_lowerCI	Correlation_upperCI	pValue	PvalueCor
IL6	0.25683	0.019565	0.463749	0.0328	0.6072
FLT1	0.41909	0.197720	0.595771	0.0003	0.0118

Biomarker	Correlation	Correlation_lowerCI	Correlation_upperCI	pValue	PvalueCor
IL6	0.25857	0.013644	0.471094	0.0372	0.6456
FLT1	0.36769	0.133163	0.559284	0.0024	0.0883

Table 12: Correlation of IL-6 and FLT1 with NIHSS 24-hours change

(Up: univariate analysis, Bottom: after adjustment on baseline NIHSS and ASPECTS)

Correlation of MESOSCALE biomarkers with infarct core volumes

Infarct core volume at 24 hours

There was no significant correlation between the MESOSCALE biomarkers and infarct core volume at 24 hours in univariate and multivariate analysis (Figure 38, supplemental Tables 7 and 8).

Of note, ICAM-1 was negatively correlated with infarct volume at 24 hours before correction for multiple comparisons ($p=0.0283$ in univariate analysis, $p=0.0065$ in multivariate analysis) but was not significant after correction for multiple comparisons ($p=0.9804$ in univariate analysis, $p=0.2423$ in multivariate analysis; Table 13).

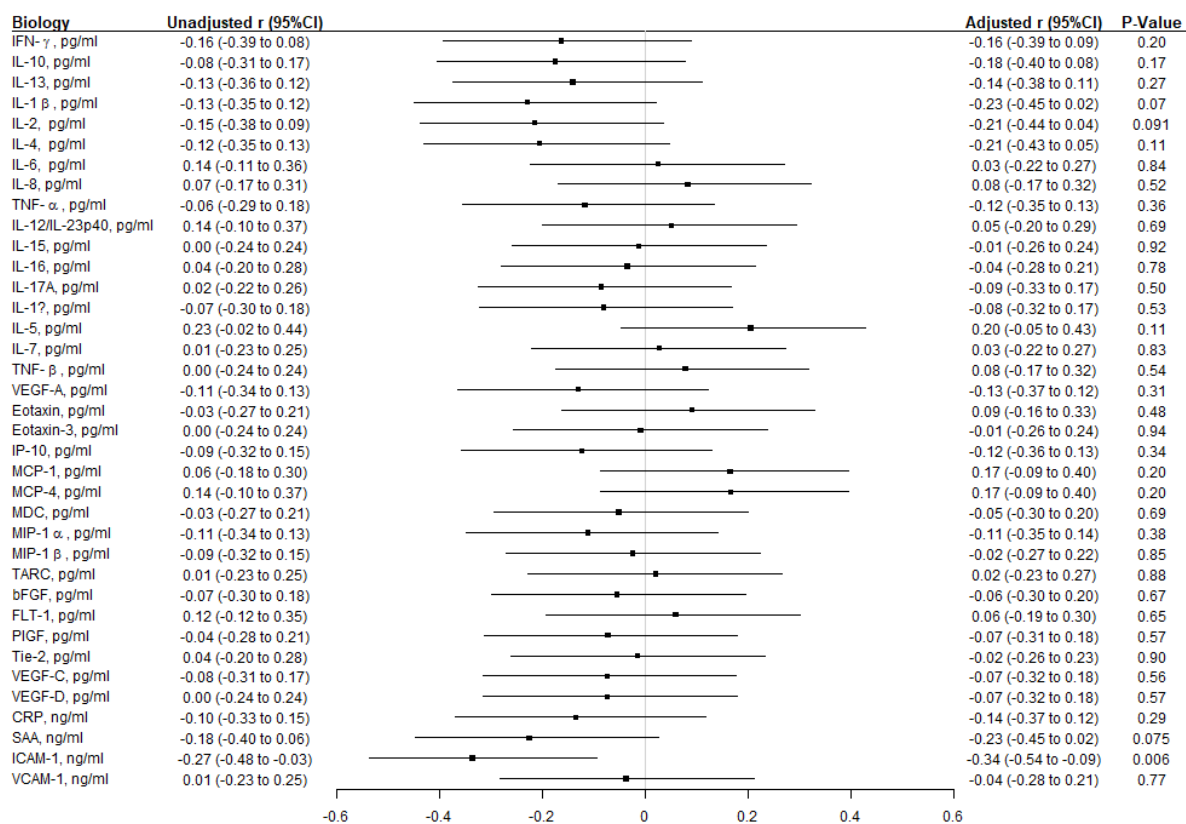


Figure 38: Association of MESOSCALE biomarkers with 24-hours Infarct Volume

Spearman's rank correlation coefficients (r) before and after adjustment on admission NIHSS and ASPECTS are reported. No p -values reached the significance level after applying False Discovery Rate controlling procedures.

Biomarker	Correlation	Correlation_lowerCI	Correlation_upperCI	pValue	PvalueCor
ICAM-1	-0.26752	-0.475503	-0.027160	0.0283	0.9804

Biomarker	Correlation	Correlation_lowerCI	Correlation_upperCI	pValue	PvalueCor
ICAM_1	-0.33728	-0.537994	-0.094981	0.0065	0.2423

Table 13: Correlation of ICAM-1 with final stroke volume at 24 hours

(Up: univariate analysis, bottom: after adjustment on baseline NIHSS and ASPECTS)

[Infarct core volume change](#)

There was no significant correlation between the MESOSCALE biomarkers and infarct core growth at 24 hours in univariate and multivariate analysis (Figure 39; Supplemental Tables 9 and 10).

Of note, ICAM-1 was associated with lower infarct volume change at 24 hours before correction for multiple comparisons ($p=0.0204$ in univariate analysis, $p=0.0142$ in multivariate analysis) but was not significant after correction for multiple comparisons ($p=0.7007$ in univariate analysis, $p=0.5255$ in multivariate analysis; Table 14).

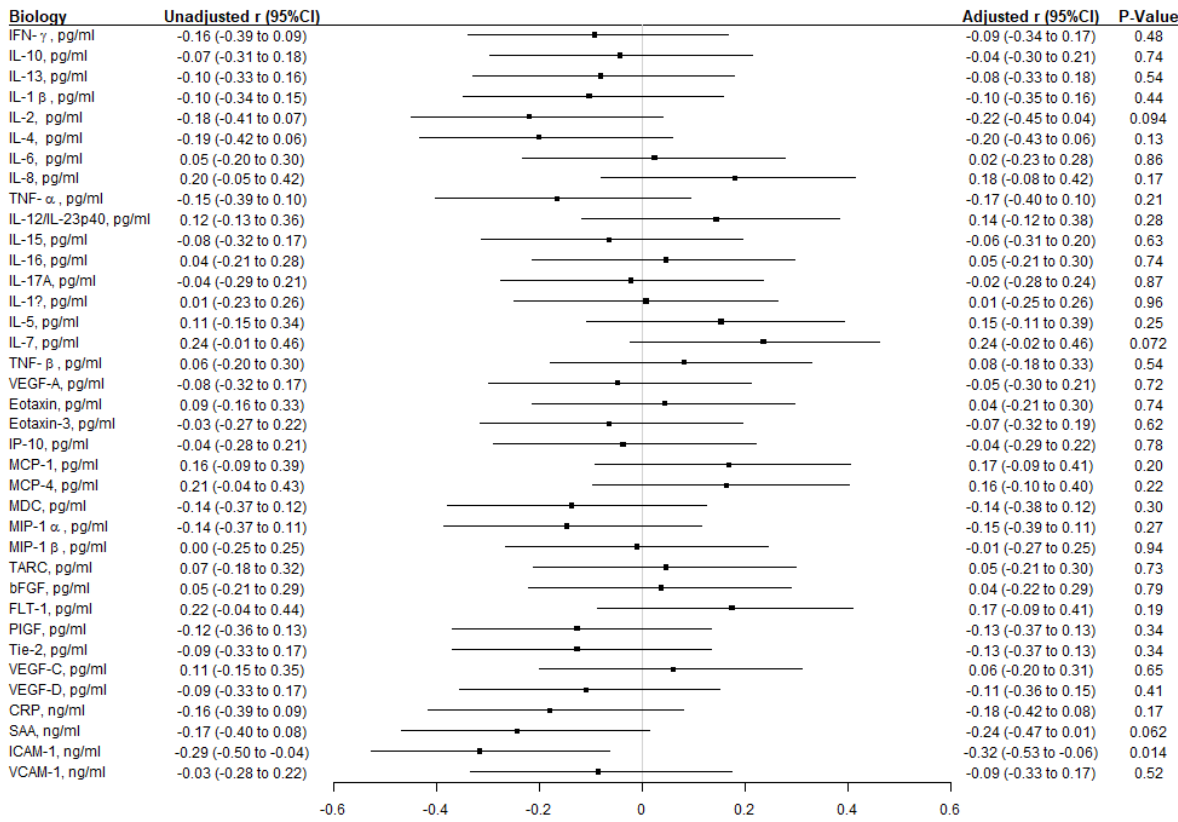


Figure 39: Association of MESOSCALE biomarkers with 24-hours Infarct Volume change (difference between H24 and admission infarct volume)

Spearman's rank correlation coefficients (r) before and after adjustment on admission NIHSS and ASPECTS are reported. No p-values reached the significance level after applying False Discovery Rate controlling procedures.

Biomarker	Correlation	Correlation_lowerCI	Correlation_upperCI	pValue	PvalueCor
ICAM_1	-0.29079	-0.500610	-0.044031	0.0204	0.7007

Biology	Correlation	Correlation_lowerCI	Correlation_upperCI	pValue	PvalueCor
ICAM_1	-0.31643	-0.527633	-0.062953	0.0142	0.5255

Table 14: Correlation of ICAM-1 with stroke volume change at 24 hours

(Up: univariate analysis, bottom: after adjustment on baseline NIHSS and ASPECTS)

Association of MESOSCALE biomarkers with stroke etiology

There was no significant association between the MESOSCALE biomarkers and stroke etiology (cardioembolic versus other causes; Figure 40 and Supplemental Table 11).

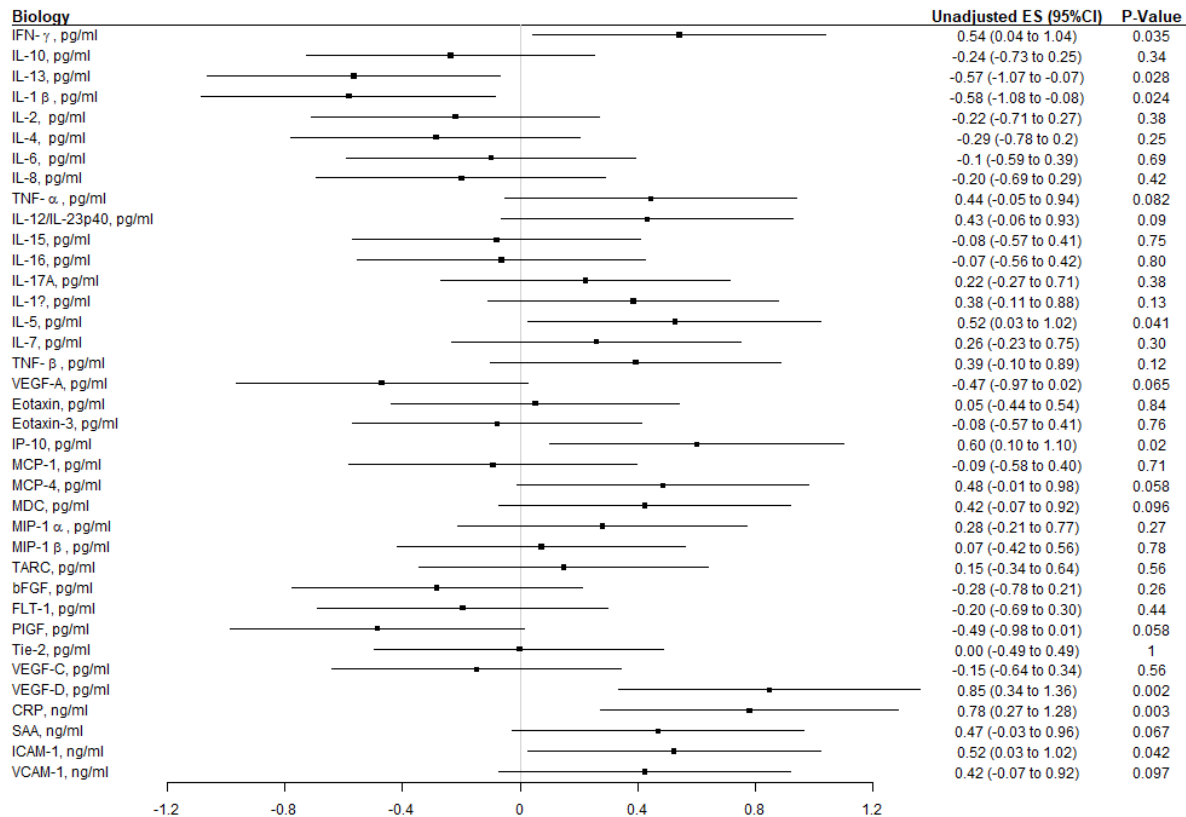


Figure 40: Association of MESOSCALE biomarkers with cardioembolic etiology

Standardized mean differences (effect size, ES) calculated on rank-transformed data. No p-values reached the significance level after applying False Discovery Rate controlling procedures.

Association of MESOSCALE biomarkers with hemorrhagic transformation

There was no significant association between the MESOSCALE biomarkers and the occurrence of any hemorrhagic transformation (Figure 41 and Supplemental Tables 12 and 13).

In univariate analysis and before correction for multiple comparisons, Eotaxin was negatively correlated to the occurrence of any hemorrhagic transformation (Spearman's rank correlation

coefficient=-0.53085, p=0.0324). Still, it was not significant after correction for multiple comparisons (p=0.5988).

TARC was positively correlated with the occurrence of any hemorrhagic transformation in univariate and multivariate analysis (Spearman's rank correlation coefficient=0.53123 and 0.55465; p=0.0305 and p=0.0247, respectively) but did not remain significant after correction for multiples comparisons.

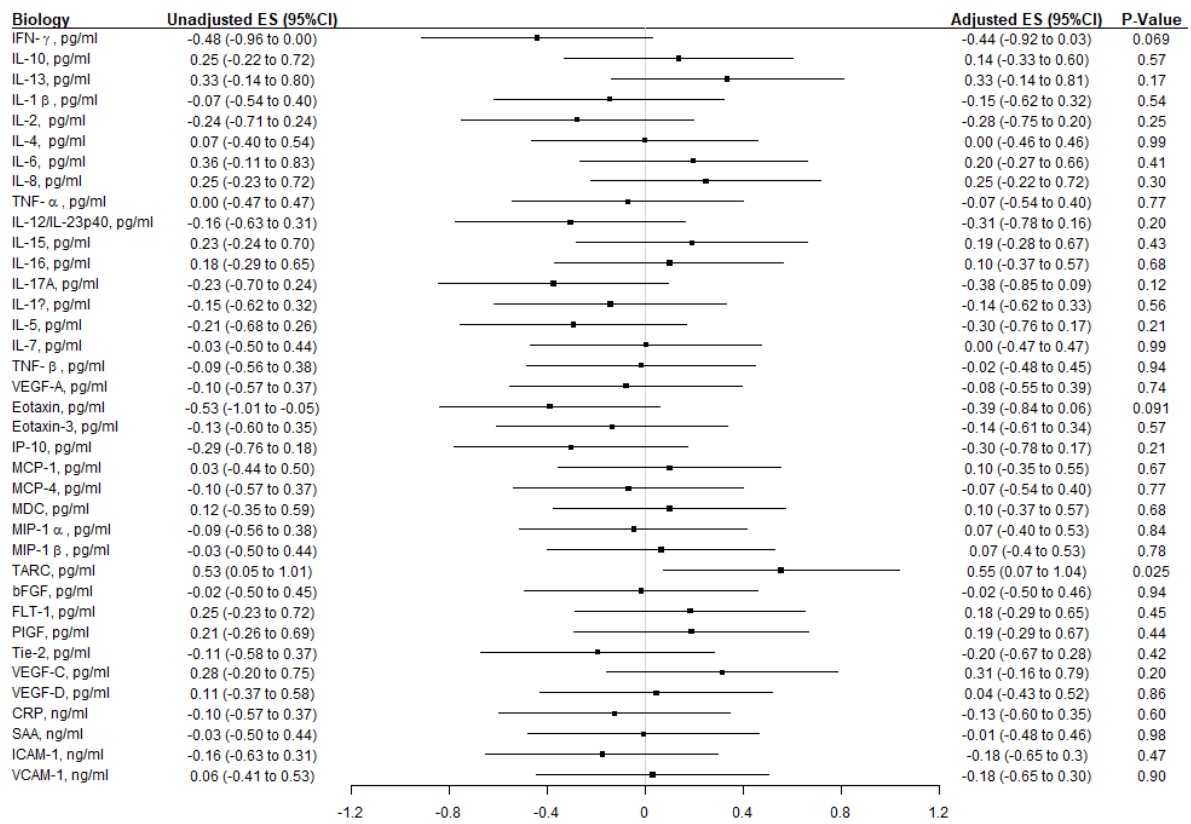


Figure 41: Association of MESOSCALE biomarker with any intracranial hemorrhage

Standardized mean differences (effect size, ES) calculated on rank-transformed data before and after adjustment on admission NIHSS and ASPECTS are reported. No p-values reached the significance level after applying False Discovery Rate controlling procedures.

Biomarker	EffectSize	EffectSize_lowerCI	EffectSize_upperCI	Pvalue	PvalueCor
Eotaxin	-0.53085	-1.00926	-0.05244	0.0324	0.5988
TARC	0.53123	0.05281	1.00966	0.0305	0.5988

Biomarker	EffectSize	EffectSize_lowerCI	EffectSize_upperCI	Pvalue	PvalueCor
TARC	0.55465	0.072765	1.03654	0.0247	0.8703

Table 15: Correlation of Eotaxin and TARC with any hemorrhagic transformation

Univariate analysis (up), multivariate analysis (bottom)

Discussion

This study analyzed the correlation between a large panel of neuroinflammation and vascular-angiogenesis biomarkers and clinical, biological, and imaging readouts in a cohort of consecutive AIS patients treated by EVT. We present the largest cohort of blood samples obtained in the intracranial ischemic arterial bed beyond the intracranial LVO.

Multivariate analysis retained three MESOSCALE biomarkers associated with stroke outcome (90-day mRS), namely IL-6, TARC and SAA.

We will first discuss the choice of this MESOCAL panel before detailing the current knowledge about these three biomarkers.

Biomarkers choice

This MESOSCALE panel allows the robust quantification of a broad range of central immune soluble factors. Several of these biomarkers were postulated to play a role in experimental and clinical AIS (Table 16).

Biomarker(s) name(s)	Role(s) demonstrated in AIS
Eotaxin-3, MCP-4	Role not known in AIS.
MIP-1 β	Also known as CCL4. Higher expression in ischemic brain. ¹³⁸
TARC	Also known as CCL-17. Low plasmatic concentration may be associated to lower stroke severity. ¹³⁹
IP-10	Interferon-inducible protein-10 (IP-10) is a chemokine with chemoattractant actions for monocytes and T cells. Brain ischemia induces IP-10. ¹⁴⁰
MDC	Also known as CCL22. Diminution of CCL22 concentration after cerebral ischemia and in systemic circulation 24 h after stroke symptoms onset. Diminution associated to increased stroke severity. ¹³⁹

MIP-1 α , IL-8, MCP-1	Enhance the migration of bone marrow stromal cells toward ischemic brain in a rodent model of stroke. ¹⁴¹
IFN- γ	Glycosylated, 19.3 kDa pro-inflammatory cytokine. Produced by lymphocytes and is a potent activator of macrophages. Involved in numerous pathways. Decreased infarct volume in IFN γ -/- mice, ¹⁴² and after systemic administration of an IFN γ neutralizing antibody ¹⁴³
IL-10	Glycosylated 20.5 kDa cytokine, also known as synthesis inhibitory factor (CSIF). produced by a variety of cell lines such as T-cells, macrophages, and mast cells. Inhibits the synthesis of numerous cytokines (including IFN- γ , IL-2, IL-3, TNF- α , TNF- β , and GM-CSF) that suppress Th1 proinflammatory responses and promote phagocytic uptake. Upregulated in both hemispheres after experimental stroke. ¹⁴⁴ Increased infarct volume when IL-10 deficiency. ¹⁴⁵
IL-13	Glycosylated, 15.8 kDa cytokine. Secreted by a variety of immune cells. Positive regulation of B-cell proliferation, macrophage activation, immunoglobulin production. Delivery of IL-13 enhances microglial/macrophage anti-inflammatory responses in vivo and in vitro, decreases ischemia-induced brain cell death. ¹⁴⁶
IL-1	Both IL-1 α and IL-1 β are created as 31-kDa precursor proteins. Induce their biological effects through binding to the IL-1 type I receptor (IL-1R1), which is expressed on several cell types. Crucial mediators of neuronal injury, and blockage of IL-1 actions is beneficial in several experimental models of brain damage, resulting in large decreases of infarct volume. ^{147,148} Mechanisms implied in IL-1 brain injury are unclear, but increasing evidence indicates the cerebrovasculature as a key target.
IL-2	Glycosylated 17.6 kDa protein produced by T-cells, also known as T-cell growth factor (TCGF). Major regulator of the immune system through T-cell proliferation and other activities. Facilitates Treg-induced neuroprotection in experimental model of stroke, associated to reduced TNF- α levels. ¹⁴⁹
IL-4	Glycosylated 17.5 kDa protein also known as B-cell stimulatory factor 1 (BSF-1) and lymphocyte stimulatory factor 1. Produced by Th2 cells and participates in activation of B- cells and other cell types. Suppresses the

	function of Th1 cells and macrophages as well as inhibits IFN-γ and IL-12 production. In response to ischemic insult, neurons produce and secrete anti-inflammatory cytokine interleukin 4 (IL-4). ¹⁵⁰ Deficiency of IL-4 leads to neural hyperexcitability and aggravates cerebral ischemia-reperfusion injury. ¹⁵¹
IL-6	23.7 kDa cytokine also known as B-cell stimulatory factor 2 (BSF-2), CTL differentiation factor (CDF), and Interferon beta-2 (IFN-β2, secreted mainly by T cells and macrophages. Involved in numerous biological processes including inflammation, aging, cell growth, apoptosis. Implied in the microglia-mediated death of neuronal cells. ¹⁵² Basal plasmatic level of IL-6 is correlated to stroke severity. ¹⁵³ Further details in the following paragraph.
IL-8	11.1 kDa CXC chemokine, also known as C-X-C motif chemokine 8 (CXCL8), granulocyte chemotactic protein 1 (GCP-1), monocyte-derived neutrophil chemotactic factor (MDNCF), monocyte-derived neutrophil-activating peptide (MONAP), neutrophil-activating protein 1 (NAP-1), and T-cell chemotactic factor. Expressed by several cell types as a response to inflammation. It attracts neutrophils, basophils, and T-cells, but not monocytes. It is also involved in neutrophil activation. High levels of circulating IL-8 are associated with larger infarct size in patients with acute ST-segment elevation myocardial infarction. ¹⁵⁴
TNF-alpha	25.6 kDa cytokine. This cytokine has been extensively studied in experimental stroke. ¹⁵⁵ Produced by resident microglia, intrathecal macro-phages, and infiltrating, monocyte-derived macrophages. Stimulates IL-1. TNF-α receptor inhibitors reduce volume of brain infarction, oedema, and oxidative stress on experimental models of AIS. ^{156,157} However, studies of TNF-deficient mice suggest that TNF may also be neuroprotective. ¹⁵⁸
IL-12	Binding of IL-12 to the receptor complex induces phosphorylation of tyrosine kinase 2 (TYK2) and Janus kinase 2 (JAK2). IL-12 has been shown to accumulate in human atherosclerotic plaques. ¹⁵⁹ IL-23 belongs to IL-12 cytokine family, and increases in patients with carotid stenosis. ¹⁶⁰
IL-15	Astrocytes are the main source of IL-15 in the inflammatory central nervous system. Chemotactic for T cells, promoting the migration of T

	cells to inflammatory tissues. May increase postischemic brain damage via propagation of CD8+ T and NK cell-mediated immunity. ¹⁶¹ Blockage of IL-15 responses after cerebral ischemia-reperfusion decreases brain injury in adult mice. ¹⁶²
IL-16	Pro-inflammatory cytokine produced by activated CD8+ T cells. Binds to CD4 and activates CD4+ T cells, monocytes, macrophages, and dendritic cells. Mediator of inflammation, increasing the production of inflammatory cytokines (TNF-a, IL-1b, and IL-6). ¹⁶³ IL-16+ cells accumulates in the necrotic lesion and at bordering peri-lesional areas of ischemic core. ¹⁶⁴
IL-5, IL-7	IL-5 and IL-7 may be predictors of oedema and infarct volume. ¹⁶⁵
VEGF-A	Dual role of VEGF in ischemic stroke. In the early stages of cerebral ischemia VEGF: increases and induces the destruction of the BBB. ¹⁶⁶ At a later phase of cerebral ischemia, VEGF regulates angiogenesis, neurogenesis, neurite growth and brain oedema.
VEGF-C	Not known
VEGF-D	Increased VEGF-D plasmatic concentrations has been associated with AF and AIS.
VCAM-1	Cerebral invasion of lymphocytes depends on the interaction of the leukocyte very late antigen-4 (VLA-4) with vascular cell adhesion molecule-1 (VCAM-1) on endothelial cells. Decreased expression of VCAM-1 on endothelial cells via downregulation of CD151 restrains neutrophil and monocyte infiltration and improves neurological outcomes after AIS in human. ¹⁶⁷
ICAM-1	Glycoprotein adhesion receptor mainly expressed on the surface of endothelial cells, inducing the recruitment of leukocytes from the circulation to the inflammation site. Serum ICAM-1 levels of AIS patients with poor outcomes are significantly higher than those with good outcomes. ¹⁶⁸ A RCT study showed that anti-ICAM therapy with enlimomab is not an effective treatment for AIS, and may worsen AIS outcome. ¹⁶⁹
CRP	Patients with AIS with plasmatic CRP levels ≥ 1.5 mg/dL at discharge have a significantly worse outcome. ¹⁷⁰

SAA	Also known as Serum Amyloid A. Blood SAA measured at baseline is an independent predictor of infection after AIS. ¹⁷¹
Tie-2	Tie2-expressing monocytes promote endogenous revascularization in the mouse brain after ischemic injury. ¹⁷² Tie-2 is a receptor of Angiopoietin-1.
Flt-1	Soluble flt-1 (sFlt-1) is a natural inhibitor of VEGF. In a rat model, sFlt-1 gene transfer significantly reduced infarct volume, brain oedema, and blood—brain barrier permeability. ¹⁷³
PIGF	Also known as Placental growth factor, member of VEGF family. Role not known in AIS.
bFGF	FGF has a protective and survival-promoting effects in stroke models, enhancing neuronal survival, angiogenesis, protection against BBB disruption, regulating microglia, reducing the infarct size and decreasing neurological impairment. ¹⁷⁴

Table 16: Overview of biomarkers quantified in the present study

Deciphering the role of intracranial post-clot blood inflammation in AIS

Pro and anti-inflammatory mechanisms are involved in the post-stroke innate and adaptative immune response. Neuroinflammation in response to ischemic insult has both beneficial and detrimental effects. The same factors may contribute to brain damage or protection depending on the temporospatial context of their expression.¹⁷⁵

The ischemic cascade corresponds to the chain of events that follows cell death and release of damage-associated molecular patterns (DAMPs), which triggers multiple molecular events leading to immune cell activation, inflammation, and programmed cell death.¹⁷⁶ Neuroinflammation occurs locally at the site of infarction but also in remote areas (“global brain inflammation”), in acute and chronic phases of stroke.¹⁷⁷

The two following paragraphs will focus on IL-6, TARC (CCL-17), and SAA, which intracranial levels we found significant correlated to functional outcomes at 3 months.

IL-6

Elevated serum IL-6 levels are implicated in a higher risk of AIS.¹⁷⁸

This cytokine is generally considered an adverse prognostic factor in AIS patients,^{179,180} and is associated with several imaging parameters (mean volume of DWI lesion at admission, perfusion deficit, final infarct size).¹⁸¹ A recent study showed that an elevated plasmatic peripheral blood circulation IL-6 is a biomarker of futile reperfusion in patients undergoing EVT.¹⁸² A lower level of IL-6 at baseline is associated with a first-pass effect (defined as complete or near-complete reperfusion achieved after a single thrombectomy attempt, predictive of a favorable outcome in AIS patients).¹⁸³ Release of IL-6 after AIS impairs cerebrovascular autoregulation in a pig model.¹⁸⁴ This cytokine also has prothrombotic properties,¹⁸⁵ contributing to upregulation of tissue factor from monocyte-macrophages, an increase of fibrinogen expression, reduced expression of protein C, and increased platelet reactivity.¹⁸⁶

However, there are also data demonstrating a direct neurovascular trophic action of IL-6. In mice, IL-6 produced locally by resident brain cells enhances post-stroke angiogenesis. IL-6 knock-out mice have fewer numbers of new endothelial cells in the infarct region, increased chronic lesion volumes, and worse long-term functional outcomes.¹⁸⁷ Older study showed that, in rats, intracerebroventricular injection of recombinant IL-6 significantly reduced ischemic brain damage after MCA occlusion.¹⁸⁸

Further studies may assess the impact of central IL-6 (high or low levels) on the BBB, using in-vitro models.¹⁸⁹

This ambivalent effect of IL-6 is not surprising. This cytokine harbors a wide range of competing effects and is an important messenger molecule between leucocytes, the vascular endothelium, and resident cells of the brain parenchyma. Biological activities (including anti-apoptotic, pro-proliferative, growth-inhibitory, and differentiation-inducing effects) of IL-6 are mediated by a dimeric membrane receptor that exists in a membrane-bound and soluble form.

IL-6 increase post-AIS is mainly driven by resident brain cells, i.e., neurons, glial cells (astrocytes), microglia and the vascular endothelium,^{187,190} highlighting the relevance of central sampling.

T cell-directed CC chemokine thymus and activation-regulated chemokine (TARC, or CCL-17)

In our study, a higher level of central TARC/CCL17 was associated to lower mRS at 3 months (better outcome).

One study showed a negative correlation between stroke severity with CCL17 level one day after AIS (the lower the CCL17 level, the higher the NIHSS score).¹³⁹ TARC/CCL17, expressed by M2 microglia, uses CCR4 as a receptor expressed in Th2 T-cells. Thus, CCL17 amplifies the immune response of type 2, and enhances the production of anti-inflammatory cytokines IL-4, IL5, IL-10, IL-13¹⁹¹. IL-4 deficiency in mice results in Th2 impairment, leading to larger infarct volume 24 hours after AIS, suggesting that Th2 response is neuroprotective.¹⁹² Th2 cells promote M2 (anti-inflammatory) polarization of microglia, having a protective effect.¹⁹³

Two immunomodulatory drugs targeting T-cell immune answer after stroke have been challenged in clinical settings:

- Natalizumab: blocks α4 integrin on leukocytes. Although this drug showed promising results in a mouse model,¹⁹⁴ its efficacy was not confirmed in a randomized double-blind, phase 2 study of patients with AIS (Natalizumab administered up to 9 h after stroke onset did not reduce infarct growth).¹⁹⁵
- Fingolimod: an oral sphingosine-1-phosphate receptor modulator (indicated in relapsing multiple sclerosis), which reduces peripheral lymphocyte numbers by inhibiting lymphocytes' exit from spleen and lymph nodes. Fingolimod enhances short and long-term neurological recovery in clinical trials with or without alteplase.^{194,196} Suggested mechanisms of action include reduced secondary injury to the brain due to the diminution of T-cells infiltration into the brain and improvement of perfusion in the distal microvasculature. However, notable limitations such as the small sample size (46 patients in the latest study) or lack of blinded treatment administration prevent generalizability of these preliminary data.

Our study did not analyze the leukocyte population in the intracranial blood.

In a previous study, flow cytometry was used to analyze leukocyte subpopulations in ischemic blood samples aspirated during EVT of AIS. A higher percentage of T cells (helper and cytotoxic) was found in the ischemic compartment compared to the systemic blood, along with a decrease in macrophages.¹⁹⁷

Serum Amyloid A (SAA)

SAA is an acute-phase protein which is upregulated by a variety of inflammatory stimuli. Increased synthesis of SAA is induced by pro-inflammatory cytokines such as IL1, TNF- α , IL-6.¹⁹⁸ It may have an active role during inflammation, activating severe pathways leading to the expression of proinflammatory factors and proteins expressed by the M2 macrophages.¹⁹⁹

Study Limits

Sampling failure

Central blood sampling was not possible in around 32% of cases. In the article of Kollikowski and al., aspiration was not possible in 52%. We did not analyze the association of collateral circulation with the rate of failure or success. We should note that in the study of Kollikowski and al., multiple logistic regression analysis was performed to identify patient characteristics influencing the ability to aspirate ischemic blood after the thrombus (successful vs. unsuccessful aspiration with the microcatheter). They found that increased collateral status and no active smoking were predictive of successful aspiration.¹⁰⁰

Limited sample size and reasons

Although our cohort is the largest to date analyzing central blood obtained by microcatheter aspiration, the sample size remains limited, and microcatheter aspiration was not attempted in 44% of AIS treated by EVT during the study period in our large volume CSC.

Finally, because our protocol excluded intracranial blood samples processed >24 hours after microcatheter aspiration, patients treated by EVT from the late afternoon of Friday to Sunday noon were not eligible.

Systemic inflammation

The MESOSCALE panel has not been performed on peripheral samples yet. These samples are available. One possibility is that elevated central cytokines may be due to systemic inflammation. Indeed, microcatheter aspiration allows access to blood flow fed through pial collateral channels, which connect the terminal branches of the occluded vascular MCA field with the ACA and PCA territories. It has been suggested that central leukocytes increase after

AIS occurs via retrograde collateral pial blood flow.¹⁰⁰ However, whether there is a central enrichment of pro and anti-inflammatory cytokines during AIS needs to be determined.

To clarify this issue, we will soon analyse the collected peripheral blood samples (MesoScale) and perform biomarkers ratio analyses (patient-specific; biomarker concentration in central samples/biomarker concentration in peripheral samples). Subgroup analysis will focus on patients with successful reperfusion after EVT (\geq TICI 2B) to assess if that ratio may be correlated to outcomes, especially infarct growth. Final infarct volume is a strong independent predictor of functional outcome.²⁰⁰ Despite successful recanalization obtained by EVT, a substantial infarct growth occurs in patients with AIS.²⁰¹ These data highlight the need for new strategies to limit infarct expansion after successful EVT reperfusion.

Correlation with etiology

We could not find an association between a specific central biomarker and an etiologic group (cardioembolic vs. other). A very recent longitudinal case-control study (September 2022) performed on 1200 patients showed that the peripheral plasma levels of inflammation-related proteins differ in large artery atherosclerosis, cardioembolic stroke, small artery occlusion stroke, and cryptogenic stroke.²⁰²

Outcomes

We fully acknowledge that the mRS at 90 days, the traditional outcome measure in AIS trials, remains a gross and unperfect outcome. Recovery after AIS depends on several factors, including patient demographics, comorbidities, stroke interventions such as tPA or EVT, poststroke rehabilitation, recurrent AIS, secondary complications (infection occurs in 30% of AIS patients)²⁰³, and genetic variations.²⁰⁴ A recent study indicates that around 50% of patients with good mRS (0-1) after an AIS will have cognitive impairment or restrictions in reintegration.²⁰⁵

Not studied biomarkers

Metalloproteinases

The biomarkers panel used in this study did not include metalloproteinases (MMPs).

Several MMPs are implicated in AIS physiopathology, the most studied being MMP-9.⁹² The effect of full and partial mechanical reperfusion on MMP-9 expression in rat brains following MCA occlusion was proposed. Authors observed increased expression of MMP-9 following occlusion in ischemic brain regions and the normal-appearing homolateral frontal cortex.²⁰⁶ MMP may degrade the extracellular matrix and tight junction component and enable BBB breakdown. MMP-9 correlates with initial and final NIHSS and final infarct core, and the incidence of hemorrhagic transformation, when dosed in AIS patients' serum.^{207,208} MMP-9 is up-regulated by tissue t-PA both in animal models and AIS patients.²⁰⁹ To our knowledge, MMP-9 has never been quantified in central blood in patients. Whether intracranial, peri-thrombi levels of MMP-9 may have a prognostic impact remains to be tested, for example, using Ultra-Sensitive Kit assay-specific of Mesoscale (<https://www.mesoscale.com/en/products/human-mmp-9-ultra-sensitive-kit-k151hac>). MMP-12 is another MMP mediating BBB disruption via tight junction protein degradation after focal cerebral ischemia in rats. A recent study showed that MMP-12 knockdown adult male mice had reduced post-ischemic infarct volume and improved motor and cognitive functional recovery after transient MCA occlusion.²¹⁰

Other chemokines

They act mainly via recruiting effector leukocytes to the ischemic brain. CC and CXC chemokines are the most relevant AIS subfamilies recruiting neutrophils and monocytes, with phagocytic activity. Several studies have analyzed the role of chemokines in AIS, showing an increased expression within the ischemic brain regions.¹³⁹ Kollikowski and al., showed that CXCL-11 (I-TAC), which has chemoattractant activity for activated T cells, was locally elevated in the ischemic blood.¹⁰⁰

CONCLUSION AND PERSPECTIVES

AIS remains a leading cause of death and disability, and therapeutic options or tools for diagnosis and prognosis are limited. Even if performed early and technically successful, EVT of AIS does not guarantee a favorable outcome.²¹¹ Modern EVT allows high recanalization rates (70–90%), but patients good functional outcome remain low (30–60%), and only 10% are without stroke symptoms at 3 months (mRS 0).²¹² Hence, a relative discrepancy exists between recanalization and good functional outcomes, with substantial room for therapeutic improvement, and advanced research is necessary to understand the complex biological processes of AIS that lead to the final infarct core.

Within this framework, we conducted a multidisciplinary approach exploiting EVT, a revolutionary opportunity to study clot and blood biology intracranially in AIS patients.

First, we showed that quantitative proteomics and SVM analysis could be feasibly combined to examine the variation of intracranial human thrombi proteomes. The SVM method used was set to identify combinations of protein trios in the intracranial thrombi, and it allowed for an 88.3% correct classification of our selected cardioembolic and atherothrombotic populations. SVM identified Factor XIII, a protein implied in the last step of the coagulation (known as “fibrin stabilizing factor”), as one potential differentiating element between the cardioembolic and atherothrombotic thrombi analyzed.

Interestingly, a follow-up paper proposed Factor XIII as a cardioembolic thrombi biomarker.¹³³ This coagulation factor could be re-tested in a validation cohort of AIS patients. Unlike the interest in the development of novel anticoagulants targeting FXIa and FXIIa,²¹³ there is no trials focusing on Factor XIII inhibition to prevent AIS in patients with atrial fibrillation. However, whether FXIII Inhibition maybe be a valid therapeutic strategy has been tested in vitro and in animal models in the context of venous thromboembolism.²¹⁴

Factor XIII Val34Leu polymorphism, which is a common genetic alteration influencing the rate of FXIII activation by thrombin and as a result clot structure, has a protective effect against myocardial infarction and venous thromboembolism.²¹⁵ Recently, it has been shown that intracranial clot burden was decreased in AIS patients harboring factor XIII Val34Leu polymorphism.²¹⁶

Patients in whom the stroke etiology remains undetermined following an exhaustive diagnostic investigation (accounting for up to a third of all cases of stroke) are problematic for clinicians, especially regarding secondary stroke prevention. If confirmed, methods allowing differentiation of cardioembolic and non-cardioembolic sources of stroke may give arguments to give anticoagulation therapy after the stroke occurrence. Moreover, thrombus biomarkers, as Factor XIII, may be used in combination with blood-based biomarkers for searching atrial fibrillation after cryptogenic AIS.²¹⁷

In the second part of this thesis, we quantified a large panel of biomarkers in the ischemic blood distal to the thrombus, showing that three biomarkers (IL-6, SAA, TARC) were correlated with stroke outcome assessed by 90-day mRS.

This second work is in line with the modern paradigm of AIS treatment. A wide range of potential neuroprotective agents has been investigated to reduce brain injury and improve patient recovery. However, despite promising results obtained in animal models, none of the tested neuroprotective strategies appeared effective in clinical trials in earlier studies.²¹⁸

One hypothesis explaining these failures might be that recanalization may be a necessary condition for effectiveness of neuroprotective treatments.

Among the bunch of published neuroprotective studies, we see that only fifteen RCT have been performed on patients benefiting of both reperfusion therapy and neuroprotection agent. Of these, in only three were patients 100% treated with EVT.²¹⁹

Of the four main neuroprotection targets (reduction of oxidative stress, of excitotoxicity, inflammation, and cellular apoptosis), two were explored by these RCT associating neuroprotection with EVT:

- **Reduction of oxidative stress:**

- A subgroup analysis of URICO-ICTUS trial (2017) included patients with LVO who received both IVT and EVT. They were randomized to intravenous 1000 mg uric acid or placebo. Neuroprotective action of uric acid involves suppression of oxyradical accumulation, stabilization of calcium homeostasis, and preservation of mitochondrial function.²²⁰ Good functional outcome

significantly better for patients treated with uric acid than those receiving placebo.²²¹ The limited sample size of this subgroup analysis (n=45) needs validation in a larger trial.

- A recent RCT considered normobaric oxygen as an adjuvant neuroprotective strategy, applied to patients with LVO in the anterior circulation treated by EVT. Patients were randomized to receive either high-flow normobaric oxygen therapy (n=88) or routine low-flow oxygen supplementation (n=87). NBO patients demonstrated increased odds favoring the distribution of global disability scores on the 90-day mRS.
- **Reduction of neuronal excitotoxicity:** in March 2020 was published a RCT (ESCAPE-NA1) using nerinetide, an eicosapeptide that interferes with post-synaptic density protein 95.²²² This agent may penetrate the BBB after intravenous administration, and due to its interactions with neurotoxic signalling proteins, lead to reduction of intracellular endogenous nitric oxide without blocking synaptic activity. That neuroprotective agent has already demonstrated to reduce ischemic damage in mice, rats and primates.²²³⁻²²⁶

The main result of that large RCT (ESCAPE NA-1 included 1105 patients) was that nerinetide did not improve the proportion of patients achieving good clinical outcomes after EVT compared with patients receiving placebo. However, the subgroup of patients not treated with alteplase had better outcomes. In the absence of tPA, the odds ratio for achieving a 90-day mRS with nerinetide was 1.6 (95% CI, 1.06-2.60; p=0.028), and nerinetide treatment in the absence of tPA reduced mortality risk by 43%. These results may suggest an interaction between nerinetide and alteplase, nullifying treatment effect, and are the reason of a new phase III trial (ESCAPE-NEXT), which will evaluate nerinetide with EVT in the absence of tPA.²²⁷

At our knowledge, there is not RCT that have targeted inflammation disturbance in AIS patients treated with EVT.

Because our results showed a correlation of local central level of IL-6 and 90-day mRS, one would enquire to assess the effect of anti-IL6 therapy administered locally in the ischemic area.

However, the first step is to assess IL-6 central/peripheral ratio in patients having achieved successful reperfusion IVT, and to correlate this ratio to stroke outcomes (infarct volume, mRS). This will allow to better individualize the specific IL-6 impact on AIS outcomes, and eventually to increase our knowledge about this cytokine described to have an ambivalent function in AIS.¹⁹⁰ To date, there is no direct evidence showing that IL-6 plays a detrimental role in acute phase of cerebral ischemia.

Tocilizumab is an humanized monoclonal antibody IL-6 receptor antagonist, indicated in some forms of rheumatoid arthritis or juvenile idiopathic polyarthritides. It has also been proposed for severe refractory primary central nervous system vasculitis and in critically ill patients with coronavirus disease 2019.^{228,229}

As a large monoclonal antibody with a molar mass of 145.0 kg/mol, it is not expected to penetrate the BBB in normal subjects. However, a recent article showed that tocilizumab prevented macro- and microcirculatory disturbances and was acutely neuroprotective after induced subarachnoid hemorrhage. Amounts of IL-6 in CSF after tocilizumab administration was higher than baseline, which seems an indirect indication that this competitive antagonist of the IL-6 receptor went through the blood brain barrier.²³⁰

Moreover, the disruption of the BBB after AIS may eventually facilitating the passage of tocilizumab.

Very interestingly, a recent cardiologic RCT showed that early treatment with tocilizumab (single intravenous infusion) augmented myocardial salvage in patients presenting with acute ST-Segment Elevation Myocardial Infarction within 6h of symptom onset and undergoing revascularization with percutaneous coronary intervention, without safety concerns.²³¹

If further developed and tested on larger cohorts, these methods have the potential to discover precise and novel pathophysiological players and biomarkers, with the ideal goal of aiding cerebrovascular stroke diagnosis and secondary prevention, with a special focus on controlling reperfusion damage.

To conclude, our work opens numerous avenues for further explorations:

1. Thrombus composition and the analysis of clot of unknown origin. Our department will shortly obtain a dedicated -20° Low Freezer, which will allow collecting thrombi (and blood) 24-hour/7-day .
2. Central intracranial blood samples: further exploitation and in vitro experiments using BBB models to unravel damage and molecular mechanisms provoked by human-derived blood samples.
3. Additional biomarkers can be tested using MESOSCALE (e.g., MMPs) to advance understanding of the molecular events associated with AIS.
4. Local injection (during EVT) of specific blocking antibodies directed at soluble pro-inflammatory players. This strategy could be an innovative and local treatment to prevent adverse outcomes such as hemorrhagic transformation.
5. The impact of central endothelial and leukocyte-derived microvesicles could also be assessed, to validate their prognostic values.²³² Microvesicles are small membrane vesicles (<1 μm) shed by cells in response to inflammatory activation, and have a regulatory role in cardiovascular diseases, promoting inflammation, endothelial activation, vascular dysfunction, thrombosis, and atherosclerosis progression. Methodological guidelines have been published for microvesicle analysis and may be applied in our work.^{233,234}
6. Finally, a better understanding of local inflammation is crucial to improve the development of cell-based therapy in AIS, including transplantation of mesenchymal stem cells (MSCs), endothelial progenitor cells (EPCs), or neural precursor cells (NPCs). Cell-based therapy can be divided into two main processes, which are the replacement of pathological affected cells and/or the activation of endogenous mechanisms leading to tissue self-renewal. Functional improvements seen after the transplantation of MSCs in ischemic stroke models are hypothesized to be due to paracrine factors(chemokines, cytokines, neurotrophic factors, and extra-cellular vesicles, commonly referred to as the MSCs secretome), more than homing withing the brain, leading to attenuation of inflammation, release of topic factors, stimulation of endogenous angiogenesis and neurogenesis.^{235,236} However, survival of transplanted cells in the pathological environment is subjected to multiple insults including inflammatory response.²³⁷ Many soluble factors are sensed by MSCs and subsequently

alter their paracrine activities. EPCs are circulating cells harboring both progenitor and stem-cell characteristics. They have the capacity to differentiate into mature endothelial cells and to self-renew.²³⁸ Inflammatory environment influences the proliferation and angiogenic function of EPCs, which is the maintenance of the endothelium by either releasing angiogenic growth factors or acting as a cellular reservoir to replace injured endothelial cells.²³⁹

REFERENCES

1. Amarenco P, Bogousslavsky J, Caplan LR, Donnan GA, Hennerici MG. Classification of stroke subtypes. *Cerebrovasc Dis. Basel Switz.* 2009;27:493–501.
2. Ornello R, Degan D, Tiseo C, Carmine CD, Perciballi L, Pistoia F, Carolei A, Sacco S. Distribution and Temporal Trends From 1993 to 2015 of Ischemic Stroke Subtypes: A Systematic Review and Meta-Analysis. *Stroke.* 2018;STROKEAHA.117.020031.
3. Yaghi S, Bernstein RA, Passman R, Okin PM, Furie KL. Cryptogenic Stroke: Research and Practice. *Circ Res.* 2017;120:527–540.
4. Brozici M, van der Zwan A, Hillen B. Anatomy and Functionality of Leptomeningeal Anastomoses: A Review. *Stroke.* 2003;34:2750–2762.
5. Benjamin EJ, Virani SS, Callaway CW, Chamberlain AM, Chang AR, Cheng S, Chiuve SE, Cushman M, Delling FN, Deo R, et al. Heart Disease and Stroke Statistics—2018 Update: A Report From the American Heart Association. *Circulation.* 2018;137:e67–e492.
6. Smith WS, Lev MH, English JD, Camargo EC, Chou M, Johnston SC, Gonzalez G, Schaefer PW, Dillon WP, Koroshetz WJ, et al. Significance of large vessel intracranial occlusion causing acute ischemic stroke and TIA. *Stroke.* 2009;40:3834–3840.
7. Dozois A, Hampton L, Kingston CW, Lambert G, Porcelli TJ, Sorenson D, Templin M, VonCannon S, Asimos AW. PLUMBER Study (Prevalence of Large Vessel Occlusion Strokes in Mecklenburg County Emergency Response). *Stroke.* 2017;48:3397–3399.
8. Rennert RC, Wali AR, Steinberg JA, Santiago-Dieppa DR, Olson SE, Pannell JS, Khalessi AA. Epidemiology, Natural History, and Clinical Presentation of Large Vessel Ischemic Stroke. *Neurosurgery.* 2019;85:S4–S8.
9. Gibo H, Lenkey C. Microsurgical anatomy of the middle cerebral artery. *J Neurosurg.* 1981;54:19.
10. Bernardo-Castro S, Sousa JA, Brás A, Cecília C, Rodrigues B, Almendra L, Machado C, Santo G, Silva F, Ferreira L, et al. Pathophysiology of Blood–Brain Barrier Permeability Throughout the Different Stages of Ischemic Stroke and Its Implication on Hemorrhagic Transformation and Recovery. *Front. Neurol.* [Internet]. 2020 [cited 2022 Jul 11];11. Available from: <https://www.frontiersin.org/articles/10.3389/fneur.2020.594672>
11. Lin HJ, Wolf PA, Kelly-Hayes M, Beiser AS, Kase CS, Benjamin EJ, D'Agostino RB. Stroke severity in atrial fibrillation. The Framingham Study. *Stroke.* 1996;27:1760–1764.
12. Rahman F, Kwan GF, Benjamin EJ. Global epidemiology of atrial fibrillation. *Nat Rev Cardiol.* 2014;11:639–654.
13. Kishore A, Vail A, Majid A, Dawson J, Lees KR, Tyrrell PJ, Smith CJ. Detection of atrial fibrillation after ischemic stroke or transient ischemic attack: a systematic review and meta-analysis. *Stroke.* 2014;45:520–526.
14. Grond M, Jauss M, Hamann G, Stark E, Veltkamp R, Nabavi D, Horn M, Weimar C, Köhrmann M, Wachter R, et al. Improved detection of silent atrial fibrillation using 72-hour Holter ECG in patients with ischemic stroke: a prospective multicenter cohort study. *Stroke.* 2013;44:3357–3364.
15. Wood W. History and Dissection of a Case, in Which a Foreign Body Was Found within the Heart. *Edinb Med Surg J.* 1814;10:50–54.
16. Harvey EA, Levine SA. A STUDY OF UNINFECTED MURAL THROMBI OF THE HEART.
17. Watson T, Shantsila E, Lip GY. Mechanisms of thrombogenesis in atrial fibrillation: Virchow's triad revisited. *The Lancet.* 2009;373:155–166.
18. Spagnoli LG, Mauriello A, Sangiorgi G, Fratoni S, Bonanno E, Schwartz RS, Piepras DG, Pistolese R, Ippoliti A, Holmes DR. Extracranial thrombotically active carotid plaque as a risk factor for ischemic stroke. *JAMA.* 2004;292:1845–1852.

19. Stoll G, Bendszus M. Inflammation and atherosclerosis: novel insights into plaque formation and destabilization. *Stroke*. 2006;37:1923–1932.
20. Meyer FB, Sundt TM, Piepgras DG, Sandok BA, Forbes G. Emergency carotid endarterectomy for patients with acute carotid occlusion and profound neurological deficits. *Ann. Surg.* 1986;203:82–89.
21. Eker OF, Bühlmann M, Dargazanli C, Kaesmacher J, Mourand I, Gralla J, Arquian C, Fischer UM, Gascou G, Heldner M, et al. Endovascular Treatment of Atherosclerotic Tandem Occlusions in Anterior Circulation Stroke: Technical Aspects and Complications Compared to Isolated Intracranial Occlusions. *Front. Neurol.* 2018;9:1046.
22. Arenillas JF. Intracranial atherosclerosis: current concepts. *Stroke*. 2011;42:S20-23.
23. Dieleman N, Yang W, Abrigo JM, Chu WCW, van der Kolk AG, Siero JCW, Wong KS, Hendrikse J, Chen XY. Magnetic Resonance Imaging of Plaque Morphology, Burden, and Distribution in Patients With Symptomatic Middle Cerebral Artery Stenosis. *Stroke*. 2016;47:1797–1802.
24. Boudiaf N, Attyé A, Warnking JM, Troprès I, Lamalle L, Pietras J, Krainik A. BOLD fMRI of cerebrovascular reactivity in the middle cerebral artery territory: A 100 volunteers' study. *J. Neuroradiol. J. Neuroradiol.* 2015;42:338–344.
25. Karenberg A, Hort I. Medieval Descriptions and Doctrines of Stroke: Preliminary Analysis of Select Sources. Part II: Between Galenism and Aristotelism – Islamic Theories of Apoplexy (800–1200). *J. Hist. Neurosci.* 1998;7:174–185.
26. Tissue Plasminogen Activator for Acute Ischemic Stroke. *N. Engl. J. Med.* 1995;333:1581–1588.
27. Emberson J, Lees KR, Lyden P, Blackwell L, Albers G, Bluhmki E, Brott T, Cohen G, Davis S, Donnan G, et al. Effect of treatment delay, age, and stroke severity on the effects of intravenous thrombolysis with alteplase for acute ischaemic stroke: a meta-analysis of individual patient data from randomised trials. *Lancet Lond. Engl.* 2014;384:1929–1935.
28. Luengo-Fernandez R, Violato M, Candio P, Leal J. Economic burden of stroke across Europe: A population-based cost analysis. *Eur. Stroke J.* 2020;5:17–25.
29. Luengo-Fernandez R, Violato M, Candio P, Leal J. Economic burden of stroke across Europe: A population-based cost analysis. *Eur. Stroke J.* 2020;5:17–25.
30. Hankey GJ, Jamrozik K, Broadhurst RJ, Forbes S, Anderson CS. Long-term disability after first-ever stroke and related prognostic factors in the Perth Community Stroke Study, 1989–1990. *Stroke*. 2002;33:1034–1040.
31. de Bekker A, Geerlings MI, Uitewaal-Poslawsky IE, de Man-van Ginkel JM. Depression in Stroke Survivors: Ten-Year Follow-Up. Determinants of the Natural Course of Depressive Symptoms in Stroke Survivors in the Netherlands: The SMART-Medea Study. *J. Stroke Cerebrovasc. Dis. Off. J. Natl. Stroke Assoc.* 2022;31:106272.
32. Badwaik DrG, Badwaik P. Influence of Psychological Disorders on the Functional Outcomes in the Survivors of Ischemic Stroke. *J. Stroke Cerebrovasc. Dis.* 2021;30:105486.
33. Camilo O, Goldstein LB. Seizures and Epilepsy After Ischemic Stroke. *Stroke*. 2004;35:1769–1775.
34. S B-C, V1 F, V P, Cm L, H S. Auckland Stroke Outcomes Study. Part 2: Cognition and functional outcomes 5 years poststroke. *Neurology [Internet]*. 2010 [cited 2022 Sep 15];75. Available from: <https://pubmed.ncbi.nlm.nih.gov/21041784/>
35. Radford K, Grant M, Sinclair E, Kettlewell J, Watkin C. What is a return to work after stroke? 12-month outcomes in a feasibility trial. *J. Rehabil. Med.* 2020;0.
36. Hacke W, Kaste M, Bluhmki E, Brozman M, Dávalos A, Guidetti D, Larrue V, Lees KR, Medeghri Z, Machnig T, et al. Thrombolysis with alteplase 3 to 4.5 hours after acute ischemic stroke. *N. Engl. J. Med.* 2008;359:1317–1329.
37. Campbell BCV, Ma H, Ringleb PA, Parsons MW, Churilov L, Bendszus M, Levi CR,

- Hsu C, Kleinig TJ, Fatar M, et al. Extending thrombolysis to 4·5–9 h and wake-up stroke using perfusion imaging: a systematic review and meta-analysis of individual patient data. *Lancet Lond Engl*. 2019;394:139–147.
38. Thomalla G, Boutitie F, Ma H, Koga M, Ringleb P, Schwamm LH, Wu O, Bendszus M, Bladin CF, Campbell BCV, et al. Intravenous alteplase for stroke with unknown time of onset guided by advanced imaging: systematic review and meta-analysis of individual patient data. *Lancet Lond Engl*. 2020;396:1574–1584.
39. Saqqur M, Uchino K, Demchuk AM, Molina CA, Garami Z, Calleja S, Akhtar N, Orouk FO, Salam A, Shuaib A, et al. Site of arterial occlusion identified by transcranial Doppler predicts the response to intravenous thrombolysis for stroke. *Stroke*. 2007;38:948–954.
40. del Zoppo GJ, Higashida RT, Furlan AJ, Pessin MS, Rowley HA, Gent M. PROACT: a phase II randomized trial of recombinant pro-urokinase by direct arterial delivery in acute middle cerebral artery stroke. PROACT Investigators. Prolyse in Acute Cerebral Thromboembolism. *Stroke*. 1998;29:4–11.
41. Furlan A, Higashida R, Wechsler L, Gent M, Rowley H, Kase C, Pessin M, Ahuja A, Callahan F, Clark WM, et al. Intra-arterial Prourokinase for Acute Ischemic StrokeThe PROACT II Study: A Randomized Controlled Trial. *JAMA*. 1999;282:2003–2011.
42. Smith WS, Sung G, Starkman S, Saver JL, Kidwell CS, Gobin YP, Lutsep HL, Nesbit GM, Grobelny T, Rymer MM, et al. Safety and efficacy of mechanical embolectomy in acute ischemic stroke: results of the MERCI trial. *Stroke*. 2005;36:1432–1438.
43. Smith WS, Sung G, Saver J, Budzik R, Duckwiler G, Liebeskind DS, Lutsep HL, Rymer MM, Higashida RT, Starkman S, et al. Mechanical thrombectomy for acute ischemic stroke: final results of the Multi MERCI trial. *Stroke*. 2008;39:1205–1212.
44. Saver JL, Jahan R, Levy EI, Jovin TG, Baxter B, Nogueira RG, Clark W, Budzik R, Zaidat OO, SWIFT Trialists. Solitaire flow restoration device versus the Merci Retriever in patients with acute ischaemic stroke (SWIFT): a randomised, parallel-group, non-inferiority trial. *Lancet Lond Engl*. 2012;380:1241–1249.
45. Nogueira RG, Lutsep HL, Gupta R, Jovin TG, Albers GW, Walker GA, Liebeskind DS, Smith WS. Trevo versus Merci retrievers for thrombectomy revascularisation of large vessel occlusions in acute ischaemic stroke (TREVO 2): a randomised trial. *The Lancet*. 2012;380:1231–1240.
46. Kidwell CS, Jahan R, Gornbein J, Alger JR, Nenov V, Ajani Z, Feng L, Meyer BC, Olson S, Schwamm LH, et al. A Trial of Imaging Selection and Endovascular Treatment for Ischemic Stroke. *N Engl J Med*. 2013;368:914–923.
47. Broderick JP, Palesch YY, Demchuk AM, Yeatts SD, Khatri P, Hill MD, Jauch EC, Jovin TG, Yan B, Silver FL, et al. Endovascular Therapy after Intravenous t-PA versus t-PA Alone for Stroke. *N Engl J Med*. 2013;368:893–903.
48. Ciccone A, Valvassori L, Nichelatti M, Sgoifo A, Ponzio M, Sterzi R, Boccardi E, SYNTHESIS Expansion Investigators. Endovascular treatment for acute ischemic stroke. *N Engl J Med*. 2013;368:904–913.
49. Berkhemer OA, Fransen PSS, Beumer D, van den Berg LA, Lingsma HF, Yoo AJ, Schonewille WJ, Vos JA, Nederkoorn PJ, Wermer MJH, et al. A Randomized Trial of Intraarterial Treatment for Acute Ischemic Stroke. *N Engl J Med*. 2015;372:11–20.
50. Jovin TG, Chamorro A, Cobo E, de Miquel MA, Molina CA, Rovira A, San Román L, Serena J, Abilleira S, Ribó M, et al. Thrombectomy within 8 Hours after Symptom Onset in Ischemic Stroke. *N Engl J Med*. 2015;372:2296–2306.
51. Goyal M, Demchuk AM, Menon BK, Eesa M, Rempel JL, Thornton J, Roy D, Jovin TG, Willinsky RA, Sapkota BL, et al. Randomized Assessment of Rapid Endovascular Treatment of Ischemic Stroke. *N Engl J Med*. 2015;372:1019–1030.

52. Saver JL, Goyal M, Bonafe A, Diener H-C, Levy EI, Pereira VM, Albers GW, Cognard C, Cohen DJ, Hacke W, et al. Stent-Retriever Thrombectomy after Intravenous t-PA vs. t-PA Alone in Stroke. *N. Engl. J. Med.* 2015;372:2285–2295.
53. Campbell BCV, Mitchell PJ, Kleinig TJ, Dewey HM, Churilov L, Yassi N, Yan B, Dowling RJ, Parsons MW, Oxley TJ, et al. Endovascular Therapy for Ischemic Stroke with Perfusion-Imaging Selection. *N. Engl. J. Med.* 2015;372:1009–1018.
54. Bracard S, Ducrocq X, Mas JL, Soudant M, Oppenheim C, Moulin T, Guillemin F, THRACE investigators. Mechanical thrombectomy after intravenous alteplase versus alteplase alone after stroke (THRACE): a randomised controlled trial. *Lancet Neurol.* 2016;15:1138–1147.
55. Muir KW, Ford GA, Messow C-M, Ford I, Murray A, Clifton A, Brown MM, Madigan J, Lenthall R, Robertson F, et al. Endovascular therapy for acute ischaemic stroke: the Pragmatic Ischaemic Stroke Thrombectomy Evaluation (PISTE) randomised, controlled trial. *J. Neurol. Neurosurg. Psychiatry.* 2017;88:38–44.
56. Nogueira RG, Jadhav AP, Haussen DC, Bonafe A, Budzik RF, Bhuvan P, Yavagal DR, Ribo M, Cognard C, Hanel RA, et al. Thrombectomy 6 to 24 Hours after Stroke with a Mismatch between Deficit and Infarct. *N. Engl. J. Med.* 2018;378:11–21.
57. Albers GW, Marks MP, Kemp S, Christensen S, Tsai JP, Ortega-Gutierrez S, McTaggart RA, Torbey MT, Kim-Tenser M, Leslie-Mazwi T, et al. Thrombectomy for Stroke at 6 to 16 Hours with Selection by Perfusion Imaging. *N. Engl. J. Med.* 2018;378:708–718.
58. Chia NH, Leyden JM, Newbury J, Jannes J, Kleinig TJ. Determining the Number of Ischemic Strokes Potentially Eligible for Endovascular Thrombectomy: A Population-Based Study. *Stroke.* 2016;47:1377–1380.
59. Forestier G, Kerleroux B, Janot K, Zhu F, Dumas V, Hak J-F, Shotar E, Ben Hassen W, Bourcier R, Soize S, et al. Mechanical thrombectomy practices in France: Exhaustive survey of centers and individual operators. *J. Neuroradiol. J. Neuroradiol.* 2020;47:410–415.
60. Marder VJ, Chute DJ, Starkman S, Abolian AM, Kidwell C, Liebeskind D, Ovbiagele B, Vinuela F, Duckwiler G, Jahan R, et al. Analysis of Thrombi Retrieved From Cerebral Arteries of Patients With Acute Ischemic. *Stroke.* 2006;37:2086–2093.
61. Niesten JM, van der Schaaf IC, van Dam L, Vink A, Vos JA, Schonewille WJ, de Bruin PC, Mali WPTM, Velthuis BK. Histopathologic composition of cerebral thrombi of acute stroke patients is correlated with stroke subtype and thrombus attenuation. *PloS One.* 2014;9:e88882.
62. Bang OY, Ovbiagele B, Kim JS. Evaluation of Cryptogenic Stroke With Advanced Diagnostic Techniques. *Stroke.* 2014;45:1186–1194.
63. Niessen F, Hilger T, Hoehn M, Hossmann K-A. Differences in clot preparation determine outcome of recombinant tissue plasminogen activator treatment in experimental thromboembolic stroke. *Stroke J. Cereb. Circ.* 2003;34:2019–2024.
64. Tomkins AJ, Schleicher N, Murtha L, Kaps M, Levi CR, Nedelmann M, Spratt NJ. Platelet rich clots are resistant to lysis by thrombolytic therapy in a rat model of embolic stroke. *Exp. Transl. Stroke Med.* 2015;7:2.
65. Choi MH, Park GH, Lee JS, Lee SE, Lee S-J, Kim J-H, Hong JM. Erythrocyte Fraction Within Retrieved Thrombi Contributes to Thrombolytic Response in Acute Ischemic Stroke. *Stroke.* 2018;49:652–659.
66. Jolugbo P, Ariëns R. Thrombus composition and efficacy of thrombolysis and thrombectomy in acute ischaemic stroke. *Stroke.* 2021;52:1131–1142.
67. Fennell VS, Nagesh SVS, Meess KM, Gutierrez L, James RH, Springer ME, Siddiqui AH. What to do about fibrin rich ‘tough clots’? Comparing the Solitaire stent retriever with a novel geometric clot extractor in an in vitro stroke model. *J. NeuroInterventional Surg.* 2018;10:907–910.

68. Berg R van den, Ribó M, Arnberg F, Estrade L, Thornton J, Weitz AT, Gontu V, Karam A, Hernández D, Clarençon F, et al. P64 NIMBUS geometric clot extractor for tough clots: SPERO study results and clot composition. *J. NeuroInterventional Surg.* 2022;14:A34–A34.
69. Tiedt Steffen, Herzberg Moriz, Küpper Clemens, Feil Katharina, Kellert Lars, Dorn Franziska, Liebig Thomas, Alegiani Anna, Dichgans Martin, Wollenweber Frank A., et al. Stroke Etiology Modifies the Effect of Endovascular Treatment in Acute Stroke. *Stroke.* 0:STROKEAHA.119.028383.
70. Jickling GC, Sharp FR. Biomarker panels in ischemic stroke. *Stroke J. Cereb. Circ.* 2015;46:915–920.
71. De Meyer SF, Andersson T, Baxter B, Bendszus M, Brouwer P, Brinjikji W, Campbell BC, Costalat V, Dávalos A, Demchuk A, et al. Analyses of thrombi in acute ischemic stroke: A consensus statement on current knowledge and future directions. *Int. J. Stroke.* 2017;12:606–614.
72. Sweeney MD, Zhao Z, Montagne A, Nelson AR, Zlokovic BV. Blood-Brain Barrier: From Physiology to Disease and Back. *Physiol. Rev.* 2019;99:21–78.
73. Librizzi L, de Cutis M, Janigro D, Runtz L, de Bock F, Barbier EL, Marchi N. Cerebrovascular heterogeneity and neuronal excitability. *Neurosci. Lett.* 2018;667:75–83.
74. Giannoni P, Badaut J, Dargazanli C, De Maudave AF, Klement W, Costalat V, Marchi N. The pericyte-glia interface at the blood-brain barrier. *Clin. Sci. Lond. Engl.* 1979. 2018;132:361–374.
75. Nation DA, Sweeney MD, Montagne A, Sagare AP, D’Orazio LM, Pachicano M, Sepehrband F, Nelson AR, Buennagel DP, Harrington MG, et al. Blood-brain barrier breakdown is an early biomarker of human cognitive dysfunction. *Nat. Med.* 2019;25:270–276.
76. Aliena-Valero A, Baixaulli-Martín J, Torregrosa G, Tembl JI, Salom JB. Clot Composition Analysis as a Diagnostic Tool to Gain Insight into Ischemic Stroke Etiology: A Systematic Review. *J. Stroke.* 2021;23:327–342.
77. Fitzgerald S, Mereuta OM, Doyle KM, Kallmes DF, Brinjikji W. Correlation of imaging and histopathology of thrombi in acute ischemic stroke with etiology and outcome. *J. Neurosurg. Sci.* 2019;63:292–300.
78. Benson JC, Kallmes DF, Larson AS, Brinjikji W. Radiology-Pathology Correlations of Intracranial Clots: Current Theories, Clinical Applications, and Future Directions. *AJNR Am. J. Neuroradiol.* 2021;42:1558–1565.
79. Liebeskind DS, Sanossian N, Yong WH, Starkman S, Tsang MP, Moya AL, Zheng DD, Abolian AM, Kim D, Ali LK, et al. CT and MRI early vessel signs reflect clot composition in acute stroke. *Stroke J. Cereb. Circ.* 2011;42:1237–1243.
80. Kim SK, Yoon W, Kim TS, Kim HS, Heo TW, Park MS. Histologic Analysis of Retrieved Clots in Acute Ischemic Stroke: Correlation with Stroke Etiology and Gradient-Echo MRI. *AJNR Am. J. Neuroradiol.* 2015;
81. Bourcier R, Mazighi M, Labreuche J, Fahed R, Blanc R, Gory B, Duhamel A, Marnat G, Saleme S, Costalat V, et al. Susceptibility Vessel Sign in the ASTER Trial: Higher Recanalization Rate and More Favourable Clinical Outcome after First Line Stent Retriever Compared to Contact Aspiration. *J. Stroke.* 2018;20:268–276.
82. McMahon Naoimh E., Banga Munirah, Benedetto Valerio, Bray Emma P., Georgiou Rachel F., Gibson Josephine M.E., Lane Deirdre A., Al-Khalidi A. Hakam, Chatterjee Kausik, Chauhan Umesh, et al. Etiologic Workup in Cases of Cryptogenic Stroke. *Stroke.* 2020;51:1419–1427.
83. Boeckh-Behrens T, Schubert M, Förschler A, Prothmann S, Kreiser K, Zimmer C, Rieger J, Bauer J, Neff F, Kehl V, et al. The Impact of Histological Clot Composition in

- Embolic Stroke. *Clin. Neuroradiol.* [Internet]. 2014 [cited 2015 Jan 2]; Available from: <http://link.springer.com/10.1007/s00062-014-0347-x>
84. Jander S, Sitzer M, Schumann R, Schroeter M, Siebler M, Steinmetz H, Stoll G. Inflammation in High-Grade Carotid Stenosis : A Possible Role for Macrophages and T Cells in Plaque Destabilization. *Stroke*. 1998;29:1625–1630.
85. Profumo E, Buttari B, Tosti ME, Tagliani A, Capoano R, D'Amati G, Businaro R, Salvati B, Riganò R. Plaque-infiltrating T lymphocytes in patients with carotid atherosclerosis: an insight into the cellular mechanisms associated to plaque destabilization. *J. Cardiovasc. Surg. (Torino)*. 2013;54:349–357.
86. Dargazanli C, Rigau V, Omer E. High CD3+ cells in intracranial thrombi represent a biomarker of atherothrombotic stroke. *PLoS ONE*. 2016;
87. Li S, Huang Y, Liu Y, Rocha M, Li X, Wei P, Misilimu D, Luo Y, Zhao J, Gao Y. Change and predictive ability of circulating immunoregulatory lymphocytes in long-term outcomes of acute ischemic stroke. *J. Cereb. Blood Flow Metab.* 2021;41:2280–2294.
88. Schuhmann MK, Bieber M, Franke M, Kollikowski AM, Stegner D, Heinze KG, Nieswandt B, Pham M, Stoll G. Platelets and lymphocytes drive progressive penumbral tissue loss during middle cerebral artery occlusion in mice. *J. Neuroinflammation*. 2021;18:46.
89. Zhou Y-X, Wang X, Tang D, Li Y, Jiao Y-F, Gan Y, Hu X-M, Yang L-Q, Yu W-F, Stetler RA, et al. IL-2mAb reduces demyelination after focal cerebral ischemia by suppressing CD8+ T cells. *CNS Neurosci. Ther.* 2019;25:532–543.
90. Liesz A, Suri-Payer E, Veltkamp C, Doerr H, Sommer C, Rivest S, Giese T, Veltkamp R. Regulatory T cells are key cerebroprotective immunomodulators in acute experimental stroke. *Nat. Med.* 2009;15:192–199.
91. Biomarkers Definitions Working Group. Biomarkers and surrogate endpoints: preferred definitions and conceptual framework. *Clin. Pharmacol. Ther.* 2001;69:89–95.
92. Dagonnier M, Donnan GA, Davis SM, Dewey HM, Howells DW. Acute Stroke Biomarkers: Are We There Yet? *Front. Neurol.* [Internet]. 2021 [cited 2022 Sep 16];12. Available from: <https://www.frontiersin.org/articles/10.3389/fneur.2021.619721>
93. Bustamante A, López-Cancio E, Pich S, Penalba A, Giralt D, García-Berrocoso T, Ferrer-Costa C, Gasull T, Hernández-Pérez M, Millan M, et al. Blood Biomarkers for the Early Diagnosis of Stroke: The Stroke-Chip Study. *Stroke*. 2017;48:2419–2425.
94. Dargazanli C, Zub E, Deverdun J, Decourcelle M, de Bock F, Labreuche J, Lefèvre P-H, Gascou G, Derraz I, Riquelme Bareiro C, et al. Machine Learning Analysis of the Cerebrovascular Thrombi Proteome in Human Ischemic Stroke: An Exploratory Study. *Front. Neurol.* 2020;11:575376.
95. Hochrainer K, Yang W. Stroke Proteomics: From Discovery to Diagnostic and Therapeutic Applications. *Circ. Res.* 2022;130:1145–1166.
96. Rao NM, Capri J, Cohn W, Abdaljaleel M, Restrepo L, Gornbein JA, Yong WH, Liebeskind DS, Whitelegge JP. Peptide Composition of Stroke Causing Emboli Correlate with Serum Markers of Atherosclerosis and Inflammation. *Front. Neurol.* [Internet]. 2017 [cited 2019 Sep 19];8. Available from: <https://www.ncbi.nlm.nih.gov/pmc/articles/PMC5585134/>
97. Lepedda AJ, Cigliano A, Cherchi GM, Spirito R, Maggioni M, Carta F, Turrini F, Edelstein C, Scanu AM, Formato M. A proteomic approach to differentiate histologically classified stable and unstable plaques from human carotid arteries. *Atherosclerosis*. 2009;203:112–118.
98. Muñoz R, Santamaría E, Rubio I, Ausín K, Ostolaza A, Labarga A, Roldán M, Zandio B, Mayor S, Bermejo R, et al. Mass Spectrometry-Based Proteomic Profiling of Thrombotic Material Obtained by Endovascular Thrombectomy in Patients with Ischemic Stroke. *Int. J. Mol. Sci.* 2018;19:498.

99. Alonso-Orgaz S, Moreno-Luna R, López JA, Gil-Dones F, Padial LR, Moreu J, de la Cuesta F, Barderas MG. Proteomic characterization of human coronary thrombus in patients with ST-segment elevation acute myocardial infarction. *J. Proteomics*. 2014;109:368–381.
100. Kollikowski AM, Schuhmann MK, Nieswandt B, Müllges W, Stoll G, Pham M. Local leukocyte invasion during hyperacute human ischemic stroke. *Ann. Neurol.* 2020;ana.25665.
101. Strinitz M, Pham M, März AG, Feick J, Weidner F, Vogt ML, Essig F, Neugebauer H, Stoll G, Schuhmann MK, et al. Immune Cells Invade the Collateral Circulation during Human Stroke: Prospective Replication and Extension. *Int. J. Mol. Sci.* 2021;22:9161.
102. Kollikowski AM, Pham M, März AG, Papp L, Nieswandt B, Stoll G, Schuhmann MK. Platelet Activation and Chemokine Release Are Related to Local Neutrophil-Dominant Inflammation During Hyperacute Human Stroke. *Transl. Stroke Res.* 2022;13:364–369.
103. Fraser JF, Collier LA, Gorman AA, Martha SR, Salmeron KE, Trout AL, Edwards DN, Davis SM, Lukins DE, Alhajeri A, et al. The Blood And Clot Thrombectomy Registry And Collaboration (BACTRAC) protocol: novel method for evaluating human stroke. *J. NeuroInterventional Surg.* 2019;11:265–270.
104. Shaw BC, Maglinger GB, Ujas T, Rupareliya C, Fraser JF, Grupke S, Kesler M, Gelderblom M, Pennypacker KR, Turchan-Cholewo J, et al. Isolation and identification of leukocyte populations in intracranial blood collected during mechanical thrombectomy. *J. Cereb. Blood Flow Metab.* 2022;42:280–291.
105. Maglinger B, Sands M, Frank JA, McLouth CJ, Trout AL, Roberts JM, Grupke S, Turchan-Cholewo J, Stowe AM, Fraser JF, et al. Intracranial VCAM1 at time of mechanical thrombectomy predicts ischemic stroke severity. *J. Neuroinflammation*. 2021;18:109.
106. Cook-Mills JM, Marchese ME, Abdala-Valencia H. Vascular Cell Adhesion Molecule-1 Expression and Signaling During Disease: Regulation by Reactive Oxygen Species and Antioxidants. *Antioxid. Redox Signal.* 2011;15:1607–1638.
107. Janelidze S, Mattsson N, Stomrud E, Lindberg O, Palmqvist S, Zetterberg H, Blennow K, Hansson O. CSF biomarkers of neuroinflammation and cerebrovascular dysfunction in early Alzheimer disease. *Neurology*. 2018;91:e867–e877.
108. Sun B, Tang N, Peluso MJ, Iyer NS, Torres L, Donatelli JL, Munter SE, Nixon CC, Rutishauser RL, Rodriguez-Barraquer I, et al. Characterization and Biomarker Analyses of Post-COVID-19 Complications and Neurological Manifestations. *Cells*. 2021;10:386.
109. Di Battista AP, Buonora JE, Rhind SG, Hutchison MG, Baker AJ, Rizoli SB, Diaz-Arrastia R, Mueller GP. Blood Biomarkers in Moderate-To-Severe Traumatic Brain Injury: Potential Utility of a Multi-Marker Approach in Characterizing Outcome. *Front. Neurol.* 2015;6:110.
110. Buonora JE, Yarnell AM, Lazarus RC, Mousseau M, Latour LL, Rizoli SB, Baker AJ, Rhind SG, Diaz-Arrastia R, Mueller GP. Multivariate analysis of traumatic brain injury: development of an assessment score. *Front. Neurol.* 2015;6:68.
111. Lee JW, Devanarayan V, Barrett YC, Weiner R, Allinson J, Fountain S, Keller S, Weinryb I, Green M, Duan L, et al. Fit-for-Purpose Method Development and Validation for Successful Biomarker Measurement. *Pharm. Res.* 2006;23:312–328.
112. Markus A, Valerie S, Mira K. Promising Biomarker Candidates for Cardioembolic Stroke Etiology. A Brief Narrative Review and Current Opinion. *Front. Neurol.* 2021;12:624930.
113. Boos CJ, Anderson RA, Lip GYH. Is atrial fibrillation an inflammatory disorder? *Eur. Heart J.* 2006;27:136–149.
114. Guo Y, Lip GYH, Apostolakis S. Inflammation in atrial fibrillation. *J. Am. Coll. Cardiol.* 2012;60:2263–2270.
115. Pisner DA, Schnyer DM. Support vector machine [Internet]. In: Machine Learning. Elsevier; 2020 [cited 2022 Aug 6]. p. 101–121. Available from:

<https://linkinghub.elsevier.com/retrieve/pii/B9780128157398000067>

116. Noble WS. What is a support vector machine? *Nat. Biotechnol.* 2006;24:1565–1567.
117. Han H, Jiang X. Overcome Support Vector Machine Diagnosis Overfitting. *Cancer Inform.* 2014;13:145–158.
118. Powers William J., Rabinstein Alejandro A., Ackerson Teri, Adeoye Opeolu M., Bambakidis Nicholas C., Becker Kyra, Biller José, Brown Michael, Demaerschalk Bart M., Hoh Brian, et al. Guidelines for the Early Management of Patients With Acute Ischemic Stroke: 2019 Update to the 2018 Guidelines for the Early Management of Acute Ischemic Stroke: A Guideline for Healthcare Professionals From the American Heart Association/American Stroke Association. *Stroke.* 2019;50:e344–e418.
119. Furie KL, Jayaraman MV. 2018 Guidelines for the Early Management of Patients With Acute Ischemic Stroke. *Stroke.* 2018;49:509–510.
120. Puetz V, Sylaja P n., Coutts SB, Hill MD, Dzialowski I, Mueller P, Becker U, Urban G, O'Reilly C, Barber PA, et al. Extent of Hypoattenuation on CT Angiography Source Images Predicts Functional Outcome in Patients With Basilar Artery Occlusion. *Stroke.* 2008;39:2485–2490.
121. Turk AS, Frei D, Fiorella D, Mocco J, Baxter B, Siddiqui A, Spiotta A, Mokin M, Dewan M, Quarfordt S, et al. ADAPT FAST study: a direct aspiration first pass technique for acute stroke thrombectomy. *J. Neurointerventional Surg.* 2014;6:260–264.
122. Dargazanli C, Fahed R, Blanc R, Gory B, Labreuche J, Duhamel A, Marnat G, Saleme S, Costalat V, Bracard S, et al. Modified Thrombolysis in Cerebral Infarction 2C/Thrombolysis in Cerebral Infarction 3 Reperfusion Should Be the Aim of Mechanical Thrombectomy: Insights From the ASTER Trial (Contact Aspiration Versus Stent Retriever for Successful Revascularization). *Stroke.* 2018;49:1189–1196.
123. Fugate JE, Klunder AM, Kallmes DF. What Is Meant by “TICI”? *Am. J. Neuroradiol.* 2013;34:1792–1797.
124. Jm P, Nl R, N H, Jc T, S M, A B, M S, W B, Df K, Km K. Comparison of Balloon Guide Catheters and Standard Guide Catheters for Acute Ischemic Stroke: A Systematic Review and Meta-Analysis. *World Neurosurg.* [Internet]. 2021 [cited 2022 Sep 15];154. Available from: <https://pubmed.ncbi.nlm.nih.gov/34280538/>
125. Swinbanks D. Australia backs innovation, shuns telescope. *Nature.* 1995;378:653–653.
126. Rogers JC, Bomgarden RD. Sample Preparation for Mass Spectrometry-Based Proteomics; from Proteomes to Peptides. *Adv. Exp. Med. Biol.* 2016;919:43–62.
127. Kiser JZ, Post M, Wang B, Miyagi M. Streptomyces erythraeus Trypsin for Proteomics Applications. *J. Proteome Res.* 2009;8:1810–1817.
128. Polaskova V, Kapur A, Khan A, Molloy MP, Baker MS. High-abundance protein depletion: comparison of methods for human plasma biomarker discovery. *Electrophoresis.* 2010;31:471–482.
129. Tubaon RM, Haddad PR, Quirino JP. Sample Clean-up Strategies for ESI Mass Spectrometry Applications in Bottom-up Proteomics: Trends from 2012 to 2016. *Proteomics.* 2017;17.
130. Yamashita M, Fenn JB. Electrospray ion source. Another variation on the free-jet theme. *J. Phys. Chem.* 1984;88:4451–4459.
131. Bateman NW, Goulding SP, Shulman NJ, Gadok AK, Szumlinski KK, MacCoss MJ, Wu CC. Maximizing Peptide Identification Events in Proteomic Workflows Using Data-Dependent Acquisition (DDA). *Mol. Cell. Proteomics MCP.* 2014;13:329–338.
132. Tyanova S, Temu T, Cox J. The MaxQuant computational platform for mass spectrometry-based shotgun proteomics. *Nat. Protoc.* 2016;11:2301–2319.
133. Rossi R, Mereuta OM, Barbachan e Silva M, Molina Gil S, Douglas A, Pandit A,

- Gilvarry M, McCarthy R, O'Connell S, Tierney C, et al. Potential Biomarkers of Acute Ischemic Stroke Etiology Revealed by Mass Spectrometry-Based Proteomic Characterization of Formalin-Fixed Paraffin-Embedded Blood Clots. *Front. Neurol.* [Internet]. 2022 [cited 2022 Jul 23];13. Available from: <https://www.frontiersin.org/articles/10.3389/fneur.2022.854846>
134. Brinjikji W, Abbasi M, Mereuta OM, Fitzgerald S, Larco JA, Dai D, Kadirvel R, Nogueira RG, Kvamme P, Layton KF, et al. Histological composition of retrieved emboli in acute ischemic stroke is independent of pre-thrombectomy alteplase use. *J. Stroke Cerebrovasc. Dis. Off. J. Natl. Stroke Assoc.* 2022;31:106376.
135. Lyden PD. Cerebroprotection for Acute Ischemic Stroke: Looking Ahead. *Stroke.* 2021;52:3033–3044.
136. Jickling GC, Liu D, Ander BP, Stamova B, Zhan X, Sharp FR. Targeting neutrophils in ischemic stroke: translational insights from experimental studies. *J. Cereb. Blood Flow Metab.* 2015;35:888–901.
137. Albers GW, Thijs VN, Wechsler L, Kemp S, Schlaug G, Skalabrin E, Bammer R, Kakuda W, Lansberg MG, Shuaib A, et al. Magnetic resonance imaging profiles predict clinical response to early reperfusion: the diffusion and perfusion imaging evaluation for understanding stroke evolution (DEFUSE) study. *Ann. Neurol.* 2006;60:508–517.
138. Ramos-Cejudo J, Gutiérrez-Fernández M, Rodríguez-Frutos B, Alcaide ME, Sánchez-Cabo F, Dopazo A, Díez-Tejedor E. Spatial and Temporal Gene Expression Differences in Core and Periinfarct Areas in Experimental Stroke: A Microarray Analysis. *PLOS ONE.* 2012;7:e52121.
139. García-Berrocoso T, Giralt D, Llombart V, Bustamante A, Penalba A, Flores A, Ribó M, Molina CA, Rosell A, Montaner J. Chemokines after human ischemic stroke: From neurovascular unit to blood using protein arrays. *Transl. Proteomics.* 2014;3:1–9.
140. Wang X, Ellison JA, Siren AL, Lysko PG, Yue TL, Barone FC, Shatzman A, Feuerstein GZ. Prolonged expression of interferon-inducible protein-10 in ischemic cortex after permanent occlusion of the middle cerebral artery in rat. *J. Neurochem.* 1998;71:1194–1204.
141. Wang L, Li Y, Chen X, Chen J, Gautam SC, Xu Y, Chopp M. MCP-1, MIP-1, IL-8 and Ischemic Cerebral Tissue Enhance Human Bone Marrow Stromal Cell Migration in Interface Culture. *Hematology.* 2002;7:113–117.
142. Yilmaz G, Arumugam TV, Stokes KY, Granger DN. Role of T lymphocytes and interferon-gamma in ischemic stroke. *Circulation.* 2006;113:2105–2112.
143. Seifert HA, Collier LA, Chapman CB, Benkovic SA, Willing AE, Pennypacker KR. Pro-Inflammatory Interferon Gamma Signaling is Directly Associated with Stroke Induced Neurodegeneration. *J. Neuroimmune Pharmacol.* 2014;9:679–689.
144. Fouda AY, Kozak A, Alhusban A, Switzer JA, Fagan SC. Anti-inflammatory IL-10 is upregulated in both hemispheres after experimental ischemic stroke: Hypertension blunts the response. *Exp. Transl. Stroke Med.* 2013;5:12.
145. Pérez-de Puig I, Miró F, Salas-Perdomo A, Bonfill-Texidor E, Ferrer-Ferrer M, Márquez-Kisinousky L, Planas AM. IL-10 deficiency exacerbates the brain inflammatory response to permanent ischemia without preventing resolution of the lesion. *J. Cereb. Blood Flow Metab.* 2013;33:1955–1966.
146. Kolosowska N, Keuters MH, Wojciechowski S, Keksa-Goldsteine V, Laine M, Malm T, Goldsteins G, Koistinaho J, Dhungana H. Peripheral Administration of IL-13 Induces Anti-inflammatory Microglial/Macrophage Responses and Provides Neuroprotection in Ischemic Stroke. *Neurother. J. Am. Soc. Exp. Neurother.* 2019;16:1304–1319.
147. Murray KN, Parry-Jones AR, Allan SM. Interleukin-1 and acute brain injury. *Front. Cell. Neurosci.* 2015;9:18.

148. Sobowale OA, Parry-Jones AR, Smith CJ, Tyrrell PJ, Rothwell NJ, Allan SM. Interleukin-1 in Stroke: From Bench to Bedside. *Stroke*. 2016;47:2160–2167.
149. Borlongan MC, Kingsbury C, Salazar FE, Toledo ARL, Monroy GR, Sadanandan N, Cozene B, Gonzales-Portillo B, Saft M, Wang Z-J, et al. IL-2/IL-2R Antibody Complex Enhances Treg-Induced Neuroprotection by Dampening TNF- α Inflammation in an In Vitro Stroke Model. *Neuromolecular Med*. 2021;23:540–548.
150. Zhao X, Wang H, Sun G, Zhang J, Edwards NJ, Aronowski J. Neuronal Interleukin-4 as a Modulator of Microglial Pathways and Ischemic Brain Damage. *J. Neurosci. Off. J. Soc. Neurosci*. 2015;35:11281–11291.
151. Chen X, Zhang J, Song Y, Yang P, Yang Y, Huang Z, Wang K. Deficiency of anti-inflammatory cytokine IL-4 leads to neural hyperexcitability and aggravates cerebral ischemia-reperfusion injury. *Acta Pharm. Sin. B*. 2020;10:1634–1645.
152. Shu J, Fang X-H, Li Y-J, Deng Y, Wei W-S, Zhang L. Microglia-induced autophagic death of neurons via IL-6/STAT3/miR-30d signaling following hypoxia/ischemia. *Mol. Biol. Rep*. 2022;49:7697–7707.
153. Li C, Hu L, Zhao J, Di M, Fan C, Han L, Zhu X. Effect of intravenous thrombolysis combined with mild hypothermia on the levels of IL-1 β , IL-6, ICAM-1 and MMP-2 in patients with acute cerebral infarction and clinical significance. *Exp. Ther. Med*. 2022;23:223.
154. Shetelig C, Limalanathan S, Hoffmann P, Seljeflot I, Gran JM, Eritsland J, Andersen GØ. Association of IL-8 With Infarct Size and Clinical Outcomes in Patients With STEMI. *J. Am. Coll. Cardiol*. 2018;72:187–198.
155. Xue Y, Zeng X, Tu W-J, Zhao J. Tumor Necrosis Factor- α : The Next Marker of Stroke. *Dis. Markers*. 2022;2022:2395269.
156. Clausen BH, Degn M, Martin NA, Couch Y, Karimi L, Ormhøj M, Mortensen M-LB, Gredal HB, Gardiner C, Sargent IIL, et al. Systemically administered anti-TNF therapy ameliorates functional outcomes after focal cerebral ischemia. *J. Neuroinflammation*. 2014;11:203.
157. Lin S-Y, Wang Y-Y, Chang C-Y, Wu C-C, Chen W-Y, Liao S-L, Chen C-J. TNF- α Receptor Inhibitor Alleviates Metabolic and Inflammatory Changes in a Rat Model of Ischemic Stroke. *Antioxidants*. 2021;10:851.
158. Lambertsen KL, Clausen BH, Babcock AA, Gregersen R, Fenger C, Nielsen HH, Haugaard LS, Wirenfeldt M, Nielsen M, Dagnaes-Hansen F, et al. Microglia protect neurons against ischemia by synthesis of tumor necrosis factor. *J. Neurosci. Off. J. Soc. Neurosci*. 2009;29:1319–1330.
159. Uyemura K, Demer LL, Castle SC, Jullien D, Berliner JA, Gately MK, Warrier RR, Pham N, Fogelman AM, Modlin RL. Cross-regulatory roles of interleukin (IL)-12 and IL-10 in atherosclerosis. *J. Clin. Invest*. 1996;97:2130–2138.
160. Abbas A, Gregersen I, Holm S, Daissormont I, Bjerkeli V, Krohg-Sørensen K, Skagen KR, Dahl TB, Russell D, Almås T, et al. Interleukin 23 levels are increased in carotid atherosclerosis: possible role for the interleukin 23/interleukin 17 axis. *Stroke*. 2015;46:793–799.
161. Li M, Li Z, Yao Y, Jin W-N, Wood K, Liu Q, Shi F-D, Hao J. Astrocyte-derived interleukin-15 exacerbates ischemic brain injury via propagation of cellular immunity. *Proc. Natl. Acad. Sci. U. S. A*. 2017;114:E396–E405.
162. Lee GA, Lin T-N, Chen C-Y, Mau S-Y, Huang W-Z, Kao Y-C, Ma R-Y, Liao N-S. Interleukin 15 blockade protects the brain from cerebral ischemia-reperfusion injury. *Brain. Behav. Immun*. 2018;73:562–570.
163. Mathy NL, Scheuer W, Lanzendorfer M, Honold K, Ambrosius D, Norley S, Kurth R. Interleukin-16 stimulates the expression and production of pro-inflammatory cytokines by human monocytes. *Immunology*. 2000;100:63–69.

164. Schwab JM, Nguyen TD, Meyermann R, Schluesener HJ. Human focal cerebral infarctions induce differential lesional interleukin-16 (IL-16) expression confined to infiltrating granulocytes, CD8+ T-lymphocytes and activated microglia/macrophages. *J. Neuroimmunol.* 2001;114:232–241.
165. Martha SR, Cheng Q, Fraser JF, Gong L, Collier LA, Davis SM, Lukins D, Alhajeri A, Grupke S, Pennypacker KR. Expression of Cytokines and Chemokines as Predictors of Stroke Outcomes in Acute Ischemic Stroke. *Front. Neurol.* 2019;10:1391.
166. Hu Y, Zheng Y, Wang T, Jiao L, Luo Y. VEGF, a Key Factor for Blood Brain Barrier Injury After Cerebral Ischemic Stroke. *Aging Dis.* 2022;13:647–654.
167. Gao C, Jia W, Xu W, Wu Q, Wu J. Downregulation of CD151 restricts VCAM-1 mediated leukocyte infiltration to reduce neurobiological injuries after experimental stroke. *J. Neuroinflammation.* 2021;18:118.
168. Wang L, Chen Y, Feng D, Wang X. Serum ICAM-1 as a Predictor of Prognosis in Patients with Acute Ischemic Stroke. *BioMed Res. Int.* 2021;2021:5539304.
169. Enlimomab Acute Stroke Trial Investigators. Use of anti-ICAM-1 therapy in ischemic stroke: results of the Enlimomab Acute Stroke Trial. *Neurology.* 2001;57:1428–1434.
170. Di Napoli M, Papa F, Bocola V. C-Reactive Protein in Ischemic Stroke. *Stroke.* 2001;32:917–924.
171. Schweizer J, Bustamante A, Lapierre-Fétaud V, Faura J, Scherrer N, Azurmendi Gil L, Fluri F, Schütz V, Luft A, Boned S, et al. SAA (Serum Amyloid A): A Novel Predictor of Stroke-Associated Infections. *Stroke.* 2020;51:3523–3530.
172. Sheng Y, Duan X, Liu Y, Li F, Ma S, Shang X, Wang X, Liu Y, Xue R, Qin Z. Tie2-expressing monocytes/macrophages promote cerebral revascularization in peri-infarct lesions upon ischemic insult. *Signal Transduct. Target. Ther.* 2021;6:1–3.
173. Kumai Y, Ooboshi H, Ibayashi S, Ishikawa E, Sugimori H, Kamouchi M, Kitazono T, Egashira K, Iida M. Postischemic Gene Transfer of Soluble Flt-1 Protects against Brain Ischemia with Marked Attenuation of Blood—Brain Barrier Permeability. *J. Cereb. Blood Flow Metab.* 2007;27:1152–1160.
174. Dordoe C, Chen K, Huang W, Chen J, Hu J, Wang X, Lin L. Roles of Fibroblast Growth Factors and Their Therapeutic Potential in Treatment of Ischemic Stroke. *Front. Pharmacol. [Internet].* 2021 [cited 2022 Sep 14];12. Available from: <https://www.frontiersin.org/articles/10.3389/fphar.2021.671131>
175. Planas AM, Gorina R, Chamorro A. Signalling pathways mediating inflammatory responses in brain ischaemia. *Biochem. Soc. Trans.* 2006;34:1267–1270.
176. Iadecola C, Buckwalter MS, Anrather J. Immune responses to stroke: mechanisms, modulation, and therapeutic potential. *J. Clin. Invest.* 2020;130:2777–2788.
177. Shi K, Tian D-C, Li Z-G, Ducruet AF, Lawton MT, Shi F-D. Global brain inflammation in stroke. *Lancet Neurol.* 2019;18:1058–1066.
178. Jenny NS, Callas PW, Judd SE, McClure LA, Kissela B, Zakai NA, Cushman M. Inflammatory cytokines and ischemic stroke risk. *Neurology.* 2019;92:e2375–e2384.
179. Smith CJ, Emsley HCA, Gavin CM, Georgiou RF, Vail A, Barberan EM, del Zoppo GJ, Hallenbeck JM, Rothwell NJ, Hopkins SJ, et al. Peak plasma interleukin-6 and other peripheral markers of inflammation in the first week of ischaemic stroke correlate with brain infarct volume, stroke severity and long-term outcome. *BMC Neurol.* 2004;4:2.
180. Waje-Andreassen U, Kråkenes J, Ulvestad E, Thomassen L, Myhr K-M, Aarseth J, Vedeler CA. IL-6: an early marker for outcome in acute ischemic stroke. *Acta Neurol. Scand.* 2005;111:360–365.
181. Hotter B, Hoffmann S, Ulm L, Meisel C, Fiebach JB, Meisel A. IL-6 Plasma Levels Correlate With Cerebral Perfusion Deficits and Infarct Sizes in Stroke Patients Without Associated Infections. *Front. Neurol.* 2019;10:83.

182. Mechtouff L, Bochaton T, Paccalet A, Da Silva CC, Buisson M, Amaz C, Derex L, Ong E, Berthezene Y, Eker OF, et al. Association of Interleukin-6 Levels and Futile Reperfusion After Mechanical Thrombectomy. *Neurology*. 2021;96:e752–e757.
183. Mechtouff L, Bochaton T, Paccalet A, Crola Da Silva C, Buisson M, Amaz C, Derex L, Ong E, Berthezene Y, Dufay N, et al. A lower admission level of interleukin-6 is associated with first-pass effect in ischemic stroke patients. *J. Neurointerventional Surg.* 2022;14:248–251.
184. Armstead WM, Hekierski H, Pastor P, Yarovoi S, Higazi AA-R, Cines DB. Release of IL-6 After Stroke Contributes to Impaired Cerebral Autoregulation and Hippocampal Neuronal Necrosis Through NMDA Receptor Activation and Upregulation of ET-1 and JNK. *Transl. Stroke Res.* 2019;10:104–111.
185. Esmon CT. Inflammation and thrombosis. *J. Thromb. Haemost.* 2003;1:1343–1348.
186. Burstein SA. Cytokines, platelet production and hemostasis. *Platelets*. 1997;8:93–104.
187. Gertz K, Kronenberg G, Kälin RE, Baldinger T, Werner C, Balkaya M, Eom GD, Hellmann-Regen J, Kröber J, Miller KR, et al. Essential role of interleukin-6 in post-stroke angiogenesis. *Brain*. 2012;135:1964–1980.
188. Loddick SA, Turnbull AV, Rothwell NJ. Cerebral interleukin-6 is neuroprotective during permanent focal cerebral ischemia in the rat. *J. Cereb. Blood Flow Metab. Off. J. Int. Soc. Cereb. Blood Flow Metab.* 1998;18:176–179.
189. Clé M, Desmetz C, Barthelemy J, Martin M-F, Constant O, Maarifi G, Foulongne V, Bolloré K, Glasson Y, De Bock F, et al. Zika Virus Infection Promotes Local Inflammation, Cell Adhesion Molecule Upregulation, and Leukocyte Recruitment at the Blood-Brain Barrier. *mBio*. 2020;11:e01183-20.
190. Suzuki S, Tanaka K, Suzuki N. Ambivalent aspects of interleukin-6 in cerebral ischemia: inflammatory versus neurotrophic aspects. *J. Cereb. Blood Flow Metab. Off. J. Int. Soc. Cereb. Blood Flow Metab.* 2009;29:464–479.
191. Arumugam TV, Granger DN, Mattson MP. Stroke and T-cells. *Neuromolecular Med.* 2005;7:229–242.
192. Xiong X, Barreto G, Xu L, Ouyang Y, Xie X, Giffard RG. Increased brain injury and worsened neurological outcome in IL-4 Knockout Mice Following Transient Focal Cerebral Ischemia. *Stroke J. Cereb. Circ.* 2011;42:2026–2032.
193. Lei T-Y, Ye Y-Z, Zhu X-Q, Smerin D, Gu L-J, Xiong X-X, Zhang H-F, Jian Z-H. The immune response of T cells and therapeutic targets related to regulating the levels of T helper cells after ischaemic stroke. *J. Neuroinflammation*. 2021;18:25.
194. Liesz A, Zhou W, Mracskó É, Karcher S, Bauer H, Schwarting S, Sun L, Bruder D, Stegemann S, Cerwenka A, et al. Inhibition of lymphocyte trafficking shields the brain against deleterious neuroinflammation after stroke. *Brain*. 2011;134:704–720.
195. Elkins J, Veltkamp R, Montaner J, Johnston SC, Singhal AB, Becker K, Lansberg MG, Tang W, Chang I, Muralidharan K, et al. Safety and efficacy of natalizumab in patients with acute ischaemic stroke (ACTION): a randomised, placebo-controlled, double-blind phase 2 trial. *Lancet Neurol.* 2017;16:217–226.
196. Tian D-C, Shi K, Zhu Z, Yao J, Yang X, Su L, Zhang S, Zhang M, Gonzales RJ, Liu Q, et al. Fingolimod enhances the efficacy of delayed alteplase administration in acute ischemic stroke by promoting anterograde reperfusion and retrograde collateral flow. *Ann. Neurol.* 2018;84:717–728.
197. Zimmermann L, Pham M, März AG, Kollikowski AM, Stoll G, Schuhmann MK. Defining cerebral leukocyte populations in local ischemic blood samples from patients with hyperacute stroke. *J. Cereb. Blood Flow Metab.* 2022;42:901–904.
198. Uhlar CM, Whitehead AS. Serum amyloid A, the major vertebrate acute-phase reactant. *Eur. J. Biochem.* 1999;265:501–523.

199. Ye RD, Sun L. Emerging functions of serum amyloid A in inflammation. *J. Leukoc. Biol.* 2015;98:923–929.
200. Boers AMM, Jansen IGH, Beenen LFM, Devlin TG, San Roman L, Heo JH, Ribó M, Brown S, Almekhlafi MA, Liebeskind DS, et al. Association of follow-up infarct volume with functional outcome in acute ischemic stroke: a pooled analysis of seven randomized trials. *J. Neurointerventional Surg.* 2018;10:1137–1142.
201. Bala F, Ospel J, Mulpur B, Kim BJ, Yoo J, Menon BK, Goyal M, Federau C, Sohn S-I, Hussain MS, et al. Infarct Growth despite Successful Endovascular Reperfusion in Acute Ischemic Stroke: A Meta-analysis. *Am. J. Neuroradiol.* 2021;42:1472–1478.
202. Stanne TM, Angerfors A, Andersson B, Bränmark C, Holmegaard L, Jern C. Longitudinal Study Reveals Long-Term Proinflammatory Proteomic Signature After Ischemic Stroke Across Subtypes. *Stroke* [Internet]. 2022 [cited 2022 Sep 27]; Available from: <https://www.ahajournals.org/doi/abs/10.1161/STROKEAHA.121.038349>
203. Westendorp WF, Nederkoorn PJ, Vermeij J-D, Dijkgraaf MG, van de Beek D. Post-stroke infection: a systematic review and meta-analysis. *BMC Neurol.* 2011;11:110.
204. Lindgren A, Maguire J. Stroke Recovery Genetics. *Stroke.* 2016;47:2427–2434.
205. Kapoor A, Lanctôt KL, Bayley M, Kiss A, Herrmann N, Murray BJ, Swartz RH. “Good Outcome” Isn’t Good Enough. *Stroke.* 2017;48:1688–1690.
206. Douglas AS, Shearer JA, Okolo A, Pandit A, Gilvarry M, Doyle KM. The Relationship Between Cerebral Reperfusion And Regional Expression Of Matrix Metalloproteinase-9 In Rat Brain Following Focal Cerebral Ischemia. *Neuroscience.* 2021;453:256–265.
207. Carbone F, Vuilleumier N, Bertolotto M, Burger F, Galan K, Roversi G, Tamborino C, Casetta I, Seraceni S, Trentini A, et al. Treatment with recombinant tissue plasminogen activator (r-TPA) induces neutrophil degranulation in vitro via defined pathways. *Vascul. Pharmacol.* 2015;64:16–27.
208. Wang L, Deng L, Yuan R, Liu J, Li Y, Liu M. Association of Matrix Metalloproteinase 9 and Cellular Fibronectin and Outcome in Acute Ischemic Stroke: A Systematic Review and Meta-Analysis. *Front. Neurol.* 2020;11:523506.
209. Ning M, Furie KL, Koroshetz WJ, Lee H, Barron M, Lederer M, Wang X, Zhu M, Sorensen AG, Lo EH, et al. Association between tPA therapy and raised early matrix metalloproteinase-9 in acute stroke. *Neurology.* 2006;66:1550–1555.
210. Arruri V, Chokkalla AK, Jeong S, Chelluboina B, Mehta SL, Veeravalli KK, Vemuganti R. MMP-12 knockdown prevents secondary brain damage after ischemic stroke in mice. *Neurochem. Int.* 2022;105432.
211. Olivot J-M, Heit JJ, Mazighi M, Raposo N, Albucher JF, Rousseau V, Guenego A, Thalamas C, Mlynash M, Drif A, et al. What predicts poor outcome after successful thrombectomy in early time window? *J. NeuroInterventional Surg.* [Internet]. 2021 [cited 2022 Sep 19]; Available from: <https://jnis.bmjjournals.com/content/early/2021/11/08/neurintsurg-2021-017946>
212. Goyal M, Menon BK, van Zwam WH, Dippel DWJ, Mitchell PJ, Demchuk AM, Dávalos A, Majoi CBLM, van der Lugt A, de Miquel MA, et al. Endovascular thrombectomy after large-vessel ischaemic stroke: a meta-analysis of individual patient data from five randomised trials. *The Lancet* [Internet]. 2016 [cited 2016 Mar 22]; Available from: <http://linkinghub.elsevier.com/retrieve/pii/S014067361600163X>
213. Bentley R, Hardy LJ, Scott LJ, Sharma P, Philippou H, Lip GYH. Drugs in phase I and II clinical development for the prevention of stroke in patients with atrial fibrillation. *Expert Opin. Investig. Drugs.* 2021;30:1057–1069.
214. Wolberg AS, Sang Y. Fibrinogen and Factor XIII in Venous Thrombosis and Thrombus Stability. *Arterioscler. Thromb. Vasc. Biol.* 2022;42:931–941.

215. Wartiovaara U, Mikkola H, Szőke G, Haramura G, Kárpáti L, Balogh I, Lassila R, Muszbek L, Palotie A. Effect of Val34Leu polymorphism on the activation of the coagulation factor XIII-A. *Thromb. Haemost.* 2000;84:595–600.
216. Szegedi I, Orbán-Kálmandi R, Nagy A, Sarkady F, Vasas N, Sik M, Lánczi LI, Berényi E, Oláh L, Crișan A, et al. Decreased clot burden is associated with factor XIII Val34Leu polymorphism and better functional outcomes in acute ischemic stroke patients treated with intravenous thrombolysis. *PLoS ONE*. 2021;16:e0254253.
217. Palà E, Bustamante A, Pagola J, Juega J, Francisco-Pascual J, Penalba A, Rodriguez M, De Lera Alfonso M, Arenillas JF, Cabezas JA, et al. Blood-Based Biomarkers to Search for Atrial Fibrillation in High-Risk Asymptomatic Individuals and Cryptogenic Stroke Patients. *Front. Cardiovasc. Med.* 2022;9:908053.
218. O'Collins VE, Macleod MR, Donnan GA, Horky LL, van der Worp BH, Howells DW. 1,026 experimental treatments in acute stroke. *Ann. Neurol.* 2006;59:467–477.
219. Vos EM, Geraedts VJ, van der Lugt A, Dippel DWJ, Wermer MJH, Hofmeijer J, van Es ACGM, Roos YBWEM, Peeters-Scholte CMPCD, van den Wijngaard IR. Systematic Review - Combining Neuroprotection With Reperfusion in Acute Ischemic Stroke. *Front. Neurol.* 2022;13:840892.
220. Yu ZF, Bruce-Keller AJ, Goodman Y, Mattson MP. Uric acid protects neurons against excitotoxic and metabolic insults in cell culture, and against focal ischemic brain injury *in vivo*. *J. Neurosci. Res.* 1998;53:613–625.
221. Chamorro Á, Amaro S, Castellanos M, Gomis M, Urra X, Blasco J, Arenillas JF, Román LS, Muñoz R, Macho J, et al. Uric acid therapy improves the outcomes of stroke patients treated with intravenous tissue plasminogen activator and mechanical thrombectomy. *Int. J. Stroke Off. J. Int. Stroke Soc.* 2017;12:377–382.
222. Hill MD, Goyal M, Menon BK, Nogueira RG, McTaggart RA, Demchuk AM, Poppe AY, Buck BH, Field TS, Dowlatshahi D, et al. Efficacy and safety of nerinetide for the treatment of acute ischaemic stroke (ESCAPE-NA1): a multicentre, double-blind, randomised controlled trial. *Lancet Lond. Engl.* 2020;395:878–887.
223. Teves LM, Cui H, Tymianski M. Efficacy of the PSD95 inhibitor Tat-NR2B9c in mice requires dose translation between species. *J. Cereb. Blood Flow Metab. Off. J. Int. Soc. Cereb. Blood Flow Metab.* 2016;36:555–561.
224. Sun H-S, Doucette TA, Liu Y, Fang Y, Teves L, Aarts M, Ryan CL, Bernard PB, Lau A, Forder JP, et al. Effectiveness of PSD95 inhibitors in permanent and transient focal ischemia in the rat. *Stroke*. 2008;39:2544–2553.
225. Cook DJ, Teves L, Tymianski M. A translational paradigm for the preclinical evaluation of the stroke neuroprotectant Tat-NR2B9c in gyrencephalic nonhuman primates. *Sci. Transl. Med.* 2012;4:154ra133.
226. Cook DJ, Teves L, Tymianski M. Treatment of stroke with a PSD-95 inhibitor in the gyrencephalic primate brain. *Nature*. 2012;483:213–217.
227. NoNO Inc. A Multicentre, Randomized, Double-blinded, Placebo-controlled, Parallel Group, Single-dose Design to Determine the Efficacy and Safety of Nerinetide in Participants With Acute Ischemic Stroke Undergoing Endovascular Thrombectomy Excluding Thrombolysis [Internet]. clinicaltrials.gov; 2022 [cited 2022 Sep 28]. Available from: <https://clinicaltrials.gov/ct2/show/NCT04462536>
228. Cabreira V, Dias L, Fernandes B, Aires A, Guimarães J, Abreu P, Azevedo E. Tocilizumab for severe refractory primary central nervous system vasculitis: A center experience. *Acta Neurol. Scand.* 2022;145:479–483.
229. Interleukin-6 Receptor Antagonists in Critically Ill Patients with Covid-19. *N. Engl. J. Med.* 2021;384:1491–1502.
230. Croci DM, Wanderer S, Strange F, Grüter BE, Sivanrupan S, Andereggen L, Casoni

- D, von Gunten M, Widmer HR, Di Santo S, et al. Tocilizumab Reduces Vasospasms, Neuronal Cell Death, and Microclot Formation in a Rabbit Model of Subarachnoid Hemorrhage. *Transl. Stroke Res.* 2021;12:894–904.
231. Broch K, Anstensrud AK, Woxholt S, Sharma K, Tøllefsen IM, Bendz B, Aakhus S, Ueland T, Amundsen BH, Damås JK, et al. Randomized Trial of Interleukin-6 Receptor Inhibition in Patients With Acute ST-Segment Elevation Myocardial Infarction. *J. Am. Coll. Cardiol.* 2021;77:1845–1855.
232. Huo S, Kränkel N, Nave AH, Sperber PS, Rohmann JL, Piper SK, Heuschmann PU, Landmesser U, Endres M, Siegerink B, et al. Endothelial and Leukocyte-Derived Microvesicles and Cardiovascular Risk After Stroke: PROSCIS-B. *Neurology*. 2021;96:e937–e946.
233. Coumans FAW, Brisson AR, Buzas EI, Dignat-George F, Drees EEE, El-Andaloussi S, Emanueli C, Gasecka A, Hendrix A, Hill AF, et al. Methodological Guidelines to Study Extracellular Vesicles. *Circ. Res.* 2017;120:1632–1648.
234. Théry C, Witwer KW, Aikawa E, Alcaraz MJ, Anderson JD, Andriantsitohaina R, Antoniou A, Arab T, Archer F, Atkin-Smith GK, et al. Minimal information for studies of extracellular vesicles 2018 (MISEV2018): a position statement of the International Society for Extracellular Vesicles and update of the MISEV2014 guidelines. *J. Extracell. Vesicles*. 2018;7:1535750.
235. Li W, Shi L, Hu B, Hong Y, Zhang H, Li X, Zhang Y. Mesenchymal Stem Cell-Based Therapy for Stroke: Current Understanding and Challenges. *Front. Cell. Neurosci.* [Internet]. 2021 [cited 2022 Oct 23];15. Available from: <https://www.frontiersin.org/articles/10.3389/fncel.2021.628940>
236. Zhang Y, Dong N, Hong H, Qi J, Zhang S, Wang J. Mesenchymal Stem Cells: Therapeutic Mechanisms for Stroke. *Int. J. Mol. Sci.* 2022;23:2550.
237. Yu SP, Wei Z, Wei L. Preconditioning Strategy in Stem Cell Transplantation Therapy. *Transl. Stroke Res.* 2013;4:76–88.
238. Hristov M, Erl W, Weber PC. Endothelial progenitor cells: isolation and characterization. *Trends Cardiovasc. Med.* 2003;13:201–206.
239. Custodia A, Ouro A, Sargentó-Freitas J, Aramburu-Núñez M, Pías-Peleteiro JM, Hervella P, Rosell A, Ferreira L, Castillo J, Romaus-Sanjurjo D, et al. Unraveling the potential of endothelial progenitor cells as a treatment following ischemic stroke. *Front. Neurol.* 2022;13:940682.

SUPPLEMENTAL DATA

Supplemental File 1: Ethics committee approval

COMITE DE PROTECTION DES PERSONNES SUD MEDITERRANEE III

Président: J-Y. LEFRANT Vice-Président: A-M. JOUBERT

Référence CPP à rappeler:	2019.10.04 quatre_19.07.30.36737	Nîmes, le:	08 Avril 2021	
Lors de sa séance du:	07 avril 2021	Présidée par Mme ou M:	J-Y. LEFRANT	
En présence des membres suivants: Mmes et MM:		Membres titulaires	Membres suppléants	
1 ^{er} Collège	Personnes qualifiées en recherche biomédicale	X J-Y. LEFRANT X S. DROUZY X D. MOTTET	X C. LECHICHE R. DE TAYRAC L. GONTIER-MAURIN	
	Compétents en biostatistique/épidémiologie	X C. DEMATTEI	X S. BASTIDE	
	Médecins généralistes	X P. SERAYET	C. GRAS-AYGON	
	Pharmacien hospitaliers	A. MOURGUES	X G. LEGUELINEL	
	Infirmiers	X G. BAVILLE	A. GIRON	
2 ^e Collège	Compétents en questions éthiques	C. BERHAULT	V. ANTOINE	
	Psychologues	X L. HERITIER	C. AYELA	
	Travailleurs sociaux	P. BERTAUDON		
	Compétents en matière juridique	X E. TOULOUSE-MULLER C. ROLLAND	M. GRIT	
	Représentants d'associations agréées de malades et usagers du système de santé	A-M. JOUBERT Y. PRIOUX	X A. MENSUELLE-FERRARI	
Personnes cooptées	Pédiatre			
	Spécialiste pour défaut de consentement			
Les membres suivants s'étant retirés: Mmes et MM:				
Le comité de protection des personnes Sud Méditerranée III a examiné les informations relatives à un projet référencé localement sous le numéro ci-dessus, et identifié par le numéro ci-dessous, relatif à:		Recherche interventionnelle de type 1 Recherche interventionnelle de type 2 X Recherche non interventionnelle de type 3 Utilisation d'éléments et produits du corps humain Collection d'échantillons biologiques		
Numéro d'enregistrement:		EudraCT	ANSM 2018-A02651-54	
Intitulé du projet:		"Analyse multimodale de l'origine des thrombi intracrâniens - MISO"		
Promoteur		CHU DE MONTPELLIER		
Investigateur principal ou coordonnateur:		PR. COSTALAT		
Lieu de recherche (si soumis à autorisation):				
Au titre d'une demande d'avis concernant:	X	Projet initial Modification substantielle N° 2	Dans le cadre de: Première soumission Nouvelle soumission d'un projet modifié en réponse aux observations du comité	
Date de réception du projet visé		03 mars 2021		
X	Le comité, ayant examiné ou réexaminé le projet soumis, exprime en séance plénière l'avis ci-contre:			
	Le projet ayant fait l'objet de réserves mineures lors de la délibération initiale, et celles-ci ayant été prises en compte, le comité exprime ce jour l'avis ci-contre:			
X	Favorable Défavorable Différé P2P (sans 2 ^{ème} passage) 2P (2 ^{ème} passage) Eclaircissements des réponses apportées			
Date de prise d'effet du présent avis:		07 avril 2021		
Le président:		X	Le vice-président:	Le président de séance:

Adresser la correspondance à : CPP Sud-Méditerranée 3, CHU de Nîmes – Site Serre Cavalier - Place du Professeur Robert Debré, 30099 Nîmes Cedex 9
 Téléphone : 04.66.23.64.33
 Secrétariat : Mme CABRERA
 e-mail : cppsudmed3@chu-nimes.fr

Page 1 sur 2

COMITE DE PROTECTION DES PERSONNES

SUD MEDITERRANEE III

Président: J-Y. LEFRANT Vice-Président: A-M. JOUBERT

Référence CPP à rappeler: 2019.10.04 quatre_19.07.30.36737

Le présent avis concerne spécifiquement les documents suivants:	Version n° :	En date du:
X Courrier de demande		16 février 2021
X Justification de la modification substantielle		
X Liste des documents transmis		
X Protocole	4	16 février 2021
X Note d'information et de non opposition destinée aux proches	1	16 février 2021
X Tableau comparatif des modifications		

REMARQUES

(1) Le comité prend en considération pour sa décision les conditions de validité de la recherche au regard de la protection des personnes, notamment l'information des participants avant et pendant la durée de la recherche y compris l'adéquation, l'exhaustivité et l'intelligibilité des informations écrites, les modalités de recueil de leur consentement, les indemnités éventuellement dues, la pertinence générale du projet et l'adéquation entre les objectifs poursuivis et les moyens mis en œuvre, ainsi que la qualification du ou des investigateurs.

(2) Quel que soit l'avis du Comité, il ne dégage pas le promoteur de sa responsabilité.

(3) Conformément à la réglementation, tout avis est transmis à l'autorité compétente et, en cas d'avis défavorable, aux autres comités.

(4) En cas d'avis différé, le promoteur est invité à transmettre au comité dans les meilleurs délais les informations complémentaires demandées et/ou le projet modifié répondant aux réserves exprimées. Il peut demander, ainsi que l'investigateur principal, à être entendu par le comité.

MOTIVATION DE L'AVIS DU COMITE

Adresser la correspondance à : CPP Sud-Méditerranée 3, CHU de Nîmes – Site Serre Cavalier - Place du Professeur Robert Debré, 30029 Nîmes Cedex 9
Téléphone : 04.66.23.64.33
Secrétariat : Mme CABRERA
e-mail : cppsudmed3@chu-nimes.fr

Page 2 sur 2

Supplemental File 2: model of informed consent



MISO
Version n°3 du 01/12/2020

NOTE D'INFORMATION ET NON OPPOSITION

MULTIMODAL INVESTIGATION OF CLOT ORIGIN

MISO - RECHMPL 18_0236

Version n°3 du 01/12/2020

Promoteur de la recherche : CHU de Montpellier

Investigateur coordonnateur/principal : Pr Vincent COSTALAT

Madame, Monsieur,

Votre médecin vous propose de participer à une recherche dont le *CHU de Montpellier* est le promoteur. Avant de prendre une décision, il est important que vous lisiez attentivement ces pages qui vous apporteront les informations nécessaires concernant les différents aspects de cette recherche. N'hésitez pas à poser toutes les questions que vous jugerez utiles à votre médecin.

Votre participation est entièrement volontaire. Si vous ne désirez pas prendre part à cette recherche, vous continuerez à bénéficier de la meilleure prise en charge médicale possible, conformément aux connaissances actuelles.

POURQUOI CETTE RECHERCHE ?

L'infarctus cérébral est un problème majeur de santé publique. Un nombre conséquent de patients, et ce même après traitement endovasculaire de l'infarctus cérébral, évolue vers l'œdème cérébral ou la transformation hémorragique. L'analyse du sang situé à proximité du thrombus permettrait d'établir une échelle de gravité des conséquences de l'occlusion.

QUEL EST L'OBJECTIF DE CETTE RECHERCHE ?

L'objectif de cette recherche est de réaliser des analyses du sang situé à proximité du thrombus pour tenter de déterminer les mécanismes d'apparition de l'œdème cérébral et la transformation hémorragique.

COMMENT VA SE DEROULER CETTE RECHERCHE ?

Le protocole ne modifie pas votre prise en charge dans le cadre de l'intervention endovasculaire.

Lors de votre installation en salle d'angiographie, un prélèvement sanguin sera réalisé dont une faible quantité sera destinée à la recherche pour réaliser des analyses biologiques de base. Ce faible volume n'implique pas de volume de prélèvement supplémentaire notable.

Au cours de l'opération, une ponction fémorale artérielle sera également réalisée. L'artère occluse sera désobstruée et au cours de la manipulation, une aspiration de sang intracérébral sera réalisée pour limiter la survenue d'embolies distales. Un échantillon de ce sang sera utilisé pour la recherche.

Cette récupération n'entraîne aucune manipulation supplémentaire que celle prévue pour votre traitement endovasculaire.

Contenu des visites :

Visite	Visite 1	Visite 2
Date	Jour 1	3 mois +/- 2 mois
Bilan d'inclusion	X	
Intervention endovasculaire	X	
Prélèvement de sang péri thrombus	X	
Bilan clinique de la pathologie		X
Examen clinique neurologique (NIHSS)		X
Evaluation du score global du handicap (mRS)		X

QUI PEUT PARTICIPER ?

Pour participer à cette étude vous devez être hospitalisé pour traitement endovasculaire d'infarctus cérébral avec occlusion d'un gros tronc artériel visible en imagerie, être non dépendant dans les actes de la vie quotidienne et être âgé de plus de 18 ans.

La participation à cette recherche n'engendrera aucun frais supplémentaire par rapport à ceux que vous auriez pour le suivi habituel de cette maladie.

SI LA RECHERCHE COMPORTE UNE SOUS ETUDE

Si vous le désirez, vous pouvez également donner votre accord pour l'utilisation de vos données dans le cadre de l'étude ANAIS. L'objectif de cette étude est d'estimer et de comparer la variation de la concentration de cytokines inflammatoires (molécule ayant un rôle dans le système immunitaire), dans la période peropératoire jusqu'à 48 heures après la thrombectomie mécanique chez les patients avec un AVC ischémique selon le protocole d'anesthésie utilisé.

Les résultats de cette étude définiront l'intérêt et la faisabilité d'un essai clinique plus large visant à évaluer l'impact des médicaments anesthésiques sur la variation des cytokines inflammatoires.

Cette recherche engendrera le prélèvement de 15ml de sang supplémentaire en 3 prélèvements distincts et de 5 prélèvements salivaire.

LA RECHERCHE INCLUT UNE COLLECTION D'ECHANTILLONS BIOLOGIQUES (sérothèque, DNAtèque,[®])

Les prélèvements constitueront une collection de sang périthrombus analysés par l'équipe collaboratrice n°3 dirigée par le Pr Hirtz à la plateforme de Protéomique Clinique au sein de l'Institut de Recherche en Médecine et Biothérapies (IRMB) . Des analyses protéomiques seront réalisées sur ces échantillons. Cette collection sera réalisée conformément à la réglementation et déclarée auprès des instances.

Si vous ne vous y opposez pas, le thrombus sera également récupéré dans le cadre du soin pour implémenter une collection déjà existante. Cette collection est stockée dans le service du Pr RIGAU (Laboratoire d'Anatomie et de Cytologie Pathologiques).

Si vous le souhaitez, vous pouvez être assisté par votre personne de confiance ou proche qui vous accompagne afin de vous aider dans vos décisions. Vous pouvez refuser de participer à cette collection et demander la destruction de ses échantillons à tout moment. Si vous le souhaitez, vous serez informé des résultats obtenus.

Sauf refus de votre part, ces collections et/ou données anonymisées associées pourront être cédées, pendant la recherche ou à l'issue de celle-ci, à d'autres équipes de recherche publiques ou privées souhaitant effectuer des recherches scientifiques.

Vos prélèvements pourront être détruits à n'importe quel moment si vous en formulez la demande auprès du médecin investigateur.

QUELS SONT LES BENEFICES ATTENDUS ?

Aucun bénéfice individuel immédiat n'est attendu pour les participants à la recherche.

Néanmoins, analyser la composition de ces prélèvements permettrait une meilleure connaissance des mécanismes d'apparition de l'oedème cérébral et la transformation hémorragique suite à un AVC.

Aucun risque surajouté pour les patients inclus, le protocole de recherche ne changeant en rien la procédure endovasculaire.

QUELS SONT VOS DROITS ?

Votre médecin doit vous fournir toutes les explications nécessaires concernant cette recherche. Si vous souhaitez vous en retirer à quelque moment que ce soit, et quel que soit le motif, vous continuerez à bénéficier du suivi médical et cela n'affectera en rien votre surveillance future.

Conformément à l'article L.1111-6 du Code de la Santé Publique, vous pouvez désigner une personne de confiance qui peut être un parent, un proche ou votre médecin traitant et qui sera consultée au cas où vous seriez hors d'état d'exprimer votre volonté et de recevoir l'information nécessaire à cette fin. Elle rend compte de votre volonté. Son témoignage prévaut sur tout autre témoignage. Cette désignation est faite par écrit et cosignée par la personne désignée. Elle est révisable et révocable à tout moment.

Si vous le souhaitez, votre personne de confiance peut vous accompagner dans vos démarches et assister aux entretiens médicaux afin de vous aider dans vos décisions.

Dans le cadre de la recherche à laquelle le *CHU de Montpellier* vous propose de participer, un traitement informatique de vos données personnelles va être mis en œuvre pour permettre d'analyser les résultats de la recherche au regard de l'objectif de cette dernière qui vous a été présenté.

Le responsable de ce traitement est le CHU de Montpellier.

Le médecin investigator de l'étude et tout autre personnel de l'étude tenu au secret professionnel et sous la responsabilité du médecin s'occupant de votre traitement recueilleront des données médicales vous concernant. Ces informations, appelées « Informations personnelles », seront consignées sur les formulaires, appelés cahiers d'observations, fournis par le promoteur. Seules les informations strictement nécessaires au traitement et à la finalité de la recherche seront collectées sur une base de données sécurisée puis conservées à l'issue de la recherche, sous la responsabilité du Pr Vincent COSTALAT pendant 15 ans.

Afin d'assurer la confidentialité de vos informations personnelles, ni votre nom ni aucune autre information qui permettrait de vous identifier directement ne seront saisis sur le cahier d'observation ou dans tout autre dossier que le médecin investigator de l'étude fournira au promoteur de la recherche ou aux personnes ou sociétés agissant pour son compte, en France ou à l'étranger.

Ces données seront identifiées par un code (*numéro d'inclusion et initiales*). Le code est utilisé pour que le médecin de l'étude puisse vous identifier si nécessaire.

Ces données pourront également, dans des conditions assurant leur confidentialité, être transmises aux autorités de santé françaises.

Conformément aux dispositions de la loi relative à l'informatique, aux fichiers et aux libertés (loi n° 78-17 du 6 janvier 1978 relative à l'informatique, aux fichiers et aux libertés modifiée par la loi n° 2018-493 du 20 juin 2018 relative à la protection des données personnelles) et au règlement général sur la protection des données (règlement UE 2016/679), vous disposez d'un droit **d'accès, de rectification, d'effacement ou de limitation** des informations collectées vous concernant dans le cadre de ce traitement.

Dans certains cas, vous pouvez également **refuser la collecte de vos données et vous opposer à ce que certains types de traitement des données soient réalisés**. Vous disposez également d'un droit **d'opposition à la transmission des données** couvertes par le secret professionnel susceptibles d'être utilisées dans le cadre de cette recherche et d'être traitées.

Vous pouvez également **accéder** directement ou par l'intermédiaire du médecin de votre choix à l'ensemble de vos données médicales en application des dispositions de l'article L1111-7 du code de la santé publique.

Vous pourrez retirer à tout moment votre accord concernant la collecte de vos données dans le cadre de ce traitement. Le cas échéant, conformément à l'article L.1122-1-1 du Code de la Santé Publique, les données vous concernant qui auront été recueillies préalablement à votre accord pourront ne pas être effacées et pourront continuer à être traitées dans les conditions prévues par la recherche.



Enfin, vous pouvez demander à ce que les informations personnelles colligées vous soient fournies, à vous ou à un tiers, sous un format numérique (**droit de portabilité**).

Vos droits cités ci-dessus s'exercent auprès du médecin qui vous suit dans le cadre de la recherche et qui connaît votre identité.

Si vous avez d'autres questions au sujet du recueil, de l'utilisation de vos informations personnelles ou des droits associés à ces informations, vous pouvez contacter le Délégué à la Protection des Données du CHU de Montpellier (mail : dpo@chu-montpellier.fr) ou le médecin investigateur de l'étude, Pr Vincent COSTALAT.

Si malgré les mesures mises en place par le promoteur, vous estimatez que vos droits ne sont pas respectés, vous pouvez déposer une plainte auprès de l'autorité de surveillance de la protection des données compétente en France, la Commission Nationale de l'Informatique et des Libertés (CNIL).

Si le responsable de traitement souhaite effectuer un traitement ultérieur des données à caractère personnel vous concernant pour une finalité autre que celle pour laquelle vos données à caractère personnel ont été collectées, vous serez informé(e) au préalable quant à cette autre finalité, à la durée de conservation de vos données, et toute autre information pertinente permettant de garantir un traitement équitable et transparent.

Conformément à la loi n°2012-300 du 5 mars 2012 relative aux recherches impliquant la personne humaine : - cette recherche a obtenu un avis favorable du Comité de Protection des Personnes de Sud-Méditerranée III.

- les personnes ayant subi un préjudice après participation à une recherche impliquant la personne humaine peuvent faire valoir leurs droits auprès des commissions régionales de conciliation et d'indemnisation des accidents médicaux
- lorsque cette recherche sera terminée, vous serez tenu(e) informé(e) personnellement des résultats globaux par votre médecin dès que ceux-ci seront disponibles, si vous le souhaitez.

Après avoir lu cette note d'information et de non opposition, n'hésitez pas à poser à votre médecin toutes les questions que vous désirez.

A QUI DEVEZ-VOUS VOUS ADRESSER EN CAS DE QUESTIONS OU DE PROBLEMES?

Pour tout renseignement concernant cette recherche ou pour exprimer votre droit, vous pouvez contacter par mail/courrier/téléphone :

VOS CONTACTS DANS L'ETUDE

Dr. DARGAZANLI Cyril : Service de Neuroradiologie, Hôpital Gui de Chauliac. Secrétariat : 0467337532.

c-dargazanli@chu@montpellier.fr

Mme MOYNIER Marinette : Service de Neuroradiologie, Hôpital Gui de Chauliac. Secrétariat : 0467337532

m-moynier@chu-montpellier.fr

Supplemental file 3: anesthesia protocol during EVT

PROTOCOLES ANESTHESIE PENDANT THROMBECTOMIE

POUR TOUS LES PATIENTS	
Paracétamol 1 g + Ondansétron 4 mg administré en 15 min	Dexaméthasone à éviter
Noradrénaline 10 mcg/ml A débuter avant l'ISR si AG Vitesse selon objectif tensionnel Utilisation d'autres vasopresseurs à noter sur Dx Care	Cible : PAS 140 – 180 mmHg avant récanalisation Soit Variation PAM < 20% PAM de base
Normoventilation (EtCO ₂ 35-45 mmHg)	

PROTOCOLE AG	
INDUCTION	
ETOMIDATE 0.3 – 0.5 MG/KG	Effet en 30 sec, durée 3 – 6 min
ROCURONIUM 1.0 – 1.2 MG/KG	Bridion à disposition 16 mg/kg
REMIFENTANIL AIVOC , C_{eff} entre 0.5 et 2 ng/ml	
Propofol si nécessaire 0.5 – 1 mg/kg	Si utilisation de propofol à l'induction, entretien anesthésie : PROTOCOLE 1
ENTRETIEN	
PROTOCOLE 1	
REMIFENTANIL MODALITE AIVOC, C_{eff} 0.5 – 2 ng/ml	
PROPOFOL MODALITE AIVOC, C_{eff} 3 – 5 mcg/ml	
PROTOCOLE 2	
REMIFENTANIL MODALITE AIVOC, C_{eff} 0.5 – 2 ng/ml	
SEVORANE, MAC 0.8	à régler selon âge du patient/dose remifentanil en cours

PROTOCOLE AL + SEDATION	
REMIFENTANIL MODALITE AIVOC, C_{eff} 0.5 – 2 ng/ml	Cible RASS 0/-2 (RASS0=Pt éveillé et calme RASS-1=contact à l'appel >10sec RASS-2=contact à l'appel<10sec)
PROPOFOL MODALITE AIVOC si nécessaire, C _{eff} max 1 mcg/ml	Masque Oxygène + Monitorage EtCO ₂ (capnomètre dans le masque pour garder une bonne FR).

Supplemental Table 1: Association between MESOSCALE central biomarkers and stroke outcome (modified Rankin Score), univariate analysis

Biomarker	Correlation	Correlation_lowerCI	Correlation_upperCI	pValue	PvalueCor
IFNy	-0.05312	-0.280978	0.181139	0.6588	0.7927
IL10	0.32344	0.096945	0.514738	0.0053	0.0739
IL13	-0.20007	-0.411441	0.034545	0.0921	0.2408
IL1B	0.19792	-0.036761	0.409597	0.0957	0.2408
IL2	-0.03514	-0.264421	0.198382	0.7703	0.8637
IL4	-0.13205	-0.352108	0.103682	0.2699	0.4938
IL6	0.40580	0.189449	0.580801	0.0003	0.0129
IL8	0.24466	0.012052	0.449407	0.0380	0.1759
TNFalpha	0.19682	-0.037895	0.408651	0.0976	0.2408
IL12_IL23p40	0.15095	-0.084698	0.368774	0.2064	0.4242
IL15	0.22228	-0.011461	0.430444	0.0604	0.2056
IL16	0.02974	-0.203532	0.259422	0.8048	0.8759
IL17A	0.22612	-0.007446	0.433710	0.0560	0.2056
IL1alpha	0.05610	-0.178261	0.283715	0.6409	0.7927
IL5	0.12925	-0.106477	0.349629	0.2803	0.4938
IL7	-0.15505	-0.372372	0.080555	0.1941	0.4225
TNFbeta	-0.05568	-0.283328	0.178668	0.6434	0.7927
VEGF_A	-0.04871	-0.276929	0.185382	0.6855	0.7927
Eotaxin	-0.11848	-0.340053	0.117210	0.3228	0.4976
Eotaxin3	0.05145	-0.182740	0.279452	0.6688	0.7927
IP_10	0.14128	-0.094429	0.360267	0.2374	0.4623
MCP1	-0.02194	-0.252179	0.210950	0.8554	0.9043
MCP4	-0.10257	-0.325833	0.132952	0.3926	0.5810
MDC	-0.06148	-0.288631	0.173071	0.6091	0.7927
MIP1alpha	0.11917	-0.116520	0.340672	0.3199	0.4976
MIP_1beta	-0.00682	-0.238068	0.225249	0.9548	0.9548
TARC	-0.30892	-0.502857	-0.081041	0.0080	0.0739
bFGF	0.16469	-0.072523	0.382266	0.1705	0.3943
FLT1	0.26336	0.030142	0.466441	0.0261	0.1587
PIGF	-0.01384	-0.246253	0.220271	0.9091	0.9344
Tie2	0.12327	-0.114166	0.345827	0.3069	0.4976
VEGF_C	-0.22325	-0.432659	0.012197	0.0611	0.2056
VEGF_D	0.06301	-0.173275	0.291606	0.6029	0.7927
CRP	0.20411	-0.030365	0.414911	0.0855	0.2408
SAA	0.31296	0.085458	0.506173	0.0071	0.0739
ICAM_1	0.25542	0.023450	0.458459	0.0300	0.1587
VCAM_1	0.26248	0.030960	0.464374	0.0256	0.1587

Supplemental Table 2: Association between MESOSCALE central biomarkers and stroke outcome (modified Rankin Score), multivariate analysis (NIHSS/ASPECTS adjusted)

Biomarker	Correlation	Correlation_lowerCI	Correlation_upperCI	pValue	PvalueCor
IFNy	-0.07918	-0.311189	0.162882	0.5224	0.7046
IL10	0.26118	0.022321	0.468801	0.0311	0.1644
IL13	-0.19776	-0.415327	0.044146	0.1062	0.3571
IL1B	0.16156	-0.081144	0.384121	0.1888	0.4991
IL2	-0.06630	-0.299532	0.175370	0.5924	0.7307
IL4	-0.13623	-0.361982	0.106635	0.2691	0.5751
IL6	0.37283	0.144797	0.559448	0.0016	0.0294
IL8	0.23066	-0.009943	0.443247	0.0583	0.2695
TNFalpha	0.14513	-0.097717	0.369788	0.2387	0.5519
IL12_IL23p40	0.08657	-0.155686	0.317842	0.4841	0.7046
IL15	0.20363	-0.038083	0.420341	0.0959	0.3549
IL16	-0.03488	-0.270808	0.205503	0.7785	0.8949
IL17A	0.15455	-0.088227	0.378023	0.2091	0.5157
IL1alpha	0.07793	-0.164100	0.310059	0.5290	0.7046
IL5	0.07841	-0.163637	0.310488	0.5265	0.7046
IL7	-0.13326	-0.359378	0.109594	0.2798	0.5751
TNFbeta	0.01108	-0.228022	0.248774	0.9288	0.9878
VEGF_A	-0.03172	-0.267894	0.208510	0.7981	0.8949
Eotaxin	-0.06931	-0.302266	0.172455	0.5757	0.7307
Eotaxin3	0.03667	-0.203795	0.272459	0.7674	0.8949
IP_10	0.11861	-0.124172	0.346438	0.3367	0.6228
MCP1	-0.08292	-0.314554	0.159249	0.5028	0.7046
MCP4	-0.09953	-0.329459	0.143000	0.4208	0.7046
MDC	-0.12637	-0.353304	0.116462	0.3057	0.5953
MIP1alpha	0.10777	-0.134887	0.336813	0.3831	0.6749
MIP_1beta	0.00421	-0.234478	0.242364	0.9729	0.9878
TARC	-0.35379	-0.544293	-0.123396	0.0029	0.0354
bFGF	0.16236	-0.080335	0.384815	0.1866	0.4991
FLT1	0.29587	0.059600	0.497424	0.0139	0.1031
PIGF	-0.00190	-0.240199	0.236650	0.9878	0.9878
Tie2	0.07714	-0.164868	0.309345	0.5332	0.7046
VEGF_C	-0.20378	-0.420463	0.037934	0.0957	0.3549
VEGF_D	-0.00255	-0.240810	0.236037	0.9836	0.9878
CRP	0.17990	-0.062482	0.399996	0.1425	0.4395
SAA	0.38745	0.161376	0.571001	0.0010	0.0294
ICAM_1	0.27138	0.033215	0.477264	0.0248	0.1531
VCAM_1	0.29979	0.063859	0.500635	0.0126	0.1031

Supplemental Table 3: Association between MESOSCALE biomarkers and favorable outcome (mRS 0-2 or mRS prestroke=90-day mRS), univariate analysis

Biomarker	EffectSize	EffectSize_lowerCI	EffectSize_upperCI	Pvalue	PvalueCor
IFNy	0.05573	-0.42526	0.53671	0.8237	0.8964
IL10	-0.69679	-1.19097	-0.20260	0.0069	0.1273
IL13	0.62891	0.13716	1.12066	0.0138	0.1479
IL1B	-0.29740	-0.78075	0.18595	0.2293	0.5574
IL2	-0.19090	-0.67281	0.29101	0.4387	0.6705
IL4	0.21398	-0.26819	0.69615	0.3855	0.6705
IL6	-0.71364	-1.20847	-0.21882	0.0058	0.1273
IL8	-0.33872	-0.82280	0.14535	0.1720	0.4948
TNFalpha	-0.37309	-0.85784	0.11166	0.1334	0.4948
IL12_IL23p40	-0.18497	-0.66682	0.29688	0.4531	0.6705
IL15	-0.31943	-0.80315	0.16430	0.1972	0.5211
IL16	-0.16620	-0.64787	0.31547	0.5002	0.6829
IL17A	-0.28991	-0.77314	0.19332	0.2410	0.5574
IL1alpha	0.19799	-0.28400	0.67998	0.4219	0.6705
IL5	-0.27095	-0.75388	0.21199	0.2728	0.5612
IL7	0.25180	-0.23086	0.73445	0.3077	0.5954
TNFbeta	0.01170	-0.46920	0.49261	0.9665	0.9665
VEGF_A	0.11299	-0.36826	0.59425	0.6475	0.7778
Eotaxin	0.33721	-0.14683	0.82126	0.1738	0.4948
Eotaxin3	0.02428	-0.45664	0.50520	0.9253	0.9510
IP_10	-0.27081	-0.75374	0.21212	0.2730	0.5612
MCP1	-0.04571	-0.52667	0.43525	0.8558	0.9047
MCP4	0.15323	-0.32832	0.63478	0.5344	0.6829
MDC	0.17631	-0.30546	0.65807	0.4745	0.6753
MIP1alpha	-0.24450	-0.72706	0.23805	0.3218	0.5954
MIP_1beta	-0.10152	-0.58271	0.37967	0.6816	0.7881
TARC	0.55316	0.06385	1.04248	0.0288	0.2130
bFGF	-0.20594	-0.69412	0.28225	0.4096	0.6705
FLT1	-0.35250	-0.84295	0.13794	0.1608	0.4948
PIGF	0.15487	-0.33281	0.64254	0.5353	0.6829
Tie2	-0.09514	-0.58239	0.39212	0.7045	0.7899
VEGF_C	0.48185	-0.01156	0.97527	0.0579	0.3241
VEGF_D	-0.11302	-0.60039	0.37434	0.6517	0.7778
CRP	-0.36704	-0.85166	0.11759	0.1396	0.4948
SAA	-0.61414	-1.10539	-0.12288	0.0160	0.1479
ICAM_1	-0.45340	-0.93997	0.03317	0.0701	0.3241
ICAM_1	-0.45340	-0.93997	0.03317	0.0701	0.3241

Supplemental Table 4: Association between MESOSCALE biomarkers and favorable outcome (mRS 0-2 or mRS prestroke=90-day mRS), multivariate analysis

Biomarker	EffectSize	EffectSize_lowerCI	EffectSize_upperCI	Pvalue	PvalueCor
IFNy	0.08831	-0.38826	0.56487	0.7175	0.8296
IL10	-0.59850	-1.08237	-0.11464	0.0158	0.1322
IL13	0.61027	0.12035	1.10020	0.0151	0.1322
IL1B	-0.21277	-0.69094	0.26540	0.3850	0.7251
IL2	-0.12874	-0.60961	0.35213	0.6011	0.8238
IL4	0.16770	-0.30206	0.63746	0.4858	0.7251
IL6	-0.64130	-1.12471	-0.15788	0.0097	0.1322
IL8	-0.27135	-0.75068	0.20799	0.2691	0.7112
TNFalpha	-0.30781	-0.79062	0.17499	0.2133	0.6640
IL12_IL2	-0.11644	-0.59232	0.35943	0.6328	0.8296
IL15	-0.29908	-0.78336	0.18520	0.2280	0.6640
IL16	-0.06819	-0.54387	0.40749	0.7795	0.8483
IL17A	-0.20637	-0.68070	0.26797	0.3956	0.7251
IL1alpha	0.19695	-0.28687	0.68077	0.4267	0.7251
IL5	-0.16536	-0.63301	0.30228	0.4899	0.7251
IL7	0.23223	-0.25035	0.71481	0.3475	0.7251
TNFbeta	-0.10629	-0.58060	0.36802	0.6617	0.8296
VEGF_A	0.09402	-0.38874	0.57679	0.7037	0.8296
Eotaxin	0.27919	-0.17808	0.73646	0.2333	0.6640
Eotaxin3	0.07636	-0.40415	0.55687	0.7563	0.8480
IP_10	-0.23769	-0.72050	0.24513	0.3365	0.7251
MCP1	0.03190	-0.42883	0.49263	0.8925	0.9302
MCP4	0.17068	-0.30738	0.64874	0.4857	0.7251
MDC	0.23593	-0.24703	0.71888	0.3402	0.7251
MIP1alph	-0.17528	-0.64870	0.29814	0.4698	0.7251
MIP_1bet	-0.08965	-0.56127	0.38196	0.7105	0.8296
TARC	0.59635	0.10510	1.08761	0.0179	0.1322
bFGF	-0.18749	-0.67616	0.30119	0.4538	0.7251
FLT1	-0.39825	-0.88308	0.08658	0.1089	0.4477
PIGF	0.13151	-0.35588	0.61890	0.5983	0.8238
Tie2r	-0.02981	-0.51781	0.45820	0.9051	0.9302
VEGF_C	0.42351	-0.06184	0.90885	0.0886	0.4097
VEGF_D	-0.01982	-0.50458	0.46493	0.9364	0.9364
CRP	-0.31036	-0.79331	0.17260	0.2097	0.6640
SAA	-0.66023	-1.15207	-0.16839	0.0088	0.1322
ICAM_1	-0.43803	-0.92592	0.04987	0.0797	0.4097
ICAM_1	-0.43803	-0.92592	0.04987	0.0797	0.4097

Supplemental Table 5: Association between MESOSCALE central biomarkers and 24-hours NIHSS change, univariate analysis

Biomarker	Correlation	Correlation_lowerCI	Correlation_upperCI	pValue	PvalueCor
IFNy	-0.12354	-0.349185	0.117449	0.3131	0.8911
IL10	0.13815	-0.102868	0.362079	0.2587	0.8911
IL13	-0.13090	-0.355696	0.110112	0.2848	0.8911
IL1B	0.12835	-0.112656	0.353444	0.2944	0.8911
IL2	-0.09652	-0.325125	0.144132	0.4315	0.9951
IL4	-0.09836	-0.326772	0.142327	0.4227	0.9951
IL6	0.25683	0.019565	0.463749	0.0328	0.6072
IL8	0.20158	-0.038336	0.417082	0.0968	0.8810
TNFalpha	-0.04053	-0.274303	0.198335	0.7418	0.9951
IL12_IL23p40	0.02153	-0.216400	0.256757	0.8611	0.9951
IL15	0.07419	-0.165921	0.305015	0.5459	0.9951
IL16	-0.05922	-0.291414	0.180402	0.6300	0.9951
IL17A	0.04988	-0.189389	0.282877	0.6851	0.9951
IL1alpha	-0.05641	-0.288853	0.183107	0.6464	0.9951
IL5	-0.07213	-0.303142	0.167928	0.5572	0.9951
IL7	-0.06872	-0.300053	0.171228	0.5760	0.9951
TNFbeta	0.02723	-0.210999	0.262036	0.8249	0.9951
VEGF_A	-0.17891	-0.397601	0.061636	0.1418	0.8810
Eotaxin	-0.00409	-0.240509	0.232845	0.9735	0.9951
Eotaxin3	0.04849	-0.190717	0.281609	0.6934	0.9951
IP_10	-0.07488	-0.305640	0.165251	0.5422	0.9951
MCP1	-0.0007501	-0.237383	0.235978	0.9951	0.9951
MCP4	0.03215	-0.206330	0.266577	0.7939	0.9951
MDC	-0.15976	-0.380993	0.081110	0.1905	0.8810
MIP1alpha	-0.06374	-0.295525	0.176047	0.6041	0.9951
MIP_1beta	-0.11734	-0.343693	0.123601	0.3382	0.8939
TARC	-0.00255	-0.239071	0.234288	0.9835	0.9951
bFGF	0.04098	-0.199682	0.276424	0.7409	0.9951
FLT1	0.41909	0.197720	0.595771	0.0003	0.0118
PIGF	-0.16136	-0.383949	0.081344	0.1894	0.8810
Tie2	-0.00241	-0.240679	0.236169	0.9845	0.9951
VEGF_C	-0.01115	-0.248839	0.227956	0.9283	0.9951
VEGF_D	-0.20798	-0.424044	0.033583	0.0888	0.8810
CRP	-0.16847	-0.388561	0.072280	0.1670	0.8810
SAA	0.03418	-0.204397	0.268450	0.7812	0.9951
ICAM_1	0.00769	-0.229458	0.243877	0.9502	0.9951
VCAM_1	0.14532	-0.095673	0.368376	0.2344	0.8911

Supplemental Table 6: Association between MESOSCALE central biomarkers and 24-hours NIHSS change, multivariate analysis

Biomarker	Correlation	Correlation_lowerCI	Correlation_upperCI	pValue	PvalueCor
IFNy	-0.05999	-0.299077	0.187095	0.6363	0.9999
IL10	0.17016	-0.078248	0.396444	0.1760	0.7237
IL13	-0.13132	-0.362685	0.117314	0.2983	0.9198
IL1B	0.17556	-0.072765	0.401082	0.1625	0.7237
IL2	-0.09184	-0.327747	0.156239	0.4683	0.9999
IL4	-0.15189	-0.380640	0.096720	0.2281	0.7671
IL6	0.25857	0.013644	0.471094	0.0372	0.6456
IL8	0.22693	-0.019733	0.444718	0.0690	0.6456
TNFalpha	-0.04748	-0.287704	0.199076	0.7083	0.9999
IL12_IL23p40	0.00394	-0.240219	0.247573	0.9752	0.9999
IL15	0.07632	-0.171335	0.313831	0.5471	0.9999
IL16	-0.03183	-0.273371	0.213970	0.8021	0.9999
IL17A	0.05197	-0.194782	0.291796	0.6821	0.9999
IL1alpha	-0.05221	-0.292010	0.194557	0.6807	0.9999
IL5	0.01054	-0.234037	0.253711	0.9338	0.9999
IL7	-0.07139	-0.309388	0.176107	0.5734	0.9999
TNFbeta	-0.00128	-0.245095	0.242702	0.9919	0.9999
VEGF_A	-0.15450	-0.382902	0.094096	0.2201	0.7671
Eotaxin	-0.05004	-0.290032	0.196635	0.6934	0.9999
Eotaxin3	0.06294	-0.184253	0.301755	0.6197	0.9999
IP_10	-0.08821	-0.324495	0.159788	0.4862	0.9999
MCP1	0.00925	-0.235249	0.252510	0.9419	0.9999
MCP4	0.01100	-0.233607	0.254136	0.9310	0.9999
MDC	-0.18406	-0.408371	0.064089	0.1427	0.7237
MIP1alpha	0.0004085	-0.243518	0.244280	0.9974	0.9999
MIP_1beta	-0.10628	-0.340599	0.142093	0.4009	0.9999
TARC	-0.02699	-0.268924	0.218545	0.8316	0.9999
bFGF	0.03572	-0.210272	0.276950	0.7784	0.9999
FLT1	0.36769	0.133163	0.559284	0.0024	0.0883
PIGF	-0.19202	-0.415176	0.055924	0.1258	0.7237
Tie2	-0.03238	-0.273878	0.213446	0.7987	0.9999
VEGF_C	-0.08682	-0.323258	0.161133	0.4931	0.9999
VEGF_D	-0.22630	-0.444184	0.020398	0.0698	0.6456
CRP	-0.18026	-0.405116	0.067972	0.1513	0.7237
SAA	0.0000218	-0.243879	0.243919	0.9999	0.9999
ICAM_1	0.00270	-0.241375	0.246419	0.9830	0.9999
VCAM_1	0.12302	-0.125562	0.355393	0.3303	0.9399

Supplemental Table 7: Association between MESOSCALE biomarkers and infarct volume at 24 hours. Univariate analysis.

Biomarker	Correlation	Correlation_lowerCI	Correlation_upperCI	pValue	PvalueCor
IFNy	-0.16484	-0.388563	0.079715	0.1832	0.9804
IL10	-0.07572	-0.309764	0.168096	0.5439	0.9804
IL13	-0.12724	-0.355710	0.117480	0.3061	0.9804
IL1B	-0.12605	-0.354661	0.118664	0.3107	0.9804
IL2	-0.15416	-0.379288	0.090515	0.2138	0.9804
IL4	-0.11749	-0.347095	0.127162	0.3450	0.9804
IL6	0.13564	-0.109108	0.363095	0.2749	0.9804
IL8	0.07349	-0.170253	0.307755	0.5559	0.9804
TNFalpha	-0.05911	-0.294715	0.184144	0.6359	0.9804
IL12_IL23p40	0.14400	-0.100740	0.370419	0.2460	0.9804
IL15	-0.00385	-0.243801	0.236609	0.9755	0.9957
IL16	0.04271	-0.199861	0.279743	0.7325	0.9957
IL17A	0.01875	-0.222598	0.257662	0.8808	0.9957
IL1alpha	-0.06568	-0.300681	0.177812	0.5988	0.9804
IL5	0.22717	-0.015509	0.441812	0.0644	0.9804
IL7	0.01035	-0.230509	0.249861	0.9340	0.9957
TNFbeta	0.00449	-0.236006	0.244402	0.9714	0.9957
VEGF_A	-0.11307	-0.343181	0.131531	0.3636	0.9804
Eotaxin	-0.03219	-0.270082	0.209873	0.7967	0.9957
Eotaxin3	-0.0006791	-0.240844	0.239573	0.9957	0.9957
IP_10	-0.09099	-0.323502	0.153222	0.4654	0.9804
MCP1	0.06144	-0.181895	0.296838	0.6226	0.9804
MCP4	0.13979	-0.104954	0.366738	0.2603	0.9804
MDC	-0.02848	-0.266666	0.213389	0.8197	0.9957
MIP1alpha	-0.10973	-0.340213	0.134832	0.3781	0.9804
MIP_1beta	-0.09177	-0.324199	0.152461	0.4616	0.9804
TARC	0.01125	-0.229664	0.250697	0.9283	0.9957
bFGF	-0.06702	-0.303650	0.178400	0.5942	0.9804
FLT1	0.12440	-0.122227	0.354887	0.3209	0.9804
PIGF	-0.03682	-0.276129	0.207328	0.7700	0.9957
Tie2	0.04453	-0.199982	0.283194	0.7236	0.9957
VEGF_C	-0.07717	-0.312818	0.168574	0.5394	0.9804
VEGF_D	-0.00176	-0.243672	0.240392	0.9889	0.9957
CRP	-0.09730	-0.329139	0.147054	0.4349	0.9804
SAA	-0.18240	-0.403718	0.061829	0.1400	0.9804
ICAM_1	-0.26752	-0.475503	-0.027160	0.0283	0.9804
VCAM_1	0.01326	-0.227766	0.252572	0.9155	0.9957

Supplemental Table 8: Association between MESOSCALE biomarkers and infarct volume at 24 hours. Multivariate analysis.

Biomarker	Correlation	Correlation_lowerCI	Correlation_upperCI	pValue	PvalueCor
IFNy	-0.16325	-0.393923	0.089386	0.2020	0.7473
IL10	-0.17540	-0.404356	0.077062	0.1698	0.7473
IL13	-0.14172	-0.375293	0.111032	0.2691	0.8799
IL1B	-0.22995	-0.450492	0.020741	0.0697	0.6631
IL2	-0.21490	-0.437876	0.036445	0.0908	0.6631
IL4	-0.20559	-0.430029	0.046096	0.1062	0.6631
IL6	0.02520	-0.224158	0.271082	0.8452	0.9420
IL8	0.08267	-0.169191	0.323210	0.5210	0.8823
TNFalpha	-0.11811	-0.354643	0.134496	0.3580	0.8823
IL12_IL23p40	0.05132	-0.199372	0.294953	0.6907	0.9127
IL15	-0.01304	-0.259869	0.235583	0.9195	0.9420
IL16	-0.03514	-0.280198	0.214768	0.7854	0.9420
IL17A	-0.08575	-0.325963	0.166200	0.5055	0.8823
IL1alpha	-0.08109	-0.321792	0.170727	0.5290	0.8823
IL5	0.20483	-0.046876	0.429391	0.1075	0.6631
IL7	0.02775	-0.221755	0.273422	0.8298	0.9420
TNFbeta	0.07818	-0.173545	0.319186	0.5440	0.8823
VEGF_A	-0.13054	-0.365542	0.122179	0.3092	0.8799
Eotaxin	0.09044	-0.161644	0.330141	0.4824	0.8823
Eotaxin3	-0.00940	-0.256497	0.238993	0.9420	0.9420
IP_10	-0.12340	-0.359288	0.129265	0.3367	0.8823
MCP1	0.16502	-0.087593	0.395449	0.1970	0.7473
MCP4	0.16585	-0.086750	0.396165	0.1947	0.7473
MDC	-0.05151	-0.295120	0.199195	0.6897	0.9127
MIP1alpha	-0.11171	-0.348998	0.140816	0.3849	0.8823
MIP_1beta	-0.02477	-0.270686	0.224564	0.8478	0.9420
TARC	0.01979	-0.229252	0.266098	0.8782	0.9420
bFGF	-0.05539	-0.298648	0.195477	0.6675	0.9127
FLT1	0.05869	-0.192324	0.301629	0.6490	0.9127
PIGF	-0.07277	-0.314333	0.178772	0.5723	0.8823
Tie2	-0.01541	-0.262063	0.233358	0.9049	0.9420
VEGF_C	-0.07421	-0.315625	0.177384	0.5647	0.8823
VEGF_D	-0.07353	-0.315008	0.178047	0.5683	0.8823
CRP	-0.13565	-0.370001	0.117096	0.2904	0.8799
SAA	-0.22605	-0.447228	0.024825	0.0748	0.6631
ICAM_1	-0.33728	-0.537994	-0.094981	0.0065	0.2423
VCAM_1	-0.03765	-0.282496	0.212386	0.7705	0.9420

Supplemental Table 9: Association between MESOSCALE biomarkers and infarct volume change at 24 hours. Univariate analysis.

Biomarker	Correlation	Correlation_lowerCI	Correlation_upperCI	pValue	PvalueCor
IFNy	-0.15919	-0.390422	0.093489	0.2136	0.7007
IL10	-0.07274	-0.314299	0.178809	0.5725	0.7845
IL13	-0.09583	-0.334941	0.156383	0.4565	0.7845
IL1B	-0.09911	-0.337857	0.153175	0.4411	0.7845
IL2	-0.18098	-0.409129	0.071375	0.1563	0.7007
IL4	-0.19328	-0.419607	0.058777	0.1295	0.7007
IL6	0.05387	-0.196936	0.297266	0.6762	0.8619
IL8	0.19737	-0.054574	0.423076	0.1213	0.7007
TNFalpha	-0.15463	-0.386488	0.098080	0.2273	0.7007
IL12_IL23p40	0.12059	-0.132048	0.356820	0.3479	0.7845
IL15	-0.07918	-0.320080	0.172579	0.5388	0.7845
IL16	0.03801	-0.212039	0.282829	0.7683	0.8619
IL17A	-0.04165	-0.286147	0.208589	0.7469	0.8619
IL1alpha	0.01488	-0.233858	0.261571	0.9082	0.9334
IL5	0.10507	-0.147343	0.343131	0.4140	0.7845
IL7	0.23664	-0.013725	0.456067	0.0617	0.7007
TNFbeta	0.05535	-0.195517	0.298611	0.6678	0.8619
VEGF_A	-0.08228	-0.322856	0.169574	0.5230	0.7845
Eotaxin	0.09329	-0.158863	0.332682	0.4686	0.7845
Eotaxin3	-0.02763	-0.273312	0.221868	0.8305	0.8780
IP_10	-0.03794	-0.282764	0.212107	0.7687	0.8619
MCP1	0.16148	-0.091177	0.392396	0.2070	0.7007
MCP4	0.21143	-0.040051	0.434952	0.0964	0.7007
MDC	-0.13579	-0.370123	0.116957	0.2899	0.7662
MIP1alpha	-0.14101	-0.374675	0.111742	0.2715	0.7662
MIP_1beta	0.00161	-0.246265	0.249264	0.9900	0.9900
TARC	0.07385	-0.177734	0.315299	0.5666	0.7845
bFGF	0.04651	-0.206016	0.292524	0.7207	0.8619
FLT1	0.21733	-0.036081	0.441615	0.0898	0.7007
PIGF	-0.12238	-0.360236	0.132392	0.3448	0.7845
Tie2	-0.08789	-0.329763	0.166212	0.4985	0.7845
VEGF_C	0.10793	-0.146629	0.347535	0.4052	0.7845
VEGF_D	-0.08582	-0.327919	0.168222	0.5087	0.7845
CRP	-0.15847	-0.389803	0.094213	0.2157	0.7007
SAA	-0.17405	-0.403201	0.078434	0.1732	0.7007
ICAM_1	-0.29079	-0.500610	-0.044031	0.0204	0.7007
VCAM_1	-0.03287	-0.278121	0.216915	0.7990	0.8695

Supplemental Table 10: Association between MESOSCALE biomarkers and infarct volume change at 24 hours. Multivariate analysis.

Biomarker	Correlation	Correlation_lowerCI	Correlation_upperCI	pValue	PvalueCor
IFNy	-0.09300	-0.340255	0.167838	0.4852	0.8713
IL10	-0.04422	-0.296592	0.214652	0.7405	0.8831
IL13	-0.08138	-0.329946	0.179102	0.5416	0.8713
IL1B	-0.10368	-0.349672	0.157432	0.4362	0.8494
IL2	-0.22005	-0.449221	0.040077	0.0941	0.7238
IL4	-0.20169	-0.433883	0.059084	0.1259	0.7238
IL6	0.02384	-0.233866	0.278032	0.8584	0.9177
IL8	0.18009	-0.081213	0.415656	0.1730	0.7238
TNFalpha	-0.16616	-0.403810	0.095339	0.2095	0.7238
IL12_IL23p40	0.14360	-0.118002	0.384447	0.2792	0.7380
IL15	-0.06412	-0.314535	0.195695	0.6309	0.8831
IL16	0.04525	-0.213680	0.297521	0.7347	0.8831
IL17A	-0.02219	-0.276527	0.235406	0.8681	0.9177
IL1alpha	0.00750	-0.249120	0.263018	0.9552	0.9552
IL5	0.15283	-0.108761	0.392396	0.2490	0.7380
IL7	0.23557	-0.023857	0.462086	0.0724	0.7238
TNFbeta	0.08195	-0.178548	0.330456	0.5388	0.8713
VEGF_A	-0.04794	-0.299959	0.211124	0.7196	0.8831
Eotaxin	0.04422	-0.214648	0.296596	0.7405	0.8831
Eotaxin3	-0.06515	-0.315457	0.194710	0.6254	0.8831
IP_10	-0.03804	-0.290987	0.220497	0.7758	0.8831
MCP1	0.16907	-0.092394	0.406294	0.2014	0.7238
MCP4	0.16413	-0.097391	0.402075	0.2152	0.7238
MDC	-0.13776	-0.379403	0.123821	0.2995	0.7388
MIP1alpha	-0.14666	-0.387088	0.114942	0.2690	0.7380
MIP_1beta	-0.01065	-0.265924	0.246187	0.9365	0.9552
TARC	0.04631	-0.212668	0.298487	0.7287	0.8831
bFGF	0.03598	-0.222445	0.289111	0.7877	0.8831
FLT1	0.17443	-0.086959	0.410858	0.1872	0.7238
PIGF	-0.12738	-0.370400	0.134123	0.3379	0.7391
Tie2	-0.12693	-0.370006	0.134571	0.3396	0.7391
VEGF_C	0.05979	-0.199837	0.310645	0.6542	0.8831
VEGF_D	-0.10987	-0.355107	0.151374	0.4091	0.8409
CRP	-0.18091	-0.416355	0.080374	0.1710	0.7238
SAA	-0.24440	-0.469363	0.014568	0.0619	0.7238
ICAM_1	-0.31643	-0.527633	-0.062953	0.0142	0.5255
VCAM_1	-0.08568	-0.333770	0.174940	0.5204	0.8713

Supplemental Table 11: Association between MESOSCALE central biomarkers and cardioembolic etiology, univariate analysis

Biomarker	EffectSize	EffectSize_lowerCI	EffectSize_upperCI	Pvalue	PvalueCor
IFNy	0.54067	0.04278	1.03856	0.0355	0.1927
IL10	-0.23726	-0.72879	0.25427	0.3453	0.5555
IL13	-0.56693	-1.06560	-0.06825	0.0279	0.1927
IL1B	-0.58366	-1.08285	-0.08447	0.0239	0.1927
IL2	-0.22082	-0.71214	0.27051	0.3796	0.5623
IL4	-0.28739	-0.77964	0.20485	0.2539	0.4697
IL6	-0.09945	-0.58972	0.39082	0.6934	0.8429
IL8	-0.20110	-0.69220	0.29000	0.4235	0.5983
TNFalpha	0.44258	-0.05272	0.93789	0.0822	0.2239
IL12	0.43145	-0.06359	0.92649	0.0898	0.2239
IL15	-0.08161	-0.57179	0.40857	0.7470	0.8429
IL16	-0.06527	-0.55538	0.42485	0.7973	0.8429
IL17A	0.22066	-0.27066	0.71198	0.3799	0.5623
IL1alpha	0.38441	-0.10960	0.87841	0.1292	0.2657
IL5	0.52456	0.02713	1.02199	0.0410	0.1927
IL7	0.25845	-0.23336	0.75027	0.3043	0.5117
TNFbeta	0.39255	-0.10163	0.88672	0.1216	0.2647
VEGF_A	-0.47115	-0.96716	0.02486	0.0649	0.2057
Eotaxin	0.05043	-0.43964	0.54049	0.8437	0.8672
Eotaxin3	-0.07864	-0.56880	0.41153	0.7561	0.8429
IP_10	0.60001	0.10031	1.09972	0.0205	0.1927
MCP1	-0.09350	-0.58374	0.39674	0.7111	0.8429
MCP4	0.48393	-0.01240	0.98027	0.0583	0.2057
MDC	0.42357	-0.07129	0.91843	0.0956	0.2239
MIP1alpha	0.27974	-0.21239	0.77186	0.2666	0.4697
MIP_1beta	0.07121	-0.41893	0.56135	0.7789	0.8429
TARC	0.14715	-0.34344	0.63773	0.5583	0.7123
bFGF	-0.28419	-0.77814	0.20976	0.2608	0.4697
FLT1	-0.19615	-0.68895	0.29664	0.4366	0.5983
PIGF	-0.48660	-0.98480	0.01161	0.0579	0.2057
Tie2	-0.00303	-0.49476	0.48871	0.9952	0.9952
VEGF_C	-0.14874	-0.64108	0.34360	0.5555	0.7123
VEGF_D	0.84639	0.33533	1.35746	0.0017	0.0620
CRP	0.77833	0.27210	1.28455	0.0034	0.0622
SAA	0.46794	-0.02799	0.96386	0.0667	0.2057
ICAM_1	0.52268	0.02530	1.02006	0.0417	0.1927
VCAM_1	0.42199	-0.07283	0.91682	0.0968	0.2239

Supplemental Table 12: Association between MESOSCALE biomarkers and any hemorrhagic transformation, univariate analysis

Biomarker	EffectSize	EffectSize_lowerCI	EffectSize_upperCI	Pvalue	PvalueCor
IFNy	-0.47943	-0.95635	-0.00251	0.0531	0.6553
IL10	0.24774	-0.22431	0.71978	0.2940	0.9308
IL13	0.33131	-0.14215	0.80476	0.1714	0.9308
IL1B	-0.07198	-0.54239	0.39844	0.7546	0.9308
IL2	-0.23681	-0.70870	0.23508	0.3216	0.9308
IL4	0.07062	-0.39979	0.54102	0.7547	0.9308
IL6	0.35960	-0.11442	0.83362	0.1422	0.9308
IL8	0.24547	-0.22654	0.71749	0.3022	0.9308
TNFalpha	0.00376	-0.46650	0.47402	1.0000	1.0000
IL12	-0.16117	-0.63219	0.30985	0.5016	0.9308
IL15	0.22894	-0.24285	0.70072	0.3426	0.9308
IL16	0.18052	-0.29069	0.65173	0.4576	0.9308
IL17A	-0.22991	-0.70171	0.24189	0.3307	0.9308
IL1alpha	-0.14883	-0.61973	0.32208	0.5398	0.9308
IL5	-0.21235	-0.68392	0.25923	0.3795	0.9308
IL7	-0.03206	-0.50235	0.43823	0.8968	0.9361
TNFbeta	-0.08728	-0.55776	0.38320	0.7210	0.9308
VEGF_A	-0.10032	-0.57087	0.37024	0.6670	0.9308
Eotaxin	-0.53085	-1.00926	-0.05244	0.0324	0.5988
Eotaxin3	-0.12528	-0.59600	0.34543	0.6081	0.9308
IP_10	-0.29030	-0.76301	0.18242	0.2292	0.9308
MCP1	0.02678	-0.44350	0.49706	0.9062	0.9361
MCP4	-0.09753	-0.56807	0.37301	0.6929	0.9308
MDC	0.11976	-0.35092	0.59044	0.6246	0.9308
MIP1alpha	-0.08891	-0.55940	0.38158	0.7016	0.9308
MIP_1beta	-0.03376	-0.50405	0.43653	0.8875	0.9361
TARC	0.53123	0.05281	1.00966	0.0305	0.5988
bFGF	-0.02461	-0.49899	0.44976	0.9088	0.9361
FLT1	0.24630	-0.22984	0.72243	0.3109	0.9308
PIGF	0.21221	-0.26347	0.68789	0.3951	0.9308
Tie2	-0.10816	-0.58286	0.36654	0.6510	0.9308
VEGF_C	0.27545	-0.20114	0.75203	0.2697	0.9308
VEGF_D	0.10691	-0.36778	0.58161	0.6597	0.9308
CRP	-0.10061	-0.57117	0.36995	0.6713	0.9308
SAA	-0.02557	-0.49585	0.44471	0.9108	0.9361
ICAM_1	-0.16164	-0.63266	0.30938	0.5321	0.9308
VCAM_1	0.05991	-0.41046	0.53027	0.7999	0.9361

Supplemental Table 13: Association between MESOSCALE biomarkers and any hemorrhagic transformation, multivariate analysis

Biomarker	EffectSize	EffectSize_lowerCI	EffectSize_upperCI	Pvalue	PvalueCor
IFNy	-0.44202	-0.91579	0.03174	0.0687	0.8703
IL10	0.13546	-0.33053	0.60144	0.5704	0.9936
IL13	0.33431	-0.14010	0.80872	0.1690	0.8703
IL1B	-0.14720	-0.61636	0.32197	0.5402	0.9936
IL2	-0.27842	-0.75269	0.19584	0.2518	0.9318
IL4	-0.00188	-0.46261	0.45884	0.9936	0.9936
IL6	0.19617	-0.26847	0.66082	0.4098	0.9936
IL8	0.24730	-0.22340	0.71799	0.3051	0.9936
TNFalpha	-0.07026	-0.54212	0.40161	0.7713	0.9936
IL12	-0.30597	-0.77590	0.16396	0.2038	0.8703
IL15	0.19064	-0.28375	0.66503	0.4327	0.9936
IL16	0.09874	-0.36875	0.56624	0.6801	0.9936
IL17A	-0.37604	-0.84508	0.09299	0.1177	0.8703
IL1alpha	-0.14370	-0.61858	0.33117	0.5547	0.9936
IL5	-0.29518	-0.75648	0.16613	0.2117	0.8703
IL7	0.00216	-0.47048	0.47479	0.9929	0.9936
TNFbeta	-0.01743	-0.48311	0.44825	0.9418	0.9936
VEGF_A	-0.07934	-0.55358	0.39490	0.7439	0.9936
Eotaxin	-0.39122	-0.84295	0.06050	0.0910	0.8703
Eotaxin3	-0.13731	-0.60979	0.33517	0.5704	0.9936
IP_10	-0.30484	-0.78035	0.17068	0.2108	0.8703
MCP1	0.09909	-0.35384	0.55201	0.6693	0.9936
MCP4	-0.06961	-0.53862	0.39940	0.7720	0.9936
MDC	0.09891	-0.37433	0.57215	0.6832	0.9936
MIP1a	-0.04832	-0.51264	0.41601	0.8390	0.9936
MIP_1b	0.06502	-0.39823	0.52827	0.7841	0.9936
TARC	0.55465	0.07277	1.03654	0.0247	0.8703
bFGF	-0.01809	-0.49559	0.45942	0.9411	0.9936
FLT1	0.18292	-0.28837	0.65421	0.4486	0.9936
PIGF	0.18812	-0.28965	0.66589	0.4421	0.9936
Tie2	-0.19568	-0.67460	0.28323	0.4251	0.9936
VEGF_C	0.31350	-0.15966	0.78665	0.1960	0.8703
VEGF_D	0.04397	-0.43070	0.51865	0.8565	0.9936
CRP	-0.12650	-0.59880	0.34579	0.6010	0.9936
SAA	-0.00734	-0.47863	0.46395	0.9757	0.9936
ICAM_1	-0.17668	-0.65168	0.29831	0.4677	0.9936
VCAM_1	0.03004	-0.44373	0.50381	0.9015	0.9936